The role of Myosin VI in epithelial morphogenesis in *Drosophila melanogaster*

Hadas Millo

Thesis presented for the Degree of Doctor of Philosophy

The University of Edinburgh

2004

Acknowledgments

I would like to thank my supervisor, Mary Bownes, for guiding me throughout my thesis. Mary gave me the confidence to do my first own steps in research and in the same time she was always there to help when an advice was needed, always optimistic and for that I am grateful.

To my second supervisor, Justin Goodrich, for his good advice at all stages.

I am gratefull to the Darwin Trust for their studentship and the B'nei B'rith fellowship for their support.

To my dear husband Yuval who encouraged me to start the PhD studies, and supported me all the way, always helpful and showing a keen interest in my research project.

To my parents who always supported me.

To Vasiliki Lazou, for all the work that she did so dedicatedly, for understanding my sentences even when I was not totally clear, and for all the enjoyable time we had together.

To George Tzolovsky for helping me so much, especially in my first year.

To Jan and Paul Barfoot, for being good friends, for contributing to the corrections of the thesis, and for sharing with me and Yuval a great time (24).

To Leanne McGurk, for the nice time we had when we worked together and for being always helpful kind and patience.

To Kathleen Rothwell who helped me to get a soft lending in the lab, during the beginning of my studies, who was caring and helpful, and a good chat during the coffee breaks.

To Hilary Anderson for all the help with printing and submitting of articles.

And finally I would like to thank to the rest of the people in the lab, for always being helpful and nice: Sheng-in Lin, Sofia Papadia, Jun Terashima, and Tim Wood.

Abstract

In this thesis the role of Myosin VI in epithelial morphogenesis was investigated. Myosins are motor proteins that move along actin filaments. Myosins are composed of a head domain (termed the motor domain), a neck domain (which serves as a lever arm), and a tail domain (which binds to the cargo). In *Drosophila melanogaster* eight myosins had been identified previously and we identified five new myosins when the *Drosophila* genome was published. The characterization of the new myosins is described.

The *Drosophila* Myosin VI is encoded by the gene *jaguar*. This Myosin VI is unique as it moves to the minus end of the actin filament which is the opposite direction to the other myosins. Previous studies showed that Myosin VI is necessary for the organization and migration of the follicle cells during oogenesis and for the morphogenesis of the imaginal discs. In order to examine the function of the whole Myosin VI molecule in epithelial tissues, the whole Myosin VI molecule or its separate domains (the head+ neck domains or the tail domain) tagged to Green Fluorescent Protein (GFP) were expressed in somatic cells under the control of Gal4 protein and their localisation in the cells was observed. The expression of the tagged proteins under the control of a *Myosin VI-Gal4* line allowed us to observe all the epithelial cells that express Myosin VI during the whole life cycle. In many epithelial cells the head domain seems to pull the whole molecule towards the cell nucleus, where the minus end of the actin filaments is localised, however it was found that the tail is the domain that anchors the whole molecule to specific areas of the cells away from the nucleus, probably by the binding to cargo molecules.

The role of Myosin VI in dorsal closure was found when four Myosin VI mutants that were produced in our laboratory failed to close the dorsal hole during embryogenesis. The genotype and phenotype of two of the mutants, jar^{R39} and jar^{R235} are described. Depletion of Myosin VI caused detachment of cells in the leading edge and the amnioserosa and folding-in of the tissue. A similar phenotype was observed when a Myosin VI dominant negative was expressed. In regions of ruptured tissue DE-cadherin and Armadillo was mislocalised, therefore Myosin VI seems to interact with these proteins during cell adhesion. Actin filaments were found to be

disorganized at the leading edge and in the lateral epidermis at regions of ruptured tissue, suggesting that Myosin VI is also necessary for actin dynamics during dorsal closure.

The mechanism of Myosin VI function during oogenesis was investigated, by a search for proteins that function downstream of Myosin VI. Myosin VI was necessary for the expression and localisation of Dlg, Bazooka, PS2α-integrin, PSβ-integrin and Ankyrin. These results suggest that through the interaction with these molecules, Myosin VI might maintain epithelium integrity by controlling follicle cells invasion, their adhesion to extracellular matrix, and cell polarity. The effect of Myosin VI on Clathrin and α-adaptin localisation suggest a possible role of Myosin VI in endocytosis.

Abbreviations

ADP- adenosine diphosphate

AMPA - α-amino-3-hydroxy-5-methylisoxazole-4-propionic acid

ATP- adenosine triphosphate

ck –crinkled

CLIP-190- cytoplasmic linker protein-190

CLIP-190 -cytoplasmic linker protein-190

CN-connective fiber

CO- commissure fiber

DAB2 -Disabled 2

Dlg- Discs Large

DMBS – *Drosophila* myosin binding unit

ERM - Ezrin, Radixin, Moesin

EtOH – Ethanol

FERM -band 4.1, Ezrin, Radixin, Moesin

GAIP - G-alpha interacting protein

GFP – Green Fluorescent Protein

GIPC – GAIP interacting protein C terminus

hr - hours

IC – individualization complex

jar -jaguar

LCE -Long Cellular Extensions

Lgl - Lethal Giant Larvae

MAGUK - membrane associated guanylate kinase homologue

MBS – myosin binding unit

MGC- midline glial cells

Mhcl -myosin heavy chain like

min - minutes

MRLC – myosin regulatory light chain

MyTH4 - Myosin tail homology 4

NM-Nonmuscle

NSAD - nonsyndromic dominant form of deafness

nucl. – nucleotides

O/N - over night

PAK -p21-activated kinase 3

PGMH-PUAST-GFP-Myosin VI Head+ Neck domain

PGM-pUAST-GFP-Myosin VI (whole molecule)

PGMT-PUAST-GFP-Myosin VI Tail domain

PS integrin-position specific integrin

Rho-Rhomboid

ROK- Rho associated kinase

RT - Room Temperature

SAP97 -synapse-associated protein 97

SAS - Stranded at second

sec - seconds

Sqh - spaghetti - squash

TEDS -glutamic or aspartic acids, threonine or serine

U - units

UAS -Upstream Activation Sequence

zip –zipper

Table of contents

List of Figures

List of Tables

Chapter 1:

Introduction

All developmental processes involve the precise localisation of cells, organelles, proteins, nucleic acids and other molecules at specific times, and this is established in part by transportation using motor proteins. Thus motor proteins have the potential to play crucial roles in development. Nevertheless, in comparison to signal proteins, very little is known about the role of myosins in the patterning of epithelial tissues. Nonmuscle Myosin II was found to participate in the patterning of epithelial tissues in the fly life cycle (this is described below) and to be necessary for dorsal closure, imaginal discs morphogenesis and oogenesis (Young et al., 1993).

The function of Myosin VI in epithelial morphogenesis emerged only five years ago. Disruption of the expression of Myosin VI caused changes in follicle cell shape, loss of the epithelial integrity and aberrant migration of the follicle cells (Deng et al., 1999). Adult files had malformed legs and wings, suggesting that Myosin VI is also necessary for the morphogenesis of imaginal discs. In a recent study in our laboratory it was found that Myosin VI mutants fail to complete dorsal closure during embryogenesis (Leaper, 2003; Millo et al., 2004). All these results show that Myosin VI is crucial for the proper development of epithelial tissues. Myosin VI was also found to be necessary for the organization of actin filaments and to interact with proteins involved in actin dynamics in the individualization complex during spermatogenesis (Rogat and Miller, 2002), and mutations in Myosin VI cause male sterility (Hicks et al., 1999).

During dorsal closure, the detachment of the cells at the leading edge, in the absence of Myosin VI suggested that Myosin VI regulates cell adhesion (Millo et al., 2004). This was supported by the interaction that was found between Myosin VI, DE-cadherin and Armadillo in oogenesis (Geisbrecht and Montell, 2002). During oogenesis, the invasion of the follicle cell into the nurse cells cluster and the arrest of the cell migration suggest that Myosin VI might have additional roles (Deng et al., 1999), such as mediation of cells invasion and cell polarity. Finally, the need for Myosin VI for the organization of the actin filaments in the individualization complex (Hicks et al., 1999; Rogat and Miller, 2002) could suggest that the maintenance of tissue integrity by Myosin VI is established by mediating the organization of the actin cytoskeleton in the cells.

The aim of this thesis was to further investigate how Myosin VI functions in epithelial cells. This was established by examining the localisation of Myosin VI molecule and its separate domains in epithelial cells and in the individualization complex. In addition, a screen was made for proteins that would function downstream to Myosin VI and that play a role in cell-cell and cell-matrix adhesion, cell polarity and cell invasion, during oogenesis and dorsal closure.

This chapter reviews existing literature on the molecular structure and the function of myosins, in particular Myosin VI. The function of Myosin VI in *Drosophila* and in other species is described in detail along with several suggested mechanisms for how the whole molecule functions. The discussion about the various functions of Myosin VI is related to the studies in this thesis examining the function of Myosin VI molecule and it separate domains.

Because this thesis describes the characterization of novel myosins, the *Drosophila* myosins that had been identified prior to these findings are also described.

1.1 The structure of myosins

Myosins are molecular motors that move along actin filaments by converting energy obtained from adenosine triphosphate (ATP) hydrolysis to a mechanical force (Mooseker and Cheney, 1995). The myosin heavy chain molecule contains three domains: the head domain (also known as the motor domain) at the N terminus, the neck domain, and the tail domain at the C terminus. This structure, as it appears in Myosin VI is shown in figure 1.1. The various structures of all *Drosophila* myosins are seen in figure 1.3.

The motor domain contains a catalytic core, which binds actin and ATP. Hydrolysis of ATP generates force that is translated into movement of myosin along actin filaments. The motor domain contains at its carboxylic terminus a converter domain that links the catalytic core to the neck domain. This region converts the energy of ATP breakdown into movement. The head domain also contains an actin-binding site. Within the actin-binding site there is a TEDS domain which includes serine, threonine, aspartic or glutamic acid. Most of the myosins have the acidic residues

(aspartic or glutamic acid). In myosins from classes I and VI this region regulates the enzymatic activity by phosphorylation of serine or threonine (Mooseker and Cheney, 1995). The head domains are highly conserved but also contain class - specific sequences.

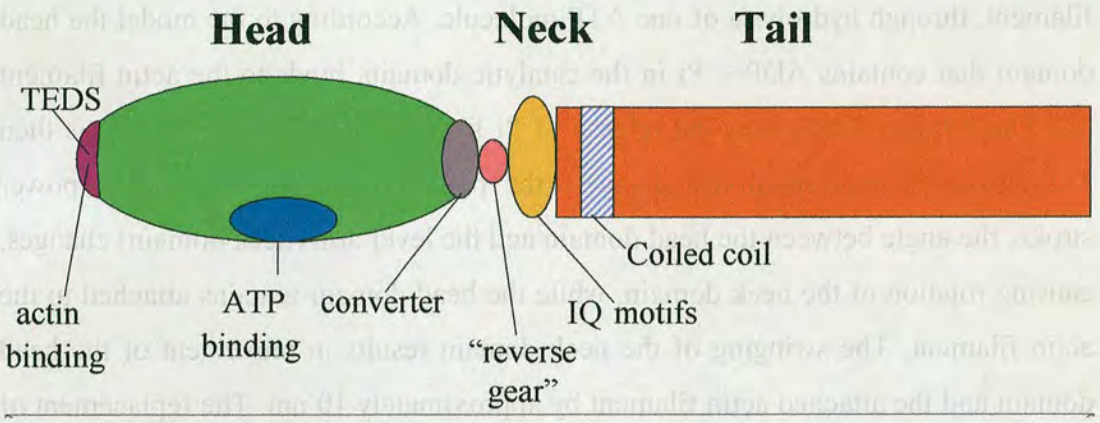

Figure 1.1: The structure of Myosin VI. The head, the neck and the tail domains are marked. The head domain contains actin binding site, ATP binding site and the converter, which converts the energy from ATP breakdown into mechanical movement. The TEDS domain lies within the actin-binding site and in Myosin VI it contains the amino acid Threonine that is phosphorylated. Between the converter and the neck domain there is an insert of the "reverse gear" domain, which changes the angle between the head and the neck domain and subsequently the direction of movement of Myosin VI. The neck domain is composed one IQ motif, which binds Calmodulin. The tail domain contains a coiled-coil region and a globular tail domain which binds to cargo proteins.

The neck domain serves as a lever arm. The movement of the converter, via ATP hydrolysis, is directly transmitted to the neck domain, so that a rotation of the converter will cause movement of the neck domain. The neck domain consists of a variable number of light - chain binding motifs, IQ motifs, containing the consensus sequence IQXXXRGXXXR (Fig. 1.1 shows one IQ motif in Myosin VI). Each IQ motif is a potential binding site for Calmodulin and/or tissue specific myosin light chains, which modulate the binding of the myosin head to actin and thus regulate myosin activity (Wolenski, 1995).

The tail domain has a structure which is specific to its class and controls the interaction of a given myosin with its cargo.

1.2 The motility of myosins along actin fragment

The model suggested for the movement of myosin along the actin filament is called the 'swinging lever arm' (Rayment et al., 1993; Vale and Milligan, 2000; Volkman and Hanein, 2000). (Described in Fig. 1.2.1) It proposes that the movement takes place through separate cycles, in each myosin makes one movement along the actin filament, through hydrolysis of one ATP molecule. According to the model the head domain that contains ADP + Pi in the catalytic domain, binds to the actin filament (a). The binding accelerates the release of Pi from the catalytic site, which is then followed by a conformational change - the power stroke (b). During the power stroke, the angle between the head domain and the lever arm (neck domain) changes, causing rotation of the neck domain, while the head domain remains attached to the actin filament. The swinging of the neck domain results in movement of the head domain and the attached actin filament by approximately 10 nm. The replacement of ADP by ATP in the catalytic site causes a conformational change in the myosin head, and a dissociation of the myosin head from actin (c). ATP is hydrolysed to ADP and Pi, both of which remain tightly bound to the myosin head (d). The hydrolysis is accompanied by an additional conformational change and a movement of the neck domain in a reverse direction to the power stroke. Finally, the binding of the motor domain to actin initiates a new cycle.

The figures in the following pages:

Figure 1.2.1. The swinging lever arm cycle. (a) ADP + Pi are bound to the catalytic domain (ATP binding site), and the motor domain is weakly bound to actin. (b) Pi is released from the catalytic domain and the neck domain undergoes a power stroke, pulling the motor domain and actin (c) The attachment of ATP to the catalytic domain dissociates the motor domain from actin. (d) ATP hydrolysis results in the rotation of the neck domain to its original position, prior to the power stroke.

Figure 1.2.2. In Myosin VI, the insert of 53 AA between the converter and the neck domain ("reverse gear", marked in red) changes the angle between the head and the neck domains, causing a change in the movement of the whole molecule towards the minus end of the actin filaments. This is in contrast to most other myosins that move towards the plus, barbed-end of the actin filaments.

Figure 1.2.1

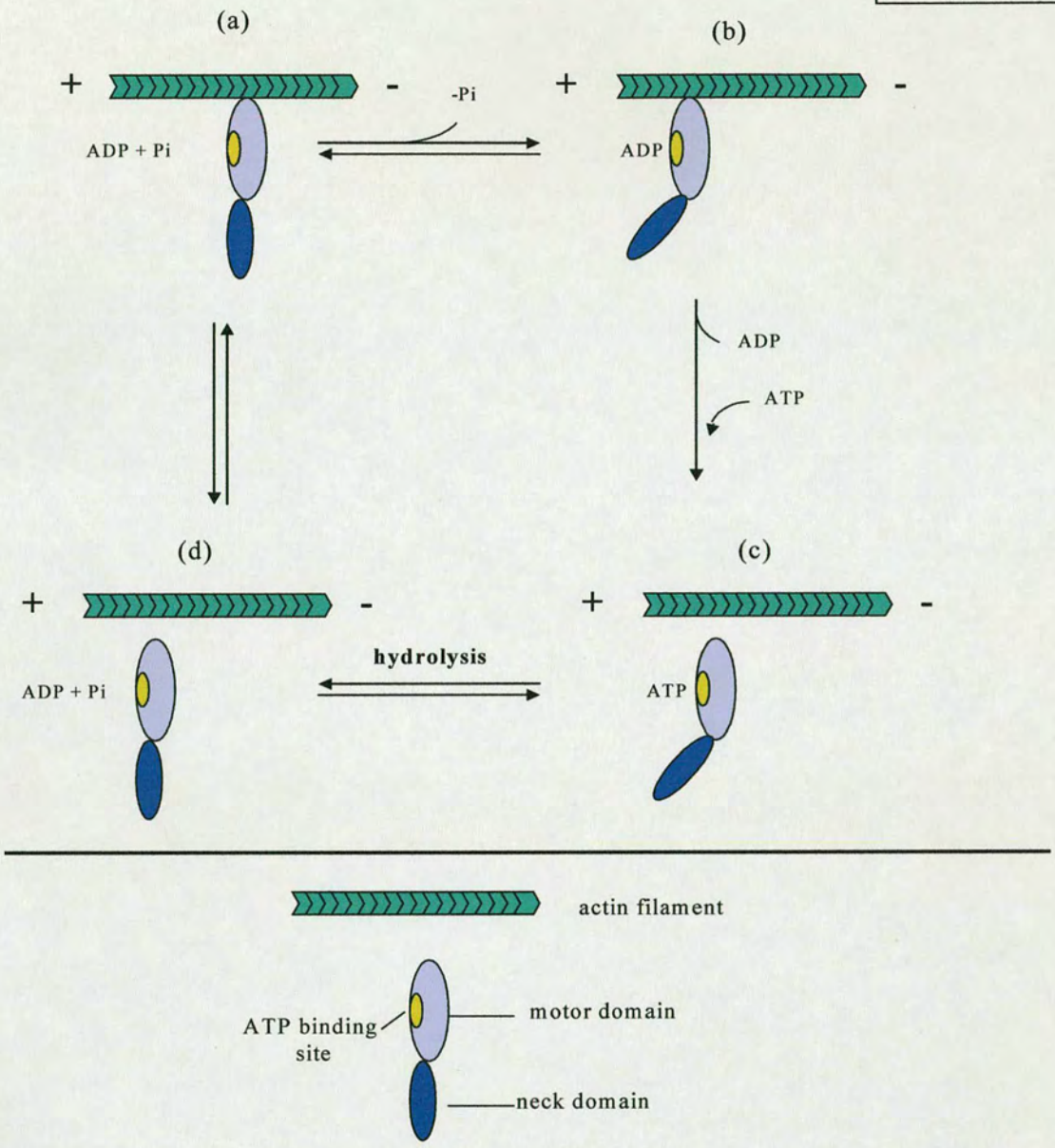

Figure 1.2.2

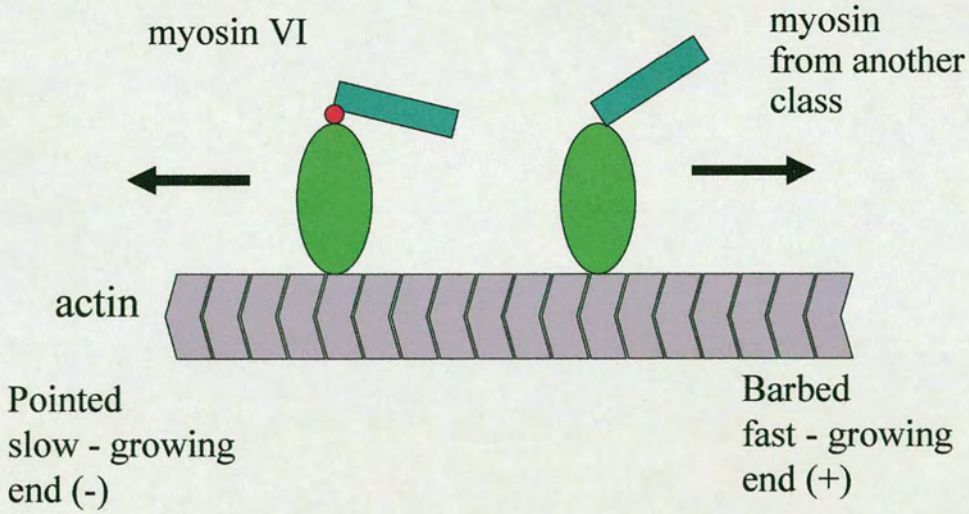

Recently it was suggested that the movement of myosins along actin filaments combines the swinging lever arm cycle along with Brownian movement (Geeves, 2002). Brownian movement causes the actin filament to move with respect to myosin and helps to re-locate myosin in a new actin site. The asymmetry of the actin filaments and the lever arm movement could bias the Brownian motion of the attachment/detachment in the same direction as the lever swings (Houdusse and Sweeney, 2001).

Apart from Myosin VI, all other myosins move towards the barbed, plus end of the actin filaments (Fig. 1.2.2). As the next section explains, Myosin VI moves towards the minus-pointed end of Myosin VI.

1.3 The classes of myosins found in Drosophila and their roles

So far, thirteen myosins have been identified in *Drosophila*, classified into eight different classes. Five novel myosins were found in our laboratory: Myo28B (VIIB), Myo10A (XV), Myo89B (Mhcl-PDZ, class XVIII), Myo29D (which forms a class of its own) and Myo95E (IC) (Tzolovsky et al., 2002). The analysis of these proteins is described in chapter 3. This section focuses on the structure and function of the myosins that had been found previously. First, Myosin VI is described in detail, followed by a description of the rest of the myosins.

1.3.1 Myosin VI

1.3.1.1 The structure and movement of Myosin VI

Class VI myosins contain the amino acid threonine (Thr^{406}) in the TEDS domain, which is phosphorylated by p21-activated kinase 3 (PAK) (Buss et al., 1998; Yoshimura et al., 2001). The phosphorylation of Thr^{406} accelerates the release of Pi. This does not seem to accelerate the movement of the motor domain along actin filaments (Morris et al., 2003). Nevertheless, the phosphorylation Myosin VI by PAK localises Myosin VI to sites of newly formed ruffles in human epidermal carcinoma cells (Buss et al., 1998), suggesting that the phosphorylation of Myosin VI does change the function of the molecule.

Figure 1.3. **A:** *Drosophila* myosins that have been identified so far. The name of the gene and the class type are indicated for every myosin: Myosin IA and IB (the gene location is indicated); muscle Myosin II, encoded by the gene *mhc*; nonmuscle Myosin II, encoded by the gene *zipper* (*zip*); Myosin III, encoded by the gene *ninaC*; Myosin V, encoded by the gene *didum*; Myosin VI, encoded by the gene *jaguar* (*jar*); and Myosin VIIa, encoded by the gene *crinkled* (*ck*). **B:** the novel myosins that have been identified. Myo95E, Myo28B, Myo10A and Myo29D are named according to their chromosomal location. Mhcl-PDZ is an abbreviation for Myosin heavy chain like containing PDZ. Myo95E was classified as Myosin IC; Myo28B was classified as Myosin VIIB; Myo10A was classified as Myosin XV; Mhcl-PDZ (located in position 89B) was classified as Myosin XVIII and Myo29D that creates a class of its own (XIX). Motor proteins are marked in red, IQ motifs in the neck domains are marked in yellow and the different domains within the tail are marked according to the key.

The neck domain includes one recognizable IQ motif that binds Calmodulin (Fig. 1.1). The binding of Calmodulin is thought to allow regulation of Myosin VI by Calcium. A recent study showed that increased Calcium levels above 10 μM slow Myosin VI motility (Morris et al., 2003).

The tail domain includes a region predicted to form a coiled – coil and a globular C - terminal domain (Fig. 1.1 and1.3). Native Myosin VI was thus predicted to exist as a two-headed dimer of the ~140 kDa heavy chains (Buss et al., 1998; Cheney et al., 1993; Mooseker and Cheney, 1995). However, gel filtration and sucrose density gradient experiments showed that the molecular weight of expressed and native Myosin VI was close to that of one single heavy chain molecule. Therefore it seems that Myosin VI may be a monomer and not a dimer (Lister et al., 2004).

Myosin VI differs from other myosins in having an insert of 53 AA between the converter domain and the neck domain. Image analysis of electron micrographs of actin filaments in the rigor state (no ATP) revealed that the neck domain (lever arm) of Myosin VI is twisted towards the pointed end of actin filaments, the opposite orientation to that found in other myosins (Fig. 1.2.2). It appears that this insert completely changes the direction in which the lever arm of Myosin VI swings (Wells et al., 1999). This domain was found to bind a Calmodulin molecule, with four Calcium ions (Bahloul et al., 2004).

Figure 1.3

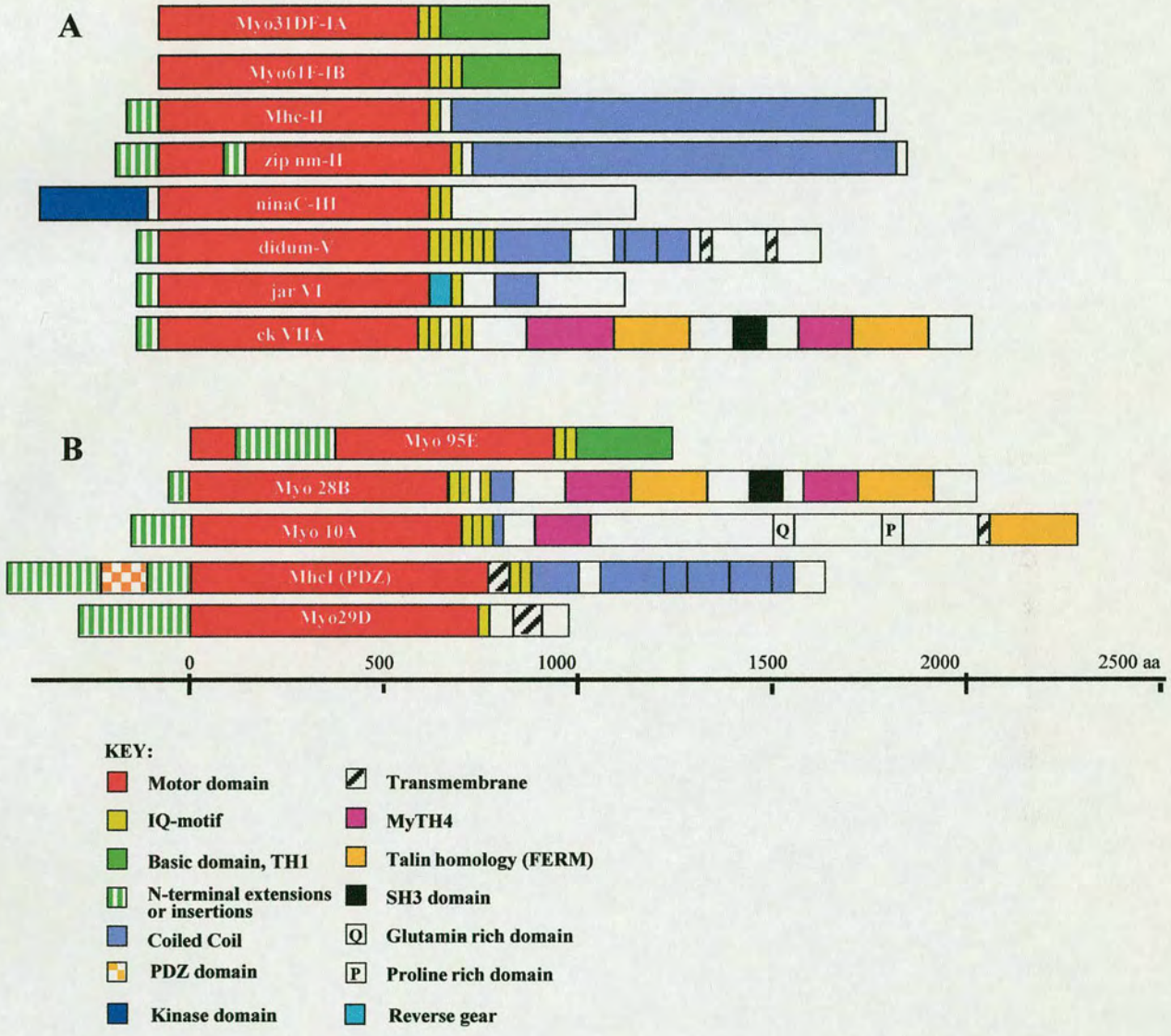
A
Myo31DF-IA
Myo61F-IB
Mhc-II
zip nm-II
ninaC-III
didum-V
jar VI
ck VIIA
B
Myo 95E
Myo 28B
Myo 10A
Q
P
MhcI (PDZ)
Myo29D
0
500
1000
1500
2000
2500 aa
KEY:
Motor domain
IQ-motif
Basic domain, TH1
N-terminal extensions or insertions
Coiled Coil
PDZ domain
Kinase domain
Transmembrane
MyTH4
Talin homology (FERM)
SH3 domain
Glutamin rich domain
Proline rich domain
Reverse gear

Because the Calcium ions do not dissociate from the Calmodulin complex bound to the insert it is suggested that this complex is structural Calmodulin that does not regulate the motor movement.

A recent study showed that Myosin VI moves in relatively big steps (36 nm) (Rock et al., 2001). According to the lever arm model, the size of the steps would be dependent on the size of the lever arm, which is defined according to the number of IQ motifs at the neck domain. This part of model is consistent with studies that showed a linear relation between the length of the lever arm and the speed of the movement in myosins engineered with different lever arm lengths (Geeves, 2002). Therefore, it was surprising to find that the size of steps made by Myosin VI-(which contains only one IQ motif), was similar to those of Myosin V that contains 6 IQ motifs. To resolve this discrepancy it was suggested that the movement of myosins along the actin filaments combines the swinging lever arm that drives the foreword steps of the head domain to bind in the next free actin site, along with Brownian movement that helps to locate and bind myosin to that site (Geeves, 2002).

It is also difficult to explain with the lever arm model the large working stroke (18 nm) of Myosin VI that was found recently, in the presence of its small neck domain (Lister et al., 2004), unless other regions in the molecule contribute to the lever arm. A possible model that explains the large stroke suggests that the size of the stroke is determined by a combination of lever arm length, orientation and position. The big stroke could be established through the swinging of the lever arm by 138°, to its final location at the rigor position or at the ADP bound position (the stroke between these two positions is only 1 nm) (Lister et al., 2004).

One of the functions proposed for Myosin VI is as an anchor of vesicles and proteins to actin filaments. The observation of single Myosin VI molecules revealed that under a backward force (load) application the movement of Myosin VI stops as it binds tightly to actin. In this way, Myosin VI is converted from a transporter to an anchor (Altman et al., 2004).

1.3.1.2 The roles of Myosin VI in Drosophila

Drosophila Myosin VI was the first to be identified in this class (Kellerman and Miller, 1992). Myosin VI is found in other species, including human, mice, pigs, rat, chicken, fish, sea urchin primates, and *C. elegans* (Avraham et al., 1995; Breckler et al., 2000; Hasson and Mooseker, 1994; Kelleher et al., 2000; Melchionda et al., 2001; Sirotkin et al., 2000; Wu et al., 2002). The structure and function of Myosin VI were described in the previous section.

The *Drosophila* Myosin VI gene (*jaguar*) is found at locus 95F on the third chromosome (Kellerman and Miller, 1992). The *jaguar* transcript is alternatively spliced within the tail domain at a site adjacent to the C - terminus of the coiled - coil domain, suggesting that at least four different protein isoforms exist. *Drosophila* Myosin VI is expressed throughout the life cycle (Kellerman and Miller, 1992), and antisense studies showed that the disruption of Myosin VI expression at various stages of development result in lethality (Deng et al., 1999).

Myosin VI seems to play a role in epithelial cell shape change and cell migration in various processes throughout life cycle. During embryogenesis, Myosin VI is expressed in the syncitial blastoderm, where it is necessary for the transport of particles (Fig. 1.3.1A), and participates in the formation of the pseudocleavage furrows between adjacent nuclei during division. Inhibition of Myosin VI function by antibody injection blocked the particle movements and caused severe defects in the syncitial blastoderm organization, including nuclear defects and disorders in cytoskeletal patterning (Mermall et al., 1994; Mermall and Miller, 1995). The invagination of the furrows could be achieved by pulling the membrane along the actin filaments towards its pointed end, which is located in the cell's interior; however the precise function of Myosin VI in this location is still not fully understood.

During later stages of embryogenesis (stage 14), Myosin VI is detected in the dorsal - lateral epidermal cells, at the leading edge of the epithelial sheet involved in dorsal closure, and in the posterior spiracles (Kellerman and Miller, 1992). During stages 14-16 Myosin VI is expressed in the central nervous system, where it is co-localised in the connectives and commissures with CLIP-190 (cytoplasmic linker protein 190), a homologue of CLIP-170. Co-immunoprecipitation studies in *Drosophila* showed

that Myosin VI interacts specifically with CLIP-190 in *Drosophila* embryos. Myosin VI and CLIP-190 are also co-expressed in the posterior pole of the early embryo (stage 2). CLIP-170 is a microtubule–binding protein and the similarity with CLIP-190 suggests that Myosin VI may participate in Transferring particles from actin filaments to microtubules and may connect between the two filaments, although the localisation of Myosin VI and CLIP-190 in the posterior pole is dependent on actin but not on the microtubule cytoskeleton (Lantz and Miller, 1998).

Myosin VI is also necessary for the asymmetric division of the neuroblasts (Petritsch et al., 2003). In *Drosophila* embryos proteins necessary for the determination of cell fate are targeted to the basal part of the neuroblasts, the spindle of the cells is rotated by 90° to align with the basal-apical axis, and the cells divide asymmetrically. In this process, Bazooka is localised to the apical region of the cell, where it recruits Inscuteable and other proteins that form the apical complex. This complex re-orients the spindle and targets the cell fate determining proteins and their adapter proteins-like Miranda to the basal part of the neuroblasts. It was found that Myosin VI is necessary for the localisation of Miranda basally and for proper spindle orientation. In Myosin VI mutants Miranda is mislocalised and the spindle in the neuroblasts is disoriented, yet the apical localisation of Inscuteable is not disrupted (as observed in stages 14-16: disrupting Myosin VI through the expression of Myosin VI dominant-negative caused Miranda mislocalisation and spindle misorientation at stage 9 (Bownes, 1975)). The direct binding of Miranda to Myosin VI supports the suggestion that the localisation of Miranda and its associated proteins basally is achieved via Myosin VI (Petritsch et al., 2003). Immunostaining shows that Myosin VI is not localised strictly at the basal crescent and this suggests that Myosin VI transports Miranda but it does not anchor it to the basal crescent. It was also found that Myosin VI has a synergistic action with the tumour suppressor protein Lethal Giant Larvae (Lgl): in *lgl* mutant embryos Miranda is present in the cell cortex, in the spindle and in the cell cytoplasm, while in the double mutant for Myosin VI and Lgl, Miranda is mostly localised in the cytoplasm.

During the third larval instar disruption in Myosin VI expression caused abnormal cuticle secretion, which suggests that Myosin VI is required for cuticle development (Deng et al., 1999). During metamorphosis, disruption in Myosin VI expression

resulted in malformed legs and wings in the adult fly, indicating that Myosin VI is essential for morphogenesis of the epithelial tissue in the imaginal disc during their development (Deng et al., 1999).

Myosin VI is necessary in the adult fly ovaries for the migration and the morphogenesis of the follicle cells epithelium, as section 1.7.1 shows. Myosin VI is also necessary for the last stage of the sperm maturation, sperm individualisation. In this process each one of the 64 spermatids is separated by a membrane that forms around it and encapsulates it. The membrane is created by an individualization complex (IC), which contains actin filaments surrounding every spermatid in a cone shape, and assembly of Myosin VI protein in a ring - shape around the spermatid, at the basement of the actin cone, between the area of the actin filaments and the site of the membrane assembly (Fig. 1.3.1B). The IC is formed at the edge of the spermatid, where the nucleus is located, and progresses along the spermatid while forming the membrane. In the Myosin VI mutants jar^{mmw14} and jar^{1} sperm individualization is inhibited and as a result the IC does not move along the spermatid and in several cases the cone structure of the IC is disrupted, which causes male sterility. This suggests that Myosin VI maintains the actin filaments at the investment cones in an organized form, and drives the membrane along the length of the spermatid (Castrillon et al., 1993; Hicks et al., 1999). The male sterility phenotype of jar^{mmw14} was rescued when Myosin VI cDNA was expressed, proving that this phenotype was caused as a result of Myosin VI depletion in the testes.

Figure 1.3.1: Myosin VI is involved in many developmental events that require membrane trafficking and assembly. **A:** An embryo during syncitial blastoderm organization. The nuclei undergo division and are separated by the formation of pseudocleavage furrows between adjacent mitotic spindles (chromosomes are drawn in blue, surrounded by microtubules). In *Drosophila*, Myosin VI is required for the invagination of the pseudocleavage furrows and for the transport particles (drawn in red), near the pseudocleavage furrows. **B:** In the testes, Myosin VI is required for the final stage of spermatogenesis - sperm individualization. In the diagram a cyst containing two out of the 64 spermatids is shown. The upper part of every spermatid is surrounded with membrane formed by the individualization complex, as it progresses towards the spermatid tail (arrow). **C:** A diagram presenting two stereocilia in the hair cells of the inner ear. Each stereocilia is separated by a coating membrane. Myosin VI is found in the circular plate, where the stereocilia are anchored (a region rich in actin filament), and in the perinuclear necklace, which is located between the cuticular plate and the plasma membrane. In *Snell's Waltzer* mice, the stereocilia are connected without having a separating membrane, (shown in dashed line), indicating that Myosin VI is required to maintain individual stereocilia separated by a coating membrane. **D:** During endocytosis two possible roles are suggested for Myosin VI: **1:** The larger isoform of Myosin VI plays a role in the creation of Clathrin coated vesicles, either by participating in the creation itself, or by cleaving the formed vesicles. **2:** The shorter isoform of Myosin VI is also necessary for the transport of the vesicles to the early endosome.

Figure 1.3.1

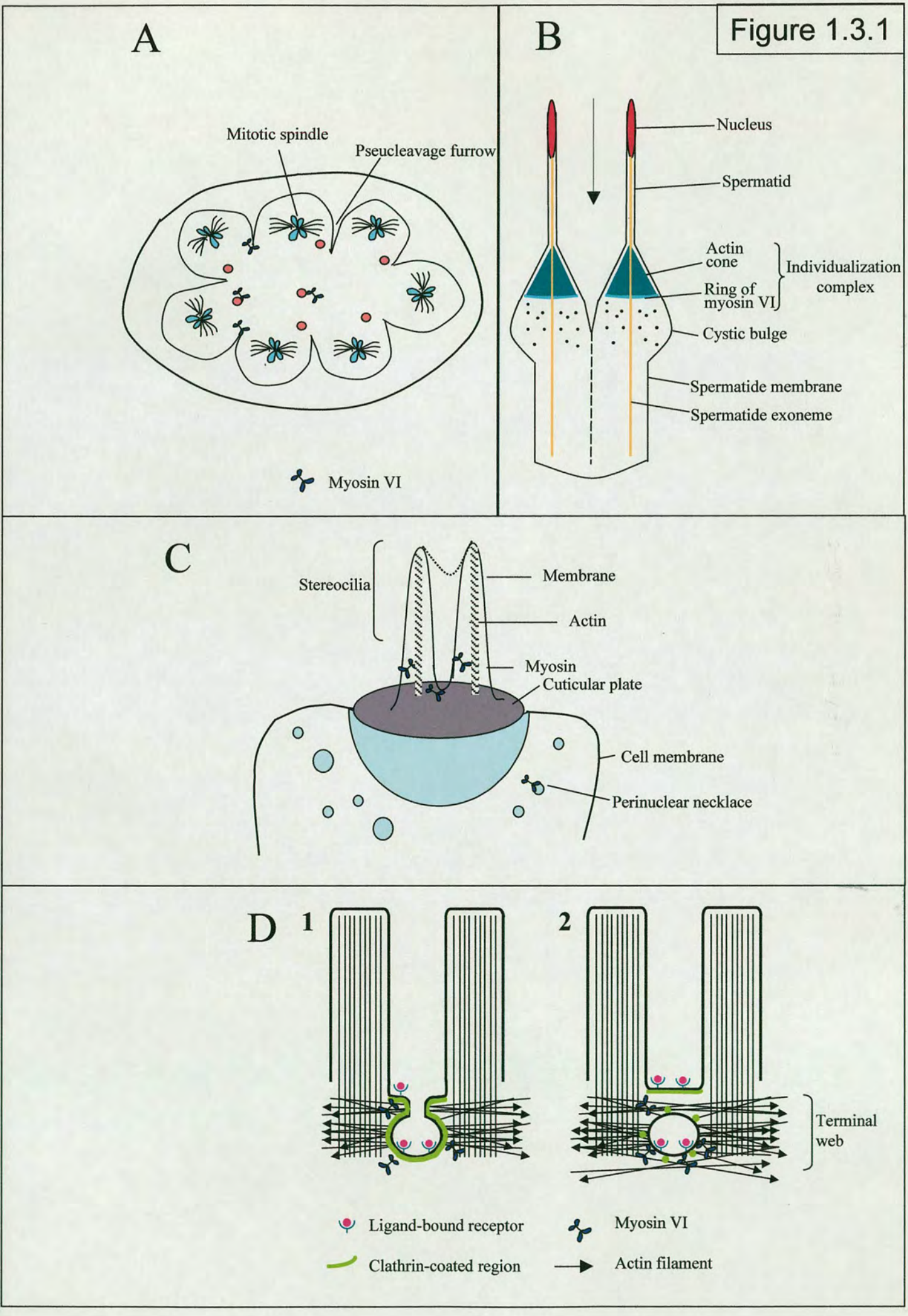
A
Mitotic spindle
Pseucleavage furrow
Myosin VI
B
Nucleus
Spermatid
Actin cone
Ring of myosin VI
Individualization complex
Cystic bulge
Spermatide membrane
Spermatide exoneme
C
Stereocilia
Membrane
Actin
Myosin
Cuticular plate
Cell membrane
Perinuclear necklace
D
1
2
Terminal web
Ligand-bound receptor
Clathrin-coated region
Myosin VI
Actin filament

Myosin VI co-localises at the base of the IC with proteins that participate in actin polymerisation: Cortactin, Arp2/3 complex and Capping protein (Rogat and Miller, 2002). Cortactin is a protein that links between actin dynamics and membrane signalling by interacting with actin polymerisation components and membrane associated-kinases; Arp2/3 is a complex of 7 proteins that binds to actin filaments at nucleation sites and initiates the synthesis of actin filaments, and Capping protein regulates actin assembly at the plus end or the filaments, at sites that Arp2/3 promotes actin assembly. In the *jar*^{1} homozygous mutants the distribution of Cortactin and Arp2/3 in the IC was abnormal, indicating that Myosin VI is necessary for the proper localisation of Cortactin and the Arp2/3 complex in the IC (Rogat and Miller, 2002).

Another protein that binds to Cortactin, Dynamin, is also expressed in the individualisation complex. Dynamin regulates actin dynamics in membrane sites where actin filaments are synthesized. The mutations of Myosin VI (*jar*^{1}) and Dynamin (*shi*^{1}) interact genetically, causing a significant decrease in the number of IC in the testes and severe defects in the stability of the IC actin filaments. This suggests that Myosin VI and Dynamin work in concert in the stabilisation of actin filaments in the IC (Rogat and Miller, 2002).

1.3.1.3 The roles of Myosin VI in other species

In the Golgi complex of mice fibroblast cells, Myosin VI is necessary for the secretion of Golgi-processed proteins and for maintaining the Golgi complex structure (Warner et al., 2003). Myosin VI is present in the leading edge and the Golgi complex of fibroblasts and epidermoid carcinoma A431 cells (Buss et al., 1998). When A431 cell surface ruffling was stimulated by EGF (epidermal growth factor), Myosin VI was phosphorylated (possibly by p21-activated kinase-PAK) and recruited into newly formed ruffles. This suggests that Myosin VI participates in the membrane trafficking involved in the ruffles creation. In immortal fibroblasts lines of the mutant *Snell's Waltzer* mice lacking Myosin VI, the size of the Golgi complex was reduced by 40% in comparison to wild-type cells. In addition, the secretion of a reporter protein (Alkaline Phosphatase) from the Golgi apparatus was reduced by 40%. When fully functional Myosin VI was expressed in these cells, the function and the morphology of the cells was restored (Warner et al., 2003).

Myosin VI is not only involved in membrane trafficking, but it also plays a role in endocytosis. In intestinal enterocytes and kidney proximal tubules Myosin VI is expressed mainly at the base of the brush border, where endocytosis of Clathrin-coated vesicles takes place (Biemesderfer et al., 2002; Buss et al., 2001; Heintzelman et al., 1994). This region of endocytosis occurs at the terminal web, where Myosin VI co-localises with Clathrin and Clathrin adapter-protein AP-2 (Biemesderfer et al., 2002; Buss et al., 2001). Following the Clathrin-mediated endocytosis, Clathrin is uncoated from the vesicles, prior to its fusion in the endosome (Hasson, 2003). It is suggested that Myosin VI plays a role in the creation of Clathrin-coated vesicles and in addition it was shown that Myosin VI is necessary in the transport of the uncoated vesicles to the endosome (Fig. 1.3.1 D).

In vertebrates two splicing forms are mainly expressed, a long form and a shorter one. The long form contains an insert of 23 amino acids between the coiled-coil region and the globular tail domain (Buss et al., 2001; Buss et al., 1998). The two splicing forms participate in endocytosis. The long spliced form is necessary for the formation of Clathrin-coated vesicles during endocytosis (Buss et al., 2001). This

form co-localises with Clathrin coated pits in cultured tissues and PCR analysis revealed that this is the main isoform that is expressed in the rat kidney and in polarised intestinal cells (Buss et al., 2001). Analysis of Myosin VI fragments revealed that the tail domain targets Myosin VI to Clathrin-coated pits only when the splice site insert is present. The expression of the long-spliced form of the tail domain dramatically reduced the endocytosis of Transferrin (a protein that undergoes receptor-mediated endocytosis), indicating that the long form of Myosin VI is necessary for the actual formation of the Clathrin coated vesicles (Buss et al., 2001).

The shorter form of Myosin VI is expressed in epithelial cells under non-polarising conditions (Aschenbrenner et al., 2003), in uncoated endocytic vesicles (Clathrin coated vesicles that undergo uncoating). Domain analysis revealed that the shorter form of the tail domain is sufficient to target Myosin VI to uncoated vesicles and also in this case, over-expression of the tail domain significantly reduces Transferrin uptake, confirming that the short form of Myosin VI also plays a role in endocytosis (Aschenbrenner et al., 2003). Under these conditions, the uptake of Transferrin (a proteins that undergoes endocytosis in mammalian cells) by Clathrin-coated pits is normal, yet the uncoated pits remain stuck to the cell periphery, inhibiting the transfer of Transferrin cargo to the endosome. Recent study shows that Myosin VI transports the uncoated vesicles out of the actin-rich network located in the epithelial cell periphery and towards the early endosome (Aschenbrenner et al., 2004). In the absence of Myosin VI motor activity, the uncoated vesicles were trapped in the actin mesh and the vesicles reached the early endosome by diffusion (the movement was significantly slowed). Expression of a mutant Myosin VI that binds tightly to actin filaments blocked the transport while de-polymerisation of the filaments rescued the transport of the vesicles to the early endosome without affecting vesicle formation. Therefore, it can be concluded that Myosin VI is necessary for the trafficking of the vesicles through the actin barrier to transfer them to the endosome (Aschenbrenner et al., 2004).

Three different proteins were found to associate with Myosin VI during endocytosis: Disabled 2 (Dab2), GAIP (G-alpha interacting protein)-interacting protein C terminus (GIPC) and synapse associated protein 97 (SAP97). Dab2 is a tumour suppressor protein implicated in cell receptor turnover, endocytosis and cell

signalling. The Dab2 molecule contains at its central region binding sites for Clathrin and AP-2 (the DFP motifs), which are sufficient for targeting Dab2 to Clathrin coated pits (Hasson, 2003). Dab2 also binds to Myosin VI at its C terminal serine and proline rich region (Inoue et al., 2002; Morris et al., 2002) (it binds to both splice forms although the insert is necessary for targeting to Clathrin coated pits). This result suggests that Dab2 serves as a bridge that links the longer form of Myosin VI with Clathrin-coated pits through association of Dab2 to Clathrin, AP-2 and other accessory proteins.

GIPC is a PDZ containing protein that contains in its C and N terminus proline-rich domains. These domains are necessary for Myosin VI binding. GIPC binds to various transmembrane proteins, and GIPG was found to transfer transmembrane proteins through the Golgi stacks (Hasson, 2003). Myosin VI was found to bind GIPG in a two-hybrid screen (Bunn et al., 1999). The precise binding region on GIPG was not defined however the PDZ domain in its own is not sufficient for binding Myosin VI in vitro. GIPC is present in small uncoated vesicles near the plasma membrane in cultured cell lines and Myosin VI co-localises with GIPC in these vesicles.

GIPC is also present in Clathrin-rich invaginations and in endocytic compartments in the proximal tubule cells, where it overlaps with Clathrin, AP-2 and Myosin VI. This evidence proposes that GIPC plays a role of in the recruitment of Myosin VI to Clathrin coated pits. Unlike Dab2, GIPC remains associated with Myosin VI after the formation of Clathrin-coated and uncoated vesicles. Therefore, this can indicate that GIPC has a role in the transport of the vesicles (Bunn et al., 1999).

Another protein that associates with Myosin VI in vesicular fractions of rat brain cells is SAP97 (synapse-associated protein 97), as described below (Wu et al., 2002).

The binding of Myosin VI with Dab2 and GIPC raises the possibility that Myosin VI participates in the formation of the Clathrin coated pits (Hasson, 2003). During the formation of the vesicles, Myosin VI either participate in the building of the vesicles, either by the re-organisation of the actin filaments and the membrane during endocytosis, or by promoting fission of the vesicles through the dissociation of the membrane. The latter hypothesis is supported by the fact that the disruption in

Myosin VI function does not alter the morphology of the Clathrin-coated pits, but causes defects in the formation of Clathrin coated vesicles.

In mice, Myosin VI was shown to play a role in maintaining the separated stereocilia membranes in cochlear hair cells (Fig. 1.3.1 C). A recessive null mutation in the Myosin VI gene in *Snell's Waltzer* mice (*Myo6*^{sv}) cause deafness and reveal degeneration of the inner and outer hair cells of the cochlea and fusion of the stereocilia soon after birth (Avraham et al., 1995; Self et al., 1999). The bundles of stereocilia appear normal at birth but gradually become disorganised and eventually fuse. In wild-type mice Myosin VI is expressed only in the inner and the outer hair cells of the cochlea, where it is found in the cuticular plate of the hair cell (the part of the cell that support the stereocilia and anchors it to the cell body), but absent from the stereocilia itself. Myosin VI is also expressed in the cell body and it is highly concentrated at the perinuclear necklace, a region between the cuticular plate (where the stereocilia is anchored into the cell body) and the plasma membrane that is rich in vesicles and is highly active in membrane transport (Hasson et al., 1997, Rodriguez and Cheney, 2000; Titus, 2000). Accordingly, several suggestions were raised about the way Myosin VI could function in the separation of the stereocilia membranes: Myosin VI could pull down the membrane towards the base of the stereocilia and the actin-rich cuticular plate (a role that would fit with a point-end directing motor), or anchor the membrane to a certain region in the actin filament. It is also possible that Myosin VI participates in the building of the membrane by transporting the vesicles found in the perinuclear necklace. Interestingly, the fused stereocilia in *Snell's Waltzer* mice created giant stereocilia (Self et al., 1999). This suggests that Myosin VI also plays a role in anchoring the stereocilia to the cuticular plate. The *Snell's Waltzer* mice have other abnormalities apart from deafness, including skeletal defects, cropped pinnae (the part of the outer ear that projects from the head). The *Myo6*^{sv} mutation has a deletion of 130 bp which cause a frame shift in the coding region and formation of a stop codon at the neck domain (Avraham et al., 1995).

Hearing loss conditions in humans were connected with mutations in the human Myosin VI gene, *Myo6*. Patients suffering from a nonsyndromic dominant form of deafness (NSAD) were found to have a missense mutation in the human Myosin VI

gene, *Myo6* (Melchionda et al., 2001) at the area encoding the core of the motor domain. Three other mutations in *Myo6* were found in patients having recessively inherited deafness (Ahmed et al., 2003). Two of the mutations were found in different places in the motor domain (a missense mutation and a frame shift mutation) and one nonsense mutation was found in the tail domain. A recent study suggested a connection between a novel missense mutation in Myosin VI, sensorineural deafness and hypertrophic cardiomyopathy (Mohiddin et al., 2004). Hypertrophic cardiomyopathy is represented by left ventricular hypertrophy, diastolic dysfunction (diastole is the part of the cardiac cycle when the ventricles relax and fill with blood) and hypercontractility. This condition is often associated with disabling symptoms, arrhythmias, and sudden death. In the studied family, the inherited sensorineural deafness co-segregated with hypertrophic cardiomyopathy. Genetic analysis suggested a linkage between the cardio-auditory phenotype and the chromosomal region of Myosin VI. In addition, all the affected members had the Myosin VI missense mutation.

The expression of Myosin VI in neurons is found not only in the *Drosophila*, but also in mammals. In rat brain cells, Myosin VI was found to associate with SAP97, a member of membrane associated guanylate kinase homologues (MAGUKs) (Wu et al., 2002). SAP97 associates Myosin VI through its N terminal. Myosin VI and SAP97 form a trimeric complex with AMPA (α-amino-3-hydroxy-5-methylisoxazole-4-propionic acid) glutamate receptor subunit, Glur1, where SAP97 links Myosin VI and Glur1. SAP97 may serve as an adaptor protein that connects Myosin VI to vesicular cargoes that carry AMPA-type glutamate receptors (Wu et al., 2002). The homologue of SAP97 in *Drosophila* is Discs Large (Dlg) and the genetic interaction between Myosin VI and Dlg will be described in chapters 4 and 6. Myosin VI is expressed in the chicken brain, along with Myosin V during embryogenesis (Suter et al., 2000). In cultured dorsal root ganglion the two myosins are expressed in the cell body, the neurites and the growth cones. In the growth cones Myosin VI and Myosin V exhibit a punctate staining pattern, each protein has a distinct cellular distribution.

In *Caenorhabditis elegans* Myosin VI is necessary for the segregation of components during spermatogenesis (Kelleher et al., 2000). Mutation in Myosin VI inhibits the delivery of mitochondria and membrane organelles (derived from endoplasmic reticulum and/or Golgi) to the budding spermatids. In addition, it was found that actin filaments are not restricted to the residual body but also appear in budding spermatids. Spermatids dissected from the mutant animals had abnormal rod-like insertions through the cell body (which did not contain actin) and other aberrant morphologies, which seem to be related to the abnormal function of the spermatids (Kelleher et al., 2000).

Recent research found that Myosin VI mRNA is expressed in the lungs of mice during embryogenesis. This expression is reduced when the levels of the transcription factor forkhead box (Fox) are low in *Foxf1(+/-)* mutant mice. Fox is essential for the development of the lung and reduced expression of *Fox* mRNA causes pulmonary hemorrhage and peripheral microvascular defects (Kalinichenko et al., 2004).

Myosin VI is expressed in large quantities in the retinas of fish (bass and rainbow trout) and primates (Breckler et al., 2000). Antibody staining revealed that within the retina Myosin VI was expressed in the photoreceptors, in horizontal cells and in Müller cells in both fish and primates as well as in the retinal pigmented epithelium. Within the bass cones, Myosin VI expression is asymmetric, suggesting a role for Myosin VI in the motility of the cone and thus the whole retina. As shown in chapter 4, Myosin VI is also expressed in the developing photoreceptors of the *Drosophila* eye disc, at the early pupal stage.

1.3.2 Myosin I

In *Drosophila*, two Myosin I members were identified (Fig. 3). Myosin IA belongs to subclass IV (Morgan et al., 1995; Morgan et al., 1994). The gene is located at locus 31DF on the second chromosome. In contrast to most of the myosins, Myosin IA does not have the typical amino acids that compose the TEDS domain (glutamic or aspartic acids, threonine or serine) and its neck domain contains two IQ motifs.
Myosin IB belongs to subclass III (Cheney et al., 1993; Morgan et al., 1995; Morgan et al., 1994). The gene is at 61F on the third chromosome. All the members of this group are characterised by a neck domain containing three IQ motifs. Like the tail domains of all other myosins from class I, the tails of *Drosophila* Myosin IA and IB contain basic residues that may affect the binding of these myosins to acidic phospholipids. *Drosophila* Myosin IA and IB are expressed in the gut epithelia: In the larval gut Myosin IA is expressed in the terminal web and Myosin IB is expressed in the apical microvilli; in the adult gut both myosins are expressed in the microvilli (Morgan et al., 1995). Myosin IB is expressed in the follicle cells during oogenesis (section1.7), initially in all the follicle cells, but by stage 10, only in the columnar cells surrounding the oocyte (Morgan et al., 1995). Antibody detection showed that the majority of Myosin IB is located at the basolateral region of the follicle cells until stage 8, and also in the apical region in subsequent stages. The role of Myosin IB in oogenesis is not clear yet. Based on the function of Myosin I in other species it is assumed that Myosin IB has a role in maintenance of the cytoskeleton of the follicle cells, or in secretion of yolk protein, the vitelline membrane and the chorion.

In yeast and *Dictyostelium* type I myosins play a role in membrane traffic (endocytosis and exocytosis), cell growth and cell movement (Baker and Titus, 1998; Kalhammer and Bahler, 2000; Soldati, 2003).

1.3.3 Myosin II

The *Drosophila* myosins of class II contain one IQ motif in the neck domain, although the myosins from class II usually contain two IQ motifs (Sellers, 2000). The tail domain consists of coiled - coil forming sequence, and terminates in a short globular non - helical segment (Fig. 1.3). Myosin II molecules have a two - headed structure, due to the dimerization of the heavy chain in the coiled - coil region of the tail. Myosin II differs from other myosins by its ability to form filaments, an ability that is based on the self-association of the rod-like coiled - coil α helical tail.

One muscle Myosin II has been found in *Drosophila*. Its gene (*mhc*) is located at 36B on chromosome 2 and produces more than 15 protein isoforms expressed in different muscles (Zhang and Bernstein, 2001).

Drosophila has a second Myosin in class II, nonmuscle Myosin II, encoded by the gene *zipper*, which is expressed in the cell cytoplasm (Kiehart et al., 1989). The gene is at 60E9 on chromosome 2 (Kiehart et al., 1989; Young et al., 1993). The *zipper* gene contains two sites for alternative splicing, thus having the potential to generate four different isoforms (Mansfield et al., 1996).

Myosin II participates in various developmental stages during the life cycle. During cellularization Myosin II is expressed in the formed pseudocleavage furrow and is necessary for basal membrane closure (Royou et al., 2004; Young et al., 1991); at the same stage Myosin II plays a role in the migration of the nuclei to the poles (Royou et al., 2002; Young et al., 1991). At later stages of embryogenesis, Myosin II controls the asymmetric localisation of proteins in neuroblasts (Barros et al., 2003) during the morphogenesis of the nervous system. Myosin II also participates in head involution (Young et al., 1993).

Nonmuscle (NM) Myosin II was the first gene whose role in dorsal closure (section 1.6) was analysed in detail (Young et al., 1993). Mutants of the *zipper* gene that lack NM Myosin II expression fails to complete dorsal closure. In the homozygous mutant $zip^{mhc\text{-}c1.3}$ that has a severe phenotype, the leading edge is disorganised, the lateral epidermis is not fused at the dorsal midline and the amnioserosa remains exposed. The shape of the cells in the lateral epidermis and the amnioserosa is aberrant, and in many cells the membrane is torn.

The strong expression of NM Myosin II at the leading edge and the co-localisation with the actin cable in that region suggested a model in which NM Myosin II pulls the epidermal cells during the hole closure like a purse string (Young et al., 1993). The function of the actin filaments in the constriction of the purse string was supported by the evidence that when the actin cable is deficient, the cells at the leading edge are not elongated as in wild type embryos (Harden et al., 1995). In NM Myosin II mutants, the cells at the leading edge remain elongated. The maintenance of the elongated cells could be established by maternal NM Myosin II (the expression level of NM Myosin II declines at late stages of embryogenesis although some material could remain in the embryos) (Young et al., 1993).

There are several factors that were found to control NM Myosin II function and expression during dorsal closure: the phosphorylation of the regulatory light (MRLC) chain of NM Myosin II stimulates activity. Myosin phosphatase regulates the phosphorylation of MRLC, and is inactivated by phosphorylation of its Myosin-binding subunit (MBS) (Mizuno et al., 2002). The Rho-associated kinases (ROKs), which function downstream of RhoA, activate NM Myosin II by promoting the phosphorylation of MRLC and MBS. Embryos lacking *Drosophila* MBS (DMBS) fail to complete dorsal closure; therefore the regulation of MRLC phosphorylation is necessary for correct dorsal closure (Mizuno et al., 2002). RhoA also regulates the expression and localisation of NM Myosin II in the lateral epidermis during dorsal closure. Expression of RhoA dominant negative reduces NM Myosin II level at the lateral epidermis and the leading edge (Bloor and Kiehart, 2002).

At the larval and pupal stages Myosin II is necessary for cytokinesis (Karess et al., 1991) and during imaginal disc morphogenesis, for normal development of the eyes and legs (Edwards and Kiehart, 1996).

Nonmuscle Myosin II was found to play several important roles in oogenesis, (section 1.7), including follicle cell migrations and cytoplasmic transport from the nurse cells into the oocyte (Edwards and Kiehart, 1996; Wheatley et al., 1995). Myosin II is expressed in the migrating follicle cells and in the nurse cells in a similar pattern to Myosin VI, being mainly concentrated in the apical and the basal parts of the follicle cells. However, the expression of Myosin II was not reduced in

the absence of Myosin VI, suggesting that Myosin VI does not control the expression of Myosin II (Deng et al., 1999). The localisation of Myosin II in the follicle cells was shown to be controlled by Lethal (2) Giant Larvae (l(2)gl). A temperature-sensitive mutation in *l(2)gl* gene has shown to disrupt the localisation of Myosin II in the follicle epithelium, creating aggregates and clumps along the apical and basal regions (De Lorenzo et al., 1999b).

The evidence that nonmuscle myosin functions in oogenesis was provided from mutation analysis of *spaghetti - squash (sqh)*, a gene encoding the regulatory light chain (RLC) of nonmuscle Myosin II (Edwards and Kiehart, 1996; Jordan and Karess, 1997; Wheatley et al., 1995). In adult females, mutations in the *spaghetti - squash* gene disrupted the migration of the border cells, the centripetal cells and the dorsal appendage follicle cells (Edwards and Kiehart, 1996). Furthermore, anterior chorion formation was disrupted, as the centripetal cells were not in the right position to secrete chorion material over the anterior end of the oocyte. The movement of the dorsal - anterior follicle cells to produce the dorsal appendages was also disrupted, and as a result, abnormal short appendages were formed. The mutation in *sqh* also changed the organisation of the follicle cells between the egg chambers: follicle cells that migrate between egg chambers failed to organize a proper stalk.

The *sqh* mutants also cause a defect in 'dumping', the process of nurse cell cytoplasm transport into the oocyte (Edwards and Kiehart, 1996; Wheatley et al., 1995). In these mutants, there is no barrier in the ring canal. The distribution of Myosin II was abnormal, suggesting that Myosin II is needed for the cytoplasmic dumping. Mutation of *sqh* in the phosphorylation sites (serine 21 and threonine-20) causes abnormal formation of the ring canals in the nurse cells, and therefore it can be concluded that Myosin II is necessary for their establishment or maintenance (Jordan and Karess, 1997). As in dorsal closure, mutation in DMBS (*Drosophila* myosin-binding subunit) also caused defects in ring canal formation, cytoplasm dumping and dorsal appendage morphogenesis, therefore the regulation of the phosphorylation of the myosin regulatory light chain is essential for the proper function of Myosin II in oogenesis (Tan et al., 2003).

Mutations in *sqh* gene also caused severe defects in proliferation and cytokinesis of the cystoblasts (Jordan and Karess, 1997).

1.3.4 Myosin III

The first myosin from this class was identified in *Drosophila*. The Myosin III gene (*ninaC)* encodes two isoforms, p174 and p132 that differ in their tail domains, which contain 420 and 54 aa, respectively, as a result of alternative splicing (Montell and Rubin, 1988). Both isoforms contain a kinase domain, N - terminal to the head domain, which seems to be needed for the phototransduction activity. Like Myosin IA, ninaC does not have the typical amino acids at the TEDS site (glutamic or aspartic acids, threonine or serine). The neck domains of the two isoforms contain two IQ motifs that bind Calmodulin (Fig. 1.3). The tail domain of p174 is rich in basic residues. Both p174 and p132 are exclusively expressed in photoreceptor cells; p174 is solely localized to the microvilli of the rhabdomere, and p132 is present in the cell body, which indicates that the tail domain of p174 is involved in targeting of this Myosin to the rhabdomere. In p174, the targeting of Calmodulin (bound to the IQ motifs) and the kinase domain to the rhabdomere is necessary in the deactivation of phototransduction process. In addition ninaC plays a role in the structural integrity of the rhabdomere (implicated by the motor domain) and P132 seems to function in membrane transport or in regulation of photoreceptor cell (Bahler, 2000).

In human, Myosin IIIa is expressed in the retina and the cochlea and was found to be necessary for normal hearing. Three different recessive loss-of function mutations in Myosin IIIa have been shown to cause nonsyndromic hearing loss (nonsyndromic means that there are no other symptoms than deafness) (Walsh et al., 2002).

1.3.5 Myosin V

Myosin V has been identified in *Caenorhabditis elegans*, yeast, rat, mouse, chicken, and human (Langford, 2002; Wu et al., 2000). The gene encoding this protein (*didum*) is on 43C, on chromosome 2. All genes corresponding to this region are essential genes and their mutants show an embryonic lethal phenotype (MacIver et al., 1998). The neck domain of Myosin V contains six IQ motifs (Fig. 1.3), and the tail domain has regions that form coiled – coil α helices, followed by a globular domain, containing two transmembrane regions. The gene has at least two transcripts that generate identical proteins (Bonafe and Sellers, 1998).

The expression of *didum* is most abundant in the adult germ line and in the early embryo (MacIver et al., 1998). *didum* is also expressed at stage 16 in the ectodermal tissue of the hindgut (Bonafe and Sellers, 1998).

Myosin V was found as one of the genes expressed in oogenesis, by using the enhancer- trap technique (MacIver et al., 1998). After cloning *didum* cDNA, whole - mount *in situ* hybridisation experiments showed that *didum* mRNA is present in the oocyte from early stages of oogenesis, suggesting that Myosin V has a role in oogenesis. At the early stages of oogenesis *didum* is expressed in the oocyte: at mid-stages (6-8) *didum* mRNA is located at the anterior pole of the oocyte; at stages 9 - 10 *didum* is expressed strongly in the nurse cells, and later on the transcript is dumped from the nurse cells to the oocyte. This last finding suggests that didum has a subsequent role in embryogenesis (MacIver et al., 1998).
Staining the egg chamber with a specific antibody for the Myosin V tail domain showed that Myosin V appears in the nurse cells during stages 1 - 13 (Tzolovsky and Bownes, unpublished). During stages 10 - 12 Myosin V appears in the oocyte- nurse cell border, forming a specific ring-shaped image, and in the anterior region of the oocyte. This supports the hypothesis that Myosin V might participate in particle transport from the nurse cells to the oocyte. Myosin V staining was also observed in the columnar follicle cells although mRNA expression was not detected there. It is likely that the concentration of mRNA was too low to be observed by the *in situ* hybridisation technique used.

Myosin V was found to have various functions in different species, including membrane and vesicle trafficking, protein and mRNA transport, organelle distribution (melanosomes and smooth endoplasmic reticulum), and cellular extension (Langford, 2002; Wu et al., 2000).

1.3.6 Myosin VIIa

Drosophila Myosin VII was the first Myosin identified in this class. This Myosin, classified as subclass VIIa, is encoded by the *crinkled* (*ck*) gene (Chen et al., 1998), and located at locus 35 B on chromosome 2.

In this myosin, the neck domain has five IQ motifs and the tail region contains two FERM domains (formally termed talin homology domains), two MyTH4 (myosin tail homology 4) domains, and an SH3 domain. FERM (named for band 4.1, Ezrin, Radixin, Moesin) is a conserved domain in band 4.1 protein superfamily, found in Talin, Filopodin, Ezrin Radixin Moesin and other proteins in this family. FERM domains are believed to be involved in membrane attachment either directly, via binding to phospholipids, or through association with integral membrane proteins. It was shown that the FERM domain mediates membrane-cytoskeleton interactions through the binding to integral membrane proteins (Sun et al., 2002). FERM proteins also interact with other proteins from the ERM (Ezrin, Radixin, and Moesin) family by binding to the C-terminal actin-binding domain that appears in the ERM proteins (Sun et al., 2002). Geli (Geli et al., 2000) found that SH3 is required for the interaction of the tail domain with actin and for triggering actin polymerisation in yeast Myosin I. It is also believed that SH3 plays a role in protein-protein interactions through the binding to proline-rich domains (Macias et al., 2002), although SH3 domains were also found to interact with non-proline peptides (Agrawal and Kishan, 2002).

Many mutations in the *crinkled* gene are homozygous lethal. Non-lethal mutations show a variety of defects in different organs, including rough eyes, thick sets of forked denticles, hairs that are basally fused, sensory hairs that are blunt, abnormal bristles and crinkled wings (Kiehart et al., 1998). Moreover, the arista laterals in the fly antenna of *crinkled* mutants are shorter, thicker and branched, suggesting that Myosin VII plays a role in the cellular extension of the epidermal cells composing the laterals (He and Adler, 2002). Interestingly, the shape of the laterals was similar to that observed after cytochalasin D (actin polymerisation inhibitor) treatment. This may suggest that Myosin VII participates in the organisation of the actin cytoskeleton during the development of the laterals.

Mutations in Myosin VIIa are responsible for hereditary deafness in both mouse and human. In mice containing a mutation in the Myosin VIIa gene (*Shaker-1*), the hair cells degenerate, suggesting that Myosin VIIa is important for the stereocilia integrity (Maniak, 2001; Wu et al., 2000). Myosin VIIa was also found in the perinuclear necklace, implying that it has a role in membrane trafficking in the inner hair cells. In humans, Myosin VIIa mutations are associated with Usher syndrome type 1B, an autosomal recessive disease resulting in hearing loss and gradual blindness, caused by degeneration of the photoreceptor cells. Myosin VII is localised in the apical domain of the retinal pigment epithelial (RPE) cells that extend long microvilli around the photoreceptor. It is possible that Myosin VIIa takes part in maintaining the structural integrity of the RPE cells and the photoreceptor cells through adhesion of the microvilli to the photoreceptor tips, or by stabilising the structure of the microvilli structure (Maniak, 2001; Tuxworth et al., 2001; Wu et al., 2000).

In *Dictyostelium* Myosin VII is involved in cell adhesion (Tuxworth et al., 2001). During the early stages of phagocytosis, the particle to be swallowed adheres to the outer surface of the *Dictyostelium* cell and a phagocytic cup is formed around the particle. Mutation in Myosin VII reduced significantly the adhesion of the particles to the cell surface, while the phagocytic cup was formed normally. Mutation in Myosin VII also reduced the adhesion between the *Dictyostelium* cells during the growth phase and reduced the adhesion of the cells to the underlying glass layer during their migration (Tuxworth et al., 2001).

1.4 Epithelial morphogenesis and the structure of epithelia in Drosophila melanogaster

Epithelial morphogenesis is the process in which an epithelial tissue obtains its specific structure and shape during development. To reach the final structure there are several dynamic events that take place, such as changes in cell shape and size, cell migration, and cell adhesion.

Epithelial tissues cover internal and external organs and serve as a barrier to the outside environment to maintain homeostasis within the developing and adult organism. Epithelial tissues are composed of cells joined to other cells via cell adhesion and through the binding to an extracellular matrix-the basal lamina. Some of the epithelial tissues are one cell thick (monolayer), like the follicle cell epithelium and the lateral epidermis (Kiehart et al., 2000), however epithelial tissues can contain several layers of cells- as in the stratified epithelium in the skin. Epithelial cells display planar polarity and basal-lateral polarity. The plasma membrane of epithelial cells contains the basal side, apical side and the lateral sides. These connect with other epithelial cells through the epithelial junctions: the adherens junction (zonula adherens) and the septate junction (Fig. 1.4). The epithelial cells connect to the extracellular matrix through their basal membrane. This structure appears in all epithelial tissues of invertebrates (Muller, 2000).

The area apical to the adherens junction is often termed the sub-apical complex, and it contains two complexes of proteins: the Crumbs complex and the Bazooka complex. These complexes create protein interactions that stabilize the membrane structures, and participate in local signalling events (Muller and Bossinger, 2003). It was suggested that this area participates in the regulation of lateral diffusion of membrane components (a function analogous to the tight junctions in vertebrate cells) (Muller, 2000).

The adherens junctions are the regions that interconnect cells by forming an adhesion belt (the zonula adherens) around each of the interacting cells in the sheet. The interaction between the cells membrane is made through the cell adhesion proteins: DE-cadherin, Armadillo and α-catenin. The adherens junctions are also the

Figure 1.4

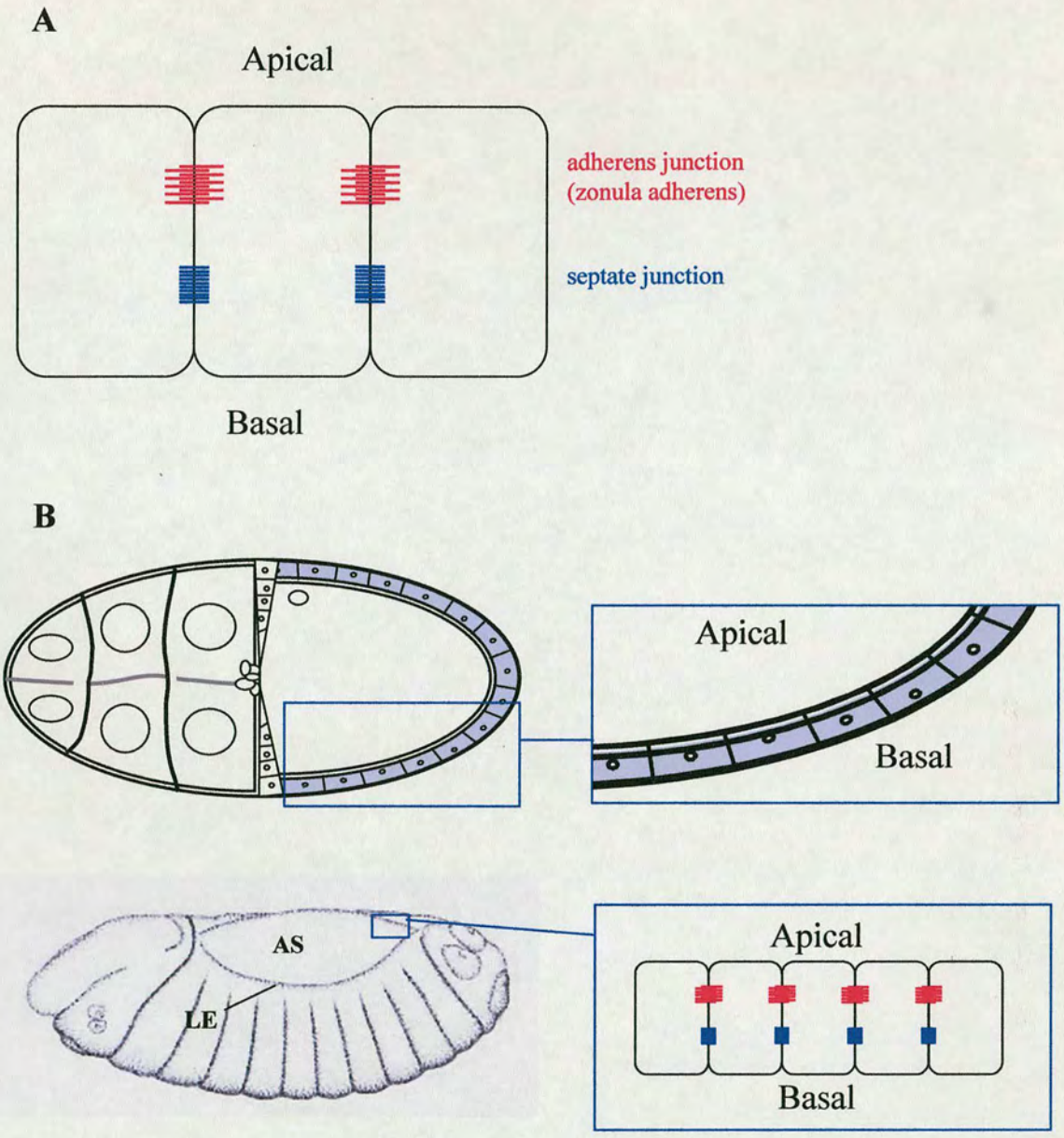

Figure 1.4. The structure of epithelial tissues. **A:** a diagram showing the basal-apical polarisation of epithelial tissues in invertebrates. Adherens junctions form the zonula adherens, a belt that surrounds the epithelial cells. The septate junctions, localised basal to the adherens junction, control the transport between the cells. Figure **B** shows the basal-apical orientation of the follicle cells epithelium in the ovaries and the lateral epidermis in the embryo.

areas that connect the bundles of actin filaments surrounding each cell, through these proteins (Muller and Bossinger, 2003).

The septate junctions control transport between cells and are often referred as gates or having a barrier function (Muller, 2000). The localisation of tumour suppressor proteins in the septate junction suggests that this area might also participate in growth control (Muller and Bossinger, 2003).

In *Drosophila* embryos, the epidermis matures after germ band extension. In the mature epidermis, the baso-lateral membrane regions contain the proteins: Neuroactin, Fasciclin III and β-spectrin (Muller, 2000). The apical membrane is specified by expression of the membrane protein Stranded At Second (SAS). The zonula adherens contains the adhesion proteins: DE-cadherin, Armadillo, Dα-catenin, βH-Spectrin and phosphotyrosyl proteins. Dlg, Scribble, Neurexin, and Coracle are localised at the septate junction.

In the follicle cell epithelium the basal membrane of the cells is connected to the basal lamina via PS1-integrin and cell-cell adhesion is mediated through DE and DN-cadherin. As in the embryonic epidermis, DE-cadherin, Armadillo, Dα-catenin localise to the zonula adherens. At the apical-lateral region, Crumbs, Bazooka and Discs Lost are present (as observed in early stages of oogenesis). βH-Spectrin expression is restricted to the apical membrane, while β-Spectrin and Ankyrin are localised to the lateral membrane and α-spectrin is present in the entire cell membrane (Lee et al., 1997). The septate junction contains the following proteins: Scribble, Dlg, Neuroglian and Fasciclin III (only in the polar cells).

The following sections discuss three processes of epithelial morphogenesis: germ band retraction, dorsal closure and oogenesis, as Myosin VI is shown in this thesis to plays an important role in these events.

1.5 Germ band retraction in Drosophila embryos

Germ band retraction begins at stage 12 of embryogenesis (Bownes stages (Bownes, 1975)) after the process of germ band extension. As germ band extension is completed, the amnioserosa, an epithelial tissue composed of large flat cells, is localised between two layers of extended germ band. The germ band tissue is composed of a mesodermal tissue and neurons of the central nervous system, covered with epidermis. During germ band retraction, the germ band tissue shortens, bringing the tail end of the germ band to the posterior of the embryo (Fig. 1.5A and the tail end is marked in figure 1.5C). The amnioserosa extends to its original position prior to germ band extension, covering the yolk sac on the dorsal side of the embryo (the yolk is shown in figure 1.5C).

The morphologic changes that take place during germ band retraction were observed in living embryos, expressing GFP tagged to different proteins (Schock and Perrimon, 2002). These observations show that during shortening the germ band doubles its height along the dorsal-ventral axis, and its width shortens by 50%. The shortening of the germ band is achieved mainly through changes in cell shape, while the re-arrangement within the tissue is minimal. The cells in the germ band slightly shorten along the anterior-posterior axis, a furrow is formed at each segment boundary and a dorso-ventral elongation occurs in the germ band cells, mainly in a row of 8 cells adjacent to the amnioserosa (Fig. 1.5B).

The amnioserosa and the germ band move together as one uniform sheet. As the amnioserosa moves, it shortens along the dorso-ventral axis, through a massive shortening of the cells along their dorsal-ventral axis (Schock and Perrimon, 2002). A close inspection at the boundaries between the amnioserosa and the leading edge of the germ band reveals that the leading edge is pulled in areas where the plasma membrane of the amnioserosa was at a right angle with the leading edge, suggesting that the amnioserosa applies forces on the germ band at the boundary of the two epithelia.

At the beginning of stage 12, the amnioserosa overlaps the germ band. As the shortening of germ band progresses, the overlap gradually decreases and at the same time the contact area between the amnioserosa and the yolk increases. Closer

inspection reveals that the connection between the amnioserosa and the germ band tissue is made through an adhesion between the tail end of the germ band and a small group of amnioserosa cells. The adhesion is made through lamellipodia that are sent from the amnioserosa, which migrates over the tail end of the germ band and adheres to it (Fig. 1.5C).

The spreading of the amnioserosa cells over the tail end of the germ band tissue is dependent on the function of α1,2 laminin and αPS3βPS integrin, two types of proteins that participate in the adhesion of cells to the extracellular matrix (Schock and Perrimon, 2003). Live images of embryos that lack βPS integrin showed that lamellipodia formation is disrupted and that there is no extracellular adhesion between the amnioserosa and the tail of the germ band tissue (Schock and Perrimon, 2003). The shape of the amnioserosa cells changes as in wild type embryos, but since there is no interaction between the amnioserosa and the germ band, the germ band retracts only partially. Expression of βPS integrin in the βPS mutants rescues the retraction defects, indicating that βPS is necessary for the process of germ band retraction.

Expression of RhoA dominant negative in the amnioserosa disrupts germ band retraction. However, no disruption occurs when RhoA dominant negative is expressed in the leading edge of the germ band (Schock and Perrimon, 2002). Germ band retraction also fails when the amnioserosa cells undergo premature death in *hindsight* mutants (Lamka and Lipshitz, 1999). These results suggest that the amnioserosa is essential for the progress of the germ band retraction.

It was proposed that the amnioserosa is needed for transmitting signals to the germ band tissue that induce cell migration (Lamka and Lipshitz, 1999), although the changes in the cells shape and the motility of the amnioserosa could also indicate that it contributes mechanical forces to the retraction (Schock and Perrimon, 2002).

The figures on the following page:

Figure 1.5: Germ band retraction. The location of the amnioserosa (AS) and the germ band (GB) tissue are shown in the diagram (taken and modified from the atlas of: The Development of *Drosophila Melanogaster* (Bates and Martines-Arias, 1993). **A:** The process of germ band shortening, as observed by time-lapse photography. The germ band cells were visualised in embryos expressing α-catenin-GFP driven by *arm-Gal4*. α-catenin-GFP is localised to the adherens junctions of the epidermal cells, enabling the cell shape to be revealed. The change in the orientation of the amnioserosa cells from the anterior-posterior to dorsal-ventral is marked by lines. **B:** One germ band cell was marked with a small dot (pointer by the arrow) and one amnioserosa cell was marked by a big dot. As germ band retraction progresses, the relative localisation of the two cells does not change, due to the attachment between the cells. Note the elongation of the germ band cells along the anterior-posterior axis, during shortening of the tissue (Schock and Perrimon, 2002). **C:** view of the amnioserosa and the tail end of the germ band tissue, during germ band retraction. The cells in the amnioserosa were marked with mEGFP, which localised both in the cytoplasm and the plasma membrane. The expression in the amnioserosa was driven by *c381-Gal4*. The amnioserosa region overlapping the tail end of the germ band is marked by an arrowhead. The triangle marks the tail end of the germ band. The arrow indicates the border between the overlapping and the non-overlapping area of the amnioserosa. The star indicates the auotofluorescense of the yolk protein (Schock and Perrimon, 2002).

Figure 1.6: Dorsal closure in a living embryo. The top diagram shows the location of the leading edge of the lateral epidermis and the amnioserosa (taken and modified from: The Development of *Drosophila melanogaster* (Bates and Martines-Arias, 1993). In order to observe the movement of the cells, the embryos express GFP targeted to actin filaments: GFP was tagged to the actin binding domain of moesin. A strong expression is observed at the actin cable in the leading edge (Kiehart et al., 2000). **A:** At the beginning of dorsal closure the actin cable starts to appear. **B-C:** As dorsal closure progresses the opposite edges adhere at the anterior and the posterior sides of the amnioserosa, and progress towards the centre of the embryo. **D:** Dorsal closure is completed. Actin expression is still observed at the dorsal midline, once closure is complete.

Figure 1.5

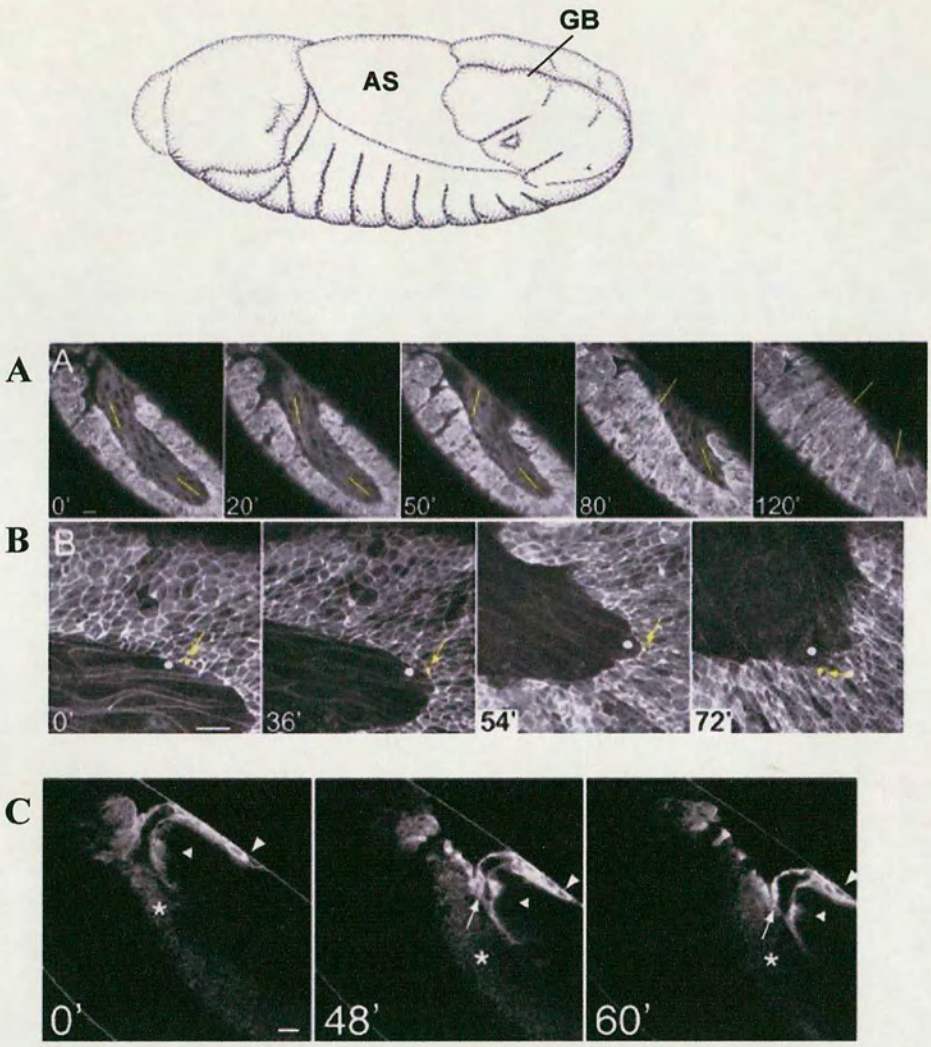

Figure 1.6

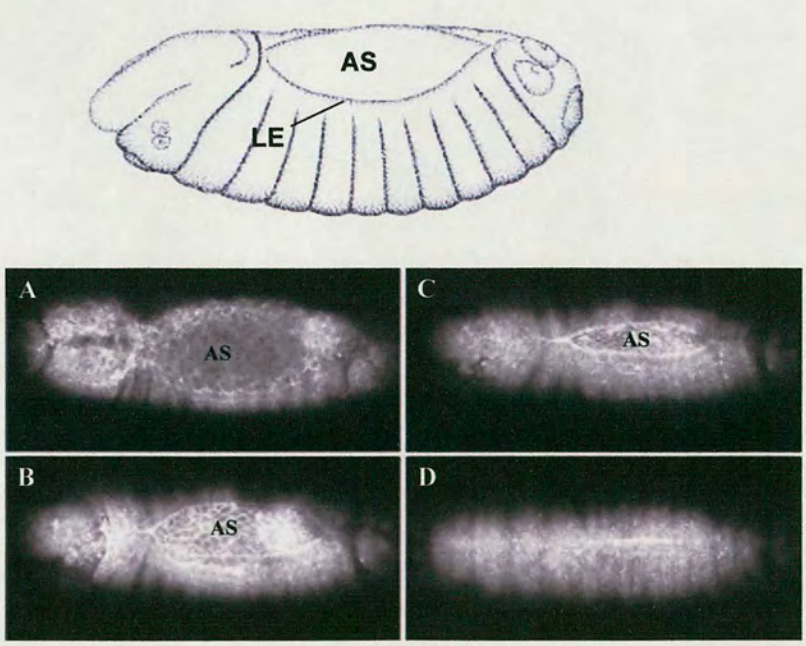

1.5.1 Myosin VI and germ band retraction

In Myosin VI mutants jar^{R39} and jar^{R235} (Leaper and Bownes, unpublished), germ band retraction is incomplete and often the germ band tissue is disconnected from the amnioserosa. A similar phenotype was observed when Myosin VI dominant negative was expressed. These phenotypes are described in chapter 5.

1.6 Dorsal closure in Drosophila embryos

Dorsal closure occurs after germ band retraction, during stages 14-15 of embryogenesis (Bownes stages (Bownes, 1975)). As germ band retraction is completed, a hole is left in the surface of the epidermis that contains the amnioserosa. During dorsal closure, the lateral epidermis that surrounds the dorsal hole migrates towards the dorsal midline, covering the amnioserosa (Fig. 1.6 A-D and Fig. 5.5 A-D in chapter 5). The migration of the lateral epidermis occurs from both sides of the embryo. The opposite tissues meet at the dorsal midline, the cells from opposite tissues adhere and the epidermis seals the dorsal opening (Martines-Arias, 1993). Initially the edges of the lateral epidermis meet at the anterior and the posterior edges. As dorsal closure progresses, the sealed areas increase and move towards the centre of the dorsal midline, in a zipping manner. At the leading edge of the migrating epidermis, an acto-myosin cable is formed, composed of actin filaments and nonmuscle Myosin II (the presence of Myosin II in the acto-myosin cable is shown in figures 5.5 A-D and 5.8.1B; the actin cable is shown in figures 5.10 A, D in chapter 5 and in figure 1.6 B-D).

The acto-myosin cable creates a ring around the amnioserosa that contracts and pulls the epidermis to close the dorsal hole at the anterior and the posterior edges. The contraction of the acto-myosin cable changes the shape of the cells at the leading edge from polygonal to an elongated shape (Fig. 5.10D in chapter 5); therefore it was proposed that the contraction of the acto-myosin cable at the leading edge is like a purse string. The change in cell shape is gradually transferred to cells located more ventrally, due to the pulling of the cells at the leading edge.

However, the purse string model is not the only force participating during dorsal closure. The forces participating in dorsal closure were studied in living embryos expressing GFP-moesin tagged protein (which binds to actin filaments in cells), by creating small cuts in the tissues with ultraviolet laser beam and examining the structural changes and the healing process in the different tissues (Kiehart et al., 2000). When a cut was made in the lateral epidermis near the leading edge, the tissue surrounding the wound moved away from the cut, causing the leading edge to move towards the dorsal midline. This suggests that under normal conditions, the lateral epidermis is put under tension that pulls the leading edge away from the dorsal midline, and hence retards dorsal closure.

Close observation of living embryos expressing GFP tagged actin confirmed that the cells at the leading edge extend filopodia and lamellipodia during dorsal closure (Jacinto et al., 2000). The filopodia and lamellipodia assist initially in the recognition of the correct cells on the opposite edge, with which they adhere, in order to close the dorsal hole neatly. As the filopodia meets a cell from the opposite edges it adheres with the cell membrane, and pulls the opposite cells together, to promote the adhesion between the cells (Martin and Wood, 2002).

The amnioserosa plays an active role in dorsal closure and it is not simply compressed by the migrating epidermis. Cuts in the amnioserosa release the tissue and the leading edge retracts away from the dorsal midline, suggesting that the amnioserosa tissue is under tension which contributes to dorsal closure, through the connection with the lateral epidermis (Kiehart et al., 2000). During dorsal closure the shape of the cells changes from elliptical to tubular. This change derives from an apical constriction of the cells and loss of cells from the tissue. The cell loss is established by invagination of cells and joining of the cells that remained on the top of them (Kiehart et al., 2000). The rupture of the amnioserosa during dorsal closure does not seem to prevent dorsal closure from proceeding; therefore the contraction of the amnioserosa might be needed to remove physical barriers during the migration of the epidermis.

1.6.1 The role of Myosin VI in dorsal closure

Kellerman and Miller (Kellerman and Miller, 1992) used antibody staining to show that Myosin VI is expressed during dorsal closure in the leading edge of the lateral epidermis. Mutations in Myosin VI cause failure in dorsal closure, and detachment of the cells at the leading edge and the amnioserosa (Millo et al., 2004). Work in this thesis suggests that Myosin VI is necessary during dorsal closure for cell adhesion and the organisation of the actin cytoskeleton

1.7 Oogenesis

Drosophila ovaries consist of 16-20 ovarioles. Each ovariole contains a string of developing egg chambers of increasing age. The most immature are in the germarium at the anterior and the most mature eggs at the posterior, ready to enter to the oviduct (Fig. 1.7.1A). The egg chambers are divided into 14 developmental stages according to their morphology (Deng et al., 1999; King, 1970; Spradling, 1993).

Oogenesis starts within the anterior region of the ovariole, in the germarium (Fig. 1.7.1A-B). A germline stem cell divides asymmetrically to produce a new stem cell and a cystoblast. Then, the cystoblast divides four more times with incomplete divisions to form a cyst of 16 cells that are connected by ring canals. One of the cells undergoes meiosis and becomes the oocyte, while the rest of the cells become nurse cells. The germarium can be divided into four regions (1.7.1B).

The stem cells and the dividing (mitotic division) cystoblasts lie within the germarium in region 1. Region 2a contains the newly formed 16 cell cysts. In region 2b, the 16 cell cysts become lens shaped with the pro-oocyte positioned at the centre of the cyst. When the cysts occupy region 3, the oocyte is located at the posterior pole, where it will remain during the subsequent stages of oogenesis. Somatic stem cells are located at the border between regions 1 and 2 of the germarium. In region 2, follicle cells (made from the somatic stem cells) migrate from the wall of the germarium to envelop the 16 cell cysts. When they reach region 3, the cysts are already surrounded by a single layer (epithelium) of follicle cells and are referred as stage-1 egg chambers. At the anterior pole of the germarium is the terminal filament, containing a stack of 6-9 non-dividing somatic cells. The terminal filament is closely

The figures in the following pages:

Figure 1.7.1 *Drosophila melanogaster* ovariole and the different developmental stages of oogenesis. **A:** Drawing of an adult wild–type ovariole. The germarium is located at the anterior edge of the ovariole (top). Several egg chambers at different developmental stages are shown: the egg chambers mature along with their movement towards the posterior. **B:** drawing of a germarium. The germarium is divided into four regions: region 1 at the anterior pole, region 2a, 2b and region 3 at the posterior pole. Region 1 contains the stem cell, the divided cystoblasts, the terminal filament at the anterior pole and the cap cells near the terminal filament. The somatic stem cells are located between region 1 and 2. Region 2a, contains the 16 cells cysts, formed after four cell divisions. In region 2b the 16 cell cysts become lens shaped. In region 3 the 16 cell cysts are surrounded by the follicle cells (their organization around the cysts started in region 2). **C:** A mature egg. The dorsal appendages and the micropyle are shown in the drawing (the operculum is marked with the arrowhead (Deng and Bownes, 1998).

Figure 1.7.2 Follicle cell migrations during the mid - stages of oogenesis. **A:** During stage 8, the follicle cells are arranged in a monolayer around the germ cells. **B:** During stage 9 a group of anterior follicle cells leave the follicle cell epithelium and migrate through the nurse cells, towards the border between the nurse cells and the oocyte (arrowhead). These cells stop migration at stage 10. In the same time, most of the follicle cells that cover the nurse cells migrate to cover the oocyte at the posterior, forming the columnar cells (arrows in **B, C**). Only a few follicle cells remain stretched covering the nurse cells. **C:** During stage 10b, the anterior columnar cells migrate centripetally along the nurse cell - oocyte border to cover the anterior side of the oocyte (arrows) (Deng and Bownes, 1998). **D:** β - galactosidase staining shows chorionic appendage formation during the migration of follicle cells from the dorsal - anterior region (arrow (Deng and Bownes, 1998)).

Figure 1.7.1

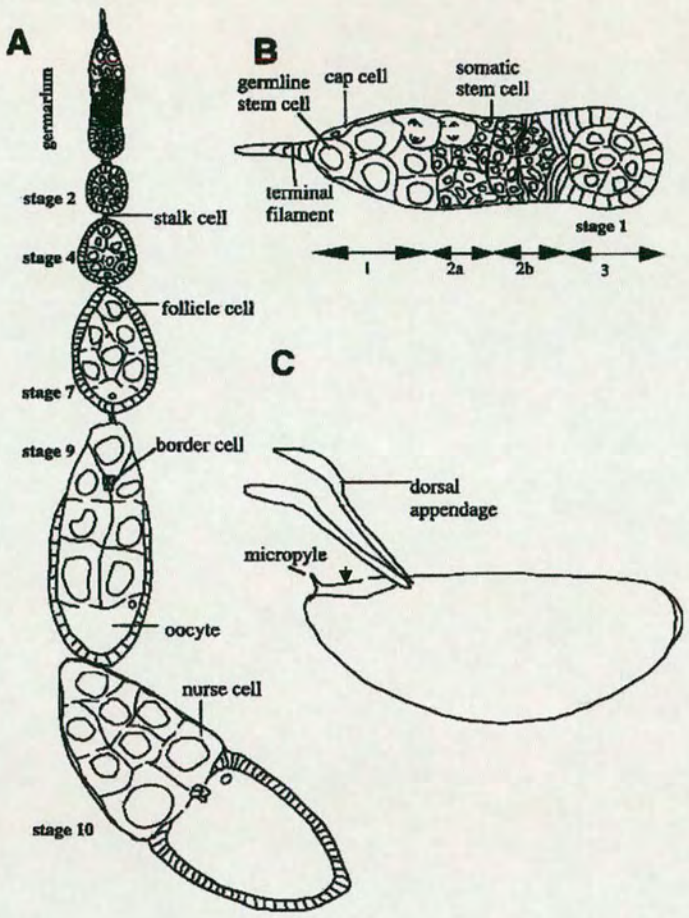

Figure 1.7.2

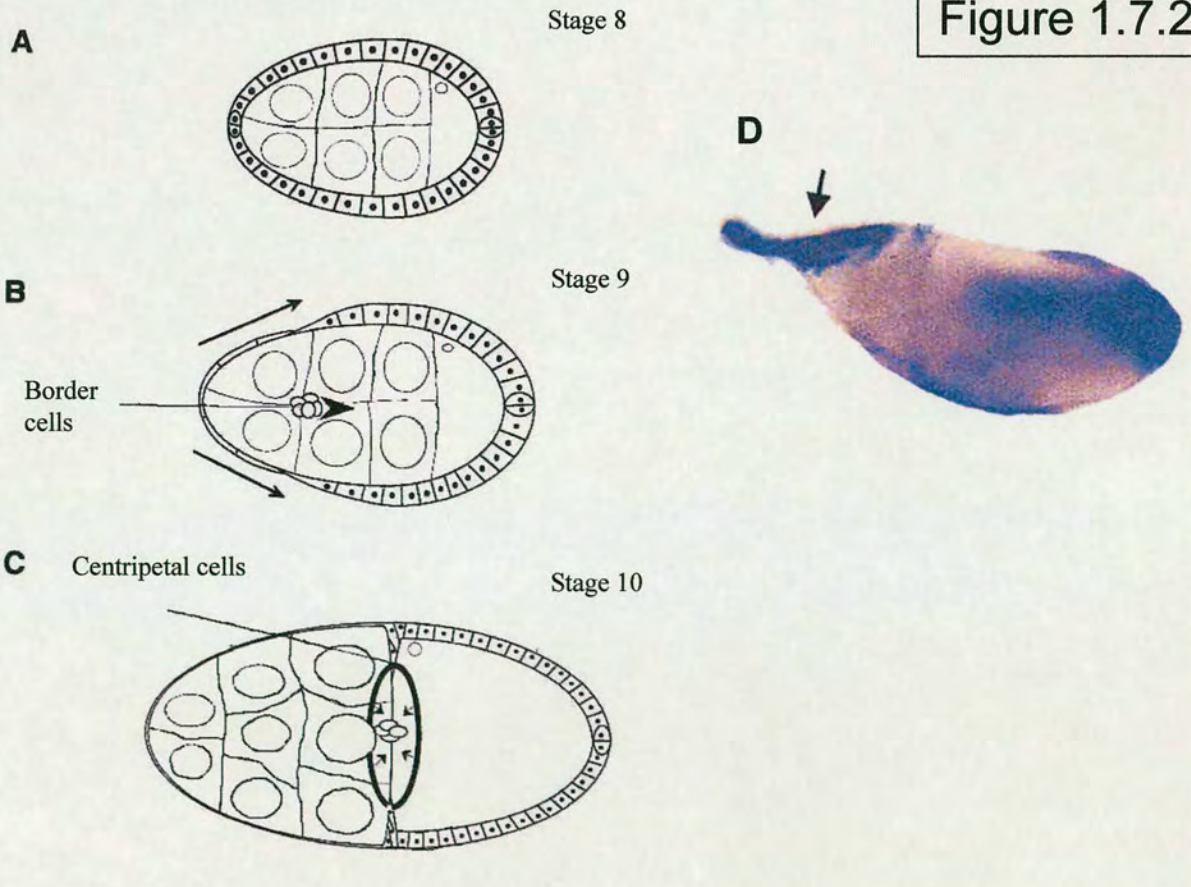

associated with another group of somatic cells called cap cells. Both the basal cells of the terminal filament and the cap cells lie adjacent to the germline stem cells (Fig. 1.7.1B). In stage 2 the egg chamber leaves the germarium (Fig. 1.7.1A). As the egg chamber leaves the germarium, five to eight follicle cells become the stalk cells. These cells form stacks that separate adjacent egg chambers. Stalk cells are not part of the follicle epithelium. Within the epithelium, the polar cells become distinct from other follicle cells. These cells are important for subsequent patterning of the egg chamber.

After leaving the germarium, the egg chamber grows in size. The germ cells enlarge due to synthesis of organelles proteins and lipids in the nurse cells, and uptake of yolk produced in the fat body (Spradling, 1993). The nurse cells and oocyte remain at approximately the same size from stage 1 to 6. In the nurse cells the nuclei divide several times forming polyploid cells. At stage 2, the oocyte nucleus, or germinal vesicle is similar in size to the nurse cell nuclei. The germinal vesicle is positioned at the posterior pole of the oocyte up to stage 7. When the egg chambers reaches stage 4 they become more elongated in shape. From stage 8 to 10b, the egg chambers grow quickly and the oocyte grows at greater rate than the nurse cells. The follicle cells and fat bodies produce yolk proteins, which are then transferred to the oocyte and allow it to grow quickly. In stage 10A egg chambers, the oocyte occupies about half of the egg chamber.

From stage 1 to 8 the somatic follicle cells are distributed in a uniform layer around the germline cells (Fig. 1.7.2A). In stage 9 the follicle cells start to undergo several migrations.

In the beginning of at stage 9, a group of 6 to 10 anterior follicle cells move through the nurse cell cluster towards the nurse cell - oocyte border (Fig. 1.7.2B). These border cells participate in the formation of the micropyle in the mature egg, thus maintaining an opening through which the sperm enters at fertilization.

At the same time, the majority of follicle cells (95%), which originally cover the nurse cells, elongate and migrate posteriorly so that by stage 10A, the oocyte is covered by a sheet of thick columnar follicle cells, while only a thin layer of 50 stretched cells are left covering the nurse cells (Fig. 1.7.2B).

By stage 10B the anterior columnar follicle cells migrate centripetally along the dorsal - ventral axis to cover the anterior end of the oocyte (the centripetal cells, Fig. 1.7.2C). These cells will secrete the anterior end of the eggshell, which, along with the eggshell secreted by the columnar cells, will eventually cover the entire egg.

At stage 11, two groups of columnar follicles cells at the dorsal-anterior region migrate anteriorly to produce a pair of dorsal appendages (Fig. 1.7.2D, 1.7.1C) (Deng et al., 1999; Spradling, 1993). The formation of the dorsal appendages is completed at stage 14. During stages 10B to 12, the cytoplasm of the nurse cells is carried through the ring canals into the oocyte. The transfer is quite rapid: most of the cytoplasm is transported into the oocyte within 30 minutes. At stages 13 to 14, the remaining nurse cells and follicle cells shrink and undergo apoptosis (King, 1970; Spradling, 1993). The mature egg is wrapped with an eggshell (chorion), containing its special structures: a pair of dorsal appendages (filaments) at the anterior end of the egg (to facilitate embryonic respiration), micropylar apparatus (for sperm entry), and operculum (located between the appendages and the micropyle, used for the larvae to hatch, Fig. 1.7.1C).

1.7.1 The role of Myosin VI in oogenesis

One role of Myosin VI in oogenesis was studied by using antibodies and fluorescence time lapse microscopy (Bohrmann, 1997). During stages 10B-12 of oogenesis, Myosin VI was found in the nurse cells, attached to cytoplasmic particles, and at the edge of the ring canals, suggesting that Myosin VI is involved in transport of cytoplasmic particles from the nurse cells, through the ring canals, into the oocyte. Microinjection of mitochondria-specific dyes has revealed that some of the transported particles are mitochondria.

Deng et al. (Deng et al., 1997) used Gal4-UAS targeted expression to detect genes expressed in the follicle cells at different stages of oogenesis. One of the cell lines had reporter gene expression in anterior follicle cells and migrating border cells, during stages 7-11 of oogenesis. After isolation of the gene by plasmid rescue techniques and sequence analysis, the gene was identified as *jaguar*, which encodes *Drosophila* Myosin VI (Deng et al., 1997; Kellerman and Miller, 1992).

The distribution of *jaguar* mRNA transcripts during oogenesis was studied by whole - mount *in situ* hybridisation. In the follicle cells, *jaguar* transcripts are present in the anterior follicle cells during stages 7-8 (Fig. 1.7.3). During stage 9, *jaguar* is expressed in the follicle cells that move from the nurse cell cluster and cover the oocyte. At stage 10 *jaguar* is expressed in the border cells, in posterior follicle cells and in the centripetally migrating follicle cells. At stages 12-13 *jaguar* is also observed in the dorsal anterior follicle cells. In the nurse cells, *jaguar* strongly expressed during stages 9-13 while Myosin VI protein expression is very low. This may indicate that stored mRNA transcripts transfer to the oocyte and less protein is translated for the function of Myosin VI in the germline.

When the expression pattern of Myosin VI during oogenesis was examined by antibody staining (Fig. 1.7.4, (Deng et al., 1999)), it was found that Myosin VI is expressed strongly in all the follicle cells that undergo migration. Myosin VI is expressed in the nurse cells at high levels up to stage 6 and at low levels in later stages. During stage 7 Myosin VI is expressed in the anterior follicle cells prior to their migration to the border cells (Fig. 1.7.4A). During stages 9-13 a strong staining appears in the follicle cells that undergo migration, including the border cells (Fig. 1.7.4B, G), the columnar cells (Fig. 1.7.4B, C), the centripetal cells (Fig. 1.7.4D, E) and the dorsal - anterior follicle cells (Fig. 1.7.4F). The expression pattern of *jaguar* (mRNA) and Myosin VI (protein) are similar. These results gave the first hint about the role of Myosin VI in the migration of the follicle cells.

The function of Myosin VI during oogenesis was studied by using the targeted gene silencing technique. This technique combines the Gal4-UAS targeted expression system and the antisense RNA technique (Deng et al., 1999). Thus, the expression of Myosin VI could be interfered with in specific somatic cells, at specific stages of development. One of the Gal4 lines used (*C532*) expressed antisense *jaguar* mRNA in all the follicle cells, except the border cells. The antisense *Jaguar* is expressed in follicle cells during stages 9 and 10 (Fig. 1.7.5). As a result, the flies had abnormal morphogenesis of the ovaries. The follicle cells developed shape defects and their migration was arrested. The integrity of the follicle cells epithelium was ruined, losing its organised monolayer structure (Fig. 1.7.5 B, D-F).

Antibody staining shows that the expression of Myosin VI is significantly reduced in most of the follicle cells (except of the border cells) when antisense *Jaguar* RNA is expressed (Fig. 1.7.5C). These results showed that Myosin VI is necessary for maintaining the integrity of the follicle cell epithelium during morphogenic changes and for the migration of the follicle cells.

When the expression of Myosin VI was disrupted in the border cells, it was found that the cells fail to migrate, thereby showing that Myosin VI is also necessary for the border cells migration (Geisbrecht and Montell, 2002; Leaper, 2003). The expression of Myosin VI was also reduced in the border cells of flies containing a mutation in the *slow border cells* (*slbo*) gene, which regulates the migration of the border cells. This suggests that the expression of Myosin VI in the border cells is controlled by *slbo*.

Since DE-cadherin is also necessary for border cell migration, interaction between the proteins was tested (Geisbrecht and Montell, 2002). In the absence of Myosin VI, the expression of DE-cadherin and Armadillo-which creates a complex with DE-cadherin-was significantly reduced in the border cell, and in the columnar follicle cells. Additionally, the expression of Myosin VI was reduced in cells lacking DE-cadherin or Armadillo. Co-immunoprecipitation tests show that Myosin VI interacts with Armadillo in ovarian cell extract. This interaction is specific since Myosin VI did not do-immunoprecipitate with Dlg, another membrane protein expressed during oogenesis. When DE-cadherin was expressed at high levels by using a heat-shock inducible transgene in ovaries depleted of Myosin VI, the migration of the border cells was rescued. Therefore, it can be concluded that it was the decline in DE-cadherin expression in the absence of Myosin VI that arrests the migration of the border cells. Border cell migration was also restored when UAS-Myosin VI or *hs*-Myosin VI was expressed, and also over-expression of UAS-slbo. These results suggest that Myosin VI plays a role in the migration through the stabilisation of the DE-cadherin-Armadillo complex. Hence, Myosin VI might promote follicle cell migration by mediating the adhesion properties of the follicle cells via DE-cadherin and Armadillo.

Figure 1.7.3

***jaguar* mRNA**

Fig. 1.7.3. The expression of *Jaguar* mRNA in the *Drosophila* egg chambers. *jaguar* mRNA is expressed in the nurse cells throughout oogenesis, with a strong signal since stage 10 and on. In the follicle cells, *jaguar* is expressed at stage 7 in the anterior cells. At stage 9, *jaguar* is expressed in follicle cells that migrate to cover the oocyte. At stage 10 expression of *jaguar* is found in the border cells and in the centripetal cells, and in stage 12 *jaguar* is expressed in the dorsal anterior cells.

Figure 1.7.4

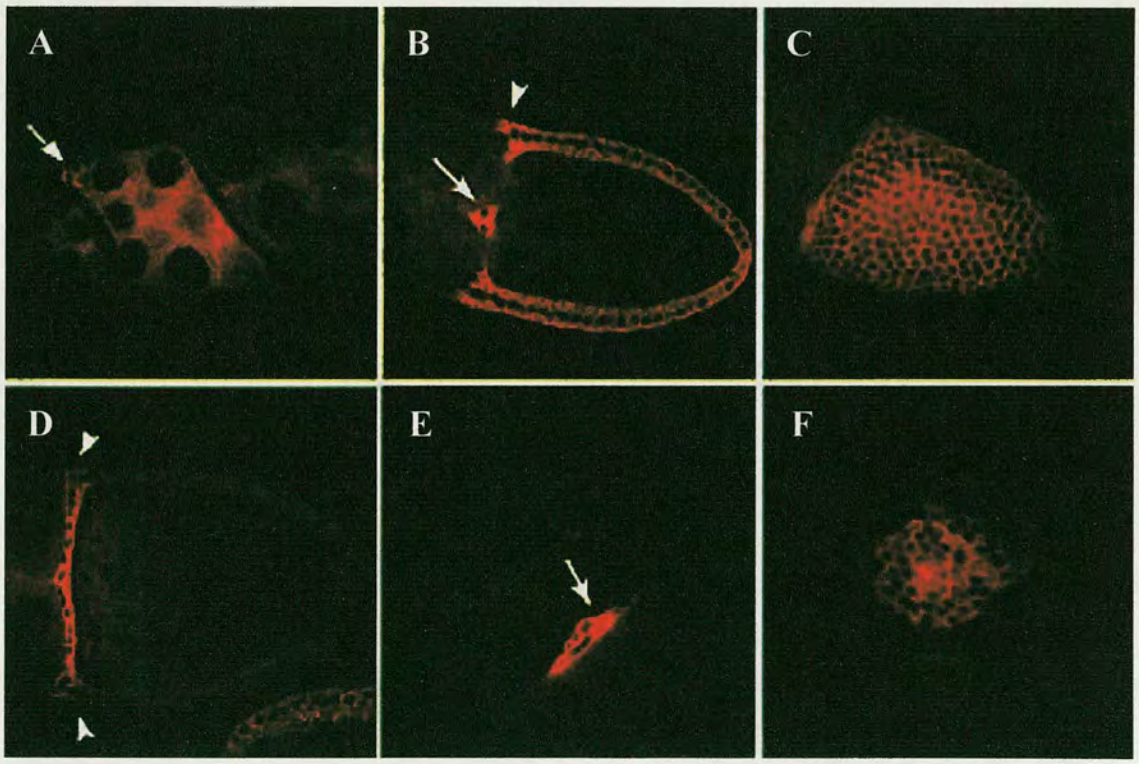

Figure 1.7.4 Expression of Myosin VI protein in oogenesis. (**A - F**) labelling of Myosin 95F. **A**: During stage 7, Myosin VI is present in the anterior follicle cells (arrow). B: Strong staining in the border cells is detected at stage 10A (arrow). During stage 10A, Myosin is present in cytoplasm of all columnar cells covering the oocyte (**B, C**). **D**: During stage 10B, when centripetal cells are migrating to cover the anterior end of the oocyte, Myosin 95F is strongly expressed in these cells (arrowhead) while staining in the columnar cells is fading. The staining remains in the leading centripetal cells, which form a contractile ring between the nurse cell cluster and the oocyte (**E**, arrow). **F**: during stages 12 - 13, Myosin VI expression is detected in dorsal anterior follicle cells [Deng, 1998 #17].

Figure 1.7.5

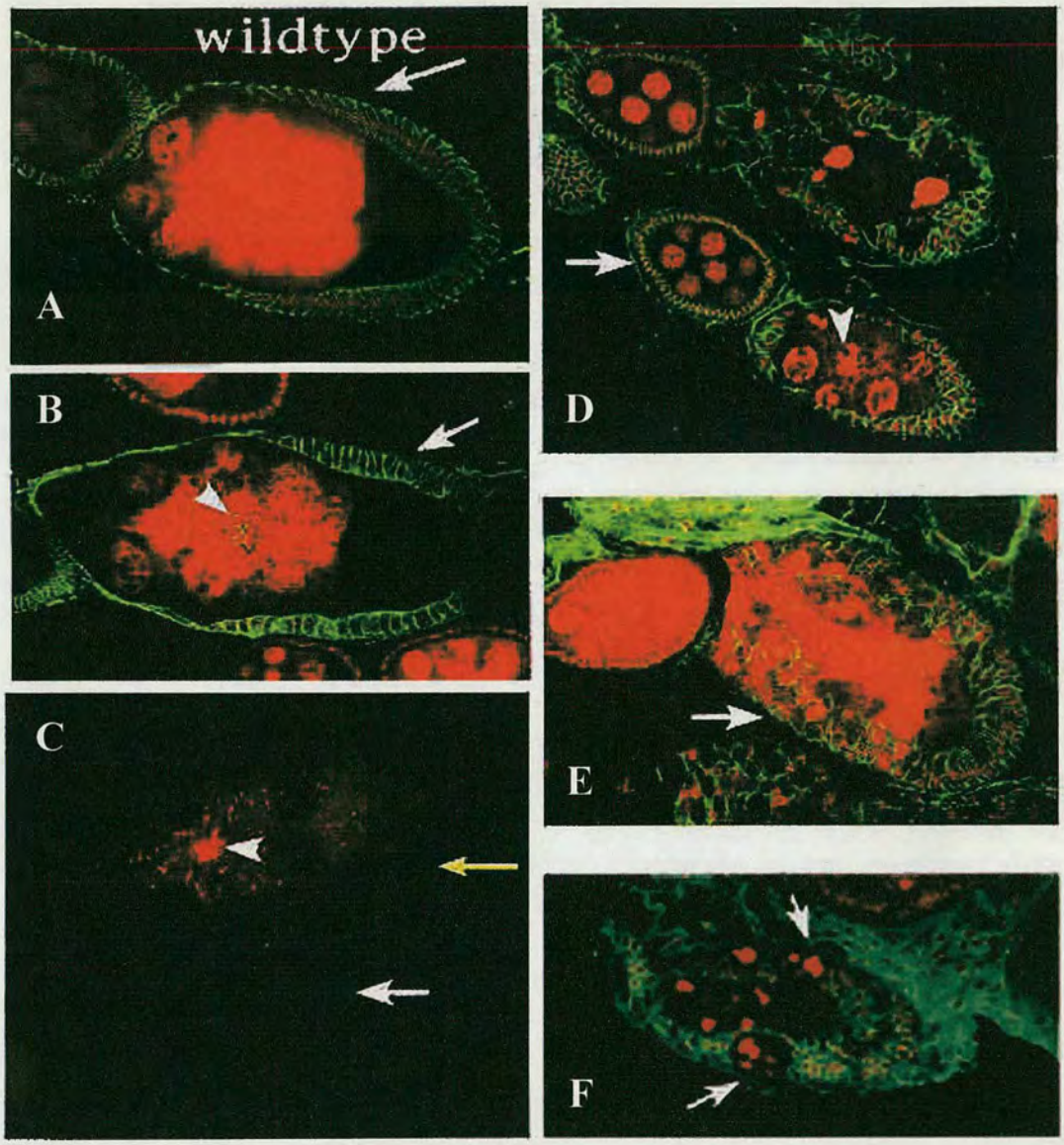

Fig. 1.7.5. Targeted *jaguar* antisense RNA expression interrupts oogenesis. Figures **A** - **D** show double label with anti-spectrin (green) to visualize follicle cell shape and propidium iodide (red) to visualize nuclei. Figure **C** show labelling of anti -Myosin 95F. **A**: A wild - type egg chamber at stage 9. The arrow shows columnar cells during their migration towards the posterior. **B**: An egg chamber of line expressing antisense (C532/Am8), at stage 9. The migrating columnar cells have an irregular morphology (arrow), however the border cell migration is unchanged (arrowhead). **C**: The expression of Myosin VI is not detected in the degenerating egg chamber (white arrow), and in the columnar cells in line C532 (yellow arrow). However, expression in the border cells (arrowhead) and nurse cells is visible. **D**: Before stage 9, *C532/Am8* egg chambers develop normally (arrow), while after stage 9 the degeneration of the egg chambers occurs (arrowhead). **E**: In a degenerating egg chamber, follicle cells have abnormal shape and the columnar follicle cells fail tomigrate. **F**: In extreme cases some of the follicle cells invade into the nurse cells cluster [Deng, 1998 #17].

Several experiments showed that the migration of the follicle cells by Myosin VI is not made through endocytosis. This possibility was tested since Myosin VI is involved in endocytosis in intestinal human cells (Buss et al., 2001). However, disruption of Myosin VI expression did not alter border cell expression of proteins involved in endocytosis, such as α-adaptin, or the expression of other cell membrane proteins. Also, reduced expression of DE-cadherin and Armadillo were not related to defects of endocytosis, since the expression of these proteins is not changed in egg chambers depleted of Dynamin, another protein necessary for endocytosis (Geisbrecht and Montell, 2002).

Border cell migration is established through cell protrusions called Long Cellular Extensions (LCE) that are sent from one of the border cells, attached to other cells membrane and pull the eight border cells cluster ("grapple and pull" model, Fulga and Rorth, 2002). In the absence of Myosin VI, LCE are not observed in the border cells, indicating that Myosin VI is necessary for the creation of these extensions (Geisbrecht and Montell, 2002). The arrest of cell migration in the absence of DE-cadherin indicates that the migration of the cells requires traction. The formation of LCE is made through actin polymerisation and membrane remodelling. These suggest that the connection of DE-cadherin and Armadillo to the cytoskeleton through Myosin VI could promote the creation of the LCE and the migration of the border cells (Schober and Perrimon, 2002).

1.8 Summary

This Introduction describes the molecular structure of Myosin VI and its functions in *Drosophila* and other species. In chapter 4 of this thesis, the function of the entire Myosin VI molecule and its separate domains is studied in more detail, by examining their localisation in organs where Myosin VI takes part in the development. The process of dorsal closure during embryogenesis is described and evidence is presented that Myosin VI is required in dorsal closure, in chapter 5.

The stages of oogenesis, focusing on the migration of the follicle cells, and the role of Myosin VI in oogenesis is described and chapter 6 details the role of Myosin VI in

follicle cell migration, through a search for proteins that function downstream of myosin VI.

The structure and function of the rest of the myosins that were found in *Drosophila* are also presented and chapter 3 describes the identification and characterisation of five new myosins in *Drosophila melanogaster.*

Chapter 2:

Materials and Methods

2.1 Materials

2.1.1 Chemicals and Radioactive isotopes

Chemicals were purchased from Sigma, BDH, Fisher Scientific and Fluka. Some materials were purchased from other suppliers, and their name will be mentioned in the text.

The isotope [^{32}P]dCTP was purchased from Amersham Biosciences.

2.1.2 Restriction endonucleases and modifying enzymes

Restriction endonucleases were obtained form New England Biolabs and Promega. Taq polymerase and accompanying buffers were supplied from Qiagen. Large fragments of DNA were amplified by using the Expand Long Template PCR kit of Roche Molecular Biochemicals. High fidelity pfu Turbo DNA polymerase was obtained from Stratagene. Klenow DNA polymerase was purchased from Roche Molecular Biochemicals.

T4 DNA ligase was purchased form New England Biolabs.

Reverse Transcriptase (SuperScript ™ II) was purchased from GIBCO BRL.

2.1.3 Buffers and Solutions

All buffers and solutions were made with sterile double distilled water (ddH_2O). Sterilization, when was required, was made by filtering the solutions through 0.22 μm filter (Satorious). Most of the solutions were stored at RT unless indicated differently.

General solutions are listed in table 2.1.3.1. When some of the reagents had similar names, they were listed in separate tables, in the sections describing their use.

Table 2.1.3.1: List of general solutions and buffers

Solution	Components/ Preparation	Final concentration
Bleaching solution	100 ml bleach solution 100 ml 1X embryo wash solution	50%
Bromophenol Blue	10 mg Bromophenol Blue Dissolve in 10 ml ddH_2O.	0.1%
$CaCl_2$	73.5g $CaCl_2.2H_2O$ (Mw: 147.0) Bring to final volume of 100 ml with ddH_2O.	5M
Carrier solution	10 mg Glycogen Dissolve in 1 ml ddH_2O. Store aliquots at -20 °C.	10 mg/ ml
Denhartd's 100X	1g BSA (Bovine Serum Albumin) 1g Ficoll (Mw: 400) 1g Polyvinylpyrolidone (Mw: 360) Bring to final volume of 50 ml with ddH_2O. Store aliquots at -20°C.	2% 2% 2%
DNA Hybridisation buffer	125 ml 20X SSPE 25 ml 10% SDS 25 ml 100X Denhartd's Bring to final volume of 500 ml with ddH_2O. Prior to the use: boil 1 ml of sssDNA (10mg/ ml) for 10 min, chill immediately on ice for 2 min and add to the solution.	5X 0.5% 5X 20 µg/ ml
DNA Sample Buffer (6X)	3 ml 0.1% Bromophenol Blue 3 ml glycerol 4 ml ddH_2O.	0.03% 30%
EDTA 0.5M pH 8.0	93g $Na_2EDTA.2H_2O$ (Mw: 372.24) Adjust to pH 8.0 with ~20g NaOH, and bring to final volume of 500 ml with ddH_2O.	0.5M
Embryo wash 10X	7g NaCl 0.5 ml Triton X-100 Bring to final volume of 100 ml with ddH_2O	7% 0.5%
Embryos Formaldehyde mix	3.25 ml ddH_2O 0.5 ml 10X PBS pH 7.4 1.25 ml 37% Formaldehyde	 1X 9.25%

List of general solutions and buffers-continuous.

Solution	Components/ Preparation	Final concentration
EtOH 70%	70 ml EtOH 100% Bring to final volume of 100 ml with ddH_2O.	70%
FISH media	5 ml 1M Tris pH 8.5 1.25g DABCO 45 ml glycerol	100mM 2.5% 90%
Fly buffer	5 ml 1M Tris-HCl pH 8.5 800 µl NaCl 5M 2.5g Sucrose 2.5 ml SDS 10% 5 ml EDTA 0.5M, pH 8.0 Bring to final volume of 50 ml with ddH_2O. Store at 4°C.	100mM 80mM 5% 0.5% 50mM
Glucose	20g Glucose Bring to final volume of 100 ml with ddH_2O. Sterilize and store at 4°C.	20%
High stringency	2.5 ml SSPE 20X 5 ml SDS 10% Bring to final volume of 500 ml with ddH_2O.	0.1X 0.1%
K Acetate	78.59g CH3COOK (Mw: 98.14) Bring to final volume of 100 ml with ddH_2O.	8M
KOH	28g KOH (Mw: 56.11) Bring to final volume of 100 ml with ddH_2O.	5M
Low stringency	50 ml SSPE 20X 5 ml SDS 10% Bring to final volume of 500 ml with ddH_2O.	2X 0.1%
Medium stringency	25 ml SSPE 20X 5 ml SDS 10% Bring to final volume of 500 ml with ddH_2O.	1X 0.1%
$MgCl_2$	9.5g $MgCl_2$ (Mw: 95.21) Bring to final volume of 100 ml with ddH_2O	1M
$MgSO_4$	24.6 gr MgSO4.7H2O (Mw: 246.5) Bring to final volume of 100 ml with ddH_2O.	1M

List of general solutions and buffers- continuous.

Solution	Components/ Preparation	Final concentration
Microinjection buffer 10X	0.186g KCl (Mw: 74.55) 5 ml PBS buffer 10mM pH 6.8 Bring to final volume of 50 ml with ddH_2O. Filter and freeze aliquots.	50mM 1mM
$MnCl_2$	39.58g $MnCl_2.4H_2O$ (Mw: 197.9) Bring to final volume of 100 ml with ddH_2O.	2M
Na Actetate, pH 5.2	40.8g CH3CooNa.3H2O (Mw: 136.08) Adjust to pH 5.2 with glacial Acetic Acid Bring to volume of 100 ml with ddH2O.	3M 5M acetate
Na_2HPO_4	17.8g $Na_2HPO_4.2H_2O$ (Mw: 178.0) Bring to final volume of 100 ml with ddH_2O. Store at 4°C.	1M
NaCl	146.1g NaCl (Mw: 58.44) Bring to final volume of 500 ml with ddH_2O.	5M
NaH_2PO_4	15.6g $NaH_2PO_4.2H_2O$ (Mw: 156.0) Bring to final volume of 100 ml with ddH_2O. Store at 4°C.	1M
NaOH	80 gr NaOH (Mw: 40.0) Bring to final volume of 20 ml with ddH_2O.	10N
NGS	50µl Normal Goat Serum 4.95 ml PBT	1%
Nipagin	1g Nipagin Bring to final volume of 10 ml with 95% EtOH.	10%
PBS pH 6.8	2.315 ml $Na_2HPO_4.2H_2O$ 1M 2.685 ml $NaH_2PO_4.2H_2O$ 1M Bring to final volume of 50 ml with ddH_2O. Store at 4°C.	46.3mM 53.7mM Total: 100mM
PBS pH 6.8	1 ml PBS pH 6.8 100mM Bring to final volume of 10 ml with ddH_2O. Store at 4°C.	10mM

List of general solutions and buffers- continuous.

Solution	Components/ Preparation	Final concentration
PBS pH 7.4 10X	40g NaCl (Mw: 58.44) 40 ml $Na_2HPO_4.2H_2O$ 1M 10 ml $NaH_2PO_4.2H_2O$ 1M Adjust to pH 7.4 with 10N NaOH Bring to final volume of 500 ml with ddH_2O	1.37M 80mM 20mM
PBT	10 ml 10X PBS pH 7.4 2.5 ml Triton X-100 Bring to final volume of 500 ml with ddH_2O. Filter and keep at 4°C.	1X 0.5%
PBTA buffer	50 ml 10XPBS pH 7.4 5g BSA 0.25 ml Triton X-100 0.1g Sodium azide Dissolve gently in 450 ml ddH_2O at 4°C. Bring to final volume of 500 ml with ddH_2O.	1X 1% 0.05% 0.02%
p-formaldehyde	4g p-formaldehyde 10 ml 10X PBS pH 7.4 Bring to final volume of 100 ml with ddH_2O. Dissolve O/N at 65°C.	4% 1X
Phenol/chloroform	5 ml Phenol (saturated with TE buffer, pH 8.0) 5 ml chloroform. Shake well before use.	
Proteinase K	10 mg proteinase K 10 µl Tris-HCl 1M, pH 7.5 590 µl ddH_2O 400 µl glycerol. Store at -20 °C	10 mg/ ml 10mM 40%
RbCl	12.09g RbCl (Mw: 120.9) Bring to final volume of 100 ml with ddH_2O.	1M

List of general solutions and buffers- continuous.

Solution	Components/ Preparation	Final concentration
Ringer's saline pH 7.2	6.8g KCl (Mw: 74.55) 13.5g NaCl (Mw: 58.44) 0.17g $CaCl_2.2H_2O$ (Mw: 147) 0.6g Tris-base (Mw: 121.14) Adjust to pH 7.2 with conc. HCl. Bring to final volume of 500 ml with ddH_2O. Filter through 0.22μm filter. Store at 4°C.	180mM 45mM 2.3mM 10mM
RNAse (DNAse free)	Dissolve 10 mg RNAse in 1 ml ddH2O. Aliquot 250 μl in 4 eppendorf tubes. Heat up to 110°C for 20 min in a closed heating block. Leave the block to cool gradually to RT. Store at -20 °C.	10 mg/ ml
SDS	50 gr SDS Bring to final volume of 500 ml with ddH_2O.	10%
Sonicated salmon sperm DNA (sssDNA)	10mg Sonicated salmon sperm DNA in 1 ml ddH_2O. Store at -20°C.	10mg/ ml
SSC 20X **pH 7.0**	87.65g NaCl (Mw: 58.44) 44.1g Na Citrate.$2H_2O$ (Mw: 294.1) Adjust to pH 7.0 with 10N NaOH Bring to final volume of 500 ml with ddH_2O.	3M 300mM
SSPE 20X **pH 7.4**	87.65g NaCl (Mw: 58.44) 15.6g $NaH_2PO_4.2H_2O$ (Mw: 156.01) 4.7g $EDTANa_2$ (Mw: 372.24) Adjust to pH 7.4 with 10N NaOH Bring to final volume of 500 ml with ddH_2O.	3M 200mM 25mM
Stripping solution	198 ml ddH_2O Boil and gently add 2 ml 10% SDS.	0.1% SDS
TAE (50X)	121g Tris Base (Mw: 121.14) 28.55 ml Glacial Acetic acid 50 ml 0.5M EDTA, pH 8.0 Bring to final volume of 500 ml with ddH_2O.	2M 50mM
TE, pH 8.0	1 ml 1M Tris, pH 8.0 200 μl 0.5M EDTA, pH 8.0 in 100 ml ddH_2O.	10 mM 1mM

List of general solutions and buffers- continuous.

Solution	Components/ Preparation	Final concentration
TFB1	1.88 ml K acetate 8M 1 ml of $CaCl_2$ 5M 12.5 ml $MnCl_2$ 2M 50 ml RbCl 1M 75 ml Glycerol Dissolve in 400 ml ddH_2O (important to add the solution in the exact order to avoid sedimentation of the salts). Adjust to pH 5.8 with Glacial Acetic acid. Bring to final volume of 500 ml with ddH_2O. Sterilize through 0.22 mm filter, and store at 4°C.	30mM 10mM 50mM 100mM 15%
TFB2	0.3g Pipes (Mw: 300) 1.5 ml $CaCl_2$ 5M 1 ml RbCl 1M 15 ml Glycerol Dissolve in 70 ml ddH_2O (important to add the solution in the exact order to avoid sedimentation of the salts). Adjust to pH 6.5 with KOH 5M. Bring to final volume of 100 ml with ddH_2O. Sterilize through 0.22 mm filter, and store at 4°C.	10mM 75mM 10mM 15%
Tris Buffer pH 8.0	Dilute 1 ml of Tris buffer pH 8.0 in 90 ml ddH_2O. Check that the pH is 8.0 and bring to final volume of 100 ml with ddH_2O. Store at 4°C.	10mM
Tris-HCl **pH 7.4** **pH 7.5** **pH 7.6** **pH 8.0** **pH 8.5**	60.55g Tris Base (Mw: 121.14) Adjust to pH 7.4 with conc. HCl (~35 ml) Adjust to pH 7.5 with conc. HCl (~32 ml) Adjust to pH 7.6 with conc. HCl (~30 ml) Adjust to pH 8.0 with conc. HCl (~20 ml) Adjust to pH 8.5 with conc. HCl (~14 ml) Bring to final volume of 500 ml with ddH_2O. Store at 4°C.	1M

2.1.4 Media preparation

All types of media were prepared by the Institute media staff. The media was sterilized by autoclaving (15 min at 15 psi) and stored at RT.

Table 2.1.4.1: Media List

Media type	Components/ preparation	Final concentration
LB (Luria Broth)	10g NaCl 10g Bacto-tryptone 5g Yeast extract Dissolve and bring to final volume of 1 lit. with ddH_2O	1% 1% 0.5%
LB Agar	10g NaCl 10g Bacto-tryptone 5g Yeast extract 15g Difco agar Dissolve in ddH_2O and bring to final volume of 1 lit.	1% 1% 0.5% 1.5%
NZY+ Broth	10g of NZ amine (casein hydrolysate) 5g of yeast extract 5g of NaCl (Mw: 58.44) Adjust to pH 7.5 using 10N NaOH. Dissolve and bring to final volume of 1 lit. with ddH_2O. Autoclave Add the following sterilized supplements prior to use: 12.5 ml 1M $MgCl_2$ 12.5 ml 1M $MgSO_4$ 20 ml of 20% (w/v) glucose	1% 0.5% 0.5%

2.1.5 Antibiotics preparation

The antibiotics were prepared at the recommended concentrations and stored at -20°C.

Table 2.1.5.1: Antibiotics list

Antibiotic	Stock solution	Working Concentration
Ampicillin	50 mg/ ml in ddH2O, kept at 20°C	50 µg/ ml
Kanamycin	25 mg/ ml in ddH2O, kept at 20°C	50 µg/ ml
Tetracycline	5 mg/ ml in EtOH, kept at 20°C covered with aluminium foil.	50 µg/ ml

2.1.6 Fly food preparation

Fly stocks were mostly grown in bottles and vials containing Staffen food. When the flies were grown in cages, a different type of food was used, as described in the table below.

Table 2.1.6: List of fly food used.

Food name	Components/ Preparation	Final concentration
Staffen	25g corn flour	2.5%
	50g Sugar	5%
	17.5g Lyophilised yeast	1.75%
	10g Agar	1%
	Dissolve in 1 Lit. boiling water. Add: 0.5 ml	
	10% Nipagin	0.005%
Apple juice plates	9g agar	2.25%
	10g sucrose	2.5%
	300 ml ddH_2O	
	Dissolve until the solution becomes transparent.	
	Add: 100 ml apple juice	25%
	Allow to cool to 60°C. Pour into plates.	

List of fly food used- continuous.

Food name	Components/ Preparation	Final concentration
Tomato juice plates	4 gr agar 160 ml ddH_2O Dissolve until the solution becomes transparent. Add: 40 ml tomato juice. Boil again Allow to cool to 60°C. Add: 500 µl nipagin (10%). Pour into plates.	1.7% 17% 2.5%
Grape juice plates	9g agar 10g sucrose 300 ml ddH_2O Dissolve until the solution becomes transparent. Add: 100 ml grape juice Allow to cool to 60°C. Add 1 ml nipagin (10%). Pour into plates.	2.25% 2.5% 25% 1.25%

2.2 Bacterial strains and plasmids

Table 2.2.1: List of bacterial strains

Host strain	Genotype/ Source
XL1 Blue (Stratagene)	*recA1 endA1 gyrA96 thi-1 hsdR17 supE44 relA1 lac[F' proAB lacI^{q}ZΔM15 Tn10 (Tet^R)]*
SoloPack®Gold Supercompetent cells (Stratagene)	Tet^R *Δ(mcrA)183 Δ(mcrCB-hsdSMR-mrr)173 endA1 supE44 thi-1 recA1 gyrA96 relA1 lac* Hte [F' *proAB lacI^{q}ZΔM15 Tn10* (Tet^r) Amy Cam^R]^a

Table 2.2.2: List of DNA constructs

Construct name	Insert	Vector	Cloning enzymes	Selection	Strain
GFP-N1	n/a	pEGFP-N1 (Clontech)	n/a	Kan^R + Neo^R	XL1 Blue
Jaguar (made by Wu-Min Deng)	Myosin VI cDNA clone (EM3)	pBluescript SK- (Stratagene)	EcoRI + XHoI	Amp^R	XL1 Blue
PGM	Myosin VI-EGFP	pUAST	EcoRI + AgeI	Amp^R	SuperGold
PGMH	Myosin VI head- EGFP	pUAST	EcoRI + AgeI	Amp^R	SuperGold
PGMT	Myosin VI tail- EGFP	pUAST	EcoRI + AgeI	Amp^R	SuperGold
pUAST	n/a	pUAST (Brand & Perrimon, 1993)	n/a	Amp^R	XL1 Blue
pUAST-GFP	pEGFP-N1	pUAST	EcoRI + Not I	Amp^R	XL1 Blue

2.2.1 Bacteria growth and storage

When bacteria cells were used from a stab, a glycerol stock, or from an old plate (3-4 weeks old), they were initially streaked on plates, to obtain independent colonies. This is done in order to reduce the likelihood of working with a culture which has become contaminated or accumulated mutations. Bacteria cells were picked under sterile conditions and applied on agar plates, containing the appropriate selection antibiotic (table 2.1.5). After incubation at 37°C O/N, separate colonies originated from single cells were obtained.

For a small scale bacteria stock, a culture was prepared in 5 ml LB medium containing the appropriate antibiotic, by inoculating a single colony from a plate,

under sterile conditions. The culture was grown O/N with shaking (150 rpm) at 37°C.

Larger scale cultures were prepared by expanding 1 ml of a small scale liquid culture in 50-500 ml LB medium containing the appropriate antibiotic and growing it O/N with shaking (150 rpm) at 37°C.

For a short-term storage, a single colony was streaked on a LB plate containing the appropriate antibiotic. The culture was grown O/N at 37°C and stored at 4°C for up to one month.

For a long-term storage (up to five years) bacterial stabs were prepared. A single colony was picked from a plate with a sterile toothpick and streaked into a LB broth containing 0.6% agar. The stab was incubated O/N at 37°C and stored at RT in dark.

For an indefinite storage of strains, a glycerol stock was prepared. 800 µl of an over-night culture were added to 200 µl of sterile glycerol, the mixture was homogenized and kept at -80°C.

2.3 *Drosophila Methods*

2.3.1 Maintenance of *Drosophila* stocks

All fly stocks were maintained in cornmeal food at 18°C or 25°C. In order to prevent mites growth, dry filter paper strips soaked with 3% (v/v, in EtOH) Benzyl Benzoate were placed in the vials and bottles, on the top of the food.

All the fly stocks used are described in table 2.3.1

Table 3.2.1 fly stocks

Fly line nickname	**Genotype**	**Phenotype**	**Source**
Oregon R +38B	Wild type	Red eyed wild type	Roote J.
wk	*w-/w-*	White eyed	
jar^{R23}	jar^{R23}/ *TM3, Sb*	*jaguar* mutant	Leaper, K.
jar^{R39}	jar^{R39}/ *TM3, Sb*	*jaguar* mutant	Leaper, K.
jar^{R39}	jar^{R39}/ *TM6, Tb*	*jaguar* mutant	Leaper, K.
jar^{R70}	jar^{R70}/ *TM3, Sb*	*jaguar* mutant	Leaper, K.
jar^{R235}	jar^{R235}/ *TM3, Sb*	*jaguar* mutant	Leaper, K.
jar^{R235}	jar^{R235}/ *TM6, Tb*	*jaguar* mutant	Leaper, K.
Jar^{mmw14}	Jar^{mmw14}/ *TM3, Sb*	*jaguar* mutant	Deng W.-M.
Am8-2	*w-; P{* w^{+}*, UAS-jar.a}Am8.2*	Myosin VI antisense	Deng W.-M.
jarΔATP	*w-; P{* w^{+}*, UAS-jar-ΔATP}/Cyo*	Myosin VI dominant negative	Jan YN.
dab	*st, dabM54/ TM3, Sb [Act-z]*	Disabled mutant	Giniger, E.
UAS RhoN19 2.1	*UAS RhoN19 2.1*	Rho dominant negative	Mlodzik, M.
UAS RhoN19 4.3	*UAS RhoN19 4.3/Cyo*	Rho dominant negative	Mlodzik, M.
$Rho1^{E3.10}$ (3176)	w^{a} $N^{fa\text{-}g}$; $Rho1^{E3.10}$/*CyO*	Rho mutant	Bloomington stock centre

Gal4 lines			
Fly line nickname	**Genotype/ transposon**	**Phenotype**	**Source**
C865	*w-;; P{w^{+}, Gal4}jar^{C865}*	Express GAL4 according to the pattern of *jar* gene.	Glover D. Kaiser K.
e22C	*y1 w-; P {w^{+}, GAL4}e22c/SM5*	Express GAL4 ubiquitously in the whole embryo.	Brand, A. and Perrimon, N.
E4	*w-;;P {w^{+}, GAL4}E4*	Gal4 expression during oogenesis in groups of follicle cells at the posterior region.	Schüpbach, T.
en	*w-; P{en2.4-GAL4}e16E*	Gal4 expression in a posterior strip of every segment. Located in chromosome 2	Brand, A.
T155 (5076)	*w-;;P{w$^{+mW.hs}$=GawB}T155*	Express GAL4 in follicle cells epithelium since stage 9. Located in chromosome 3	Bloomington Stock Centre
C532	*P {w^{+}, GAL4}C532*	Express GAL4 in follicle cells (except of the border cells) and Imaginal discs	
Balancer chromosome lines			
Fly line nickname	**Genotype**	**Balancer/ Phenotype**	**Source**
TM6-GFP	*w^{1118}; Ly^{1}/TM6B, P{w$^{+mW.hs}$=Ubi-GFP.S65T}PAD2, Tb^{1}*	3rd chromosome balancer. Fluorescent during embryogenesis	Thummel, C.S.
TM3/TM6	*w-;TM3, Sb, e/ TM6, Tb, e*	3rd chromosome balancer. White eyed, stubble, tubby and ebony	Cribbs, D.

2.3.2 Collection of embryos

In order to create embryos with a desired phenotype, a cross was set with virgin females (as in section 2.3.4) and males originated from specific lines. The flies were left to mate and lay eggs in vials containing yeast during 2-3 days, at 25°C. Afterwards the flies were transferred to a cage containing grape juice, or apple juice plates, smeared in the centre with yeast paste (made with yeast and water). The cages were held at 25°C. The change of the plates and the incubation time is indicated in every case. The embryos were collected by rinsing the plate with embryo wash solution (1X), removing the embryos from the plate with a brush and collecting the embryos into a fine plastic sieve.

2.3.2.1 Collection of fluorescent or non fluorescent embryos

Fluorescent embryos (expressing GFP) were distinguished from non-fluorescent embryos by examining them under dissecting GFP microscope (Leika) with the filter combination required for GFP observation (450-90/515). Unlike an auto-fluorescent objects, The fluorescent light coming from a GFP expressing tissue is observed only the specific GFP filter. The embryos were collected with a fine brush and used for further growth in a separate plate, or used for antibody staining

2.3.3 Collection of larvae, pupae and adults

In order to collect larvae, flies were kept in a cage and the plate (grape juice) was replaced daily. First instar larvae were collected 24 hours after the replacement of the plate, third instar larvae were collected from the plates after 3-5 days. If fluorescent larvae were to be collected, they were examined under dissecting GFP microscope as described in section 2.3.2.1.

Larvae at late third instar stage were selected from vials, 4 days after egg laying, by their ability to crawl up the bottle walls. The larvae were gently collected with forceps.

Early pupae were collected 5 days after egg laying with a wet paintbrush.

Adult flies were generally collected up to 2 weeks after their hatch. The flies were anaesthetized with CO_2 (occasionally with diethyl ether) and collected. Male and

female were distinguished according to the difference in the size, abdomen shape, and the presence of sex combs in male.

2.3.4 Collection of virgin flies and crosses

Virgin flies were collected early in the morning and during the day, at interval of 2-4 hr. Virgin flies were identified by the bright colour of the body and the presence of a dark greenish spot (the meconium, the remains of their last meal before pupating) on the underside of the abdomen (right side). Newly hatched flies were also recognized by the folded wings.

Generally, 3-5 virgin flies were mated with 1-3 males, in a vial containing fresh food and yeast. The flies were incubated at 25°C until larvae and pupae started to emerge.

2.3.5 Generation of transgenic flies

The creation of transgenic flies was made according to Rubin and Spradling (Rubin and Spradling, 1982).

2.3.5.1 Preparation of the microinjection solution.

The construct plasmids to be injected (PGM, PGMH, PGMT), and the helper plasmid pΔ2-3 were prepared as a plasmid midiprep (section 2.4.1.3) and purified as described in sections 2.4.3.1-2.4.3.3. The construct and the helper plasmids were brought to final concentrations of approximately 1μg/ μl, and 500ng/ μl respectively. The microinjection solutions, prepared with 10X microinjection buffer, had a final concentration of 400μg/ ml of the transforming plasmid and 100μg/ ml of the pΔ2-3 plasmid, in 1X injection buffer (5mM KCl, 0.1mM sodium phosphate, pH 6.8).

2.3.5.2 Microinjection of embryos

3-5 days old wk flies (homozygous w^-, white–eyed) were incubated in apple-juice plates. The plates were changed every 30 min in order to collect embryos at stages 1-2 (prior the formation of pole cells). The embryos were gently collected with a fine brush and transferred to a double sided sticky tape (Scotch Brand 3M No. 666). The

embryos were manually dechorionated and transferred to a 22 X 22 mm coverslip (attached to a 76X26 mm slide) which had a very thin strip of double sided tape on it. The embryos were oriented with their posterior ends over the edge of the tape and the coverslip. Normally, around 30 embryos were placed on each coverslip. The coverslip was placed in a Petri dish containing desiccant (silica gel) for 6-10 min and immediately covered with K-elf oil. The slide was placed on the stage of the microscope with the posterior end of the embryos towards the needle. The eggs were injected at 1500 psi for 0.3-0.5 sec. During the injection, damaged and improperly aged embryos were killed. The coverslip containing the injected embryos was placed onto a tomato juice plate smeared in the centre with yeast paste. The embryos were incubated for 2-3 days at 25°C. After one day most of the larvae started to emerge, few emerged after 2-3 days. Every larva was transferred into a separate vial containing fresh Staffen food and kept at 25°C. The adult flies that eclosed from the pupal case were crossed with 3 wk flies from the opposite sex (using virgin females). Progeny of the cross were examined for red-eyed transformants. Every transgenic fly was crossed again with wk flies to create a separate line. In every line, the red-eyed flies were selected routinely every two generations, during the food change.

2.3.5.3 Selection of transgenic lines.

About 100 transgenic lines were collected for every construct plasmid injected (PGM, PGMH, and PGMT). In order to select the lines that have the highest level of GFP tagged protein expression, all the flies were crossed with the Gal4 lines: *T155* (to observe expression in the follicle cells) and *C865* (to observe a strong expression in the larvae salivary glands). Approximately 20 lines were selected from every construct group. The list of all the selected lines is described in chapter 4.

2.4 Nucleic Acid techniques

2.4.1 Plasmid DNA preparation

2.4.1.1 All purpose plasmid miniprep

A 5 ml culture grown O/N was centrifuged and the bacterial pellet was resuspended in 250 µl Resuspension buffer. 350 µl of Lysis solution were added and mixed gently by rotating six times. After incubation for 5 min 350 µl of Neutralising solution were added and mixed gently by rotating six times. The mixture was centrifuged at 22,000g for 15 min, the supernatant was transferred to a clean eppendorf tube and the DNA was recovered from the solution by isopropanol precipitation (section 2.4.3.2).

Table 2.4.1.1: list of solutions for plasmid miniprep

Solution	**Components/ preparation**	**Final concentration**
Resuspension buffer	500 µl 1M Tris-HCl pH 7.6 200 µl 0.5M EDTA pH 8.0 100 µl RNAse (DNAse free) 10 mg/ ml Bring to final volume of 10 ml with ddH_2O.	50 mM 10 mM 100 µg/ ml
Lysis solution	2 ml 10N NaOH 10 ml 10% SDS Bring to final volume of 100 ml with ddH_2O.	0.2M 1%
Neutralising solution	3.24g CH3CooK (Mw: 98.14) Adjust the pH 4.8 with Glacial Acetic acid. Bring to final volume of 25 ml with ddH_2O. Store at 4°C.	1.32M

2.4.1.2 High purity plasmid miniprep

High quality DNA was required for sequencing and cloning experiments. QIAprep®Spin Miniprep kit (Qiagen) was used to isolate and purify 20-30 µl of plasmid DNA. The protocol is according to the supplier instructions.

2.4.1.3 High purity plasmid midiprep

QIAfilter™ Plasmid midiprep kit (Qiagen) was used to isolate up to 150 µg of highly purified plasmid DNA. This kit was used for the preparation of DNA for

microinjection. After growing 150 ml of cell culture O/N, the cells were pellet and kept at -20 for future use (up to 1 year). The purification of the plasmid DNA was according to the supplier instructions, using sterile water (pH≥7.0). Afterwards, the DNA concentration was measured. When the DNA concentration was lower than the necessary, the plasmid DNA was precipitated and resuspended in sterile water O/N at 4°C. The solution was spun for 10 min at 22,000g at 4°C in order to remove DNA aggregates, and the DNA concentration of the collected supernatant was measured again.

2.4.2 Genomic DNA preparation

Approximately 130 mg of flies (0.5 ml) were homogenized in 250 µl Fly buffer for 3 min. 750 µl of fly buffer, was added and RNA was digested with 4 µl RNAse solution one hour at 37°, followed by protein digestion with 30 µl of proteinase K solution added to the mixture for one hour at 50°. The sample was spun for 10 min at 15,000g at 4°C and the collected supernatant was mixed with one volume of phenol: chloroform solution by gentle rotation for 5 min at RT. The sample was spun for 3 min at 10,000g at RT and the collected supernatant was mixed with one volume of chloroform solution by gentle rotation for 5 min at RT. After spinning the mixture again the supernatant was pellet by mixing with 0.6 vol. of isopropanol for 5 min and centrifugation for 20 min at 15,000g at 4°C, washed in 75% EtOH, dried and resuspended in 70 µl Tris buffer (10mM Tris-HCL, pH 8.0).
The DNA concentration was measured as described in section 2.4.3.3.

2.4.3 DNA purification

2.4.3.1 Phenol/chloroform extraction

This protocol was generally used with plasmid DNA, and PCR amplified DNA. The genomic DNA was purified in a different manner, as described in section 2.4.2. Protein impurities were removed from nucleic acid preparations by phenol/ chloroform extraction. The DNA solution was brought to volume of at least 200 µl with ddH2O. Na Acetate solution was added to final volume of 10% (22 µl) and mixed well. One volume of phenol/chloroform solution (220 µl) was added; the mixture was shaken vigorously by hand for 3 min and spun for 3 min at 10,000g at RT. The supernatant was collected, one volume of chloroform (220 µl) was added, and the mixture was again shaken vigorously by hand for 3 min and spun for 3 min at 10,000g at RT. The supernatant was collected and extracted again in chloroform, in order to remove phenol remains. The supernatant was collected to a new tube.

2.4.3.2 Precipitation of nucleic acids

One volume of DNA (200 µl) was mixed with 2.5 volumes of ice-cold isopropanol (500 µl, alternatively used 3 volumes of ice-cold 100% Ethanol) and 1 µl of carrier solution (used mainly when low amount of DNA is purified). Add 10% (22µl) of Na Acetate solution (no need to add if the DNA was previously extracted with phenol/chloroform). The sample was gently mixed and centrifuged at 15,000g at 4°C for 15 min. The pellet was washed with 500 µl of 70% EtOH and centrifuged at 15,000g at 4 °C for 5 min. The DNA pellet was air dried and resuspended in the appropriate volume of 10 mM Tris-HCl, pH 8.0, or in sterile ddH2O (pH ≥7).

2.4.3.3 Estimation of nucleic acids concentration by UV spectrophotometry

The determination of DNA and RNA concentration was made by UV spectrophotometry. The absorbance of DNA/RNA was measured at 260nm and 280nm using a two-beam Hitaci spectrophotometer. The concentration of the samples was calculated using the following formula:

$$\text{DNA/ RNA concentration (ng/ µl)} = \frac{\text{A260 X DF X Sc}}{1000}$$

DF = dilution factor

Sc = Spectrophotometric conversion (Specific DNA/ RNA absorption value): Sc=50 for double stranded DNA, and Sc=40 for single-stranded DNA of RNA.

The purity of DNA was estimated by assessing the ratio A260/A280: DNA and RNA were considered to be highly pure when the ratio was greater than 1.8 and 2.0, respectively.

When a low concentration of DNA was to be detected, the amount of DNA was estimated by gel electrophoresis as described in section 2.4.5.

2.4.4 RNA preparation

All the tips and tubes used for RNA preparation were DEPC treated, and all the solutions were made with DEPC treated water.

30 first instar (approximately 500 µg) larvae were homogenized in 150 µl Trizol® reagent (Invitrogen) and incubated with additional 350 µl of Trizol for 5 min at room temperature. The RNA was extracted by mixing with 200 µl chloroform (shake vigorously for 15 sec) and spinning for 15 min at 12,000g at 4°C. The upper phase was mixed with 500 µl isopropanol and incubated at RT for 10 min. After spinning the sample for 15 min at 12,000g at 4°C, the pellet was washed in 1 ml 75% EtOH, and air dried for 15-20 min at RT. The dried pellet was resuspended in 12 µl H_2O, and used for cDNA preparation, or kept at -80°C for few days.

2.4.5 DNA agarose gel electrophoresis

Agarose gel electrophoresis was used to separate DNA molecules according to their size.1% agarose gel (in 1X TAE buffer) was used for up to 10kb DNA molecules and 0.7% gel was used for DNA molecules in the size of 10-20kb. EtBr was added to the gel to final concentration of 0.2 mg/ ml. Prior to the loading, the samples were mixed with loading buffer (Table 2.1.3.2) to a final concentration of 1X. The DNA samples were loaded on the gel and electrophoresed at 4-7V/cm in 1XTAE buffer, until the desired separation was obtained. The DNA, stained with EtBr, could be visualized on a long-wavelength UV transilluminator (365 nm). The gel was photographed by a UV camera.

In order to determine the size of DNA fragments, molecular standards were used. Approximately 0.5 μg of 1KB DNA ladder was applied per gel. To estimate the approximate amount of DNA in an unknown band, Bioline HyperLadder I was used. 5 μl of the ladder would produce a set of bands with a known amount of DNA in each band. The amount of DNA was estimated by comparing the intensity of the DNA band in the sample to the intensity of the bands in the ladder.

2.4.6 Purification of DNA from agarose gel

QIEX®II Gel Extraction Kit (Qiagen) was used to extract up to 15kb DNA fragments from agarose gels. The supplier procedure was modified as follows: the DNA fragment was excised from the gel and dissolved in 3 volumes of QX1 buffer at 65°C for 5-10 min. Once the whole gel was dissolved, 2 volumes of ddH_2O (according to the gel weight), 10 μl of 3M Na Acetate and 10 μl QIEX II resin were added. The sample was gently rotated during 6 min at RT, and the QIEX II particles were pellet at 14,000g for 1 min. The particles were washed once with QX1 buffer and two times with PE buffer (Qiagen). The pellet was air-dried at 37°C for 5-10 min. To elute the bond DNA, 30 μl of 10mM Tris-HCl, pH 8.0 were added to the pellet, the mixture was incubated for 5 min at 65°C. The sample was centrifuged at 22,000g and the cleared supernatant was transferred into a new eppendorf tube. The elution was repeated and the eluted DNA solutions were combined.

When the obtained DNA fragments were used for subsequent ligation, the DNA fragments were cleaned as described in section 2.4.3.

2.4.7 Enzymatic modifications of DNA

2.4.7.1 Endonuclease restriction of DNA

The reaction was carried out in a 20-50 µl reaction mixture, according to the manufacturer's instructions. The reaction mixture contained: DNA sample (1 µg), reaction buffer (10% of the final volume), restriction enzyme (4-10U) and ddH_2O to final volume of 20µl or 50µl. The reaction mixture was incubated at the recommended temperature (usually 37°C) for 4-20 hr, depends on the type of restriction enzyme used: when the restriction enzyme has a star activity (an aberrant restriction of DNA after a long restriction period and under abnormal conditions like high enzyme concentration), like Eco RI, it was incubated for a shorter time. In general the amount of enzyme added and the incubation time was calculated to restrict an amount of DNA that will be 4-20 times higher, in order to ensure a complete restriction, without initiation of star activity. The reaction was stopped by inactivation of the enzymes at 65°C for 15 min. When the sample had to be restricted with two enzymes or more, all the enzymes were added together with a reaction buffer selected for the optimal activity of all the enzymes. Alternatively, the DNA sample was precipitated after the first restriction (as in section 2.4.3.2), the DNA was resuspended in ddH_2O in the appropriate volume, and the second restriction reaction was carried out with a new enzyme and its appropriate buffer.

2.4.7.2 DNA ligation

The ligation reactions were made with DNA fragments and linearised cloning vectors containing cohesive ends after endonuclease restrictions. When the ligation was made during the formation of the GFP DNA constructs, all the DNA fragments were purified as described in section 2.4.3.1-2.4.3.3.

DNA ligation was performed by incubating a DNA fragment with a linearised cloning vector in the presence of a 1X ligation buffer (with ATP) and 400U T4 DNA ligase (New England Biolabs), in 10-20 µl reaction volume. The reaction was

incubated at 12-18°C for O/N and heat inactivated for 15 min at 65°C. 2µl of the reaction was used to transform into competent cells (after purification), and 8µl were loaded on a gel in order to verify the ligation.

2.4.8 DNA transformation to chemically competent cells

2.4.8.1 Preparation of competent cells

XL1 Blue culture was grown O/N on LB plate containing tetracycline. A single colony was inoculated in 5 ml LB medium and incubated O/N at 37°C. The whole culture was inoculated into 100 ml of pre-warmed (37°C) LB medium and 2 ml of 1M $MgSO_4$ were added (to final conc. of 20 mM). The cells were grown until the intensity of the cells at OD_{550} reached the value of 0.4-0.6 (after 3-5 hours). The cells were pellet at 4500g for 10 min and kept from this stage onwards at 4°C. The cells were gently resuspended in 2 ml of ice-cold TFB1 solution, by using a pipette tip. 18 ml of TFB1 were added and the cells were incubated in ice, in the cold room for 5 min. The cells were pellet at 4500g for 5 min at 4°C and gently resuspended in 4 ml ice-cold TFB2 solution. After incubation of the cells for 15-60 min in ice, in the cold room, aliquots of 100 µl were made (in the cold room) and the cells were immediately frozen and stored at -80°C.

2.4.8.2 Transformation

100 µl aliquot of competent cells were thawed on ice for 5 min. 10-50 ng of plasmid DNA (maximum volume of 10 µl) was added to the aliquot and mixed gently with a pipette tip. The cells were incubated in ice for 45 min. Then the cells were incubated for 90 seconds (not more) in 42°C pre-heated water bath. After cooling the cells for 2 min on ice, 600 µl of LB medium were added and the culture was incubated for 45 min at 37°C with agitation at 180 rpm. The cells were plated on LB plates containing the appropriate selective antibiotic, and incubated at 37°C for O/N.

When a transformation was made to GFP DNA construct after ligation, the DNA was purified once again as in section 2.4.3.1-2.4.3.3; and the transformation was made

with SoloPack®Gold Supercompetent cells (Stratagene), according to the manufacturer's instructions.

2.4.9 Colony lift hybridisation

2.4.9.1 Colony lifts

Colony lift hybridisation was used in order to identify colonies transformed with a plasmid containing the desired inserts. A round Hybond™ N+ nylon membrane (Amersham Biosciences) was marked and applied on a plate containing colonies after 16-24 hr incubation, allowing all the colonies to attach to the membrane. The position of the membrane on the plate was marked by stabbing the membrane and the agar and marking the pinching position on the plate. After 2 min the membrane was carefully removed and placed over a filter paper soaked with denaturing buffer (the side of the membrane without the colonies face to the paper). After 7 min of DNA denaturation, the membrane was aligned on a new filter paper soaked with neutralizing buffer for 3 min. Then the membrane was rinsed in rinsing buffer, and the colonies' debris was removed with a brush. The membrane was dried on a plain paper and exposed to UV light for 10 min, in order to fix the DNA to the membrane.

Table 2.4.9.1: List of solutions used for preparing the colony lifts

Solution	**Components/ Preparation**	**Final concentration**
Denaturing Buffer	150 ml NaCl 5M 25 ml NaOH 10N Bring to final volume of 500 ml with ddH_2O.	1.5M 0.5M
Neutralising Buffer	150 ml NaCl 5M 250 ml 1M Tris-HCl, pH 8.0 Bring to final volume of 500 ml with ddH_2O.	1.5M 0.5M
Rinse Buffer	50 ml 20X SSC 100 ml 1M Tris-HCl, pH 7.5 Bring to final volume of 500 ml with ddH_2O.	2X 0.2M

2.4.9.2 Radio labelling of DNA probes

The radioactive DNA probes were made by using Ready-To-Go™ DNA labelling Beads

(-dCTP) (Amersham Biosciences) along with [^{32}P]dCTP (Amersham Biosciences), according to the manufacturers' instructions. 200 ng of denatured DNA was used per labelling. Unincorporated nucleotides were removed by eluting the probe through NICK™ Columns (Amersham Biosciences) with TE buffer, pH 8.0. The columns contained Sephadex for gel filtration that allowed the high molecular weight DNA to pass faster through the column than the unincorporated nucleotides. The probe was denaturated by adding 1 µl 10N NaOH to 100 µl of probe.

2.4.9.3 Hybridisation with [^{32}P]dCTP hybridisation probes

All the incubations were made at 65°C, with continuous rotation. The membrane was incubated in 50 ml DNA hybridisation buffer for 3-24 hr. The denaturated radioactive probe was added and the membrane was incubated for O/N. The radioactive probe was stored for an additional use for up to 4 weeks in Perspex box. The membrane was washed for 15 min in low stringency solution, 20 min in medium stringency solution, and 15 min in high stringency solution. The membrane was sealed in polyethylene bag, placed in an autoradiography cassette, and exposed to a blue sensitive film (Kodak) at -70°C. The films were developed in an X-ograph compactX2 automatic film processor.

2.4.9.4 Use of two different probes.

When two probes had to be used, the first probe was removed from the membrane by placing the membrane in boiling stripping solution and allows it to cool to RT. This process was repeated until no radioactive signal was detected on the membrane. If the signal was too strong and the probe could not be removed, a new membrane had to be made, using the original colony plate for the colony lift.

2.4.10 DNA sequencing and sequence analysis

A typical (1X) sequencing reaction consisted of 8 μl Labelling Mix (BigDye™ Terminator for Cycle Sequencing, ABI PRISM, Applied Biosystems), 3.2pmol of the appropriate primer, 50-200 ng (PCR product) of 400ng (plasmid DNA) high quality DNA template and water to final concentration of 20 μl. The PCR program applied was as follows: 25 cycles, 95°C for 30 min, 50°C for 20 sec, and 4 min extension step at 60°C. In order to remove unincorporated dye terminators the sequencing reaction was passed through a purification column (Edge Gel Filtration Cartridge, ver. 11 from Edge Biosystems, or genCLEAN columns from Genpack) according to the manufacturer's instructions.

The amplified and labelled products were analysed on ABI PRISM 377 DNA sequencer (Perkin-Elmer Corporation), and on ABI PRISM 3100 DNA sequencer by staff from ICMB and ICAPB at Edinburgh University.

2.4.11 Polymerase Chain Reaction (PCR)

2.4.11.1 Standard PCR

The standard PCR was made using the Qiagen PCR kit, and the following mixture of PCR reagents was made: DNA template (60-500 ng) or 2 μl of cDNA template (reverse-transcribed mRNA); 1X Q solution; 1X Taq buffer; 0.2mM dNTP (dATP, dCTP, dGTP, dTTP); 1mM forward primer; 1mM reverse primer; 2.5U Taq polymerase, 0.4U pfu turbo polymerase (Stratagene) and sterile ddH_2O to final vol. of 50 μl.

The PCR cycle used was: 94°C for 2 min (1 cycle); 94°C for 40 seconds, 50-62°C (depends on the Tm) for 40 seconds, 72°C for 2 min per every kb pair expected in the PCR product (35 cycles); 72°C for 10 min (1 cycle). When the reaction was completed, 5-10 μl of the reaction mixture was analysed by gel electrophoresis. Table 2.4.12 shows the sequence of all the primers that have been used.

2.4.11.2 Proof-reading PCR

A proof-reading PCR was made when the amplified DNA, as a part of a DNA construct, would be translated into a protein. Since the translated template has to be accurate, the DNA amplification should be made with a minimal number of mistakes. For that reason the reaction mixture was made with pfu turbo polymerase kit (Stratagene), as follows:

100 ng DNA template (Myosin VI cDNA); 1X pfu buffer; 0.2mM dNTP; 1mM foreword primer; 1mM reverse primer; 2.5 U pfu turbo polymerase (Stratagene) and sterile ddH_2O to final vol. of 50 µl.

The PCR cycle used was: 94°C for 2 min (1 cycle); 94°C for 30 seconds, 45-50o (depends on the Tm) for 30 seconds, 72°C for 2 min and 40 sec per every kb pair expected in the PCR product (35 cycles); 72°C for 10 min (1 cycle).

2.4.11.3 Long template PCR

When PCR was undertaken for large fragments of DNA (7-15kb), the Expand Long Template PCR kit of Roche was used according to the manufacturer's instructions.

Two reaction mixtures were composed separately and combined prior to the reaction initiation: mixture 1: 500ng genomic DNA; 0.5mM dNTP; 0.3mM foreword primer; 0.3mM reverse primer; mixture 2: 1X buffer 3; 3U enzyme mix.

The PCR cycle used was: 94°C for 2 min (1 cycle); 94°C for 10 seconds, 51-59°C (depends on the Tm) for 40 seconds, 68°C for 2 min per every kb pair expected in the PCR product (10 cycles); 94°C for 10 seconds, 51-59°C for 40 seconds, 2 min per every kb pair expected in the PCR product with increment of 20 seconds per cycle (20 cycles);68°C for 10 min (1 cycle).

2.4.11.4 Single colony PCR

A single PCR was made to select bacteria transformed with plasmids containing the desired insert. In the single-colony PCR, the plasmid within the bacteria served as the DNA template. By using a sterile toothpick, a single colony was smeared at the bottom of a PCR tube (the remains of the bacteria in the toothpick was used to inoculate in a selective plate and in 5 ml selective LB medium, in order to preserve the bacteria for later use), the rest of the ingredients were added to the tube and the

reaction was carried out in the standard way as in section 2.4.11.1.

Table 2.4.11: primers used for general purposes

Primer	Sequence (5'>3' direction)	Length (nucl.)	Annealing temp. °C
529R	GTC CCG ACA AGT GGA TCA G	19	60
5k3*C865*	CGG GCT GAA AAG GGA AAA G	19	46-50
C865 for	GCG GAT CCA AAT CTT CTT GCT TTG CTG	27	51-55
C865 Rev	TTT GAA CAG GAA ACT GAA ACG	21	51-55
EXC2For	GTG CTT GTT GTT TTT CGG	18	50-52
EXC2Rev	ACA TGG AAT AGG GTG CAT GG	20	52-55
GFPR	GGT CAG CTT GCC GTA GGT	18	50
HEC2	TAT TTA CCG GTC CCT TGC CAA TAC CCT GGT AG	32	45
HKC865F	TGT TGC TAC CCA TTG CTT TTC AAT C	25	46-50
mmw14 delfor	TGC AGG TGT TGC AGA AGA GTG	21	55
mmw14 delrev	TTA TCC CCT TAC CCC TAT TCC	21	55
MYC2	ATT TAC CGG TCC TTG TTT CTG CAT TGC TGC	30	40-50
MYN	ATT TCC GAA TTC TTC GAC TCG ACT CAT CCA ACG	33	45-50
P1	GAG TTC GAC TCG ACT CAT CCA AC	23	52
P1027	TAG TGC GAT ATG TAA CCA CCG ACC	24	52-55
P517-1	ATC ACG ATG ACA ACT GCG AAC	21	55
PR491	AAG CCC AAG GGT ATC GAC AAC	21	62
PR492	ATT GAA CTC GGC ACT GGC ACA	21	62
pUASTF	AAG CAA ATA AAC AAG CGC AG	20	50
TAN	CAT TTC CGA ATT CGG CAA GAT CAA CAA GAT CCG G	34	40
TRIF	AAT CAC AGC TTC AGC CAC AC	20	60

2.4.12 Reverse transcription and PCR (RT-PCR)

Reverse transcription was done using Superscript™ II kit (GIBCO BRL). The following ingredients were added: 500-2000 ng of mRNA (the whole 12 µl of mRNA purified as described in section 2.4.4), 1µM oligo$(dT)_{18}$ primer, 0.5mM dNTP (dATP, dCTP, dTTP, dGTP). After a gentle mix the sample was heated at

65°C for 5 min and immediately cooled on ice for 2 min. The following ingredients were added to the tube: 1X RT buffer, 10mM DTT, 40U RNase OUT Recombinant Ribonuclease Inhibitor (Roche Molecular Biochemicals). The ingredients were gently mixed, and pre-incubated at 42°C for 2 min. Then 200U of SUPERSCRIPT II were added by pipetting up and down and the mixture was incubated for 50 min at 42°C, followed by inactivation at 70°C for 15 min.

2 µl of the cDNA were used for a PCR reaction, in standard conditions, as described in section 2.4.11.1.

2.4.13 Inverse PCR

Genomic DNA was prepared from flies containing p-element insertion(s) as described in section 2.4.2. 10mg of genomic DNA were restricted with Sau IIIA (15U) during 6 hr at 37°C. The reaction was stopped by heating the sample at 65°C for 20 min. The digested DNA was ligated in a 200 µl reaction containing 800U of T4 DNA ligase (New England Biolabs), O/N at 18°C. The DNA was recovered by EtOH precipitation and resuspension in 150 µl Tris buffer, 10mM, pH 8.0. 5µl of the relegated genomic DNA was used as a template for subsequent PCR reaction with primers specific for the p element (Table 2.4.13). The PCR reaction was made in standard conditions as described in section 2.4.11.1.

Table 2.4.13: Primers used for inverse PCR

Primer	Sequence (5'>3' direction)	Length (nucl.)	Annealing temp. °C
PGAWB 5b (5' PZ)	GAA AGG TTG TGT GCG GAC GA	20	55
Pry1 (3' PZ)	CCT TAG CAT GTC CGT GGG GTT TGA AT	26	58-62
Pry4 (3' PZ)	CAA TCA TAT CGC TGT CTC ACT CA	23	58-62
SP1 (5'PZ)	ACA CAA CCT TTC CTC TCA ACA A	22	55

2.5 Protein Techniques

2.5.1 Preparation of embryos for antibody staining

2.5.1.1 Embryo fixation

Embryos were collected in a plastic sieve dipped with 1X embryo wash solution, within a small Petri dish. The buffer was removed and the embryos were dechorionated in the Petri dish with 50% bleaching solution. The dechorionation process was observed under a dissecting microscope, the dechorionation was completed when the dorsal appendages were completely dissolved. The bleaching was stopped after 3 min or when 80% of the embryos were dechorionated (the shortest period); by removing the sieve from the Petri dish, rinsing it with ddH_2O and 1X embryo wash solution. The sieve was fitted on the neck of a 10 ml scintillation vial containing 1X embryo wash solution. A screw cup closed the vial and the embryos were transferred into the solution by tilting the vial. The sinking embryos were collected into a 2 ml scintillation vial with a cut pipette tip. The remains of embryo solution were removed. 1 ml of Embryos formaldehyde mix (made with formaldehyde of Fluka, 47608) and 1 ml of heptane were added and the embryos were rotated at RT for 20 min.

2.5.1.2 Methanol devitellination

In most of the antibody stains the embryos were devitalinated with methanol. After fixing the embryos, the embryo formaldehyde mix was removed (lower phase), 1 ml of 100% methanol was added, and the embryos were vigorously shaken for 15 sec. The sinking embryos were collected into an eppendorf tube with a cut pipette tip. The embryos were washed twice with fresh methanol, followed by two washed in 100% ethanol. When necessary, the embryos were stored in PBTA for 2-3 days, at 4°C, after washing in PBT for 15 min.

2.5.1.3 Manual devitellination

Manual devitellination was used when a stain of actin filaments was made with phalloidin. The fixed embryos were collected on a filter paper. After drying the remains of heptane and formaldehyde from the filter paper, the embryos were gently attach to a double sticky tape (Scotch brand, High performance coated tape 3M 9573) attached in one side to a small Petri dish, using a paintbrush. Sticking of the embryos was observed in a dissecting microscope. The embryos were immediately covered with PBTA solution. The devitellination was made with a 23g needle fitted to a 2 ml syringe. The removal of the embryos from the vitelline membrane was made by piercing the membrane in one end of the embryo and pushing the embryo from the other end, through the hole. The devitalinated embryos were collected with a cut pipette tip. The embryos could be kept in PBTA solution for few days at 4°C.

2.5.2 Preparation of ovaries and other tissues for antibody staining

Ovaries, testes and other tissues were dissected in Ringer's saline (prepared by the Institute media staff) warmed to RT. The tissue was fixed for 20 min in 4% p-formaldehyde and washed for 15 min in PBT solution. Occasionally ovarioles were separated with tungsten needles at this stage. When the tissues had to be stored, they were left in PBTA solution for up to 3 days.

2.5.3 Whole-mount in situ antibody staining

The tissue was washed 3 times for 15 min in PBT, in 0.2 ml eppendorf tubes. The blocking of the tissue was done in 1% NGS (Normal Goat Serum) for 1 hr, followed by incubation with a primary antibody for O/N at 4°C, at the concentrations described in table 2.5.3.1. The diluted antibodies were usually kept at 4°C and re-used for 2 more times. When two primary antibodies were used, the sample was washed in NGS for 10 min and incubated with the second primary antibody for 3 hours at RT. The sample was washed 3 times for 15 min in PBT, and blocked again

in NGS for 30 min. The incubation with secondary antibody was done for 1.5-2 hr at RT, covered with aluminium foil, with the dilutions described in table 2.5.3.2. When two secondary antibodies were used, the sample was washed in NGS for 10 min and incubated with the second antibody for 1.5-2 hr at RT. The tissue was washed 2 times for 30 min in PBT, followed with a wash in 1XPBS for 10 min.

Table 2.5.3.1: List of primary antibodies used.

Antigen	**Host animal**	**Working concentration**	**Source**
Drosophila α-adaptin	Rabbit	1:200	Jackson A.P.
Drosophila Ankyrin	Rabbit	1:100	Dubreuil R.
Drosophila Armadillo	Mouse	1:6	Wisechaus, E. No. N2 7A1*
Drosophila Bazooka	Rabbit	1:500	Wodarz, A
Drosophila E-Cadherin	Rat	1:20	Uemura, T.
Mosquito Clathrin	Rabbit	1:500	Kokoza, V, Raikhel, A.
Drosophila CLIP-190	Rabbit	1:50	Miller, K.
Drosophila Crumbs	Mouse	1:1	Knust, E. No. cq4*
Drosophila Dlg	Rabbit	1:250	Bryant P. J.
Rat Dynamin	Mouse	1:500	BD transduction laboratories D25520
Drosophila PS2α-integrin	Mouse	1:500	Brower D. L. No. CF2 C7
Drosophila PSβ-integrin	Mouse	1:1	Brower D. L.
Drosophila Myosin VI	Mouse	1:3 in embryos 1:10 in ovaries	Miller, K No: 3C7
Drosophila Nonmuscle myosin II	Rabbit	1:50	Kiehart and Fegali (1986) No: 656
Drosophila α-spectrin	Mouse	1:6	Branton, D., Dubreuil, R. No: 3A9 (323 or M102)*
Porcine Myosin VI	Rabbit	10μg/ ml	Hasson, T.

* Purchased from Developmental Studies Hybridoma Bank

Table 2.5.3.2: List of secondary antibodies used.

Antigen	Host animal	Labelling	Working concentration	Source
Mouse IgG	Goat	AlexaFluor®568	1:500	Molecular Probes, A-11004
Mouse IgG	Goat	FITC	1:100	Sigma F-4018
Rat IgG	Goat	FITC	1:50	Sigma F-6258
Rabbit IgG	Goat	AlexaFluor®568	1:500	Molecular Probes, A-11011
Rabbit IgG	Goat	FITC	1:100	Sigma F-9887

2.5.3.1 Actin filaments staining

The staining of actin filaments was made with Alexa Fluor ® 568 conjugated phalloidin (Molecular probes, A-12380). After the staining with the secondary antibody, the tissue was incubated for 1 hour with phalloidin (diluted 1:50 in PBS or PBT), and washed in PBT and PBS as described previously.

2.5.3.2 Sample mounting

In embryos, the 1XPBS solution was removed from the tube after the staining and 40µl of VECTASHIELD® Mounting Medium (Vector Laboratories) was added. 20-25µl of the and medium containing the embryos was mounted on a slide, covered with 20 nmX20 nm coverslip and the coverslip was sealed with nail varnish. The slides were kept at 4°C in a dark box for up to 6 months. Imaginal discs were separated in a dissecting dish containing 1XPBS and mounted on a slide containing mounting solution.

In ovaries the 1XPBS solution was removed from the tube after the staining and 150µl of FISH media was added. The samples were left for 15 min-O/N at 4°C. The tissue was mounted on a slide with 20-25µl of mounting solution. The ovarioles were separated (up to two pairs of ovaries were mounted in a slide), and the slide was covered and sealed. Testes were mounted in a similar way.

2.5.3.3 Sample observation

The stained samples were observed and photographed on a confocal microscope (Leika) or on fluorescent microscope (Zeiss AxioskopII) fitted with a digital camera. The pictures were processed with Adobe Photoshop program.

2.5.4 Preparation of slides from tissues expressing GFP

Tissues expressing GFP were fixed as described in sections 2.5.1-2.5.2. After the fixation the samples were washed with 1XPBS two times for 10 min and mounted as described in section 2.5.3.2.

Chapter 3:

Identification of novel *Drosophila* myosins

This work was undertaken in collaboration with George Tzolovsky, Stephen Pathirana, Timothy Wood, and published in Molecular Biology and Evolution, in 2002 (Tzolovsky et al., 2002).

3.1 Introduction

As described in the Introduction, eight different myosins have been found in *Drosophila*, classified into six different classes. The publication of the complete *Drosophila melanogaster* genome allowed us to screen for new potential myosins in *Drosophila*. Having the information about the new myosins enabled us to investigate if they function during oogenesis.

The search for new myosins was performed using the following steps:

1. Search for new potential myosins in the *Drosophila* genome.
2. Structural analysis of the new myosins.
3. Classification of the new myosins by phylogenetic analysis.

Screening for new myosins in *Drosophila* was undertaken as follows (Cope et al., 1996): proteins with high homology to the head domain of chicken skeletal Myosin II were searched for by using the BLAST program. Identity of 30-40% is needed for classification of a new myosin into a given myosin class, and identity of 25-30% is needed for classifying a new protein as a myosin. Five potential new myosins were identified: Myosin 95E (on the third chromosome), Myosin heavy chain like-PDZ (Mhcl-PDZ, location: 89B7, third chromosome), Myosin 28B (on the second chromosome), Myosin 10A (on the X chromosome) and Myosin 29D (on the second chromosome) (Tzolovsky et al., 2002).

The borders and the conserved regions of the head domain in the four myosins found was determined by alignment of the four myosins with chicken skeletal myosin motor domain, as in early classification schemes (Cheney et al., 1993; Mooseker and Cheney, 1995). The motor domains of the new myosins have a similar pattern of conserved regions to the chicken skeletal myosin motor domain (Mooseker and Cheney, 1995).

After finding the new myosins (George Tzolovsky), I participated in the analysis of their molecular structure. The RT-PCR analysis described in thesis chapter was established by George Tzolovsky (Tzolovsky et al., 2002).

3.2 The programs used for the structural analysis of the new myosins:

The search for proteins with high homology to the head and tail domain of the newly found myosins was performed by using the BLAST program (http://www.ncbi.nlm.nih.gov/blast/).

Alignment of similar regions in the myosins and other proteins was performed with CLUSTALW program in the GCG software package, version 10.1, for x-windows, or with the program installed on the website: http://www.ebi.ac.uk/clustalw.

Pairwise comparison was also performed by using the program Bestfit in the GCG software package.

Coiled - coils were predicted by using the Paircoil program developed by Berger et al. (Berger et al., 1995). The domains in the neck and tail regions were also identified by with Pfam program from the Sanger centre
(http://www.sanger.ac.uk/Software/Pfam/),
(http://www.isrec.isb-sib.ch/software/PFSCAN_form.html),
and SMART program (http://smart.embl-heidelberg.de/ (Schultz et al., 1998).

3.3 The structural analysis of the novel myosins

The results of the protein sequence analysis are summarized in Figures 3.3.1-3.3.2. The analysis made for each myosin is described in a separate section.

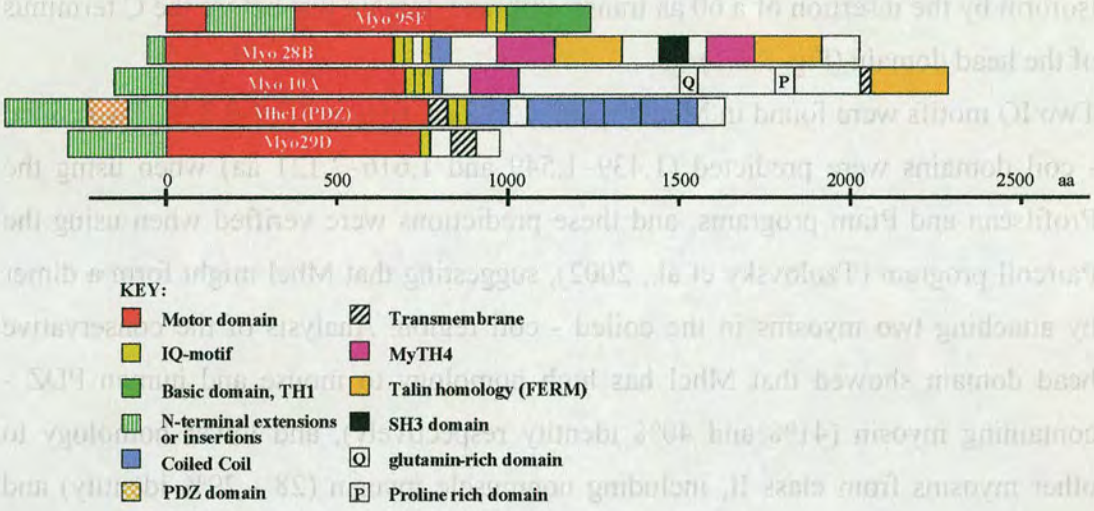

Figure 3.3.1: The protein structure of the newly found myosins: Myosin 95E, Myosin 28B, Myosin 10A, Mhcl-PDZ (89B), and Myosin 29D.

```
RISELAVLIQTMFRMYHARKRFQ          Myo95E IQ1
RMRHSQMIISSAWRTWRECRFGI          Myo95E IQ2A
RMRHSQMIISSAWRTWRAREEYR          Myo95E IQ2B

LMLKSIVTIQRGIRRVLFRRYMK          Myo28B IQ1
RYREAIITVQRYWRGRLQRRKYQ          Myo28B IQ2
VMRQGFHRLGACIAAQQLTTKFT          Myo28B IQ3
MVRCRTIKLQALSRGYLVRKDFQ          Myo28B IQ4

RLRRAAVSVQRHVRGMLVRRQLA          Myo10A IQ1
RRQAAATRLQARWRGQRAQQRYE          Myo10A IQ2
RLRKGALTAQRLWRGRQARRRVQ          Myo10A IQ3

LLSDRIIQLQAFCRGYLARKKMSQRR       Myo89B IQ1
VQELAVRCIQRNVKAFLAVRDWPWWR       Myo89B IQ2

IRHKSATLMQATWRGWWWRKKMGNGG       Myo29D IQ1
AKRSKIPGLQQAPLPNNKTTPNSAAQ       Myo29D IQ2
```

Figure 3.3.2: The IQ motifs identified in Myosin 95E, Myosin 28B, Myosin10A, Myosin 89B, and Myosin 29D. The conserved amino acids are in colour. Myosin 95E was found to have two different variants in its second IQ motif, as a result of alternative splicing (Tzolovsky et al., 2002).

3.3.1 Mhcl

Initial analysis revealed that Mhcl has two predicted isoforms (alt1 and alt2) composed of 1646 and 1706 amino acids (aa), respectively. The head domains of the two isoforms start 68 aa from the N termini. The alt2 isoform differs from the alt1 isoform by the insertion of a 60 aa transmembrane domain just before the C terminus of the head domain (Fig. 3.3.1).

Two IQ motifs were found in Mhcl (1,379–1,428 aa, figures 3.3.1-3.3.2). Two coiled - coil domains were predicted (1,439–1,549 and 1,616–2,121 aa) when using the Profilscan and Pfam programs, and these predictions were verified when using the Paircoil program (Tzolovsky et al., 2002), suggesting that Mhcl might form a dimer by attaching two myosins in the coiled - coil region. Analysis of the conservative head domain showed that Mhcl has high homology to mouse and human PDZ - containing myosin (41% and 40% identity respectively), and lower homology to other myosins from class II, including nonmuscle myosin (28 - 29% identity) and skeletal muscle (25% identity). Also the tail domain showed higher homology (32% identity) with myosins containing PDZ domains compared to other class II myosins (25% identity).

The high homology of the Mhcl motor domain with other myosins containing a PDZ domain could suggest that Mhcl also contains a PDZ domain. A sequence search (George Tzolovsky) revealed that a PDZ sequence exists 4.8 KB upstream to the predicted start of *Mhcl* mRNA, and RT-PCR analysis confirmed that this PDZ domain is indeed part of the *Mhcl* gene (Tzolovsky et al., 2002).

The initial analysis of Mhcl structure was started using the partial sequence of the gene as published by Biru (Biru, 1999). When the full sequence of this gene was published by Celera (Adams et al., 2000.), additional analysis of the sequence, in combination RT-PCR analysis, sequence analysis of expressed sequence tags (ESTs) of the *Mhcl* gene, and Promoter-predicting program (http://www.fruitfly.org/ seqptools /promoter.html) was undertaken (George Tzolovsky). The gene was found to be composed of 19 exons, creating seven different transcripts by the use of four predicted promoters (Tzolovsky et al., 2002).

3.3.2 Myosin 28B

The amino acid sequence of the head domain has 61% identity with the head domain of *crinkled - Drosophila* Myosin VIIa. It also showed 58% identity with the zebrafish Myosin VIIa, suggesting that Myo28B belongs to class VII.

Analysis revealed that Myo28B has four IQ motifs (753–845 aa, Figures 3.3.1-3.3.2), the third being poorly conserved. A subsequent coiled - coil domain (849–908 aa) was predicted with the Profilscan, Pfam and Percoil programs.

Two myosin tail homology 4 (MyTh4) domains (1,070–1,246 and 1,681–1,826 aa), were identified in Myo28B. Sequence alignment of Myo28B with other myosins from class VII and XV showed that the first MyTh4 domain has an insert of 61 amino acids (Fig. 3.3.2.1). An insert of about 88 aa, in the same place, was also found in human class VII myosin (Chen et al., 1996), in *Drosophila* Myosin VIIa, and in the hypothetical protein T10H10.1 (*Caenorhabditis elegans*). The two domains have more than 40% identity to MyTh4 domains in type VII and type XV myosins. The function of MyTH4 is unknown, but it appears in several motor proteins (including microtubule motor proteins), suggesting that it might share similar mechanisms of interaction with the cargo (Oliver et al., 1999).

Two FERM domains (named for band 4.1, Ezrin, Radixin, Moesin) were identified (1,246–1,454 and 1,826–2,039 aa). These domains have the highest homology with talin and filopodin in the band 4.1 superfamily, and a high homology with the talin – like domains in class VII myosins. Figure 3.3.2.2 shows the percentage of identity between the FERM domain in myosins VII and XV with the FERM domain in *C. elegans* Talin. The FERM1 motifs from Myosin VII show 12%–21% similarity to proteins from the FERM family and approximately 16% similarity to the band 4.1 protein. FERM2 domains in Myosin VII show a higher similarity of 17%–18% to band 4.1 protein and 18%–20% to proteins from the FERM family. When comparing the FERM domains in Myo28B and *Drosophila* Myosin VIIa, the first FERM domains share 42% identity (and 67% similarity) and the second FERM domain shares 20% identity (50% similarity). The tandem arrangement of MyTH4 and FERM domains (Fig. 3.3.1) is also conserved in myosins from classes VII and X, although it does not appear uniformly in all the myosins. Proteins from the band 4.1

family play a role in the stabilization of cells membrane, and the FERM domain was shown to mediate membrane-cytoskeleton interactions, through the binding to integral membrane proteins (Sun et al., 2002). In addition, the FERM domain was found to form interaction with other proteins from the ERM (Ezrin, Radixin, Moesin) family, by the binding with the C-terminal actin-binding domain that appears in ERM proteins (Sun et al., 2002).

Unlike other myosins from class VII, none of the programs used have identified SH3 (Src homology 3) domains in Myo28B. However, sequence alignment of SH3 domains from Myosin VII and Myosin XV with region 1551 - 1628 in Myo28B revealed that this region has high homology with SH3 domains, especially in the conserved regions (Fig. 3.3.2.3). SH3 was found in many proteins associating with cytoskeleton and in membrane proteins that are involved in signal transduction (Parsons, 2003). This domain seems to play a role in protein-protein interactions through the binding to proline-rich domains (Macias et al., 2002), although SH3 domains were also found to interact with non-proline peptides (Agrawal and Kishan, 2002). In yeast Myosin I (Myo5p), the SH3 domain was found to be required for interaction of the tail domain with actin filaments and for triggering actin polymerisation (Geli et al., 2000). In two types of yeast Myosin I, Myo3p and Myo5p, the SH3 domain interacts with Bee1p and Vrp1p, two adapter proteins that link actin assembly and signalling molecules.

Figure 3.3.2.1: ClustalW alignment of the MyTh4 domains in unconventional myosins. Identical amino acids are dark shaded and similar residues are light shaded. The sequences included in the alignment are: **CeHp**, hypothetical protein T10H10.1 *Caenorhabditis elegans* (T25888); **HsM7a** , human Myosin VII (Q13402); **DmCk**, Myosin VIIa (*ck*) – *Drosophila melanogaster* (AAF44915); **HsM15**, human Myosin XV (Q9UKN7), and **Myo28B** (AAF52536). The first MyTh4 domain in HsM7a, DmCk, CeHp, and Myo28B contain inserts of 61 – 88 AA (regions 1057 – 1144; 1048 – 1135; 971 – 1055; 1107 – 1168, respectively) that were subtracted from the sequences.

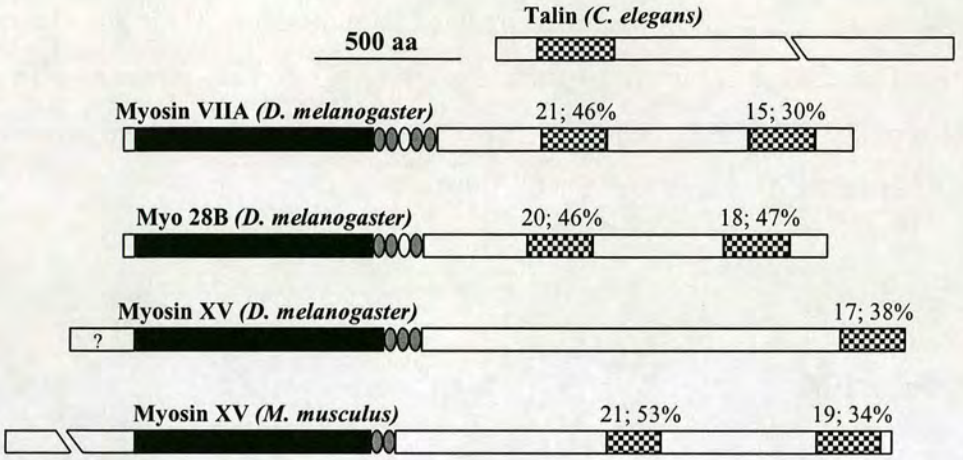

Fig. 3.3.2.2: A diagram representing the percent of identity (left value) and similarity (right value) between the FERM domains in *Drosophila* myosins VII and XV and the talin domain from *Caenorhabditis elegans* (CE, AAA74747). The FERM domains were aligned separately with the talin domain of *C. elegans*. Multiple alignment was not made since the similarity between FERM1 and FERM2 and the talin domain (from the Talin protein) was very low and resulted in unordered alignment. The comparison was preformed by using CLUSTALW (http://www2.ebi.ac.uk/clustalw/). The FERM domains of mouse Myosin XV are also presented in the diagram. The motor domain of the myosins is drawn in black, the IQ motifs in grey, and the FERM domains in patterned boxes. Accession numbers are: *C. elegans* (Talin): AAA74747; *D. melanogaster* (Myosin VIIA):CAC05418, (Myo 28B): AAF52536, (Myosin 10A-XV): AAF47980; *M. musculus* (Myosin XV): AAF05904.

```
DrM7a     1562 LRKRSKFVVALQDNPSPAADDSTFLSFLKGDLIVLDQDT-GEQVMTSGWAHG--TND--R
MmM7a     1601 LRKRSKYVVALQDNPNPAGEESGFLSFAKGDLIILDHDT-GEQVMNSGWANG--INE--R
DmCk      1556 LKKRSKYVIALQDYRAPS-DGTSFLSFFKGDLIILEDESCGESVLNNGWCLG--RCD--R
myo28B    1551 LRQRSSYGVALD--FVVEGDLEDCLVLNFGDLIEFEAGVTGAQLM-AGNAQD--CYRGCV
HsM15     2865 LKKDSDYVVAVR---NFLPEDPALLAFHKGDIIHLQPLEPPRVGYSAGCVVRRKVVYLEE
MmM15     2846 LKKDSDYVVAVR---NFLSEDPELLSFHKGDIIHLQSLEPTRVGYSAGCVVRKKLVYLEE

DrM7a     1617 TKQRG-DFPADCVYVLPT----VVRPPHD
MmM7a     1656 TKQRG-DFPTDCVYVVNSGWANGINERIK
DmCk      1611 SQERG-DFPAETVYVLPT----LSKPPQD
myo28B    1606 NGQWG-QFLAGNVRVLAT----LTK-PSE
HsM15     2922 LRRRGPDFGWRFGTIHGR----VGRFPSE
MmM15     2903 LRRRGPDFGWRFGAVHGR----VGRFPSE
```

Fig. 3.3.2.2. ClustalW alignment of region 1551 – 1628 in Myo28 and SH3 domains in unconventional myosins from class VII and XV. **DrM7a**, Myosin VIIa (*Danio rerio*, CAC05418); **MmM7a,** mouse Myosin VIIa (P97479); DmCk, Myosin VIIa *Drosophila melanogaster* (AAF44915.1); **HsM15**, human Myosin XV (Q9UKN7); **MmM15**- mouse Myosin XV (Q9QZZ4).

Also in *Dictyostelium,* the SH3 domain is involved in actin dynamics in the class I myosins, MyoB and MyoC, however in this case the SH3 domain interacts with a protein called p116, which in turn binds to Arp 2/3 and capping protein, two proteins that play a role in actin dynamics (Jung et al., 2001).

3.3.3 Myosin 10A

A Blast search with the head and tail domains of Myo10A showed identity of 47% and 42%, respectively, to mouse and human Myosin XV. The motor domain of Myosin 10A also shares 42% identity and 58% similarity with human and mouse Myosin VII.

Myosin 10A (Myo10A) has a specific N terminal domain of 149 aa, which does not share similarity with other N terminal domains of other myosins from class XV.

Three IQ domains were identified in the neck domain (841–910 aa, figure 3.3.2), followed by a short coiled - coil domain (919–946 aa, Fig. 3.3.1). Analysis of the tail domain revealed one MyTh4 domain (1014-1173aa), a glutamine - rich domain (1611 – 1647 aa), a proline - rich domain (1937 – 1991 aa), a short transmembrane motif (2,194-2,214 aa) and FERM - like domain at the C terminal (2,220–2,424 aa). The FERM - like domain was not identified using Pfam and SMART programs, probably because it is shorter by 75 aa than other FERM domains, however it has high homology with FERM domains in mouse and human Myosin XV (in the mouse it shares 40% identity with the first FERM domain, and 13% identity with the second FERM domain) and it shares 17% identity with the FERM domain in Talin (Fig. 3.3.2.2).

RT-PCR analysis revealed that Myo10A has at least two transcript variants, the longer is composed of all the five exons and the shorter lacks the second exon (Tzolovsky et al., 2002).

3.3.4 Myosin 29D

Analysis of the conserved head domain revealed that Myosin 29D (Myo 29D) is not similar to any of the known classes of myosin. It showed 29% identity (45% similarity) to myosin VII, X, and V from different species. This homology is not enough to classify Myo 29D as a class - specific myosin, suggesting that it forms a class of its own.

The head domain of Myo10A has an N terminal extension of 338 aa. Two IQ motifs were found in the neck domain (1,089–1,136 aa,), the second is poorly conserved followed by a short transmembrane motif (1,144–1,279 aa, Fig. 3.3.1- 3.3.2).

RT-PCR analysis revealed two transcripts, the first includes all the five exons composing the gene, and the second lacks exon 5 and produces a truncated form of the protein, lacking most of the motor domain (Tzolovsky et al., 2002). The two transcripts are present during all the stages of development; however the first transcript is expressed at a higher level (Tzolovsky et al., 2002).

3.3.5 Myosin 95E

This gene was not found in the initial searches. In the search for novel myosins, one of the proteins that came out with a high homology to myosins appeared to only be 59 aa long. The detailed search for the proper size of the protein was made by George Tzolovsky (Tzolovsky et al., 2002). The whole gene sequence was found in the AE003746 genome scaffolding by considering the initial gene sequence, the published sequence of the ESTs of the gene found and the homology of the translated genomic DNA with other proteins. The splice sites were predicted using the programs: The Neural Network at http://www.fruitfly.org/seqptools/splice.html and GENSCAN Server at http://genes.mit.edu/GENSCAN.html. Finally, the precise sequence of the cDNA was identified by TRPCR. The gene is composed of 16 exons. The head domain of the protein reveals 33% sequence identity and 53% similarity with the vertebrate border class I myosins, and structural analysis showed that this myosin has a similar structure as class I myosins (Tzolovsky et al., 2002). Therefore it was termed Myosin IC (myosins IA and IB were already identified). Myosin 95F contains 2 IQ motifs (928–974 aa), the second being poorly conserved (fig. 3.3.2),

and a basic tail domain (974–1,278 aa in the first isoform, 974–1,258 aa in the second isoform), as described in figure 3.3.1. The basic tail domain is found to bind to the acidic phospholipids in the cell membrane and to actin filaments (Lee et al., 1999; Tang et al., 2002).

TR-PCR analysis reveals that the gene produces at least three different transcripts, one which is composed of all the sixteen exons of the gene, the second lacks exon 12 and the third exon has an insert of several nucleotides in the fourth exon, causing shift of the open reading frame and an insert of a stop codon in exon 5 (Tzolovsky et al., 2002). The third transcript could hypothetically encode two types of truncated protein: the first composed of 464 aa encoding only a part of the head domain; and the second protein, composed of 864 aa, encoding a large part of the head domain, two IQ motifs, and the tail domain (Tzolovsky et al., 2002).

3.4 Conclusions

Eight myosins were found to exist in *Drosophila melanogaster*, prior to the publication of the *Drosophila* genome. These myosins belonged to class I (2 myosins), II (2 myosins), III, V, VI and VII. Five novel myosins have been identified, four of them belong to classes I, VII, XV, XVIII and one creates a new class.

By the time that our article was prepared, a paper was published by Yamashita et al. (Yamashita et al., 2000) showing the identified novel myosins in *Drosophila* after a blast search, classifying myo28B in class VII, myo10A in class XV and Mhcl in class XVIII. Our work complements this publication, by describing the domain composition of all the novel myosins and by classifying Myo95E as Myosin I and Myo29D in a unique class (class XIX). In addition, a transcription analysis that was made for the myosins Myo95E, Myo10A, Mhcl, and Myo 29D (Tzolovsky et al., 2002). The analysis of the transcripts for these myosins confirmed the expression of these genes in *Drosophila* (along with the identification of ESTs for every gene), showed the various splicing forms in which each myosin is expressed and served as a useful tool for verifying the sequence of the genes.

The *Drosophila* myosins are classified in nine different classes, which share different structures of the tail domain and participate in a variety of cell functions, including membrane and mRNA transport, cell adhesion, and actin dynamics (the function of the known myosins is described in chapter 1). It would be interesting to examine the function of the new myosins in *Drosophila*, especially the function of myo29D which has a unique structure which could be needed for a new purpose. RTPCR analysis revealed that Myo95E is expressed during oogenesis; Myo10A is expressed from the larval stage onwards, while Mhcl and Myo 29D are expressed throughout the life cycle (Tzolovsky et al., 2002). In situ hybridisation to ovaries undertaken in our lab by the honour student, Holy Jones, revealed that Myo10A is expressed during stages 1-13 in the nurse cells and the follicle cells, and the transcripts from the nurse cells are transferred to the oocyte. Myo29 transcripts are present in the nurse cells in stages 1-3 and weakly expressed in the follicle cells from stage 6. Mhcl transcripts are expressed in the nurse cells from stage 3 and transported to the oocyte at stage 12. Myo95E is strongly expressed in the nurse cells from stage 8 and has a moderate expression in the follicle cells from stage 7. Now that the mRNA expression pattern is established, it would be interesting to test the protein expression pattern of these myosins. Generally, the function of these myosins during oogenesis could be verified by disrupting their expression using a targeted silencing technique or by creating mutants of the myosins observing the phenotype of clones of mutant cells, or by over-expression of the proteins.

Chapter 4:

The function of Myosin VI in *Drosophila*: functional analysis by expression of Myosin VI-GFP fusion proteins

4.1 Introduction:

Myosin VI participates in the organization and patterning of many epithelial tissues as they develop, and for building membrane constructs through membrane trafficking (Deng et al., 1999; Hicks et al., 1999; Kellerman and Miller, 1992; Lantz and Miller, 1998). The function of Myosin VI was studied by observing Myosin VI within the tissue, using Myosin VI antibody, and by comparing the morphology of cells and tissues in wild-type flies and in mutant flies or flies in which the expression of Myosin VI was disrupted. In all these experiments, the function of Myosin VI was studied as a whole molecule. The function of Myosin VI and its separate domains was studied in mammalian epithelial cells (normal rat kidney cells), during endocytosis (Buss et al., 2001). However, very little is known about the way Myosin VI molecule and its separate domains function during *Drosophila* development. Myosin VI is composed of three domains: the head which is the motor domain and moves along actin filaments, the neck which regulates the movement of Myosin VI, and the tail domain which serves as a cargo for other molecules. Myosin VI is involved in dynamic processes, such as the migration of follicle cells, where it might be needed for asymmetric localization of molecules within the cells. Information about the localization of the tail and the head domains, and the whole myosin during the migration of the follicle cells, and in other processes, will give us a better understanding of the way Myosin VI and its separate domains work in the cell.

To do this Myosin VI and its domains, tagged to Green Fluorescent Protein (GFP) were produced. The expression of the GFP-tagged proteins in flies allows us to observe the expressed proteins in real time in living tissues, as well as in fixed tissues.

4.1.1 Design of the fusion proteins

Three different tagged proteins were expressed: full length Myosin VI, the head + neck domain and the tail domain, each tagged in-frame with GFP, at its N terminus (Fig 4.1.1).

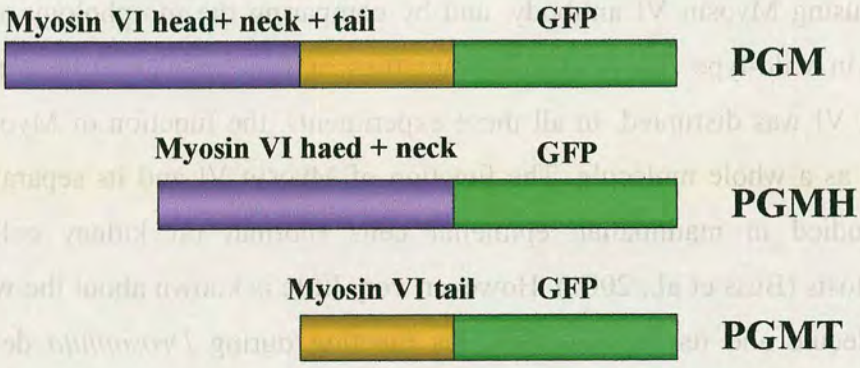

Figure 4.1.1: The three fusion proteins expressed in *Drosophila*: whole Myosin VI (PGM), the head and neck domains (PGMH) and the tail domain (PGMT), tagged to GFP. The head + neck domain is coloured in purple; the tail domain is coloured in yellow.

4.2 *Expression of the fusion proteins using the Gal4/ UAS system*

The expression of the fusion protein is achieved by using the Gal4/ UAS system (Brand and Perrimon, 1993). The DNA construct contains the cDNA corresponding to the *jaguar* gene (encoding Myosin VI) fused in - frame to *EGFP* DNA sequence (expressing GFP), cloned within the pUAST plasmid, which contains two P elements and an UAS (upstream activation sequence) target sequence (Fig. 4.2.1).

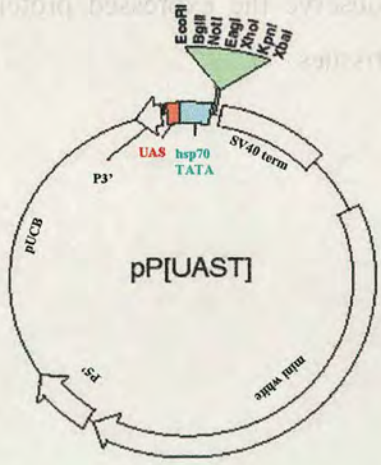

Figure 4.2.1: The structure of the pUAST plasmid: The plasmid contains the UAS (Upstream Activation Sequence) target sequence, adjacent to the hsp 70 promoter containing a TATA box; a multiple cloning site is followed by the SV40 termination domain, that includes a stop codon and a polyadenylation site; mini - white marker, two P - elements (5' and 3'), and pUCB region for Ampicillin resistance in bacteria.

The UAS target sequence and the genes are incorporated into the chromosomes by its two p-element ends catalysed by a transposase from another insertion (using the PΔ2-3 plasmid), which cannot transpose by itself. The transgenic flies are crossed with flies that express Gal4 in specific tissues (Fig. 4.2.2). The *Gal4* gene encodes a specific transcriptional activator (Gal4) which binds to the UAS target sequence. The binding of Gal4 to the UAS sequence triggers the expression of the *jaguar - EGFP* fusion gene, which is translated into a Myosin VI - GFP fusion protein

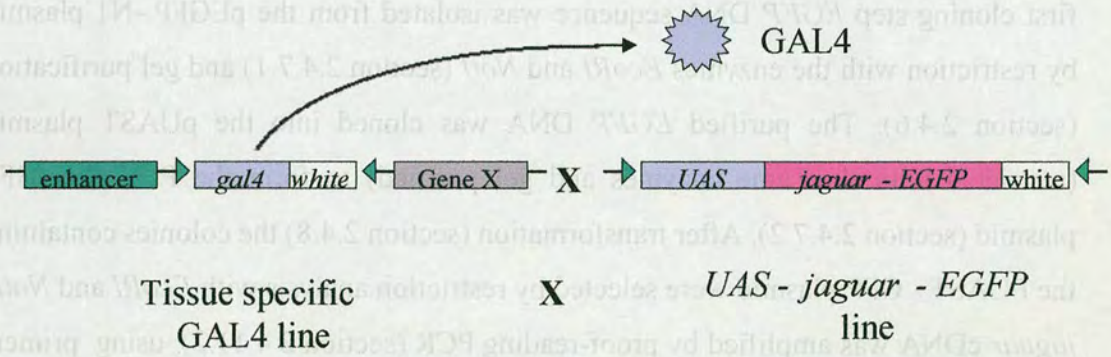

Figure 4.2.2: Activation of *jaguar - EGFP* expression by the Gal4/UAS system. The *P[Gal4]* element, which contains a reporter gene *Gal4* , a marker gene white and sequence from pBluescript plasmid, was inserted into a fly genome. The expression of the Gal4 gene is regulated by the enhancer of the gene, X, close to the P insertion. In a different fly line, the *UAS - jaguar - EGFP* construct is incorporated into the *Drosophila* genome. When the two lines are crossed, the expressed GAL4 transcriptional factor interacts with the UAS sequence and triggers the expression of *jaguar - EGFP* sequence.

4.3 Creation of the DNA constructs

Three different DNA constructs were created: **PGM** (PUAST-GFP-Myosin VI), containing the whole *jaguar* cDNA; **PGMH** (PUAST-GFP-Myosin VI Head), containing the *jaguar* cDNA encoding the head and neck domains of Myosin VI, and **PGMT** (PUAST-GFP-Myosin VI Tail), containing the *jaguar* cDNA encoding the tail domain of Myosin VI. In all the constructs, *jaguar* cDNA was fused in-frame with the *EGFP* gene, and cloned within the pUAST gene.

All the constructs were made by two cloning steps (described in Fig. 4.3.1). In the first cloning step *EGFP* DNA sequence was isolated from the pEGFP -N1 plasmid by restriction with the enzymes *EcoRI* and *NotI* (section 2.4.7.1) and gel purification (section 2.4.6). The purified *EGFP* DNA was cloned into the pUAST plasmid (restricted with the same enzymes and gel purified) to form the PUAST - GFP plasmid (section 2.4.7.2). After transformation (section 2.4.8) the colonies containing the PUAST - GFP plasmid were selected by restriction analysis with *EcoRI* and *NotI*. *jaguar* cDNA was amplified by proof-reading PCR (section 2.4.11.2), using primers that were designed to contain the restriction sites for the enzymes *EcoRI* in the 5' end and *AgeI* in the 3' end. In order to connect in-frame of *jaguar* and *EGFP* genes, the primers at the 3' end (HEC2, MYC2) contained two C nucleotides inserted between the *AgeI* restriction site and the 3' end of the *jaguar* gene, to encode the amino acid glycine. The coding region of the whole Myosin VI was amplified using the primers: MYN and MYC2; for the head domain the primers used were MYN and HEC2, and for the tail domain the primers used were TAN and MYC2. The amplified cDNA fragments and the pUAST - GFP plasmid were restricted with *EcoRI* and *AgeI* enzymes, gel purified, and cleaned (section 2.4.3). Then the plasmid and the cDNA fragments were ligated, cleaned again and transformed into competent cells. In parallel the DNA was analysed on gel to verify ligation.

Figure 4.3.1: The cloning steps used to build the pUAST - *jaguar* - *EGFP* DNA construct. **(A)** In the first stage pEGFPN1 and pUAST plasmids were restricted with *EcoRI* and *NotI* restriction enzymes. *EGFP* DNA was isolated and cloned into pUAST plasmid to form PUAST - GFP plasmid. **(B)** In the second stage *jaguar* cDNA was amplified by PCR, forming specific restriction sites (*EcoRI*, *AgeI*) at the two edges. The PCR product and the pUAST - GFP plasmids were restricted with *EcoRI* and *AgeI* restriction enzymes, and *jaguar* cDNA was cloned into the pUAST - GFP plasmid.

Figure 4.3.1

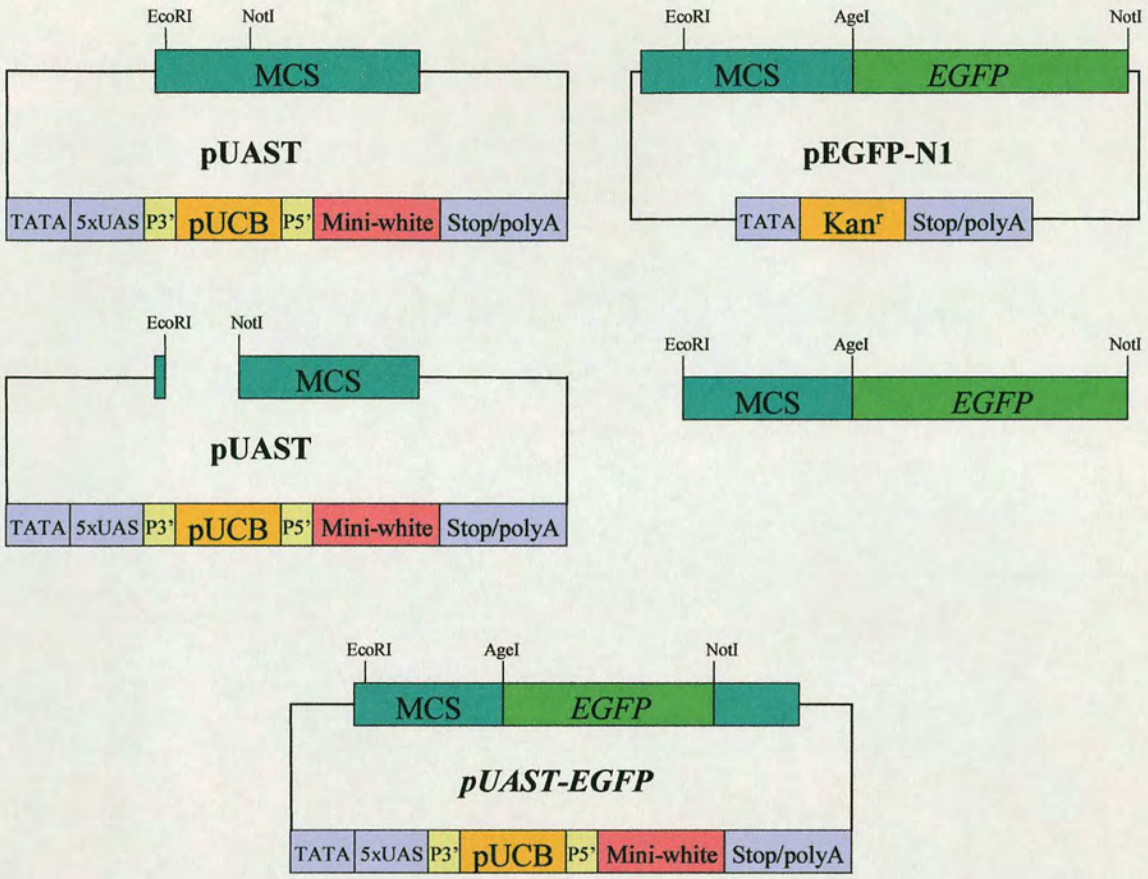
EcoRI
NotI
MCS
pUAST
TATA
5xUAS
P3'
pUCB
P5'
Mini-white
Stop/polyA
EcoRI
AgeI
NotI
MCS
EGFP
pEGFP-N1
TATA
Kan^r
Stop/polyA
EcoRI
NotI
MCS
pUAST
TATA
5xUAS
P3'
pUCB
P5'
Mini-white
Stop/polyA
EcoRI
AgeI
NotI
MCS
EGFP
EcoRI
AgeI
NotI
MCS
EGFP
pUAST-EGFP
TATA
5xUAS
P3'
pUCB
P5'
Mini-white
Stop/polyA

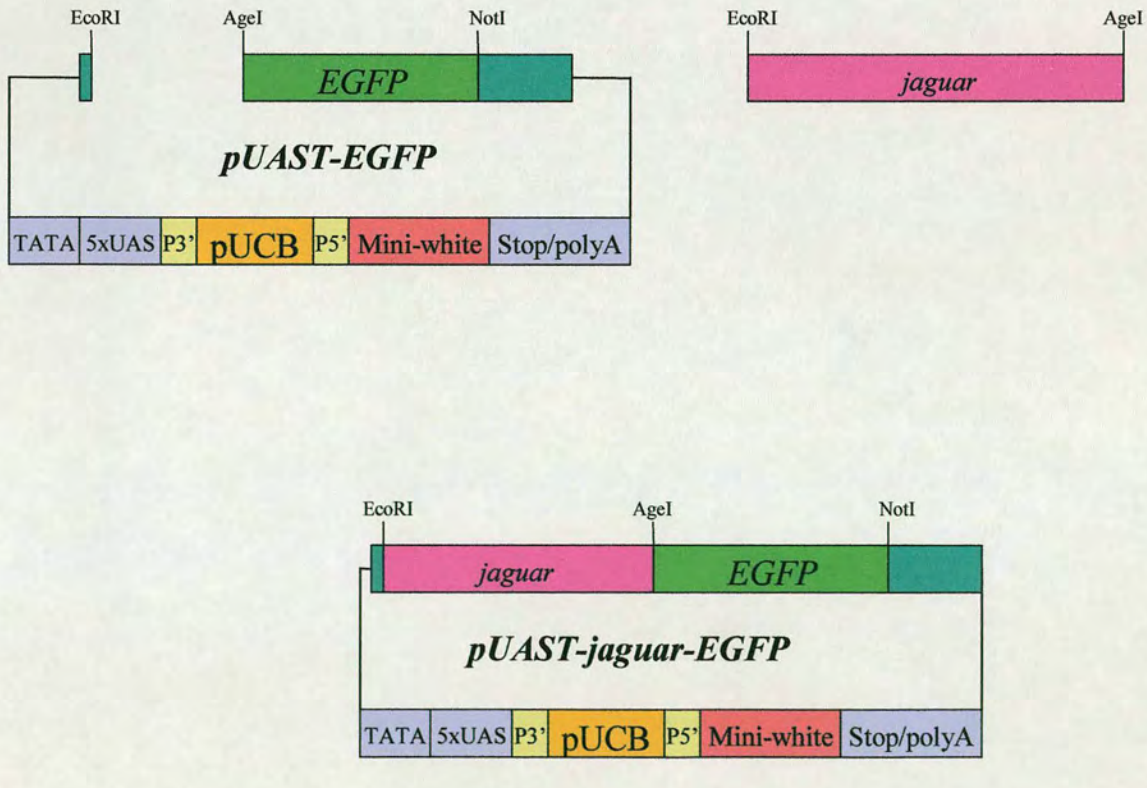
EcoRI
AgeI
NotI
EGFP
pUAST-EGFP
TATA
5xUAS
P3'
pUCB
P5'
Mini-white
Stop/polyA
EcoRI
AgeI
jaguar
EcoRI
AgeI
NotI
jaguar
EGFP
pUAST-jaguar-EGFP
TATA
5xUAS
P3'
pUCB
P5'
Mini-white
Stop/polyA

The colonies containing the insert of the *jaguar* and *EGFP* were selected by colony lift hybridisation (section 2.4.9) and single colony PCR (section 2.4.11.4). The cloning steps are described in figure 4.3.1.

The plasmids from the selected colonies were restriction-analysed with the enzymes *EcoRI*, *NotI*, and *AgeI* in order to verify the presence of *EGFP* and *jaguar* cDNA within the PGM, PGMH and PGMT plasmids (Fig. 4.3.2).

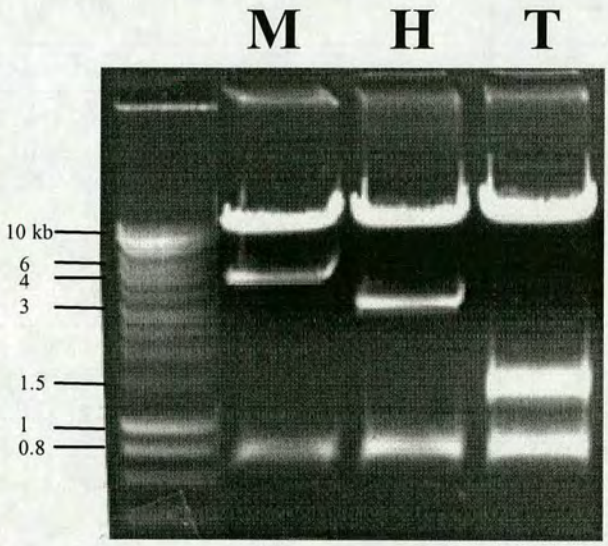

Figure 4.3.2: Restriction analysis for the three DNA constructs made: PGM (M), PGMH (H), and PGMT (T) with EcoRI, NotI and AgeI restriction enzymes. All the constructs contain the pUAST plasmid with the size of 8.9 kb, and the EGFP gene (0.8 kb). PGM contains the whole *jaguar* cDNA (4.2 kb), PGMH contains the coding region of the head and neck domains (2.85 kb) and PGMT contains the coding region of the tail domain (1.35 kb).

Finally, the connection in-frame of *jaguar* cDNA with *EGFP* sequence was verified by sequencing the region between the two genes in all the three constructs, using the GFPR primer. In order to ensure the accurate amplification of *jaguar* cDNA in the three constructs, various fragments in *jaguar* cDNA were sequenced, using the primers MYC2, MYN, TAN, HEC2, and pUASTF (thus sequenced the region connecting the pUAST plasmid and *jaguar* cDNA). In all the DNA constructs, *jaguar* cDNA was fused in-frame with *EGFP*, and the sequence of *jaguar* cDNA in all the three constructs was amplified accurately, without mistakes.

4.4 Creation of transgenic flies

The creation of transgenic flies was as described in section 2.3.5. The number of flies injected and the number of transgenic flies created for the constructs: PGM, PGMH and PGMT are described in table 4.4.1

Table 4.4.1: Microinjection summary

The injected construct	No. of embryos injected	No. of larvae survived	No. of hatching flies (crossed)	No. of crosses that gave progeny	No. of injected flies producing transgenic flies
PGM	1077	279	205	134	54/109[B]
		26%[A]	19%[A]	12.4%[A]	6.6%[A] (49.5%[C])
PGMH	1055	276	192	134	54/134[B]
		35.6%[A]	18.2%[A]	12.7%[A]	5%[A] (40.3%[C])
PGMT	1068	322	217	165	40/138[B]
		31.1%[A]	20.3%[A]	15.5%[A]	4.5%[A] (30%[C])

[A] The percentages in the table indicate the recovery out of the number of the embryos injected
[B] The number of crosses that were examined.
[C] The recovery is number of injected flies creating transgenic progeny/ number of crosses that were examined.

The main decline in the survival rate was after the microinjection. About 6-10% of the animals died during the larval and pupal stages. Among the injected flies that hatched, 65-76% were fertile. The loss of fertility in the rest of the flies could have been caused by the loss of the pole cells from the embryos during the microinjection. In spite of the low recovery of flies after the injection, the percentage of transgenic flies generated was high.

The expression level of the GFP tagged proteins depends on the location of the insert. Transgenic flies that came from the same injected embryo can have the insertion in the same place within the chromosome, if all the flies are originated from the same stem cell. However, if the transgenic flies collected are originated from different injected flies, the variability in the location of the inserts in the chromosomes increase and therefore the chance of getting flies with a good expression of the tagged proteins increases as well.

Table 4.4.2: List of the jar-GFP flies created.

PGM lines					
Fly line nickname	**Insertion genotype**	**Chr[A]**	**Fly line nickname**	**Insertion genotype**	**Chr[A]**
PGM17-1	*P{ w+, UAS-PGM}17.1*		*PGM75-5-2*	*P{ w+, UAS-PGM}75.5.2*	
PGM17-2	*P{ w+, UAS-PGM}17.2*		*PGM75-10*	*P{ w+, UAS-PGM}75.10*	3
PGM22-1	*P{ w+, UAS-PGM}22.1*	2	*PGM109-1*	*P{ w+, UAS-PGM}109.1*	
PGM22-3	*P{ w+, UAS-PGM}22.3*	4	*PGM125-2*	*P{ w+, UAS-PGM}125.2*	2
PGM25-3	*P{ w+, UAS-PGM}25.3*		*PGM128-4*	*P{ w+, UAS-PGM}128.4*	2
PGM38-2	*P{ w+, UAS-PGM}38.2*		*PGM167-2*	*P{ w+, UAS-PGM}167.2*	
PGM41-1	*P{ w+, UAS-PGM}41.1*		*PGM172-2*	*P{ w+, UAS-PGM}172.2*	
PGM41-2	*P{ w+, UAS-PGM}41.2*		*PGM196-2*	*P{ w+, UAS-PGM}196.2*	X
PGM43-2	*P{ w+, UAS-PGM}43.2*	2	*PGM214-1*	*P{ w+, UAS-PGM}214.1*	
PGM45-1	*P{ w+, UAS-PGM}45.1*		*PGM226-9*	*P{ w+, UAS-PGM}226.9*	3
PGM45-2	*P{ w+, UAS-PGM}45.2*		*PGM228-1*	*P{ w+, UAS-PGM}228.1*	2
PGM58-1	*P{ w+, UAS-PGM}58.1*	2	*PGM238-2*	*P{ w+, UAS-PGM}238.2*	
PGM75-5-1	*P{ w+, UAS-PGM}75.5.1*	3	*PGM238-5*	*P{ w+, UAS-PGM}238.5*	

[A] The chromosome location of some of the inserts is indicated.

PGMH lines					
Fly line nickname	**Insertion genotype**	**Chr[A]**	**Fly line nickname**	**Insertion genotype**	**Chr[A]**
PGMH8-2	*P{ w+, UAS-PGMH}8.2*		*PGMH114-2*	*P{ w+, UAS-PGMH}114.2*	3
PGMH56-1	*P{ w+, UAS-PGMH}56.1*	2	*PGMH119-1*	*P{ w+, UAS-PGMH}119.1*	
PGMH57-1	*P{ w+, UAS-PGMH}57.1*	2	*PGMH130-2*	*P{ w+, UAS-PGMH}130.2*	2
PGMH90-1	*P{ w+, UAS-PGMH}90.1*	3	*PGMH156-1*	*P{ w+, UAS-PGMH}156.1*	
PGMH90-2	*P{ w+, UAS-PGMH}90.2*		*PGMH181-3*	*P{ w+, UAS-PGMH}181.3*	3
PGMH94-1	*P{ w+, UAS-PGMH}94.1*	3	*PGMH197-2*	*P{ w+, UAS-PGMH}197.2*	
PGMH94-2	*P{ w+, UAS-PGMH}94.2*		*PGMH224-1*	*P{ w+, UAS-PGMH}224.1*	
PGMH106-2	*P{ w+, UAS-PGMH}106.2*		*PGMH235-2*	*P{ w+, UAS-PGMH}235.2*	
PGMH114-1	*P{ w+, UAS-PGMH}114.1*				

[A] The chromosome location of some of the inserts is indicated.

PGMT lines					
Fly line nickname	**Insertion genotype**	**Chr[A]**	**Fly line nickname**	**Insertion genotype**	**Chr[A]**
PGMT 33-2	*P{ w+, UAS-PGMT}33.2*		*PGMT 84-1*	*P{ w+, UAS-PGMT}84.1*	
PGMT 41-1	*P{ w+, UAS-PGMT}41.1*		*PGMT 84-3*	*P{ w+, UAS-PGMT}84.3*	
PGMT 59-2	*P{ w+, UAS-PGMT}59.2*		*PGMT 85-1*	*P{ w+, UAS-PGMT}85.1*	
PGMT 59-3	*P{ w+, UAS-PGMT}59.3*		*PGMT 85-2*	*P{ w+, UAS-PGMT}85.2*	
PGMT 59-5	*P{ w+, UAS-PGMT}59.5*		*PGMT 106-1*	*P{ w+, UAS-PGMT}106.1*	
PGMT 61-1	*P{ w+, UAS-PGMT}61.1*		*PGMT 127-2*	*P{ w+, UAS-PGMT}127.2*	
PGMT 61-2	*P{ w+, UAS-PGMT}61.2*		*PGMT 231-2*	*P{ w+, UAS-PGMT}231.2*	
PGMT 61-3	*P{ w+, UAS-PGMT}61.3*	X	*PGMT 236-1*	*P{ w+, UAS-PGMT}236.1*	
PGMT 69-1	*P{ w+, UAS-PGMT}69.1*		*PGMT 239-1*	*P{ w+, UAS-PGMT}239.1*	
PGMT 69-2	*P{ w+, UAS-PGMT}69.2*		*PGMT 291-1*	*P{ w+, UAS-PGMT}291.1*	
PGMT 69-3	*P{ w+, UAS-PGMT}69.3*		*PGMT 291-2*	*P{ w+, UAS-PGMT}291.2*	
PGMT 79-1	*P{ w+, UAS-PGMT}79.1*		*PGMT 315-2*	*P{ w+, UAS-PGMT}315.2*	
PGMT 83-1	*P{ w+, UAS-PGMT}83.1*				

[A] The chromosome location of some of the inserts is indicated.

For that reason, from every injected fly that produced transgenic flies, only 2-3 lines were selected. After collecting 100 transgenic flies for every injected construct, the flies having the highest expression level of GFP were selected as described in section 2.3.5.3, and the selected lines are described in table 4.4.2. Some of the fly lines we purposed to use in subsequent experiments were balanced and the chromosome location of the transposon is indicated. The expression of

PGM, PGMH and PGMT did not affect the normal function of native Myosin VI and viability. All the flies expressing the fusion proteins had progeny.

There was no correlation between the eye colour and the expression level of the fusion proteins: fly lines having bright orange eyes showed a strong expression of PGM when crossed with Gal4 lines, while several lines having dark red eyes had a weak expression of PGM. Probably the reason for the differences is that the *mini-white* gene is activated by certain activators, near the insertion site, whilst PGM expression is activated by Gal4, but which is still manipulated by different enhancers. However, it seems that there are other factors affecting the expression of PGM since the transgenic flies have different levels of PGM expression.

4.5 Expression pattern of Myosin VI during the whole fly life cycle

The fly line *C865* contains the *Gal4* gene inserted within the *jaguar* gene, in its 5'UTR region, at bp 306 in the first exon (Millo et al., 2004). In this line, Gal4 is expressed according to the expression pattern of Myosin VI. By crossing line *C865* with PGM and PGMH fly lines, it was possible to detect in which tissues and at which stages Myosin VI is expressed during the entire fly life cycle. Because PGM and PGMH expression is controlled by Gal4, the two fusion proteins showed expression in all the tissues described.

Figure 4.5.1 shows various tissues expressing PGM (the whole Myosin VI tagged to GFP) and PGMH (Myosin VI head and neck domains tagged to Myosin VI) during embryogenesis. In late embryogenesis (stages 13-15) PGM is expressed during dorsal closure, mainly at the leading edge and in the amnioserosa (A, B). PGM and PGMH are observed in the neurons of the central nervous system (F) and the

peripheral nervous system (C, D) in stages 13-15, according to Bownes stages, (Bownes, 1975; Campos-Ortega, 1985).

In *Drosophila* embryos at stage 16, Myosin VI has a physical interaction with Miranda, and is necessary for the localization of Miranda in the basal cell membrane of metaphase neuroblasts. In addition, Myosin VI is necessary for rotating the spindle in the neuroblasts by 90°C (Petritsch et al., 2003): in the Myosin VI mutant, jar^{322}, the neuroblasts spindles were disorientated and Miranda was mislocalised to the cytoplasm. Similar results were obtained when the expression and the function of Myosin VI in the neurons were disrupted by different approaches (Petritsch et al., 2003). The expression of PGM or PGMH in the neurons is consistent with the expression of Myosin VI, which is necessary for their asymmetric cell divisions, and for the proper development of the nervous system.

At stages 13-15 PGM and PGMH were also observed in the developing trachea (E), having expression at the posterior spiracle (Fig. 4.5.1 B, D). In the final stages of embryogenesis, the expression of PGM and PGMH is found in the developed salivary glands (F, G) and in the midgut mesoderm (marked MG in G and H), after the fusion of the anterior and posterior midgut.

In the third instar larvae (Fig. 4.5.2), PGM continues to be expressed in the trachea and in the epithelial cells at the dorsal trunk (Fig. 4.5.2 A, B). In the cuticle, PGM is expressed in epidermal cells appearing at the posterior part of each segment (Fig. 4.5.2 C, D). In the salivary gland PGM show a strong expression (Fig. 4.5.2 E): the strongest expression of PGM appeared within the salivary gland main duct (Fig. 4.5.2 F). PGM appears to be concentrated in groups in the salivary duct. Perhaps PGM forms a complex with proteins that have been transferred from the secretory cells to the duct. The expression of PGM and PGMH in the neurons continues to appear from embryogenesis to the moult stage, in the larval brain hemispheres and the ventral ganglion (Fig. 4.5.2 G, H).

Figure 4.5.3 shows the expression of PGM in the leg, halter and wing discs. In the leg wing and halter discs, PGM expression appears in a punctate form (A). However in some flies, PGM expression appeared all over the leg and wing discs (B). As the leg disc evaginates, PGM is expressed in the entire leg (C), suggesting that Myosin VI is necessary for the migration of the epithelial cell as the leg spreads.

The figures in the following pages:

Figure 4.5.1: Expression of PGM during embryogenesis. **A:** During dorsal closure PGM is expressed in the amnioserosa (AS) and at the leading edge (LE). The embryos were stained with phalloidin to visualise the actin filaments. In the amnioserosa Myosin VI is localized mainly in the cytoplasm and is excluded from the nuclei. **B:** A picture showing PGM expression as dorsal closure progress. The cells expressing PGM, at the leading edge are more elongated. **C-E:** Expression of PGM and PGMH in the neurons (NEU) of the peripheral nervous system and the trachea. The strong expression of PGM and PGMH in the posterior spiracle (PS) is marked. Figure **F** shows expression of PGMH in the neurons of the central nervous system (CNS). In the late stages of embryogenesis (stage 15 onwards) PGM is expressed in the salivary glands (SG) and in the midgut endoderm. **G-H**: expression of Myosin VI in the midgut (MG).

Figure 4.5.2: Expression of PGM in third instar larvae. PGM expression appeared in the first and second instar larvae, but it was more obvious at the third larval instar stage. PGM is expressed in the dorsal trunk of the larval trachea (**A, B**); in the cytoplasm of the epidermal cells producing the cuticle (**C, D**); strong expression of PGM (**E**) appears in the salivary glands, where PGM is localized at the cell membrane and in the cell cytoplasm. **F**: A strong concentration of PGM is observed in the salivary gland duct, some of it is appears as in aggregates, probably connected to vesicles. PGM is also expressed in the brain neurons, in the brain hemispheres (BH) and the ventral ganglion (VG, figures **G-H**).

Figure 4.5.3: Expression of PGM in the imaginal discs of the larvae (third instar) and pupae. **A, B**: leg wing and halter imaginal discs of third instar larvae. Figure A was taken through red and green filters in order to produce a clearer image of the cells expressing PGM. **C**: An evaginating leg disc. **D** and **E** are legs at the pupal stage. PGM is expressed in the nerve cells (microcheates) in the femur and the tibia. **F, G**: Evaginating wing discs. PGM is expressed in the wing epithelial sheet prior to the spreading of the wing, and at the basal side of the epithelial cells, where the two epithelial sheets face to each other (arrow). **H:** A wing of a *en/AM8-2* pupae, showing malformation and blistering of the wing in the posterior part of the wing (PST), where Myosin VI is disrupted (see asterisk). The anterior remains normal (ANT) **I:** Expression of PGM in the wings (arrow) and legs (asterisk) during metamorphosis within the pupal case.

Figure 4.5.4: Expression of PGM in the eye-antennal imaginal discs and in the testes of the adult fly. PGM is expressed throughout the eye-antenna disc during the third larval instar (**A**). In the pupae PGM is expressed in the ommatidia of the developing eye (**B, C**), in the evaginating antenna disc (**E**), and in the antenna (**F**). **D**: when Myosin VI is disrupted in the posterior part, the hairs are slightly thinner. In the adult fly, during spermatogenesis PGM is expressed in the individualization complexes, showing a strong expression mainly at the base of the cone (**G**). Myosin VI is also expressed in cells within the accessory gland (**H**).

Figure 4.5.5: PGM is expressed during oogenesis in all the migrating follicle cells. **A:** During stage 7 PGM is expressed in the anterior follicle cells and in the border cells as they start to migrate towards the oocytes. **B:** At stage 9 PGM is expressed in the columnar follicle cells as they migrate, note the strong expression at the apical side of the cells; **C:** A view of the expression in the columnar follicle cells as they cover the oocyte. **D:** During stage 10B, PGM expression is observed in the centripetal follicle cells as they migrate to cover the anterior part of the oocyte. **E:** Expression of PGM in the border cells as they reach the oocyte-nurse cell border, and in the contractile ring formed at the anterior of the oocyte. **F:** Expression of PGM in the columnar cells, PGM is expressed in the cytoplasm and excluded from the nucleus. **G:** Expression of PGM in the dorsal-anterior follicle cells at stages 12-13. The dorsal appendages start to develop (arrow). The border cells still show strong PGM expression. **H:** Expression of PGM in the follicle cells around the dorsal appendages.

Figure 4.5.1

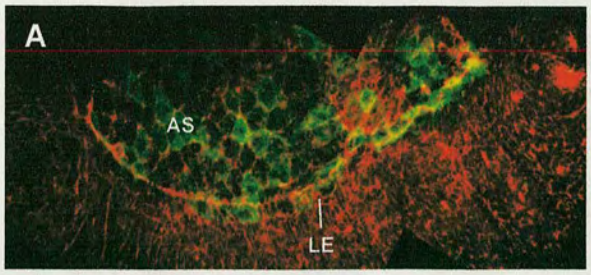

PGM 75-5-2 X C865

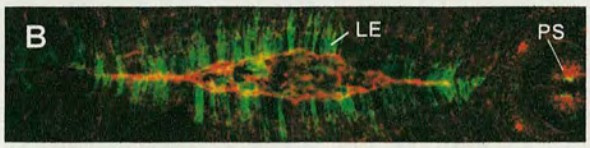

PGM 43-2 X C865

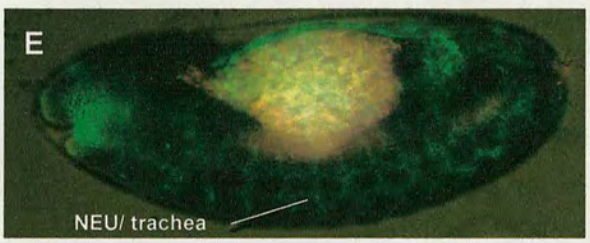

PGMH 90-2 X C865

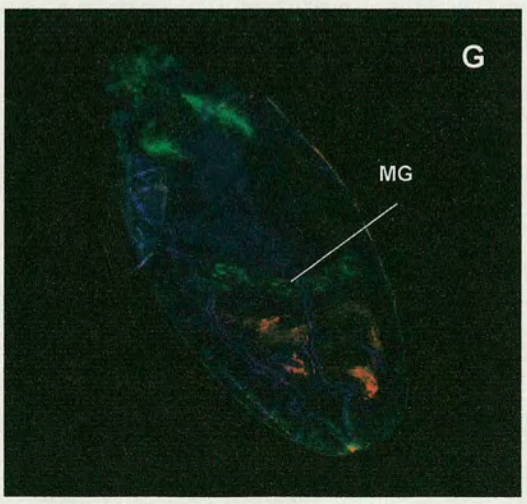

PGM 22-1 X C865

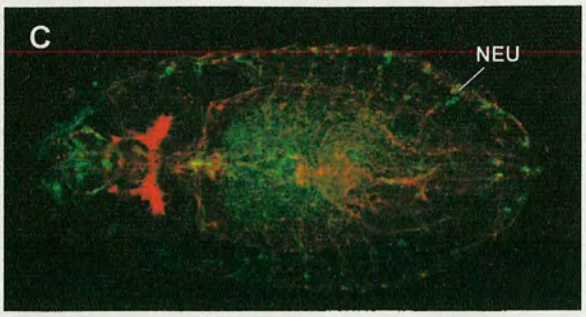

PGM 75-5-2 X C865

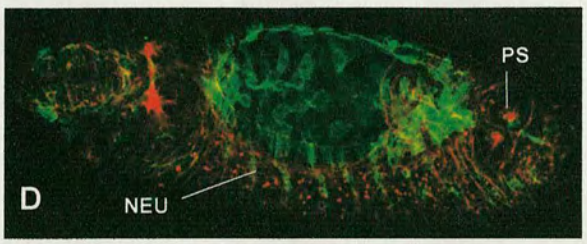

PGMH 181-3 X C865

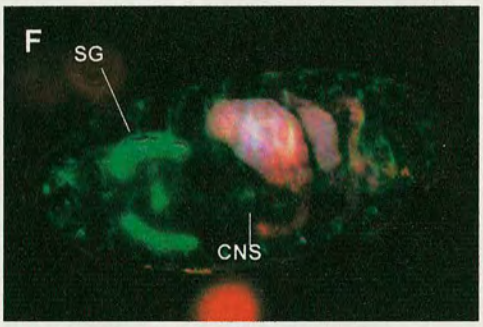

PGMH 181-3 X C865

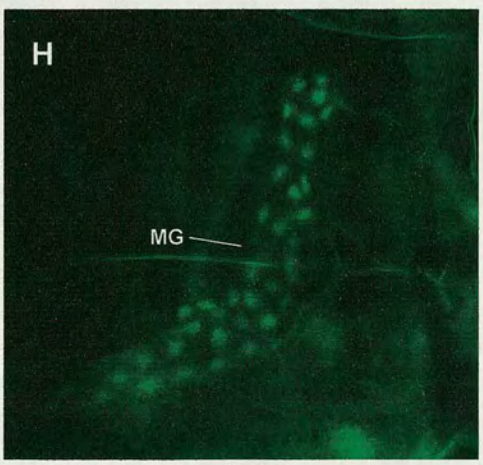

PGM 22-1 X C865

Figure 4.5.2

Larvae trachea

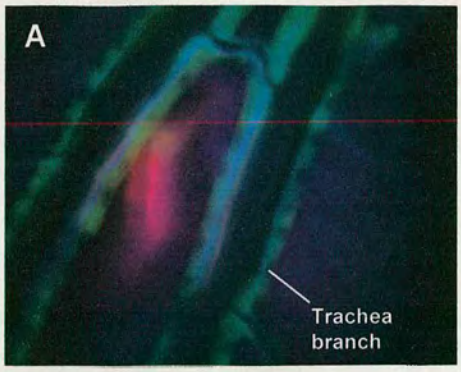

PGM 238-2 x C865

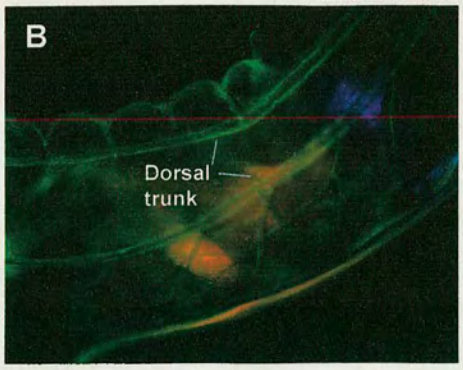

PGM 238-2 x C865

Larvae skin

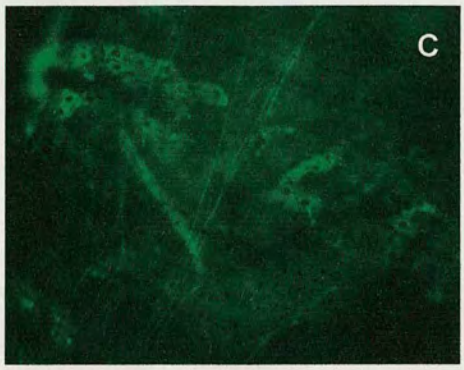

PGM 10X C865

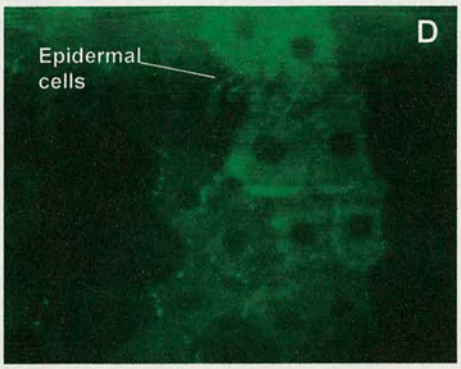

PGM 38-2 x C865

Salivary glands

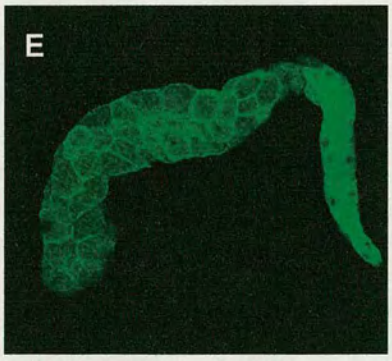

PGM 17-2 x C865

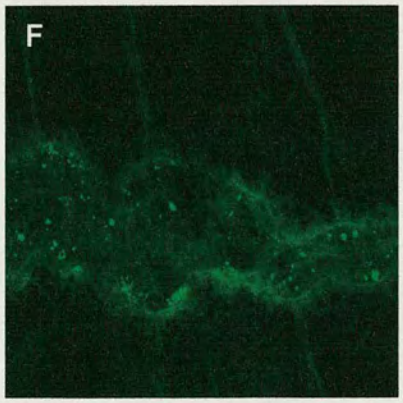

PGM 22-3 x C865

Brain

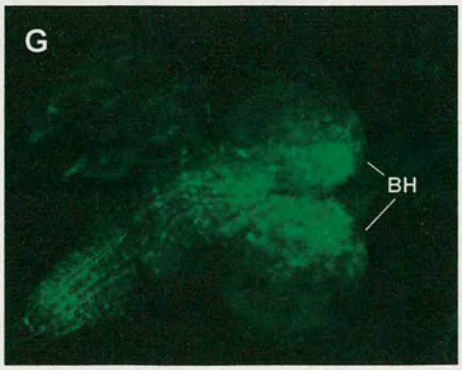

PGM 17-2 X C865

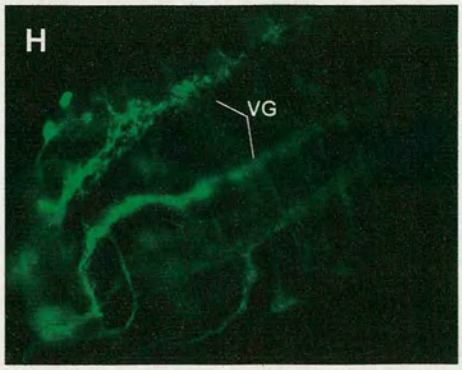

PGM 17-2 X C865

Figure 4.5.3

Imaginal discs-leg wing and halter

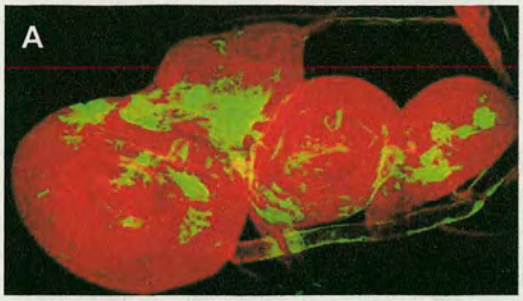

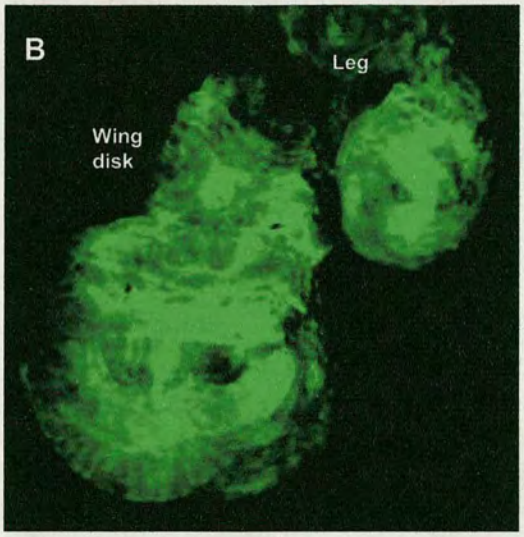

PGM 58-1 x C865

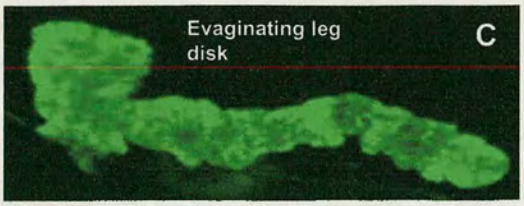

PGM 22-1 x C865

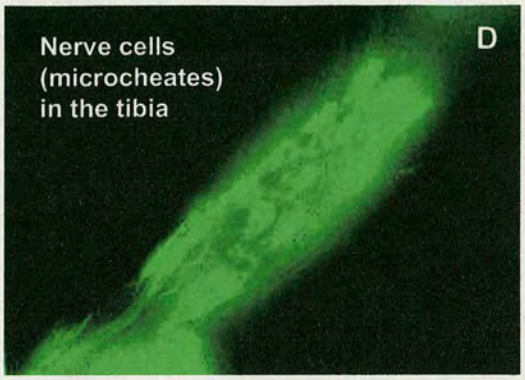

PGM 38-2 X C865

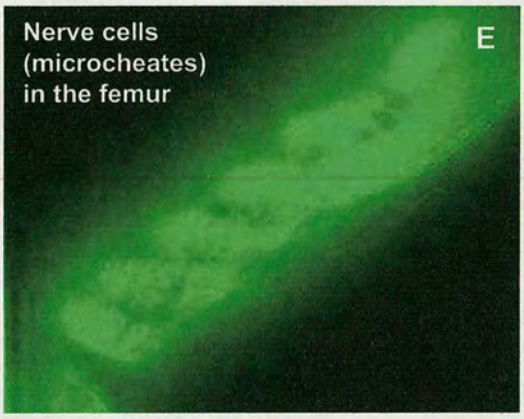

PGM 38-2 X C865

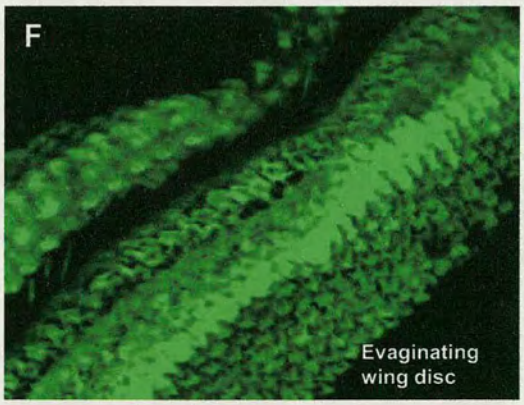

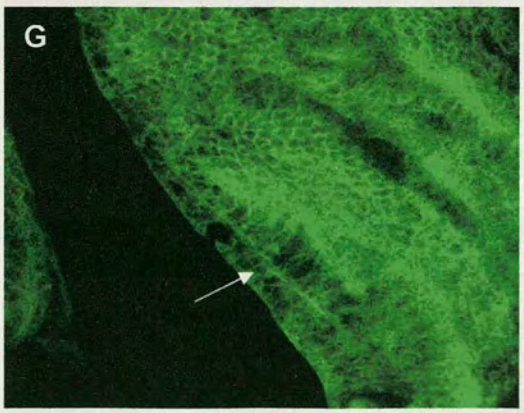

PGM 125-2 x C865

en/Am8-2

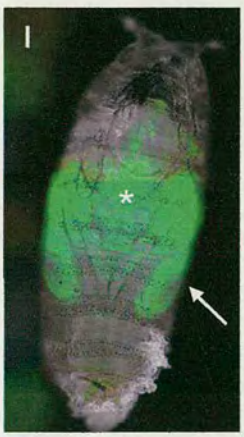

PGM 228-1 x C865

Figure 4.5.4

Imaginal discs-eye and antenna

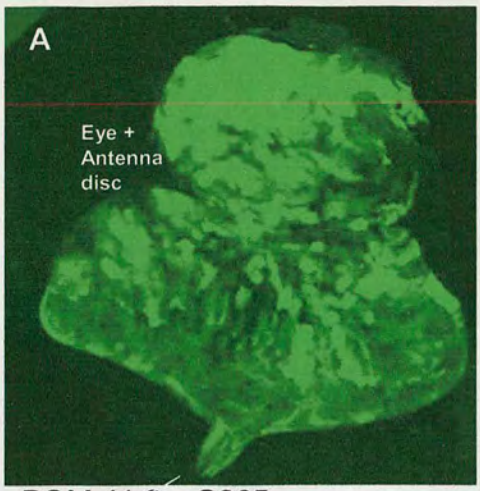

PGM 41-2 x C865

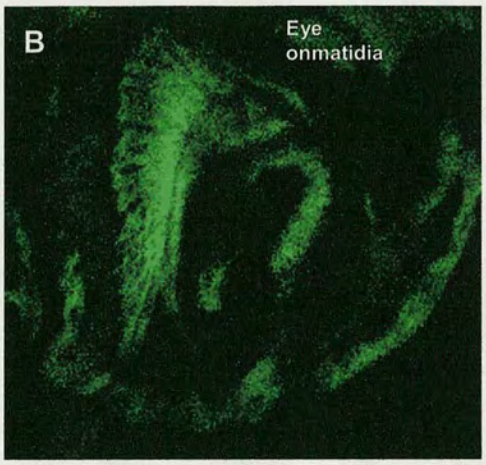

PGM 75-10 x C865

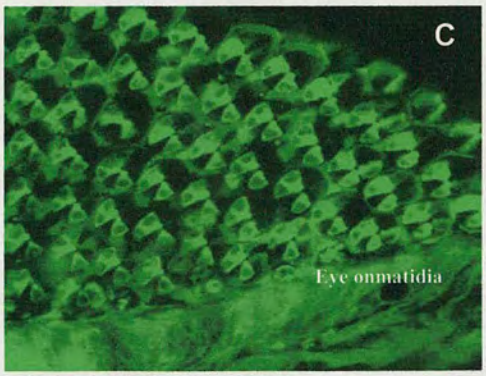

PGM 196-2 x C865

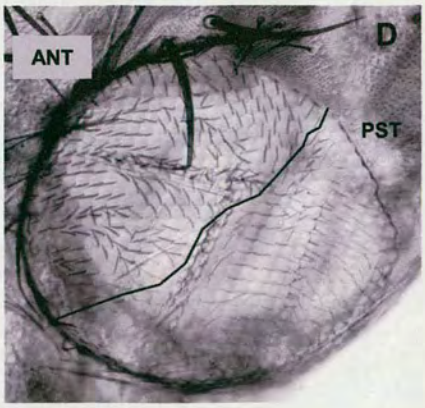

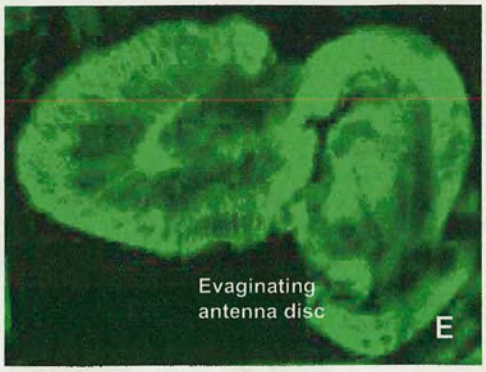

PGM 75-10 x C865

PGM 17-2 x C865

Spermatogenesis

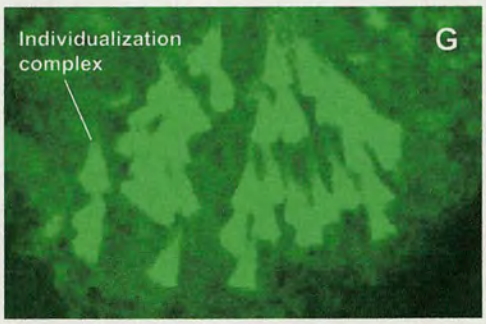

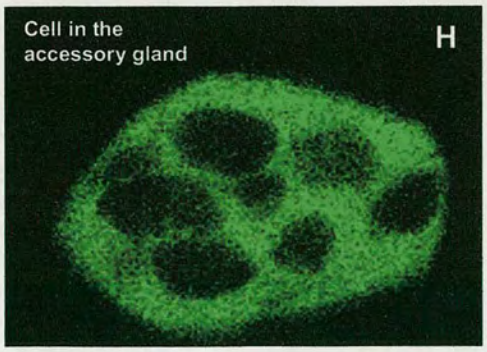

en/Am8-2

Figure 4.5.5

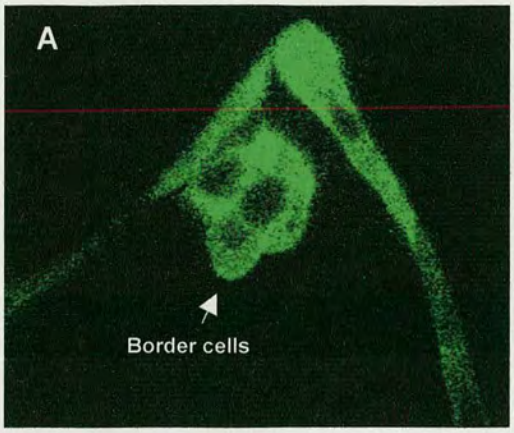

PGM 58-1 X C865

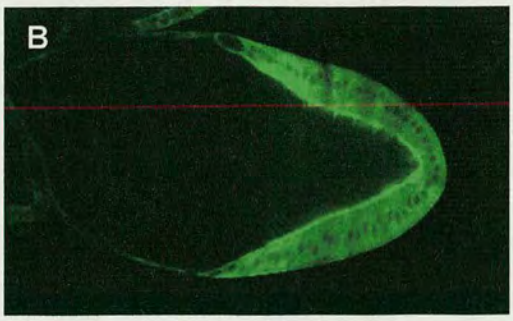

PGM 228-2 X C865

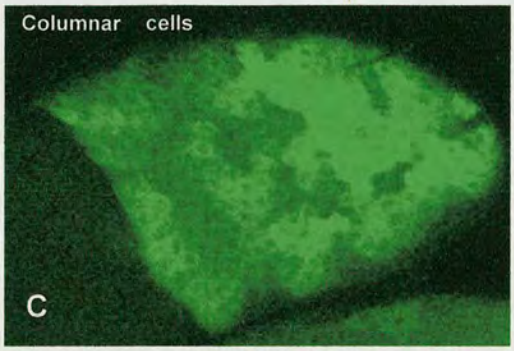

PGM 75-5-2 X C865

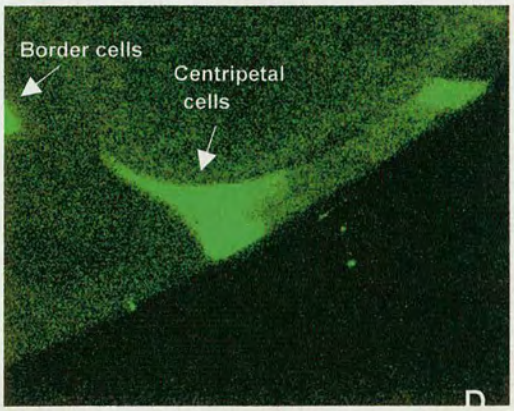

PGM 228-1 X C865

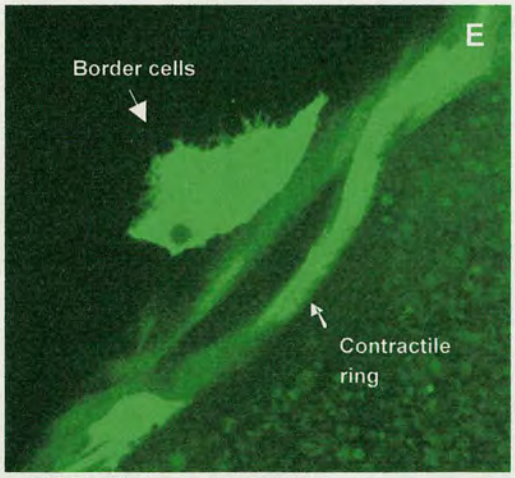

PGM 75-5-2 X C865

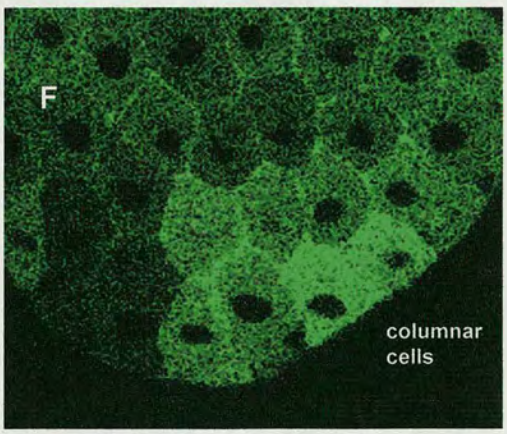

PGM 75-5-2 X C865

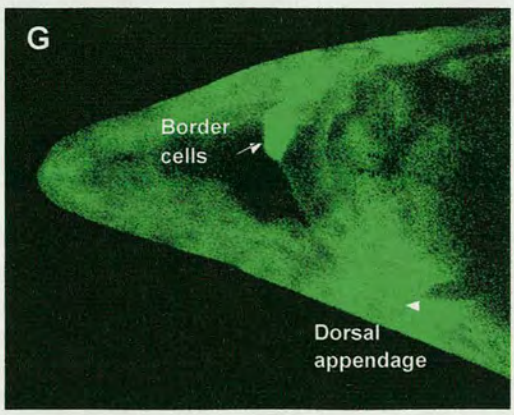

PGM 196-2 X C865

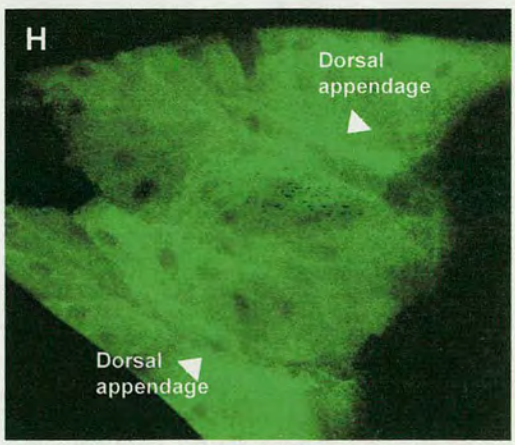

PGM 196-2 X C865

When the leg reaches its full extension, PGM is expressed in the neurons (microcheates) within the leg. Figures 4.5.3 D and E show expression of PGM in the microcheate neurons within the tibia and femur, respectively.

Disruption in Myosin VI expression by induction of Myosin VI antisense driven by the Gal4 line *C532* caused malformed legs to form (Deng et al., 1999). The malformation seems to be caused due to abnormal organization of the epithelial tissue in the evaginating disc. The expression of PGM in the leg disc during the larval and pupal stages is consistent with these results.

In the evaginating wing disc, PGM is expressed in the cells of the epithelial sheets, prior to their evagination (Fig. 4.5.3 F). The induction of Myosin VI antisense by the *C532 Gal4* line caused malformations in the wings of the adult fly (Deng et al., 1999). In many cases the wings remain folded after hatching from the pupa, and were not able to form properly. This suggests that the expression of Myosin VI in the wings is necessary for spreading the wing as the fly hatches, however, the inability of the wings to spread could be due to an abnormal organization of the wing epithelium at the pupal stage. PGM is also seen in the basal side of the epithelial cells, at the connection area of the two epithelium sheets in the wings (Fig. 4.5.3 G). In another approach for understanding the specific role of Myosin VI in the imaginal discs, we crossed the fly line *Am8-2* with an *engrailed* Gal4 line to generate a progeny with disrupted expression of Myosin VI only in the posterior compartment of the imaginal discs. In the pupa, the posterior of the wing lost its organized, folded form, forming blisters (Fig. 4.5.3 H). These results suggest that Myosin VI is necessary for patterning the organized, compact folded form of the wing as it appears in the pupae, and for keeping the epithelial sheets attached, during the wing morphogenesis. All these results suggest that Myosin VI plays a role in the migration and patterning of the epithelial sheet of the wing as it develops.

In the eye-antenna disc PGM expression appeared in the whole disc (Fig. 4.5.4 A). In later stages PGM is expressed in the eye ommatidia (Fig. 4.5.4 B, C) and in the evaginating antenna (Fig. 4.5.4 F, G). It is not clear what role Myosin VI plays in the development of the eye and the antenna. When the expression of Myosin VI is disrupted in *en/Am8-2* flies, the hairs in the posterior part of the eye seem to be slightly thinner (Fig. 4.5.4 D).

In the adult testes, PGM is expressed in the individualization complexes (Fig. 4.5.4 G). Myosin VI has been shown previously to be necessary for the creation of the individualization complex during sperm individualization (Hicks et al., 1999; Rogat and Miller, 2002) this is also mentioned in the mutant rescue test, in the following section). In the mutation jar^{mmw14}, Myosin VI is not expressed in the testes, the individualization complex is not formed and as a result the male flies are sterile. Antibody staining showed the expression of Myosin VI in the individualization complex (Hicks et al., 1999; Rogat and Miller, 2002), and the expression of PGM, in the individualization complex is consistent with these results. PGM is located in the whole individualization complex, with a strong expression at the base of the cone where Myosin VI creates a ring around every maturating spermatid. Myosin VI showed a strong expression in cells within the accessory gland as well (Fig. 4.5.4 G).

During oogenesis, PGM is expressed in all the follicle cells as they undergo migration (Fig. 4.5.5). During stage 7, PGM is expressed in the anterior follicle cells and in the border cells as they start their migration (Fig. 4.5.5 A). At stages 9-10 PGM is expressed in the migrating columnar cells (Fig. 4.5.5 B,C). At stage 10b, PGM is expressed in the centripetal follicle cells as they migrate towards the anterior part of the oocyte (Fig. 4.5.5, D-F), and in the contractile ring connecting the centripetal cells (Fig. 4.5.5 E). In figure D the stronger expression of PGM in the centripetal cells compared with the columnar cells, indicates a specific expression in the follicle cells that undergo migration. At stages 12-13 PGM is expressed in the dorsal-anterior follicle cells as they create the dorsal appendages (Fig. 4.5.5 G-H). Figure H shows a specific strong expression of PGM in the region of the developing dorsal appendages.

Because gene expression induced by Gal4 appears only in somatic cells (Gustafson and Boulianne, 1996), PGM is not expressed in the germ line. Therefore in spite of

the presence of Myosin VI in the nurse cells (Bohrmann, 1997; Deng et al., 1999), PGM is not expressed as this technique does not permit analysis of the location of Myosin VI in the nurse cells. However, in the follicle cells, the expression is similar to this observed in egg chambers stained with Myosin VI antibody. The antibody staining of the columnar cells showed a uniform expression of Myosin VI while PGM expression showed various levels of expression in different groups of cells. It is possible that the expression of PGM shows a more realistic picture of the expression pattern of Myosin VI in the follicle cells than antibody staining, since PGM expression is triggered by a Myosin VI Gal4 line (*C865*), according the expression pattern Myosin VI. It is also possible that a different turnover of *jaguar-EGFP* mRNA and PGM protein would cause different levels of expression in different cells.

Expression of Myosin VI antisense RNA in the follicle cells disrupts Myosin VI expression, the follicle cells have an abnormal shape and the migration of the cells is arrested, causing a creation of an abnormal cell epithelium (Deng et al., 1999). The expression of PGM, driven by Myosin VI-Gal4, in the migrating follicle cells, gives a clear picture of the expression of Myosin VI in the follicle cells, which is needed for their migration, and for the creation of the organized follicle cell epithelium around the oocyte, and it maintains the shape of cells shape as they move.

4.6 The rescue of Myosin VI mutants by the expression of PGM

In order to use the fusion proteins in further experiments, it was necessary to verify that PGM functions in a similar way to the native Myosin VI, and that the tagging of GFP to the C terminus of Myosin VI did not interfere with its function. To test this possibility, I made two mutant rescue studies. The first study examined the ability of PGM to rescue the embryonic lethal phenotype observed in the homozygous mutants: jar^{R23}, jar^{R39}, jar^{R70} and $jarR^{235}$. The second study examined the ability of PGM to rescue the male sterility phenotype of the mutants: jar^{R39}/jar^{mmw14}, and jar^{R235}/jar^{mmw14}.

4.6.1 Study 1: examination of embryonic lethal phenotype rescue by PGM expression, in jar^{R23}, jar^{R39}, jar^{R70} and $jarR^{235}$

In the homozygous mutant flies jar^{R23}, jar^{R39}, jar^{R70} *and* $jarR^{235}$ Myosin VI expression is disrupted (Millo et al., 2004, and chapter 5). Maternal Myosin VI is used for early embryogenesis, however the lack of new Myosin VI production in later stages (stage 12 onwards), in Myosin VI mutants causes failure in germ band retraction and dorsal closure. Many embryos died though some survived to the first larval instar using maternal Myosin VI. The purpose of this study was to examine whether or not the expression of PGM in the embryos would increase the survival rate of the homozygous mutant embryos, by increasing the number of larvae hatching from eggs.

4.6.1.1 Creation of fluorescent heterozygous mutants

In order to express PGM in mutant embryos, heterozygous mutant flies (jar^{R23}, jar^{R39}, jar^{R70} or $jarR^{235}$) were created, containing the *jaguar-EGFP* gene expressing PGM on the X chromosome, the *e22C-Gal4* gene on the second chromosome, and the mutant gene jar^{R23}, jar^{R39}, jar^{R70} or $jarR^{235}$ on the third chromosome, balanced with the chromosome TM3. *e22C-Gal4* expresses the Gal4 protein ubiquitously during embryogenesis, and hence triggers the expression of PGM throughout the

embryo during the late stages of embryogenesis. The crosses undertaken using *jar*^{R23} as an example, is described as follows:

1. In the first cross, flies from lines expressing Gal4 ubiquitously in the embryo were crossed with PGM flies, to create embryos which are ubiquitously fluorescent. They were fluorescent in the brain region at the larval stage, and had straight wing due to the loss of the balancer of the second chromosome, SM5, in the cross. In all the stages a reciprocal cross was made.

$$\frac{+;}{y/+}\ \frac{P[W^{+}(GAL4)]^{e22C}}{SM5} \quad X \quad \frac{UAS\text{-}PGM;}{+}\ \frac{+}{+}$$

Curly colour eyed male/female, colour eyed male/female

$$F1:\ \frac{PGM\ ;}{y/+}\ \frac{P[W^{+}(GAL4)]^{e22C}}{+}$$

Male/female larvae, fluorescent in the brain region, adults with straight wings.

---

2. In the second cross, the fluorescent flies UAS-*PGM* ; e22C were crossed with the balancer fly line *TM3/ TM6*. The selected progeny were fluorescent, and contained the balancer chromosome *TM3* (Stubble phenotype), or *TM6* (Tubby phenotype).

$$\frac{UAS\text{-}PGM;}{y/+}\ \frac{P[W^{+}(GAL4)]^{e22C}}{+} \ X\ \frac{+;}{+}\ \frac{+;}{+}\ \frac{TM3,\ Sb,\ e^{+}}{TM6,Tb\ e^{+}}$$

Fluorescent larvae male/female — Stubble, Tubby and ebony adult male/female

F1:

$$\frac{UAS\text{-}PGM;}{y/+}\ \frac{P[W^{+}(GAL4)]^{e22C}}{+}\ ;\ \frac{TM3,\ Sb,\ e^{+}}{+}$$

Fluorescent (brain) larvae, Stubble adult male/female

$$\frac{UAS\text{-}PGM;}{y/+}\ \frac{P[W^{+}(GAL4)]^{e22C}}{+}\ ;\ \frac{+}{TM6,\ Tb,\ e^{+}}$$

Fluorescent (brain) larvae, Tubby adult male/female

3. In the third cross the fluorescent flies *UAS-PGM; e22C; TM3* and *UAS-PGM; e22C;* TM6 were crossed again with the fly line *TM3/ TM6.* The selected progeny were fluorescent, and contained the two balancer chromosomes *TM3* and *TM6*, having the phenotype: Stubble, Tubby and ebony (a recessive phenotype that appears in the presence of the two balancer chromosomes).

$$\frac{UAS\text{-}PGM}{+/y};\ \frac{P[W^{+}(GAL4)]^{e22C}}{+};\ \frac{TM3,\ Sb,\ e^{+}}{+} \quad X \quad \frac{+}{+};\ \frac{+}{+};\ \frac{TM3,\ Sb,\ e^{+}}{TM6,\ Tb,\ e^{+}}$$

Fluorescent larvae,
Stubble adult male/female

Stubble, Tubby and
ebony male/female adult

$$\frac{UAS\text{-}PGM}{+/y};\ \frac{P[W^{+}(GAL4)]^{e22C}}{+} \quad \frac{+}{TM6,\ Tb,\ e^{+}} \quad X \quad \frac{+}{+};\ \frac{+}{+};\ \frac{TM3,\ Sb,\ e+}{TM6,\ Tb,\ e+}$$

Fluorescent larvae ,
Tubby adult male/female

Stubble, Tubby and
ebony adult male/female

F1:

$$\frac{UAS\text{-}PGM}{+/y};\ \frac{P[W^{+}(GAL4)]^{e22C}}{+};\ \frac{TM3,\ Sb,\ e^{+}}{TM6,\ Tb,\ e^{+}}$$

Fluorescent (brain) larvae, Tubby, Stubble, and ebony adult male/ female

---

4. In the fourth cross the selected flies were crossed with the heterozygous mutant jar^{R23}/ *TM3*. The progeny had four possible combinations of third chromosomes, as described in the diagram below. The homozygotes carrying the balancer chromosome *TM3* are lethal therefore all the flies that are stubble will be heterozygous for the mutant jar^{R23} (marked in box). Since the homozygous mutant flies had a *Gal4* gene inserted on the third chromosome, an additional expression pattern of PGM appeared the salivary glands (and in

the ovaries and the testes in later stages). Therefore the selected larvae were fluorescent in the brain region and in the salivary glands.

$$\frac{UAS\text{-}PGM;}{+/y}\ \frac{P[W^{+}(GAL4)]^{e22C}}{+};\ \frac{TM3,\ Sb,\ e^{+}}{TM6,\ Tb,\ e^{+}}\ X\ \frac{\pm;\ \pm;}{+\ +}\ \frac{P[W^{+}(GAL4)]^{jarR23}}{TM3,\ Sb,\ e^{+}}$$

Fluorescent larvae,
Tubby, Stubble, and ebony
adult male/ female

Stubble, mutant
adult male/ female

$$F1:\ \frac{UAS\text{-}PGM;}{+/y}\ \frac{P[W^{+}(GAL4)]^{e22C}}{+};\ \frac{P[W^{+}(GAL4)]^{jarR23}}{TM3,\ Sb,\ e^{+}}$$

selected: Fluorescent larvae (brain and/or s.gland), Stubble, but not Tubby adult male/ female

The cross combinations that appeared in the third chromosome were (in adults):

$\frac{TM3,\ Sb,\ e^{+}}{TM3,\ Sb,\ e^{+}}$	$\frac{TM3,\ Sb,\ e^{+}}{P[W^{+}(GAL4)]^{jarR23}}$	$\frac{TM6,\ Tb,\ e^{+}}{jar^{R23}\_}$	$\frac{TM6,\ Tb,\ e^{+}}{TM3,\ Sb,\ e^{+}}$
Homozygous lethal	heterozygous mutant, Stubble	heterozygous mutant, Tubby	Stubble Tubby ebony

After creating heterozygous flies, jar^{R23}, jar^{R39}, jar^{R70} and jar^{R235} that express PGM ubiquitously in the embryo, the fluorescent heterozygous flies (selected in the larval stage) were crossed with the non-fluorescent heterozygous flies.

$$\frac{UAS\text{-}PGM;}{y/+}\ \frac{P[W^{+}(GAL4)]^{e22C}}{+};\ \frac{P[W^{+}(GAL4)]^{jarR23}}{TM3,Sb\ e^{+}}\ X\ \frac{\pm;}{y/+}\ \frac{\pm}{+};\ \frac{P[W^{+}(GAL4)]^{jarR23}}{TM3,Sb\ e+}$$

In fluorescent heterozygous female, it was found that PGM was expressed in the follicle cells during oogenesis (data not shown). In order to test if maternal PGM affected embryonic survival , the survival rates of the embryos were examined when crossing fluorescent males and females separately. The fluorescent and non-

fluorescent embryos obtained from every cross were selected separately (100 eggs from each group) and the survival rates of embryos was calculated as the number of larvae hatching from the eggs during the following the following two days.

This cross created fluorescent and non-fluorescent progeny; each group contained the same genotype composition of the third chromosome (for simplicity $P[W^+(GAL4)]^{jarR23}$ was written as jar^{R23}):

$\frac{jar^{R23}}{jar^{R23}}$	$\frac{jar^{R23}}{TM3,Sb\ e^+}$	$\frac{TM3,Sb\ e^+}{TM3,Sb\ e+}$
25% homozygous mutant non-Stubble	50% heterozygous mutant Stubble	25% homozygous **lethal**

In the non-fluorescent flies, most of the homozygous mutant embryos die, and the *TM3* homozygous embryos die as well. Since only the heterozygous embryos survive, at least 50% of all the eggs are expected to hatch (the percentage is approximate since some of the homozygous mutant embryos survive until first instar larvae). In the fluorescent flies, the survival rate of the heterozygous flies and the lethality of the homozygous TM3 flies should not be affected by the expression of PGM. However, if the PGM does function like a native Myosin VI, it would then rescue the embryonic lethal phenotype, and the number of fluorescent larvae hatching from the eggs would be significantly higher than with non-fluorescent embryos. Therefore the increase in the survival rate will be due to the rescue of the homozygous mutant group only.

As a control the effect of PGM expression on the survival of non-homozygous mutant embryos was examined by setting the following cross (described for jar^{R23}):

$$\frac{UAS\text{-}PGM;\ P[W^+(GAL4)]^{e22C};\ P[W^+(GAL4)]^{jarR23}}{y/+\qquad +\qquad TM3,Sb\ e^+} \quad X \quad \frac{+;\ \ +\ ;}{y/+\ \ +} \quad \frac{TM6,\ Tb,\ e^+}{TM3,Sb\ e^+}$$

This cross created fluorescent and non-fluorescent flies; each group is expected to produce 75% viable embryos, heterozygous and non-mutant (for simplicity $P[W^{+}(GAL4)]^{jarR23}$ was written as jar^{R23}):

$\frac{jar^{R23}}{TM6,\ Tb,\ e^{+}}$	$\frac{jar^{R23}}{TM3,Sb\ e^{+}}$	$\frac{TM3,Sb\ e^{+}}{TM6,\ Tb,\ e^{+}}$	$\frac{TM3,Sb\ e^{+}}{TM3,Sb\ e+}$
25% homozygous mutant Tubby	25% heterozygous mutant Stubble	25% non-mutant Stubble Tubby	25% homozygous **lethal**

In the majority of the cases fluorescent and non-fluorescent embryos were clearly distinguishable; however, in the few cases where fluorescent larvae hatched from eggs considered to be non-fluorescent, the number of non-fluorescent eggs collected was multiplied with the correcting factor:

No. of non-fluorescent eggs collected =

$$\text{No. of eggs collected} \times \frac{\text{No. of non-fluorescent larvae}}{(\text{No. of fluorescent larvae} + \text{No. of non-fluorescent larvae})}$$

The percentage of larvae hatched from the eggs was calculated as follows:

$$\textbf{\% of larvae hatched} = \frac{\text{No. of larvae hatched} \times 100}{\text{No. of eggs collected}}$$

4.6.1.2 The different groups in the experiment:

For every mutant, there were four test groups and four control groups according to the following table (the mutant selected as an example is R23, for simplicity $P[W^{+}(GAL4)]^{jarR23}$ was written as jar^{R23}):

Table 4.6.1.2: the crosses for mutant rescue test 1

Test groups

jar^{R23}/ TM3 ♂ X UAS-PGM; e22C; jar^{R23}/ TM3 ♀	UAS-PGM; e22C; jar^{R23}/ TM3♂ X jar^{R23}/ TM3♀
test group 1 fluorescent progeny	test group 3 fluorescent progeny
test group 2 non- fluorescent progeny	test group 4 non- fluorescent progeny

Control groups

TM3/ TM6 ♂ X UAS-PGM; e22C; jar^{R23}/ TM3 ♀	UAS-PGM; e22C; jar^{R23}/ TM3♂ X TM3/ TM6 ♀
control group A fluorescent progeny	control group C fluorescent progeny
control group B non- fluorescent progeny	control group D non- fluorescent progeny

The survival rates of test groups 1 and 2 were compared with the rates in the control groups A and B. The survival rates of test groups 3 and 4 were compared with the rates in control groups C and D.

4.6.1.3 Chi square test:

If there is no rescue of the mutants by the fusion protein, it would be expected that similar survival rates would appear in the fluorescent and the non-fluorescent test groups, and that the *difference* in the survival rates between fluorescent and non fluorescent groups would be similar to that of the control group. For example, if in the control group A 57% of the larvae hatched, and in group B 50% of the larvae

hatched, the survival rate in group A is higher by 7% from group B. In this case, the null assumption (H_0) will be that in the test group the survival rate of group 1 will be higher by not more than 7% than group 2. H_0 will be rejected if the difference between survival rate of groups 1 and 2 is significantly higher compared to the difference in the control groups A and B. H_0 was rejected when the p values were lower than 0.05 (5%).

4.6.1.4 Results

The survival rate of the fluorescent and non-fluorescent flies in the test and the control groups is described for the four mutants in the following chart:

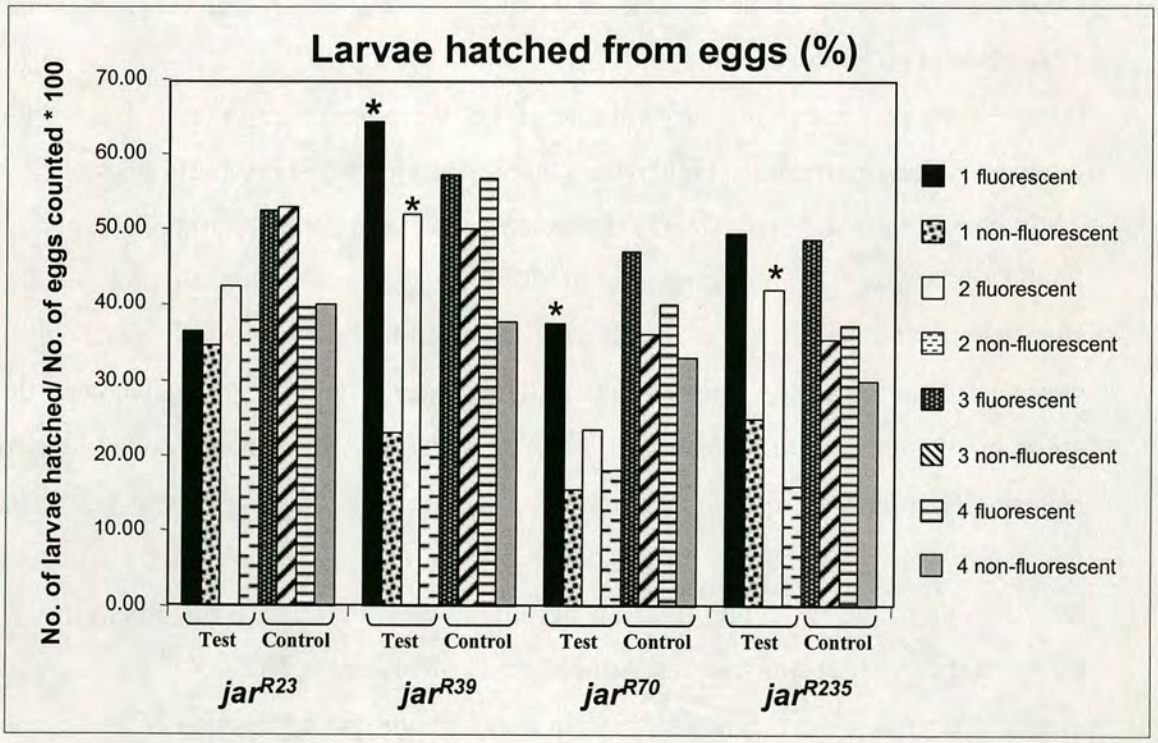

Figure 4.6.1.4: The survival rate of fluorescent and non-fluorescent embryos in the test and the control group, as made for the mutants: jar^{R23}, jar^{R39}, jar^{R70} and jar^{R235}. Crosses 1 and 2 were made in the test group and crosses 3 and 4 were made in the control group. Crosses1 and 3 (the first two columns) were made with heterozygous female expressing PGM protein (fluorescent) and non-fluorescent male. Crosses 2 and 4 were created with fluorescent heterozygous male and non-fluorescent female. The difference between the survival of fluorescent and non-fluorescent embryos was compared between groups 1 and 3, and between groups 2 and 4 and examined statistically with chi-square test. The asterisks indicates significant increase in the survival rate of fluorescent embryos ($p<0.005$).

For an unknown reason, fluorescent embryos had a higher survival rate than the non-fluorescent embryos in both the control and the test groups. However, the difference between the survival of fluorescent and non-fluorescent embryos (larvae) in the test group was significantly higher, compared to the control group, for the three mutants: jar^{R39}, jar^{R70} and jar^{R235}. When a cross was set with female fluorescent heterozygous flies (group1), the embryos survival rate was slightly higher than in the reciprocal cross, suggesting that maternal GFP protein could contribute to the survival of the embryos. The survival rate of all the embryos was lower than the expected. This could be related to the decrease in viability due to the manual collection of the embryos and extensive handing to check fluorescence. The survival rate of *OrR* flies collected was 74% (data not shown), indicating that at least 25% of the flies die due experimental procedures.

In jar^{R235} the increase in the survival rate of the fluorescent flies in cross 1 at the test group was not significantly higher than in control group 3. This could be related to the increase in the survival rate of fluorescent embryos in control group, 3.

In the mutant jar^{R23} the expression of PGM in the test groups did not increase significantly the survival rate of the fluorescent embryos. A Western blot analysis that was made for all the four mutants, at late stages of embryogenesis showed that the homozygous mutant embryos jar^{R23}/jar^{R23} and jar^{R70}/jar^{R70} had reduced level of Myosin VI compared to wild-type embryos, while in the embryos jar^{R39}/jar^{R39} and jar^{R235}/jar^{R235}, no Myosin VI was detected (Millo et al., 2004). In addition, the survival rate of the jar^{R23} non fluorescent mutants was higher than the one in the rest of the mutants. It seems that the reduced level of Myosin VI in jar^{R23} homozygous mutant embryos is sufficient for them to survive, and the expression of PGM does not make a significant contribution their survival, while in the mutants lacking Myosin VI, (jar^{R39} and jar^{R235}) the expression of PGM is vital for their survival.

In jar^{R70}, the increase in the survival rate changed significantly only in test cross 1. It is possible that the maternal contribution of PGM helped the survival of the mutant embryos in this cross.

Taken together, these results show that the expression of PGM rescues the embryonic lethal phenotype in at least one of the test groups of jar^{R39}, jar^{R70} and jar^{R235} mutants.

4.6.2 Study 2: PGM rescues male sterility phenotype in the heteroallelic mutants: jar^{R39}/jar^{mmw14}, and jar^{R235}/jar^{mmw14}

Myosin VI is necessary during sperm individualization for the creation of the individualization complex. In the mutant jar^{mmw14}, Myosin VI is not expressed in the testes, as a result, the individualization complexes are not created properly and the male flies are sterile (Hicks et al., 1999). The homozygous mutants: jar^{R39} and jar^{R235} are embryonic lethal, however, when crossed with jar^{mmw14}, these heteroallelic lines survive until adulthood. Because the mutations in the three mutants are located in the same region of the Myosin VI molecule, jar^{R39} and jar^{R235} cannot complement the male sterility phenotype of jar^{mmw14}, and as a result, jar^{R39}/jar^{mmw14}, and jar^{R235}/jar^{mmw14} males are sterile (Millo et al., 2004), and chapter 5). Previous experiment showed that the expression of Myosin VI cDNA restores the fertility phenotype of jar^{mmw14} homozygous males (Hicks et al., 1999). In this experiment I tested whether the expression of PGM could also rescue the sterility phenotype of the heteroallelic mutants.

The rescue of the embryonic lethal phenotype described in the previous section proved statistically that PGM rescues the embryonic lethal phenotype. In this test, because none of the heteroallelic flies are fertile, if PGM restores fertility, it will show clearly that PGM functions as a native Myosin VI.

The creation of heteroallelic flies, which will express PGM in the testes, is described as follows (described for jar^{R39}):

Fluorescent heterozygous female flies jar^{R39} and jar^{R235} (created in the previous test, in the last cross), were crossed with the male heterozygous mutant: jar^{mmw14}. As mentioned previously, jar^{R39} and jar^{R235} have a Gal4 gene expressed in the testes individualization complex. All the mutants are balanced over the TM3 chromosome, having the dominant phenotype Stubble.

$\frac{+}{y}$;; $\frac{jar^{mmw14}}{TM3, Sb, e^{+}}$	X	$\frac{UAS\text{-}PGM}{+}$;; $\frac{P[W^{+}(GAL4)]^{jarR39}}{TM3, Sb, e^{+}}$
Heterozygous mutant White - eyed, Stubble, adult male		Heterozygous mutant fluorescent in testes Stubble, adult female

In the progeny, male and female flies were created, having four different combinations in the third chromosome from this cross (for simplicity $P[W^+(GAL4)]^{jarR39}$ was written as jar^{R39}):

$\frac{jar^{R39}}{jar^{mmw14}}$	$\frac{jar^{mmw14}}{TM3,\ Sb,\ e^+}$	$\frac{jar^{R39}}{TM3,\ Sb,\ e^+}$	$\frac{TM3,\ Sb,\ e^+}{TM3,\ Sb,\ e^+}$
heteroallelic mutant non-Stubble adult	heterozygous mutant Stubble adult	heterozygous mutant Stubble adult	homozygous lethal

The heteroallelic mutant differs from the heterozygous mutants by having non-Stubble bristles in the adult fly.

Therefore two groups of heteroallelic male were selected:

1. $\frac{UAS\text{-}PGM;;}{y}\ \frac{P[W^+(GAL4)]^{jarR39}}{jar^{mmw14}}$

Adult male, non-stubble, fluorescent in testes

2. $\frac{+;;}{y}\ \frac{P[W^+(GAL4)]^{jarR39}}{jar^{mmw14}}$

Adult male, non-stubble, non-fluorescent

The fluorescent and non-fluorescent heteroallelic males were tested for fertility by crossing them with *OrR* virgin females. The following table summaries the No. of crosses made with each heteroallelic fly and the Number of fertile males in every group (for simplicity $P[W^+(GAL4)]^{jarR39/235}$ was written as $jar^{R39/235}$).

Table 4.6.2: results of mutant rescue test 2

	jar^{R39}/jar^{mmw14}		jar^{R235}/jar^{mmw14}	
	Fluorescent	**Non fluorescent**	**Fluorescent**	**Non fluorescent**
No. of crosses	**11**	**1**	**20**	**14**
Fertile	**9**	**0**	**18**	**0**
Sterile	**2**	**1**	**2**	**14**

The non-fluorescent heteroallelic male were sterile as expected, while the majority of the fluorescent males were fertile: 9 males out of 11 were fertile in jar^{R39}/jar^{mmw14} mutants, and 18 out of 20 males were fertile in jar^{R235}/jar^{mmw14}. These results show that the expression of PGM in the heteroallelic flies rescued their male sterility phenotype.

When the testes of heterozygous male $jar^{R39}/TM3$ were stained with Myosin VI antibody and phalloidin, the expression of Myosin VI in the individualization complexes was obvious (Fig. 4.6.2.1 A-C); however Myosin VI or phalloidin were not detected in antibody stain in the heteroallelic mutant males (Fig. 4.6.2.1 D-I). Myosin VI is necessary for the proper formation of the individualization complex (Fig. 1.3.1B in Introduction). Previous studies showed that in the mutant jar^{mmw14}, the actin filaments are present, however the actin cone is not organized properly (Hicks et al., 1999). A very weak stain of the actin filaments appeared also in the individualization complexes of the double mutant Myosin VI-Dynamin (*shi 1 /Y;* jar^{1}/jar^{1}) (Rogat and Miller, 2002). Perhaps the stability of the actin filaments is dramatically reduced when the two *jar* alleles are present.

In the fluorescent heteroallelic flies, PGM was expressed in the individualization complex (Fig. 4.6.2.2). The localization of PGM in the individualization complex of heteroallelic flies was similar to that of PGM and native Myosin VI, in the individualization complex of the fertile heterozygous flies $jar^{R39}/TM3$ (Fig. 4.6.2.3): PGM appeared in the all the individualization complexes, concentrated mainly at the base of the cone. In addition, the actin filaments appeared in the individualization cones of the heteroallelic flies, although their staining was weaker than the one in $jar^{R39}/TM3$. We conclude that the expression of PGM in the testes of the heteroallelic flies allowed the creation of the individualization complexes in their proper form, the maturation of the spermatides and the recovery of the sterility in the heteroallelic males. These results show that PGM functions like the native Myosin VI, therefore the tagging of Myosin VI in its C terminus with GFP does not disturb its function.

In figures 4.6.2.1-4.6.2.3, *P[W$^+$(GAL4)]^{jarR39}* and *P[W$^+$(GAL4)]^{jarR235}* are written as *jar^{R39}* and *jar^{R235}* for simplicity.

Figure 4.6.2.1: The expression of Myosin VI and actin in the individualization complexes of the testes. In the heterozygous males jar^{R39} /TM3, Myosin VI and actin co-localise in the individualization complexes (IC, arrows in A-C), however no expression of Myosin VI nor actin are observed in the heteroallelic flies *jar^{R39} /jar^{mmw14}* (D-F,) and *jar^{R235}/jar^{mmw14}* (G-I).

Figure 4.6.2.2: PGM expression in the individualization complexes of the fluorescent heteroallelic males *UAS-PGM;;jar^{R235}/jar^{mmw14}*(**A-C**) and *UAS-PGM;;jar^{R39}/jar^{mmw14}*(**D-F**).

Figure 4.6.2.3: A similar pattern of antibody stained Myosin VI (**A-C**) and PGM (**D-F**) was observed in the fertile heterozygous male: *jar^{R39}/TM3*. Myosin VI and PGM are expressed mainly at the base of the individualization cone. A similar localization of PGM appeared in the heteroallelic flies (Fig. 4.6.2.2).

Figure 4.6.2.1

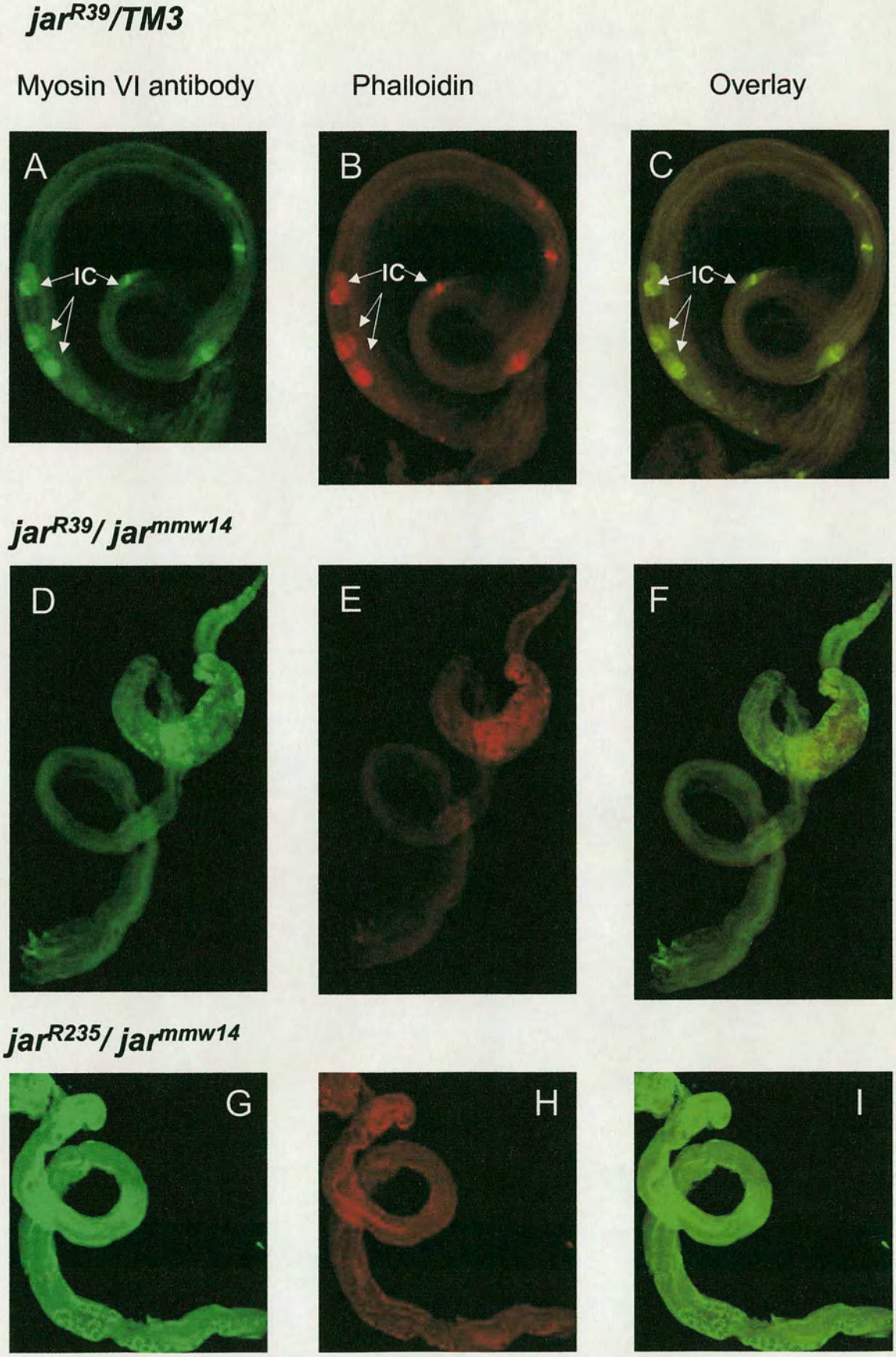
jar^R39/TM3
Myosin VI antibody
Phalloidin
Overlay
A
IC
B
IC
C
IC
jar^R39/ jar^mmw14
D
E
F
jar^R235/ jar^mmw14
G
H
I

Figure 4.6.2.2

PGM; ; jar^{R235}/mmw14

GFP (PGM)

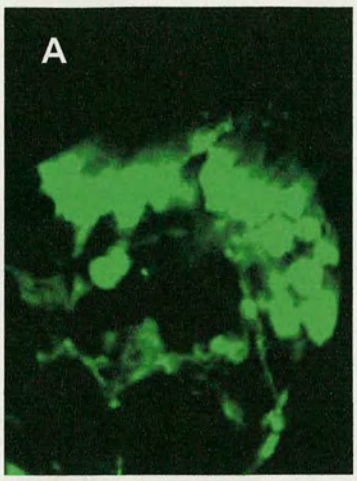

Phalloidin

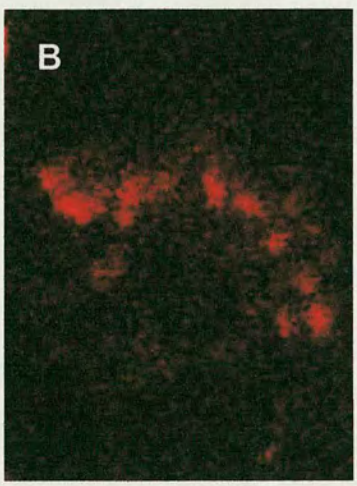

Overlay

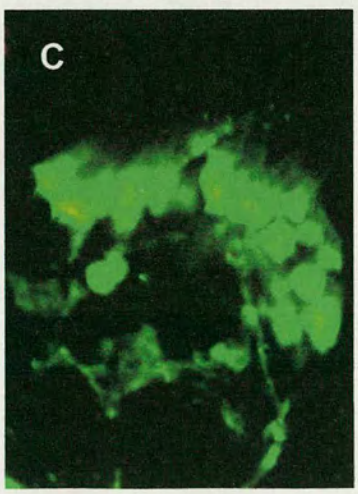

PGM; ; jar^{R39}/mmw14

GFP (PGM)

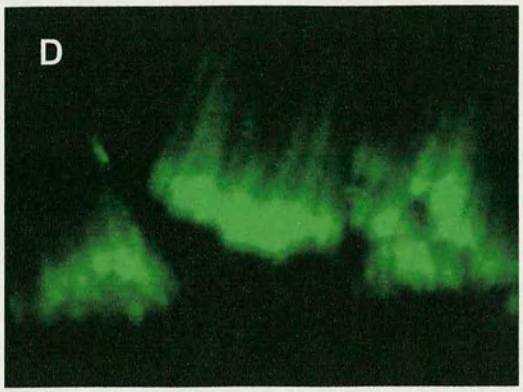

Phalloidin

Overlay

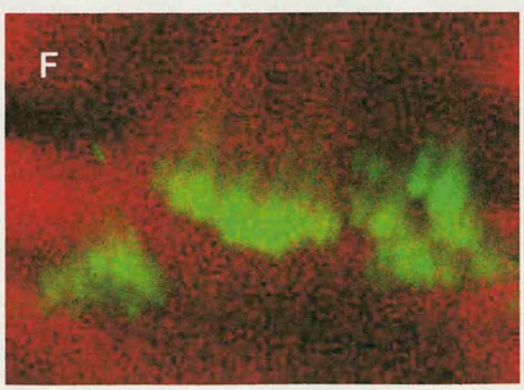

Figure 4.6.2.3

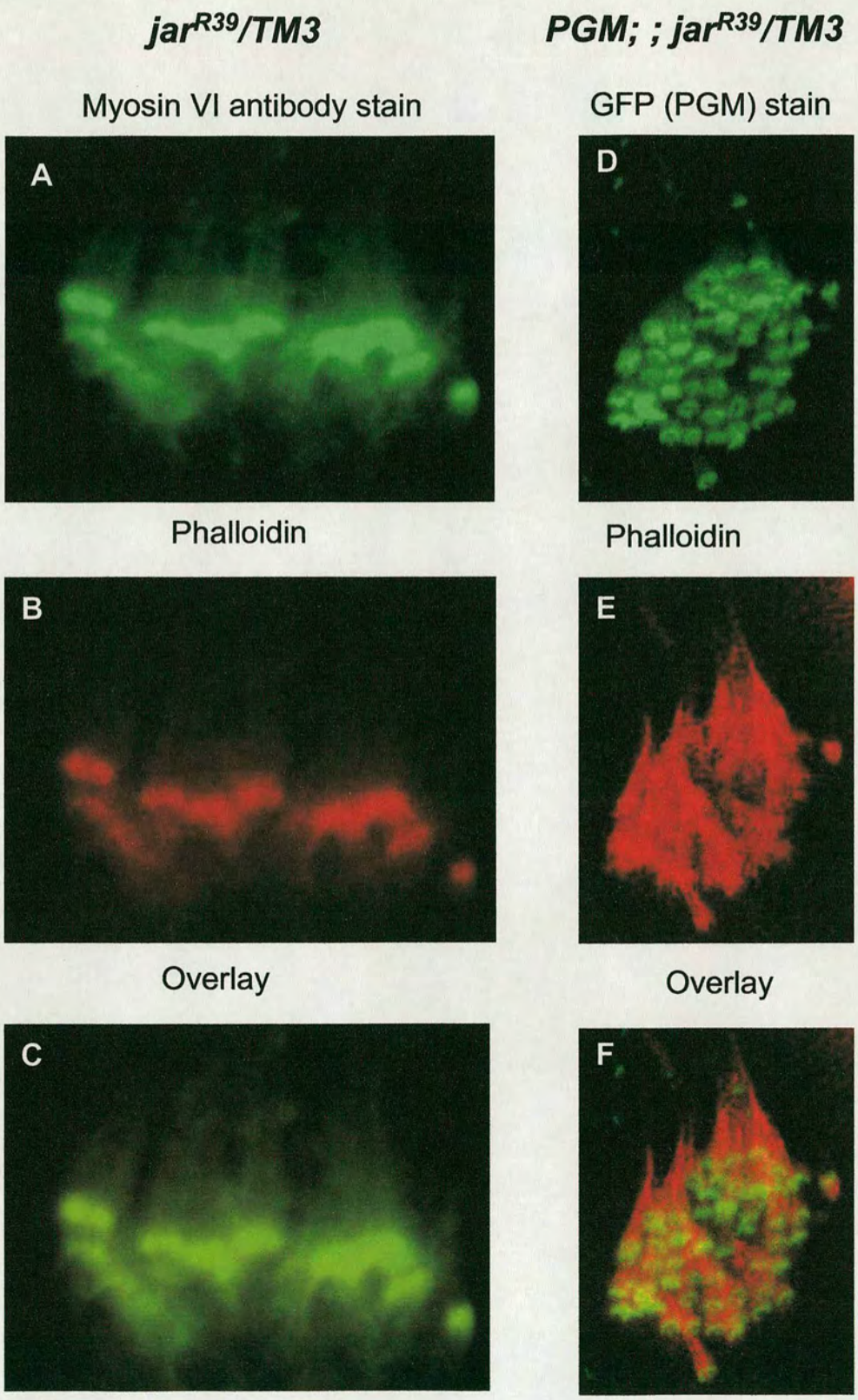
jar^R39/TM3
PGM; ; jar^R39/TM3
Myosin VI antibody stain
GFP (PGM) stain
A
D
Phalloidin
Phalloidin
B
E
Overlay
Overlay
C
F

4.7 Comparison of PGM, PGMH and PGMT expression patterns

The expression of the head, the tail and the whole Myosin VI, tagged to GFP was made in order to have a better understanding of how Myosin VI and its domains function in different tissues during development. After expressing the three proteins, tissues that showed obvious differences in the expression pattern of the three constructs were examined further. By comparing the location of the separate domains with the location of the whole myosin it became possible to conclude about the location of the region in which the tail domain binds to the cargo, the region where the head domain binds to the actin filaments, and which domain determines the final localization of Myosin VI within the cells. This can also give us a clue to how Myosin VI functions in the cells.

4.7.1 The location of the PGM, PGMH and PGMT in the salivary glands.

One of the epithelial tissues that showed the most striking differences in the expression pattern of the head, the tail, and the whole Myosin VI, was the salivary gland. This tissue had the highest expression intensity of Myosin VI, and since it contains big cells, it was relatively easy to observe the differences between constructs.

The whole Myosin VI is present in the cytoplasm and in the cell membrane (Fig. 4.7.1.1 A-C). PGM was excluded from the cell nucleus. In contrast, the head domain was present in the nucleus, but excluded from the nucleolus. PGMH has also a strong expression in the cell membrane (Fig. 4.7.1.1 D-F). The tail domain had a similar localization in the cell to the whole Myosin VI, although its expression was weaker: it was found in the cytoplasm and the cell membrane, but not in the nucleus (Fig. 4.7.1.2 A-C).

Because the head domain contains the motor domain that moves along actin filaments, PGMH is expected to co-localize with actin filaments. Therefore the salivary gland expressing PGM, PGM and PGMT were stained with phalloidin. Surprisingly, in the early stages of the third larval instar, the actin filaments showed

a complete co-localization with the expression pattern of the three different proteins, and the expression intensity of actin was proportional to the expression intensity of the fusion proteins: in salivary glands expressing the whole Myosin VI (PGM), the actin filaments were present mainly in the cell membrane and at lower levels in the cytoplasm, but excluded from the nucleus. When the head domain was expressed, a strong expression of the actin filaments appeared in the cell membrane and the cell nucleus surrounding the nucleolus (Fig. 4.7.1.1 D-F). At a later stage, the actin filaments surrounded the nucleus, which still contained the PGMH protein (Fig. 4.7.1.1G-I). When the tail domain was expressed, a net of actin and tail domain was created in the cytoplasm, surrounding the nucleus (Fig. 4.7.1.2 D-F, arrows). The actin filaments also had a strong expression at the cell membrane, where the tail domain was also present. These results were surprising. Not only that the head domain was localised in the cell nucleus, but that the actin filaments organization was also affected and followed the localization of the head domain.

When the entire Myosin VI is expressed on its own, the filaments are not created within the nucleus. This fact may indicate that the head domain plays a part in the creation of the actin filaments. Similarly, the ring created around the nucleus when PGMT was expressed, was absent when the whole Myosin VI was expressed (PGM), suggesting that in the salivary gland cells, Myosin VI plays a role in directing actin filament polarization.

Figure 4.7.1.1: The expression of the whole myosin (PGM) and the head domain (PGMH) in the salivary gland cells during third instar larvae. PGM has a strong expression in the cell membrane and a weaker expression in the cell cytoplasm (**A, C**). PGM also is located at the periphery of the nucleus. The actin filaments co-localised with PGM in the cell membrane and the cytoplasm, although at the ring of PGM surrounding the nucleus, the co-localization is weaker (**B, C**). In the early third larval instar, the head domain, expressed by PGMH, is localized within the cell nucleus, but not in the nucleolus, and the actin filaments are also located in the nucleus, and co-localise with PGMH in the entire cell (**D-F**, arrowhead). In later stages, prior to pupariation, actin filaments surround the nucleus while the head domain remains in it (**G-I**).

Figure 4.7.1.2: The expression of the tail domain (PGMT) in the salivary gland cells during the third larval instar. Like PGM, PGMT has a strong expression in the cell membrane and a weaker expression in the cytoplasm, with no expression in the nucleus (**A, C**, arrows). The actin filaments co-localise with PGMT at the cell membrane (**B**). In the cytoplasm there is an area circling the nucleolus, where PGMT is localised at higher concentration (**D-F**, arrows), and the actin filaments co-localise with PGMT in this area. PGMT had weaker expression than PGMH and PGM.

Figure 4.7.1.1

PGM expression

PGM | actin | overlay

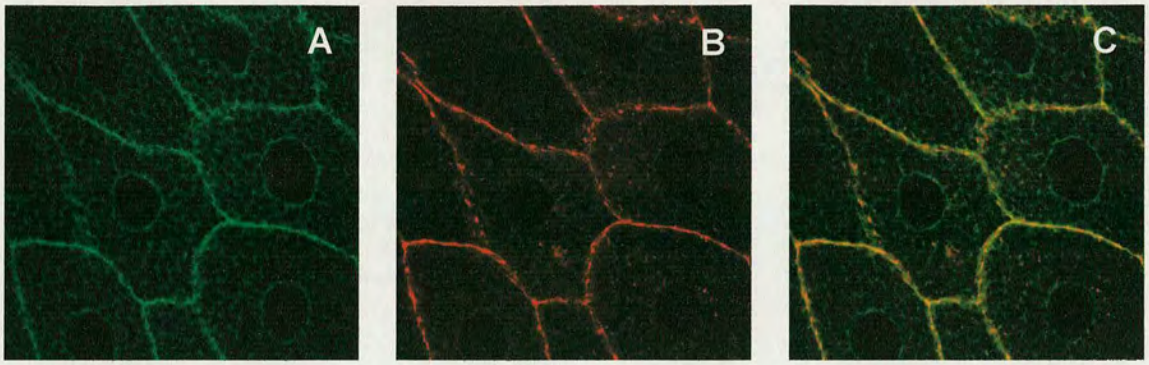

PGM 22-3 X C865

PGMH expression

Third instar-early stage

PGMH | actin | overlay

third instar-late stage

PGMH 181-3 X C865

Figure 4.7.1.2

PGMT expression

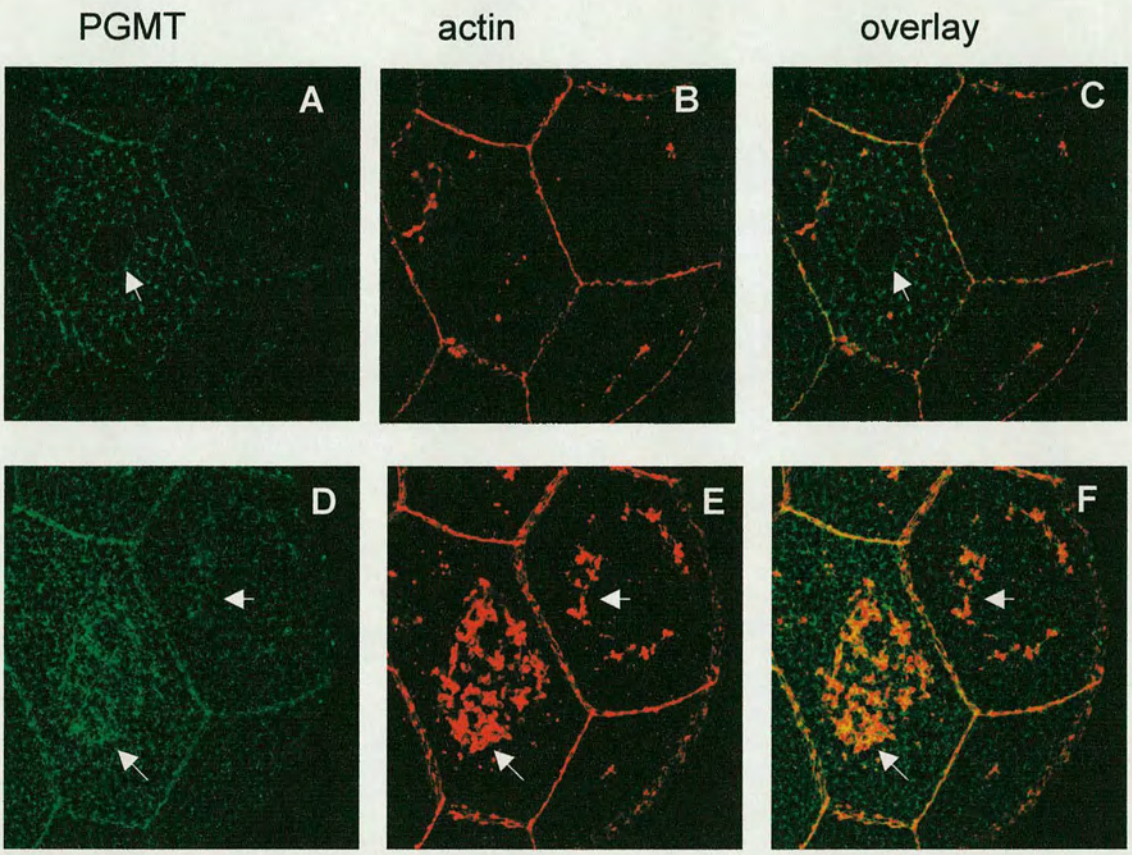

PGMT 33-2 X C865

PGMH is bigger than PGMT (130kd compared to 75kd approximately), therefore if PGMH could enter the nucleus through diffusion, HGMT would also be able to enter the nucleus. This suggests that the entry of PGMH into the nucleus is directed by the movement of the head domain to the minus end, of the actin filaments, which face towards the inner part of the cells (see discussion). Perhaps the tail domain interacts with other proteins and the whole protein complex anchors the tail away from the nucleus.

The different locations of the head domain and the tail domain in the cytoplasm can represent two different forces that are applied to the Myosin VI molecule in the salivary gland cells: the head domain pulls the molecule to the cell nucleus and the tail domain is concentrated in the cytoplasm mainly in a sphere surrounding the nucleus but slightly distant to it. The whole Myosin VI has a uniform expression in the cytoplasm, without clustering like the tail domain. This could suggest that the location of Myosin VI in the cytoplasm is dynamic and in equilibrium between the two different forces applied.

It is not clear why the clustering of PGMT around the nucleus is created. It is possible that this is the region where the cargo is located. In the cell cortex, the whole Myosin VI and its separate domains were localised, the head domain attached to the cortical actin, and the tail domain to the cargo. The similar localization of the different domains shows that in this region there are no forces that attract the domains in separate directions. Perhaps this is the last destination of the cargo molecules. Alternatively, Myosin VI could be playing a different role in this region, keeping the cargo attached to the cell membrane rather than dragging the cargo through the cell.

The exclusion of PGM and PGMT from the nucleus suggests that the tail domain is the part that anchors the whole myosin away from the nucleus. This phenomenon is also observed in other tissues such as: in the follicle cell epithelium and the embryonic epidermis.

4.7.2 The location of PGM, PGMH and PGMT in the follicle cells during oogenesis.

During oogenesis, the whole Myosin VI and the tail domain are expressed in the cell membrane and the cytoplasm, but not in the nucleus (Fig. 4.5.5, F., 4.7.2.1). In the columnar and centripetal follicle cells, PGMH is strongly expressed in the cell nucleus. In order to test whether or not the different localization of the head, the tail and the whole Myosin VI affect the organization of actin filaments within cells, ovaries expressing the three different fusion proteins were stained with phalloidin (Fig. 4.7.2.1 F-H). In columnar cells expressing PGM (F), PGMT (G), or PGMH (H) the actin filaments appeared at the cell membranes, without any significant change in their organization, suggesting that unlike the salivary gland cells, the expression of the head and the tail domain did not affect the normal organization of the actin filaments. Possibly the changes in actin organization are more difficult to observe in the follicle cells, which are much smaller.

Figure 4.7.2.1: A-C: The expression of the head domain (PGMH) in the columnar and centripetal follicle cells. The head domain is strongly expressed in the nucleus, but not in the nucleolus (arrow), and a weaker expression is seen in the cell membrane and the cytoplasm. In the centripetal cells at the anterior of the oocyte, the strong expression of PGMH in the nucleus is not obvious, possibly due to the strong expression of PGMH over the entire cell. **D-E**: The tail domain (PGMT) is localised in the cell membrane and the cell cytoplasm and excluded from the nucleus. PGMT had weaker expression than PGMH and PGM, and the protein appeared in punctate form. In figures **A-E** PGMH and PGMT were crossed with the Gal4 line *T155* that had a stronger expression in the follicle cells. Figures **F-H**, show columnar follicle cells of ovaries expressing PGM (F), PGMT (G) and PGMH (H), stained with phalloidin to view the actin cytoskeleton. The whole Myosin VI (F) and the tail domain (G) show a similar pattern of expression in the cell cytoplasm and the cell membrane, while the head domain (H) has a strong expression in the nucleus. The different pattern of expression did not significantly change the organization of the actin filaments: the actin filaments appeared in the cell membrane, and the expression of the head domain did not trigger actin polymerisation in the nucleus. The head domain had the strongest co-localization with actin filaments (H)

Figure 4.7.2.2: The expression of PGM, PGMH and PGMT at the leading edge of the border cells. Figure **A** shows the border cells with a strong expression of PGM at the leading edge, as they arrive at the nurse-cell-oocyte border. Figures **B, E**, and **H** show the expression of the whole Myosin VI (PGM), the head domain (PGMH), and the tail domain (PGMT), respectively. Figures **C, F** and **I** show the location of the actin filaments in the respective cells and the overlay images are shown in **D, G** and **J**. **B-D**: When the whole Myosin VI is expressed, it has a strong expression in the leading edge and some expression in the cell cytoplasm. **F-G**: The head domain shows a weaker expression in the leading edge and more expression in the cell cytoplasm. **H-J**: At some levels of focus the tail domain has a strong expression in the leading edge only. The actin filaments co-localise with the leading edge of all the proteins, but the tail domain and the whole Myosin VI were more concentrated in the region of the actin filaments.

Figure 4.7.2.1

PGMH

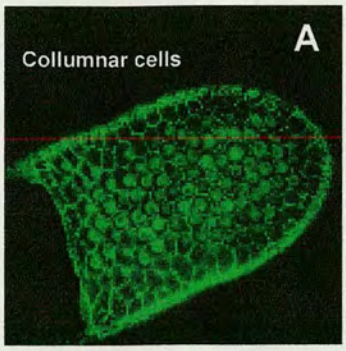

PGMH 57-1XT155

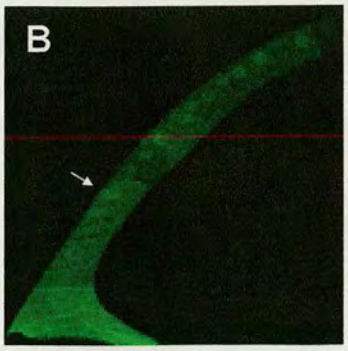

PGMH 181-3XT155

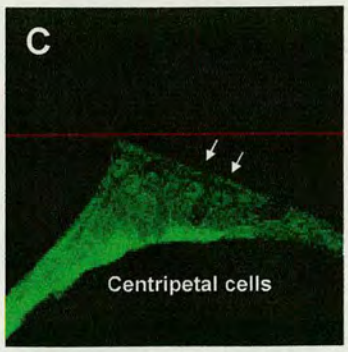

PGMH 197-1XT155

PGMT

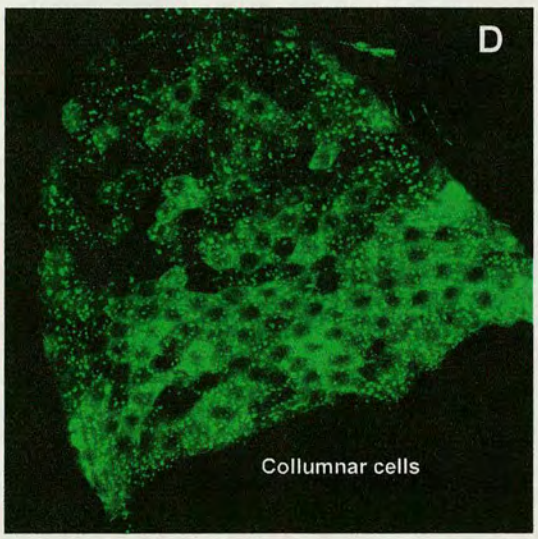

PGMT 33-2XT155

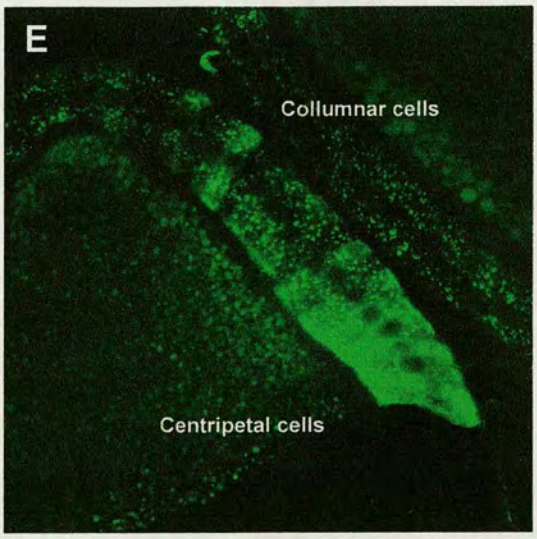

PGMT 33-2XT155

Expression of PGM/H/T in Collumnar follicle cells

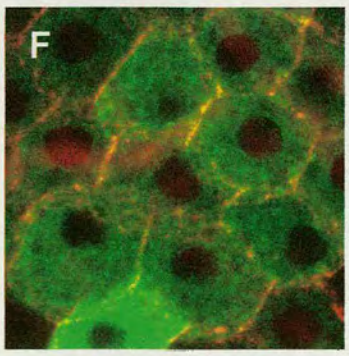

PGM 22-3 X C865

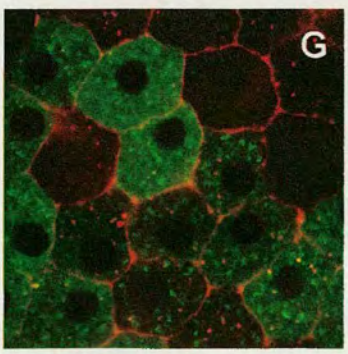

PGMT 33-2 X C865

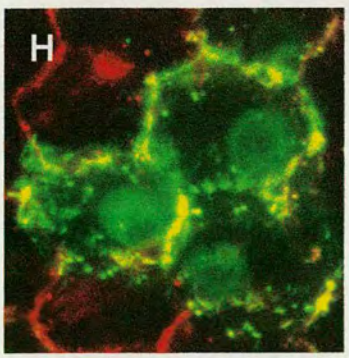

PGMH 181-3 X C865

Figure 4.7.2.2

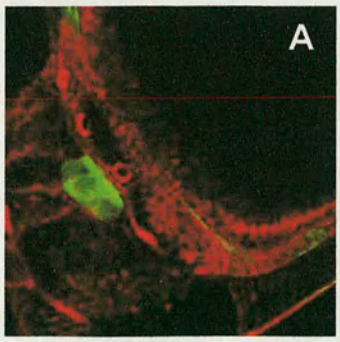

PGM Phalloidin Overlay

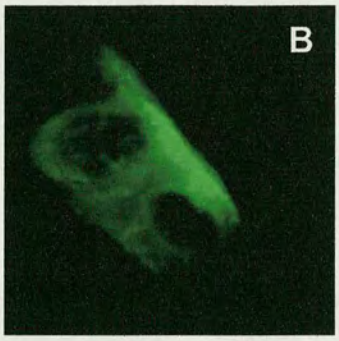

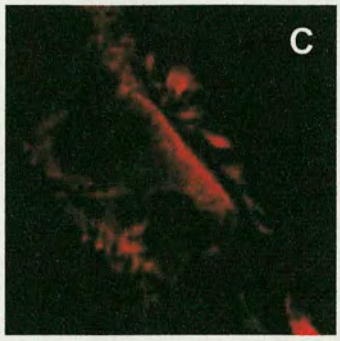

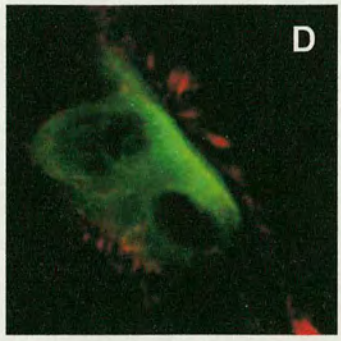

PGM 22-3X C865

PGMH Phalloidin Overlay

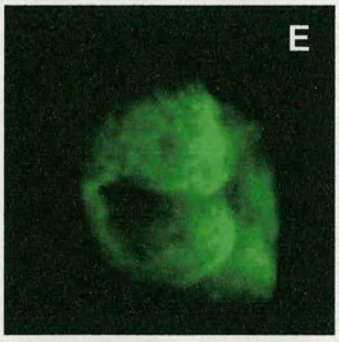

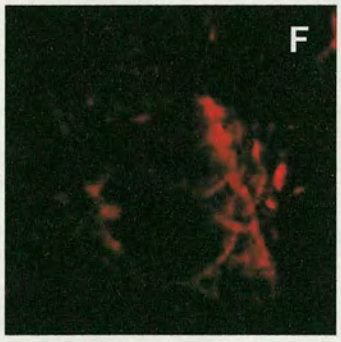

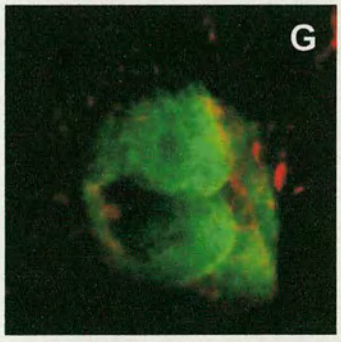

PGMH 181-3 X C865

PGMT Phalloidin Overlay

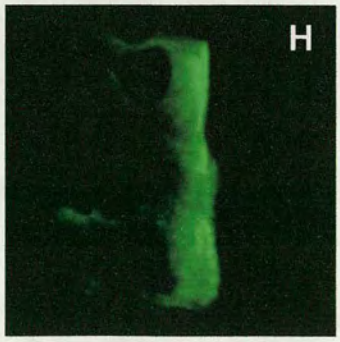

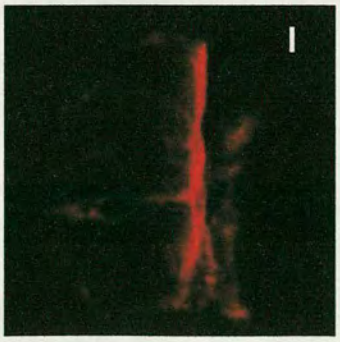

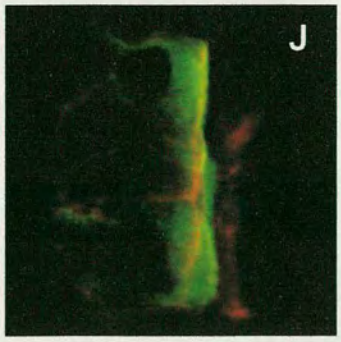

PGMT 33-2 X C865

PGMT had a weaker expression and appeared in a punctate form. This pattern also appeared in other tissues. Initially it seems that PGMT forms random aggregates, but as discussed in section 4.8, the tail domain co-localised with cargo molecules that genetically interact with Myosin VI within the cell.

As the border cells migrate, the expression pattern of PGM, PGMH and PGMT within the cells was similar: the proteins were localised in the cell cytoplasm. Antibody staining and PGM expression showed that when the border cells arrive at the nurse cell-oocyte border, a stronger expression of Myosin VI is observed at the leading edge, and the protein at the leading edge co-localises with the actin filaments at the border. Figure 4.7.2.2 shows border cells arriving to the nurse cell-oocyte border. The three proteins were expressed in the cell cytoplasm; however PGM and PGMT had a stronger expression at the leading edge.

The photographs presented are taken from sections showing the strong expression of the proteins at the leading edge, and are compared with the localization of the actin filaments. PGM has a strong expression at the leading edge and it co-localises with the actin filaments (Fig. 4.7.2.2 A-D). PGMH is spread throughout the cell cytoplasm, but also shows expression at the leading edge (Fig. 4.7.2.2 E-G). In contrast, the tail domain (PGMT) is localized in an organized area at the leading edge, which co-localises with the actin filaments (Fig. 4.7.2.2 H-J).

Myosin VI is necessary for the migration of the border cells: disruption in its expression significantly inhibits cell migration (Geisbrecht and Montell, 2002). However, the strong expression of Myosin VI at the leading edge of the border cells appeared mostly as the migration was ending. This suggests that the strong expression of Myosin VI in the leading edge may be connected the borders cells ceasing migration.

The expression of the tail domain at the leading edge, where the actin filaments are localised, is probably the region where Myosin VI binds to its cargo. It seems that when the border cells migrate, Myosin VI is spread though the cell cytoplasm, and as the migration stops, Myosin VI is blocked by attachment of the tail domain at the leading edge to a specific cargo at the nurse cell-oocyte border. DE-cadherin and Armadillo are necessary for the migration of the border cells, but not for the recruitment of the cells to the nurse cell-oocyte border (mutations in the genes encoding these proteins have reduced border-cell migration, but not invasion into the oocyte (Montell, 2003). Perhaps there are other proteins that anchor of the border cells to the oocyte-nurse cell border, and these affect the concentration of Myosin VI at the leading edge.

4.7.3 The location PGM, PGMH and PGMT in the epidermal cells at the leading edge during dorsal closure

During embryogenesis Myosin VI is expressed and necessary for the process of dorsal closure (Kellerman and Miller, 1992; Millo et al., 2004) and see chapter 5). Throughout dorsal closure, PGM expression shows that the whole Myosin VI is located in the cells at the leading edge and in the amnioserosa (Fig. 4.5.1A and 4.7.3A). Within the cells at the leading edge, PGM is localised in the cytoplasm and the cell membrane and excluded from the nucleus (4.7.3 A see magnification). PGMH shows a strong expression of the head domain in the cell membrane and co-localization with the actin filaments (Fig. 4.7.3 B-C, see magnifications).

Figure 4.7.3: The pattern expression of the head, the tail and the whole Myosin VI in the embryos, during dorsal closure. All the embryos were stained with phalloidin to visualize the actin filaments. **A**: In the leading edge cells, the whole Myosin VI (PGM) is expressed in the cell cytoplasm and the cell membrane and excluded from the nucleus. **B-C**: The head domain is strongly expressed in the cell membrane of the epidermal cells, where it co-localise with the actin filaments (see magnifications). The expression of PGMH in the cell is observed in the cytoplasm and the nucleus, although it does not seem to be concentrated in the nucleus. The tail domain (**D**, PGMT) localizes to the cell membrane and cell cytoplasm. At the apical surface of the cells PGMT has a strong expression (see magnification).

Figure 4.7.3

PGM

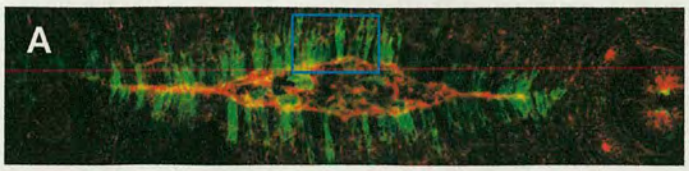

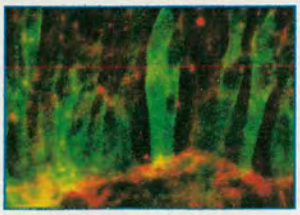

PGM 43-2 X C865

PGMH

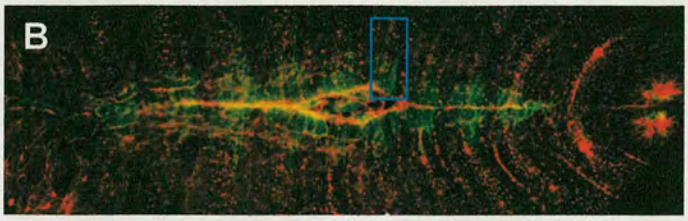

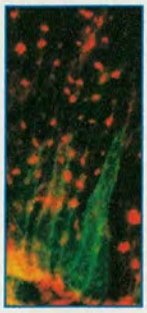

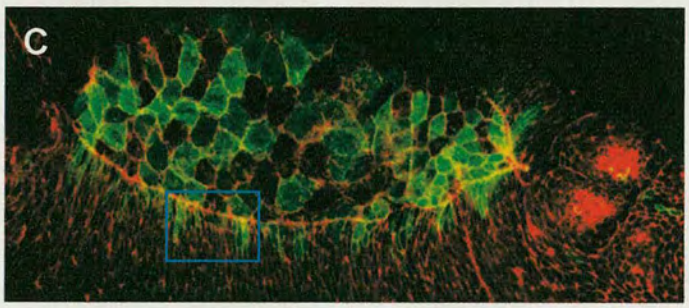

PGMH 181-3 X C865

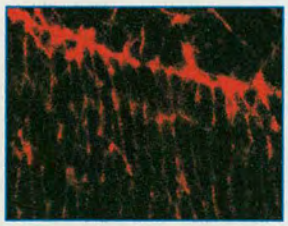

Phalloidin

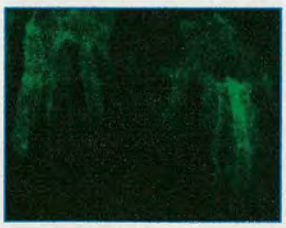

PGMH

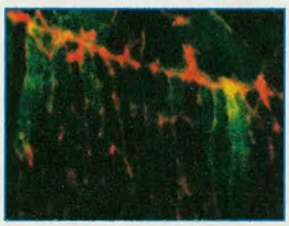

Overlay

PGMT

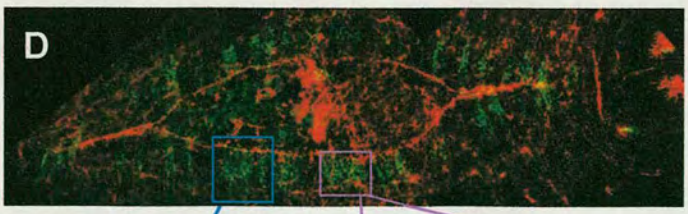

PGMT 33-2 X C865

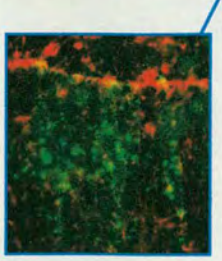

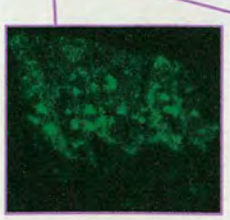

Upper section

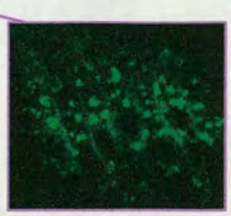

Lower section

The head domain is also located in the cytoplasm, but it is not excluded from the nucleus. PGMT was localised in the leading edge cells, in the membrane and cytoplasm and excluded from the nucleus. When looking at the apical surface of the cells, PGMT has a strong expression at the cell surface, mainly in the area closer to the leading edge. Thus we assume that the cargo of Myosin VI is located in high concentration at the apical surface of the cells. Antibody staining of Myosin VI showed a strong expression of Myosin VI at the apical surface of the cells at the leading edge, suggesting a possible role in maintaining the rigidity of the cells as they move and cover the amnioserosa. Because PGMT is expressed in cells that also have normal Myosin VI, PGMT can bind to the cargo as the cargo migrates or at its final destination. If Myosin VI is necessary for the localisation of its cargo to a specific place, it could be assumed that if would have a strong expression at its final destination, therefore, the strong expression of Myosin VI and PGMT at the apical surface of the cells could indicate that this it the one of the destinations to which Myosin VI brings its cargo.

In the amnioserosa PGM and PGMH had a similar expression pattern although the exclusion from the nucleus was slightly stronger in PGM (Fig. 4.7.3 A and C). PGMT had a very weak expression in the amnioserosa (Fig. 4.7.3 D).

As in other tissues, PGM and PGMT are excluded from the cell nucleus. This indicates that it is the tail domain that anchors Myosin VI away from the nucleus.

The expression of PGMH is not localisaed at the cell nucleus but rather at the cell membrane. When Myosin VI function is disrupted, the cells at the leading edge and the amnioserosa start to detach. This suggests that the direction of Myosin VI to the cell surface by the head domain could be necessary for the role of Myosin VI in cell-cell adhesion.

4.7.4 The location of the head, the tail and the whole Myosin VI in the individualization complex of the testes.

During sperm individualization, Myosin VI is expressed in the individualization complex and is necessary for the building of an individual membrane every created spermatid (Hicks et al., 1999; Rogat and Miller, 2002). In order to compare the localization of the head, the tail and the whole Myosin VI in the individualization complex, I have compared their expression to that of Dynamin. Dynamin functions along with Myosin VI in the regulation of actin dynamics in the individualization complex. Dynamin is localised along the length of actin cones, and a double staining of Myosin VI and Dynamin showed localization of Myosin VI at the front of the Dynamin-stained cones (Rogat and Miller, 2002). The Dynamin – stained cone allow us to compare the localization of the head and the tail domain. When PGM was expressed (Fig. 4.7.4 A-C), it was localised at the front of the Dynamin-stained cone, and several pictures showed that there is also some expression of PGM along the actin cone (Fig. 4.5.4. G), like the native Myosin VI. The head domain (PGMH) was localised along the Dynamin-stained cone, and in front of the cone. This suggests that the head domain is attached to actin filaments along the cone (Fig. 4.7.4 D-F). The tail domain was localised at the front part of the cone, some of it localised at the base of the cone and some localised on the cone itself (Fig. 4.7.4 G-I). Taken together it seems that the tail domain, attached to its cargo, anchors the whole Myosin VI to the base of the cone, while the head domain is attached to the actin filaments and pulls the whole molecule towards the base of the cone, where Myosin VI would interact with the actin polymerisation regulatory proteins: Arp2/3 and Cortactin (Rogat and Miller, 2002).

Figure 4.7.4: The expression of Myosin VI, the head and the tail domain in the individualization complexes during spermatogenesis. Testes expressing PGM (**A-C**), PGMH (**D-F**) and PGMT (**G-I**) were stained with Dynamin, which is located along the actin cone, in order to compare the localization of each protein. **A-C**: The whole Myosin VI is localised at the base of the cone. **D-F**: The head domain is localised along the actin cone. **G-I**: The tail domain is localised mainly at the base of the actin cone, with some expression along the lower part of the cone.

Figure 4.7.4

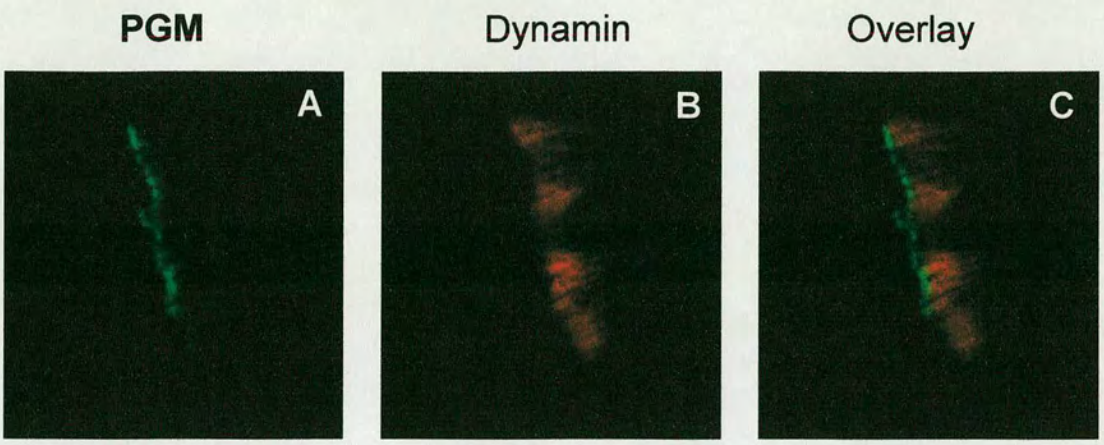

PGM 22-3X C865

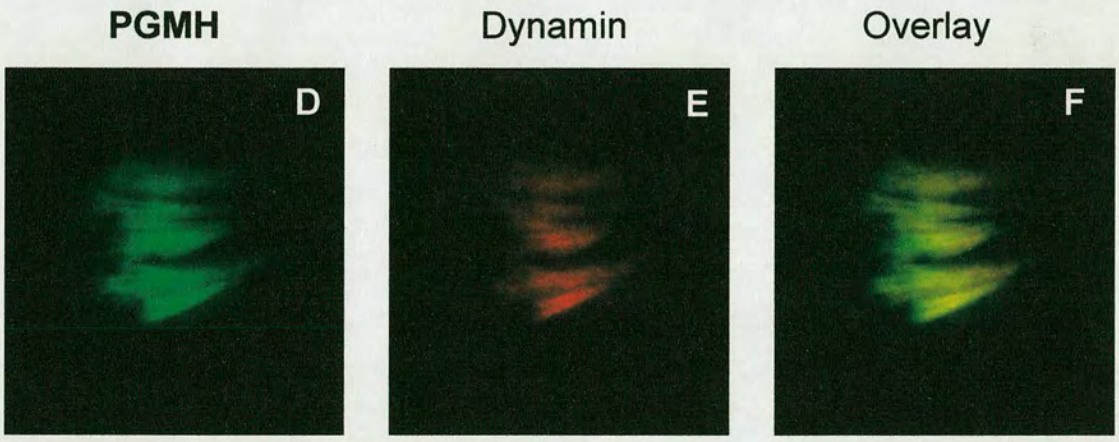

PGMH 181-3 X C865

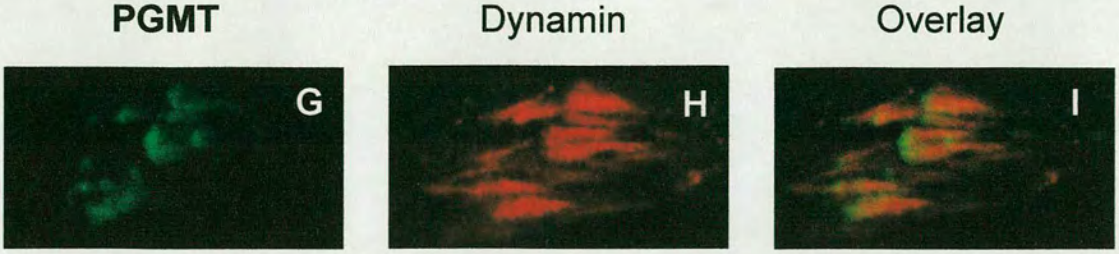

PGMT 33-2 X C865

Myosin VI was found to co-localise with Capping Protein, at the base of the cone (Rogat and Miller, 2002). Capping Protein is localised at the growing plus, barbed-end of the actin filaments, where it regulates actin polymerisation. Therefore the plus end of the actin filaments is located at the base of the cone. It was surprising to find that Myosin VI was located at the barbed end and not at the pointed end. However, the anchoring of the tail domain to the base of the cone as it is observed here can explain the orientation of Myosin VI at the base of the actin cone, at the barbed end of the actin filaments.

4.8 The tail domain co-localizes with proteins interacting with Myosin VI during oogenesis.

When looking at the expression of the tail domain (PGMT) in the egg chambers and in other tissues it is punctate, suggesting the presence of aggregates in the cell cytoplasm. The specific localization of the tail domain in the testes and the epithelial cells suggest that the tail in PGMT functions in a similar way to the regular tail domain. Why does the tail domain form aggregates in the cell cytoplasm? It seems possible that the aggregates of PGMT were created by vesicles and particles containing the cargo. Since the head domain which pulls Myosin VI to the actin filaments was missing, the tail domain could gather freely around the cargo and create aggregates around it.

To test this assumption we stained egg chambers expressing PGMT with antibodies for proteins that genetically interact with Myosin VI, as described in chapter 6.

All the proteins that were located in vesicles within the cytoplasm, had few vesicles that co-localised with PGMT aggregates: In the columnar cells, Ankyrin vesicles at the basal side co-localise with PGMT (Fig. 4.8.1 A-F, see arrows), while Armadillo vesicles co-localise at the apical side of the columnar cells (Fig. 4.8.1 G-L, arrows). PGMT protein seems to be associated with Bazooka vesicles, at the basal side of the columnar cells (Fig. 4.8.2 A-G, arrows). Unlike the results observed here, an antibody staining that was previously made in egg chambers revealed a strong expression of Bazooka in the apical side of the follicle cells, however the stain was made to egg chambers at early stages (6-8) and it could be that the staining pattern

changes during oogenesis. PS2α-integrin showed co-localization with PGMT all over the columnar cells (Fig. 4.8.2. H-J, arrows). Myosin VI genetically interacts with PSβ-integrin, and with Discs large (Dlg). PSβ-integrin is weakly expressed in vesicles (Fig. 4.8.3 B) and Dlg is not expressed in vesicles at all (Fig. 4.8.3 E), therefore we did not expect to see co-localization of PGMT aggregates with vesicles containing those proteins (Fig. 4.8.3 A-F).

α-spectrin, which does not interact with Myosin VI, did not show a co-localization with PGMT aggregates (Fig. 4.8.3 H-J). These results support the assumption that the clustering of PGMT in the cell cytoplasm is not a random aggregation but an assembly with vesicles containing proteins that seem to interact with Myosin VI. The co-localization of the tail domain with vesicles containing Ankyrin, Armadillo, Bazooka and PS2α-integrin could suggest that Myosin VI physically interacts with these proteins. It must be stressed that direct physical interactions should be tested in vivo. In order to verify that the tail domain does not accelerate creation of vesicles in the follicle cells, the existence of vesicles expressing Ankyrin, Armadillo, Bazooka and PS2α-integrin was tested in OrR egg chambers (Fig. 4.8.4).

Figure 4.8.1: Antibody staining of Ankyrin and Armadillo in columnar follicle cells expressing the tail domain (PGMT).(**A-F**) Images of PGMT (**A, D**) Ankyrin (**B, E**) and their co-localization (**C, F**). (**G-L**) Images of PGMT (**G, J**), Armadillo (**H, K**) and their co-localization (**I, L**). Arrows indicate co-localizing vesicles.

Figure 4.8.2: Antibody staining of Bazooka and PS2α-integrin in columnar follicle cells expressing the tail domain (PGMT). (**A-G**) Images of PGMT (**A, D**) Bazooka (**B, E**) and their co-localization (**C, F**, and **G**). (**H-J**) Images of PGMT (**H**), PS2α-integrin (**I**) and their co-localization (**J**). Arrows indicate co-localizing vesicles.

Figure 4.8.3: Antibody staining of PSβ-integrin, Dlg and α-spectrin in columnar follicle cells expressing the tail domain (PGMT). (**A-C**) Images of PGMT (**A**) PSβ-integrin (**B**) and their co-localization (**C**). The tail domain weakly co-localizes with PSβ-integrin, probably due to the low number of vesicles containing this protein (**D-F**) Images of PGMT (**D**), Dlg (**E**) and their co-localization (**F**). Dlg does not seem to have vesicles, therefore no co-localization is observed with PGMT aggregates. (**G-I**) Images of PGMT (**G**), α-spectrin (**H**) and their co-localization (**F**). α-spectrin does not interact with Myosin VI, and no vesicles were found to co-localization with PGMT. Arrows indicate co-localizing vesicles.

Figure 4.8.4: Antibody staining of Ankyrin (**A-B**), PS2α-integrin (**C-D**), Armadillo (**G-H**), and Bazooka (**I-J**) in OrR follicle cells.

Figure 4.8.1

PGMT 33-2 X T155

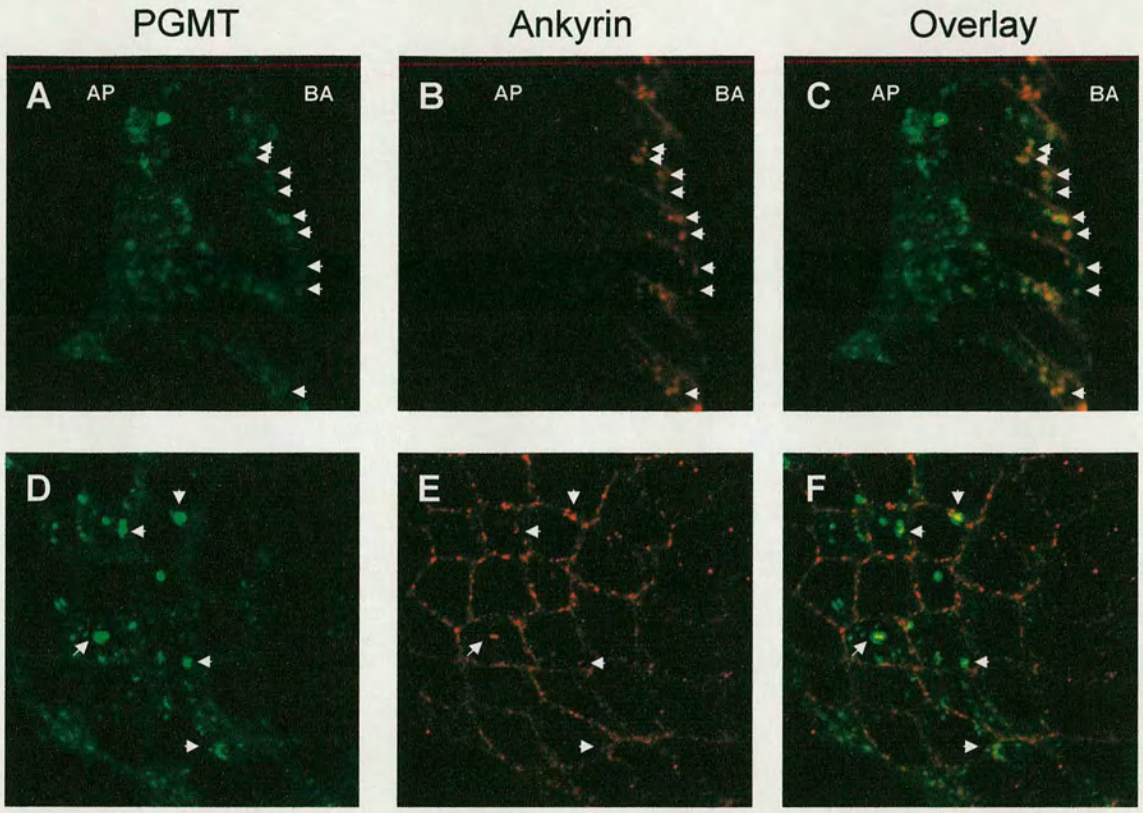

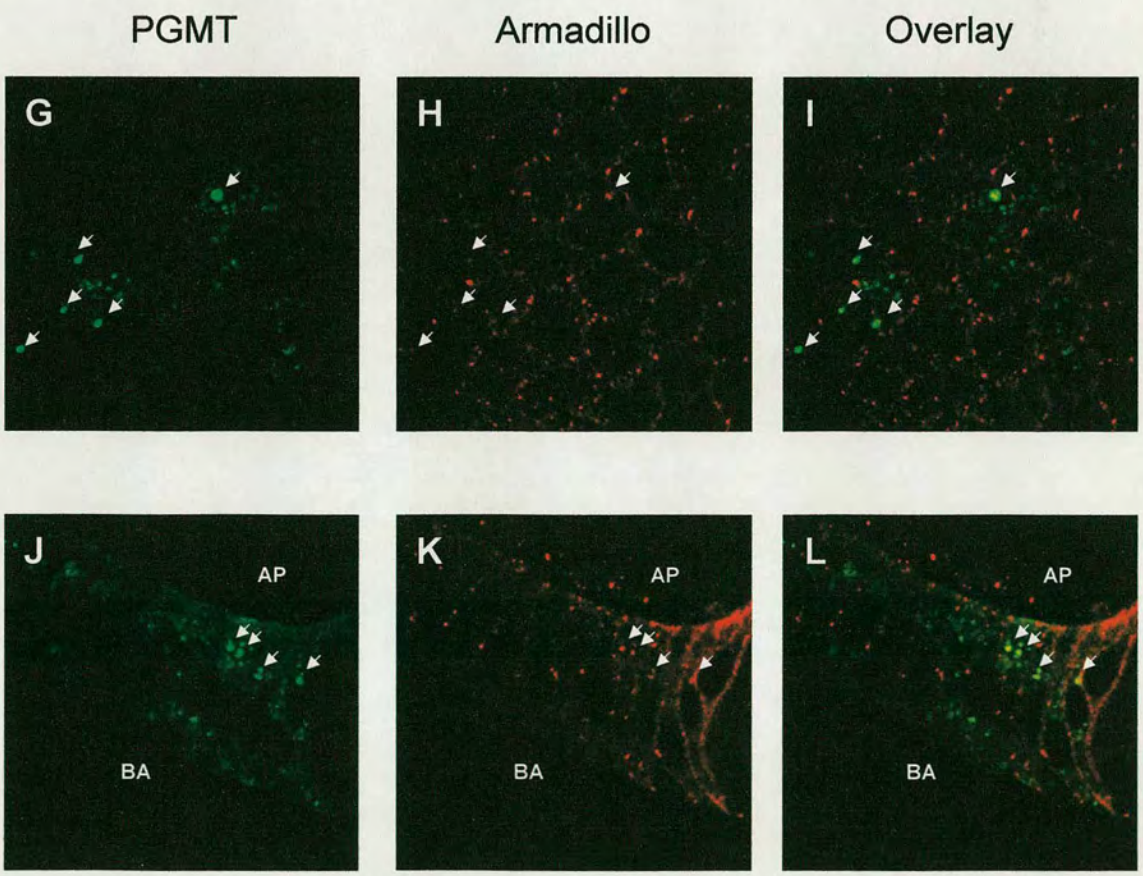

Figure 4.8.2

PGMT 33-2 X T155

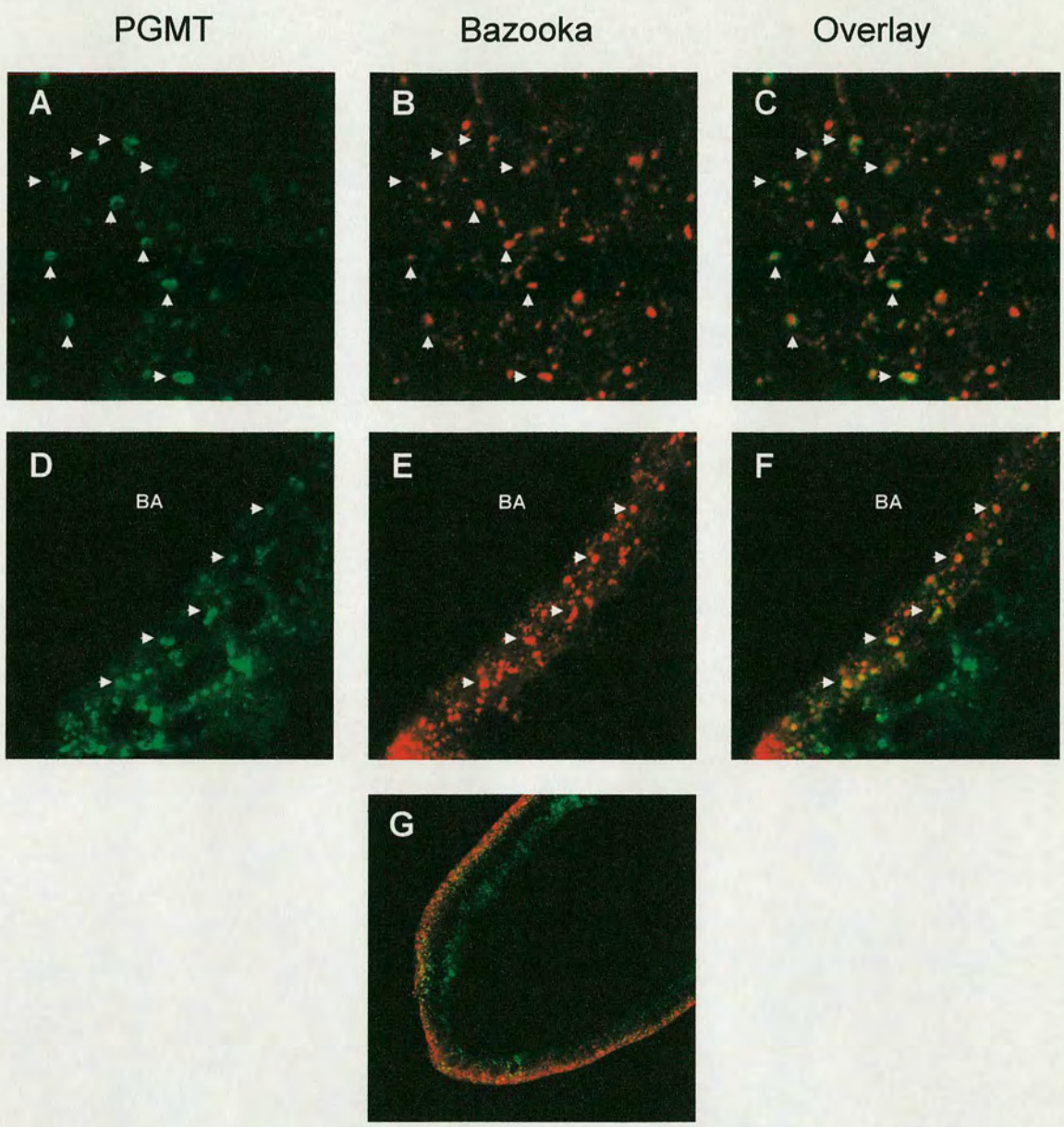

Figure 4.8.3

PGMT 33-2 X T155

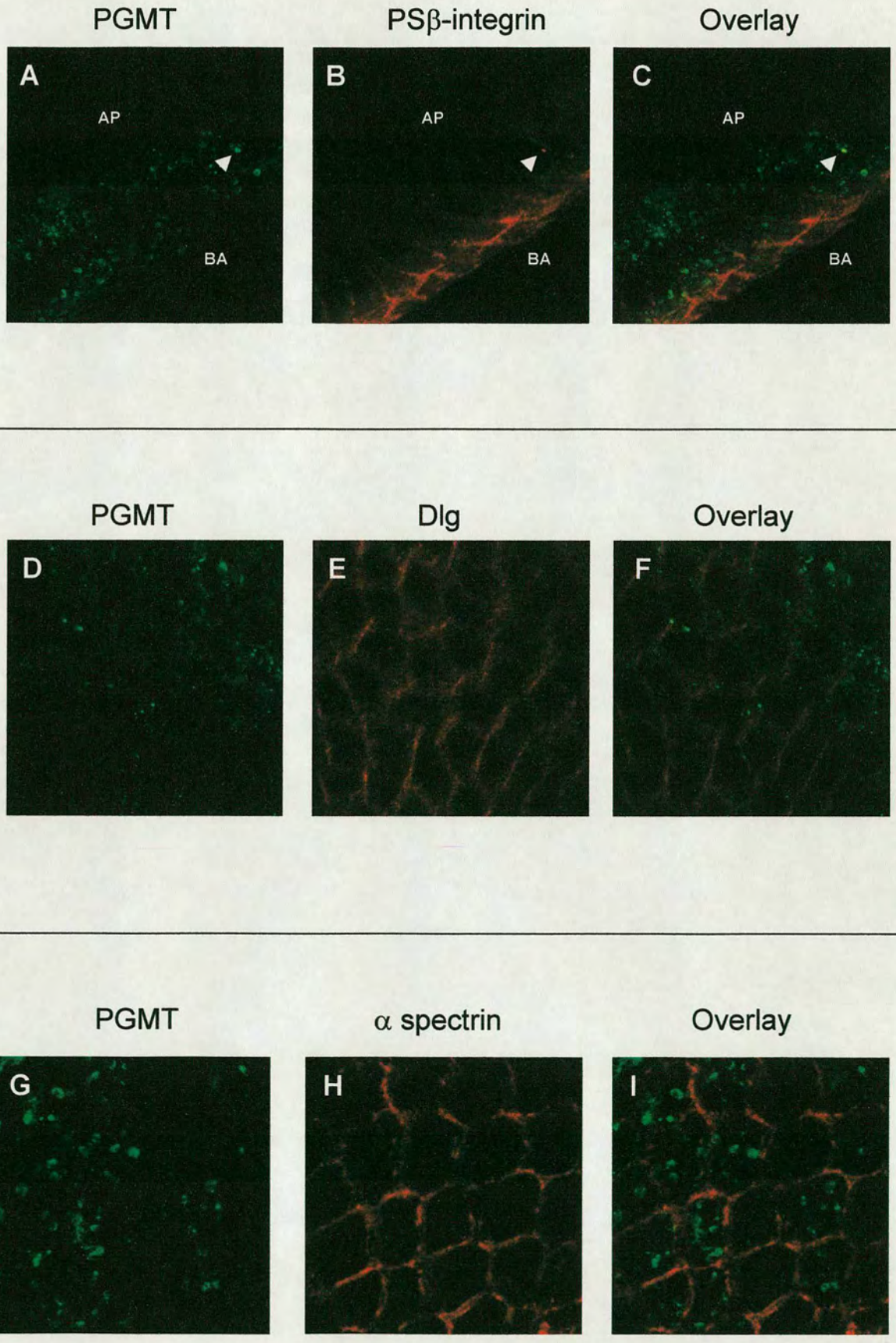

Figure 4.8.4

OrR flies

Ankyrin

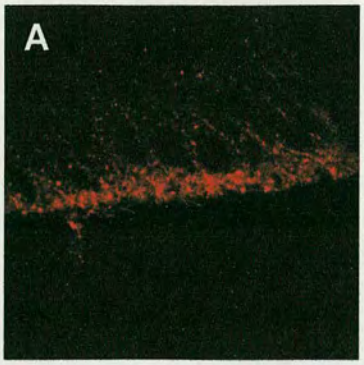

Ankyrin

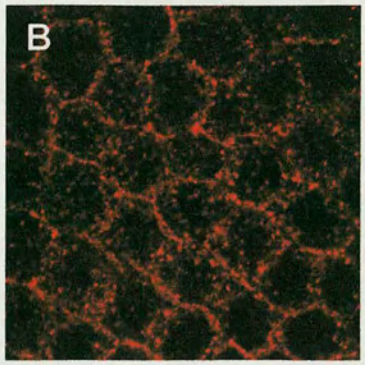

PS2α-integrin

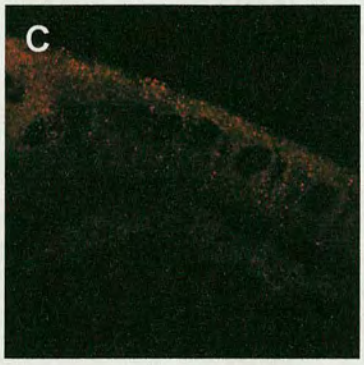

PS2α-integrin

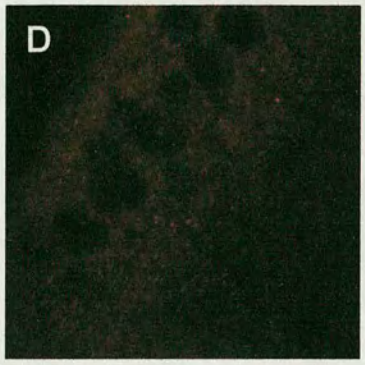

Armadillo

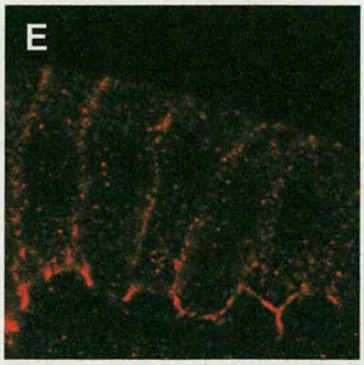

Armadillo

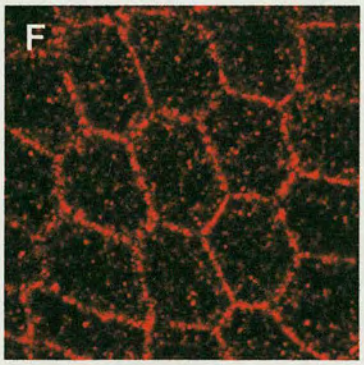

Bazooka

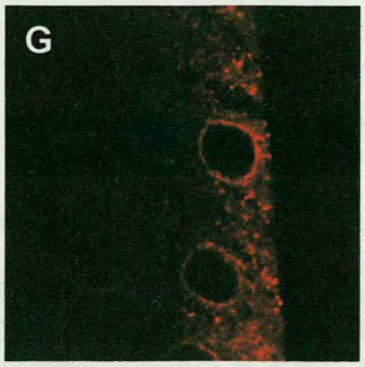

Bazooka

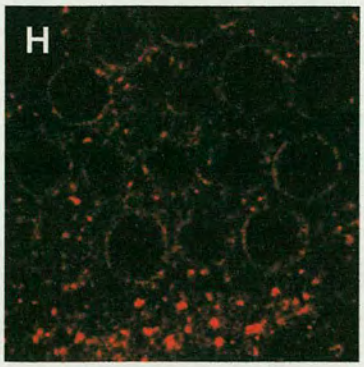

Figure 4.8.3

PGMT 33-2 X T155

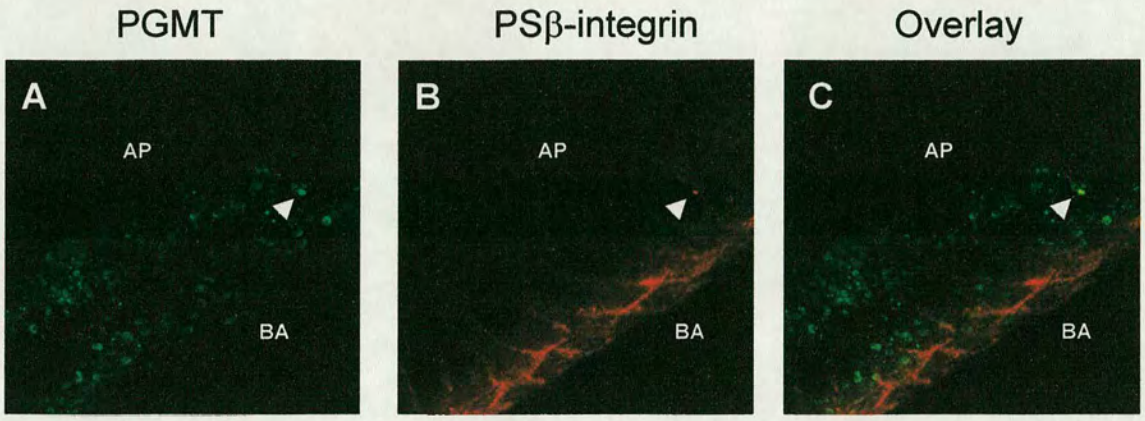

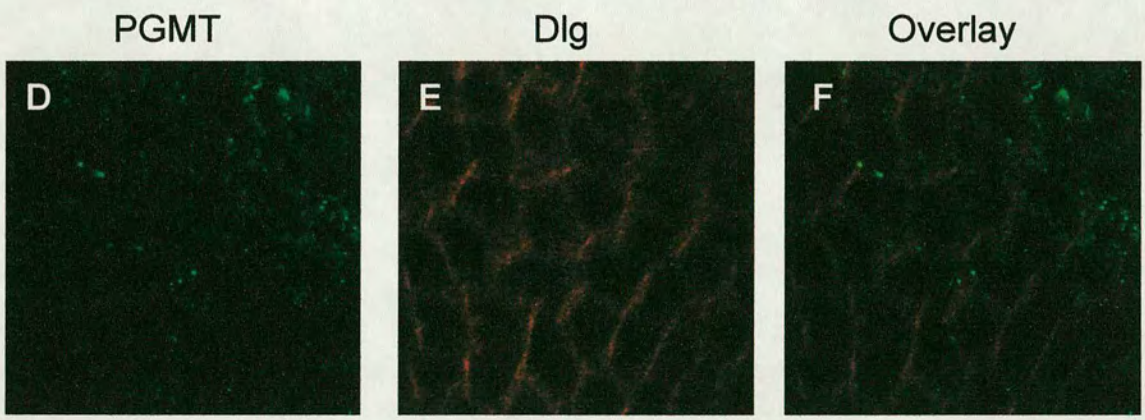

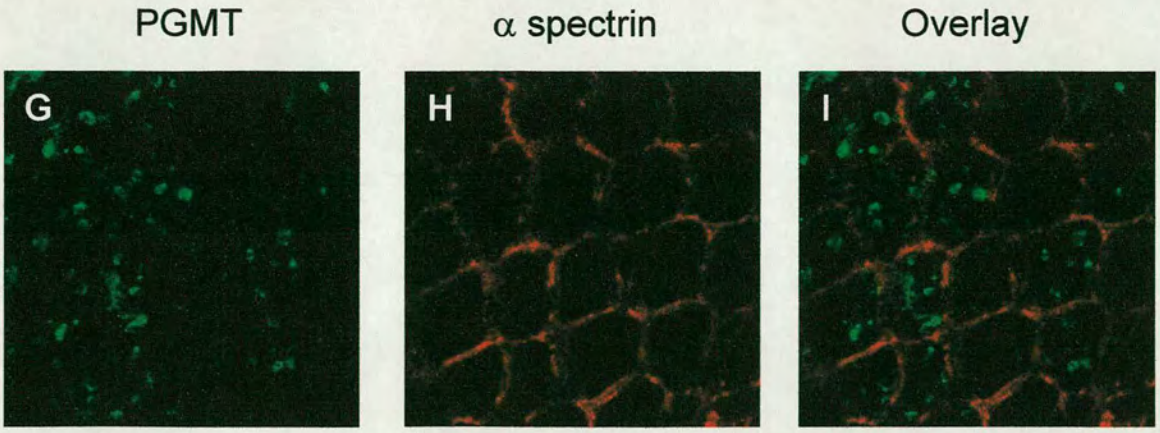

Figure 4.8.4

OrR flies

Ankyrin

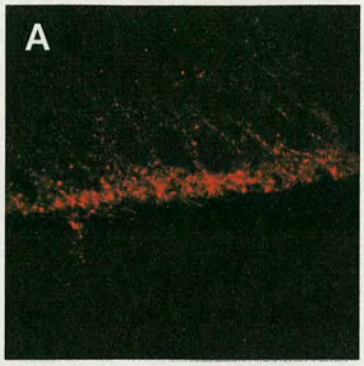

Ankyrin

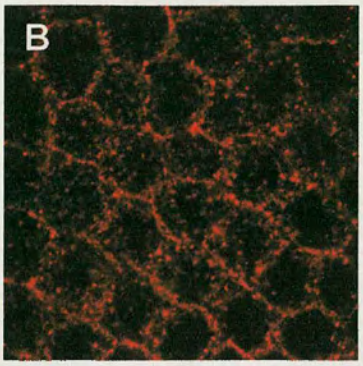

PS2α-integrin

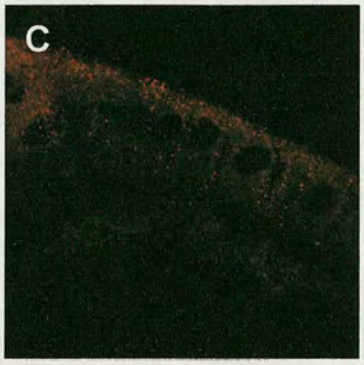

PS2α-integrin

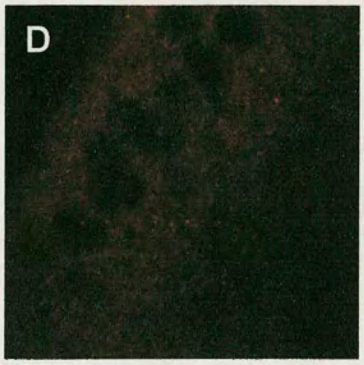

Armadillo

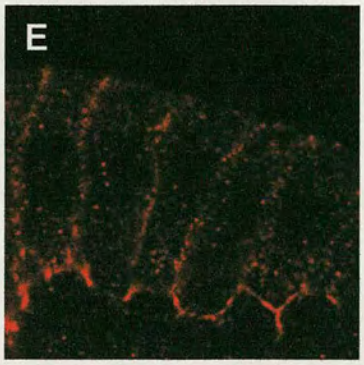

Armadillo

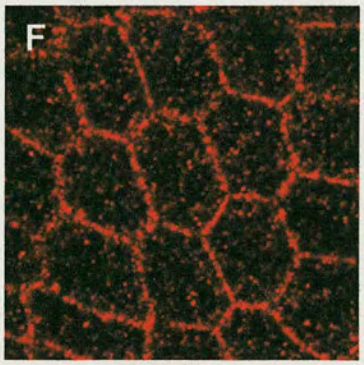

Bazooka

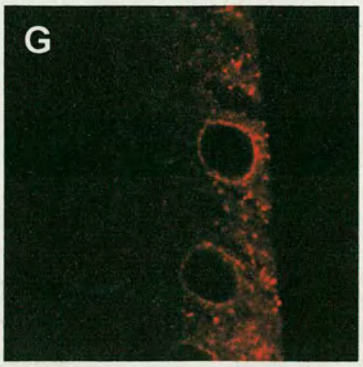

Bazooka

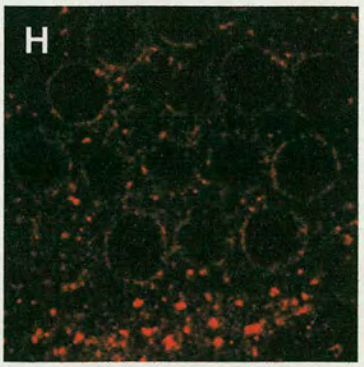

All these proteins appeared in vesicles at a similar concentration in follicle cells of wild-type egg chambers, therefore the expression of the tail domain does not accelerate the creation of vesicles bearing these proteins.

4.9 Conclusions

This chapter describes the expression of Myosin VI and its domains, tagged to GFP. In the first stage the DNA constructs expressing the fusion proteins were created, followed by the creation of the transgenic flies. The expression of Myosin VI-GFP (PGM), driven by Myosin VI-Gal4 allowed us to detect all the epithelial tissues expressing Myosin VI during *Drosophila* development. PGM expression rescued the homozygous lethality of the mutants: jar^{R39}, jar^{R70} and jar^{R235}, and the male sterility phenotype of the heteroallelic mutants: jar^{R39}/jar^{mmw14}, and jar^{R235}/jar^{mmw14}. This proved that PGM functions in a similar way to the native Myosin VI. Finally, the molecular function of the whole Myosin VI was examined by testing the localization of the head, the tail and the whole Myosin VI in the salivary gland excitatory cells, in the columnar follicle cells, in the leading edge during dorsal closure and in the individualization complexes during spermatogenesis. In all epithelial tissues, PGM, PGMH and PGMT were concentrated at the cell membrane. PGM and PGMT were concentrated in the cell cytoplasm and excluded from the nucleus. PGMH was not excluded from the nucleus, and in the columnar follicle cells and the salivary gland cells PGMH was concentrated in the nucleus. In the salivary gland cells, the concentration of PGMH in the nucleus triggered actin polymerisation in the nucleus. Finally, in the individualization complex of the testes, the tail domain was found to anchor the whole molecule to the base of the actin cone.

Driving PGM expression by a *Myosin VI-Gal4* line revealed various tissues where Myosin VI is expressed during morphogenesis. PGM was expressed in tissues that Myosin VI was shown to be expressed in and necessary for their correct morphogenesis (Deng et al., 1999; Hicks et al., 1999; Kellerman and Miller, 1992; Petritsch et al., 2003). However, PGM was also expressed in tissues, in which the expression of Myosin VI had not being previously described, including: the trachea,

the midgut, the salivary glands, the larval epidermis, the halter and eye-antenna imaginal discs, and the brain.

PGM was also expressed in tissues undergoing different processes of epithelial morphogenesis and membrane remodelling. For example, in the trachea and the salivary glands, PGM was expressed as the tissues undergo tubular morphogenesis (Nelson, 2003). During oogenesis, the follicle cells interconnect between themselves as they migrate. The position of the cells between themselves does not change during the migration (Spradling, 1993). Also during dorsal closure the whole epidermal tissue moves together to cover the amnioserosa (Martin and Wood, 2002) and during the evagination of the imaginal discs the epithelial cells migrate as the organs stretch to obtain their final shape (Fristrom and Fristrom, 1993). Although Myosin VI seems to be expressed in epithelial tissues seem to be shaped by various mechanisms of cells migration, perhaps Myosin VI plays a common role during their morphogenesis.

Myosin VI is not only necessary for the migration of the cells in epithelial tissues, but also for the attachment of tissues during their morphogenesis. In the evaginating wing disc, PGM was found to be expressed at the basal side of the epithelial cells, where the two epithelial sheets creating the wing connect, and when the expression of Myosin VI was disrupted, in the posterior compartment, the wing developed blisters. This suggest that Myosin VI is necessary for interactions with the extracellular matrix, and this is consistent with the need for Myosin VI for the attachment of the germ band to the amnioserosa during germ band retraction and the attachment of the leading edge to the amnioserosa during dorsal closure (this is discussed in chapter 5). When Myosin VI antisense was induced by *C532-Gal4* line, the wings in the adult flies were unfolded and malformed although no blistering was observed. It seems that in this case Myosin VI antisense was induced after the adhesion of the wing sheets was completed (30 hours after pupariation (Brabant et al., 1996).

PGM had a very strong expression in the salivary gland ducts, with some of the protein appearing in clustering (Fig. 4.5.2 F). The salivary gland is largest secretory tissue in the larvae, and many genes involved in the secretory pathway such as vesicular transport from the ER to the Golgi, are highly expressed. In mammalian

cells, Myosin VI is localised in the Golgi complex as a peripheral membrane protein and is necessary for secretion from the Golgi complex, and for preserving its proper morphology (Buss et al., 1998; Warner et al., 2003). The strong expression of PGM in the salivary gland, mainly in the salivary duct could suggest a role of Myosin VI in secretion from the salivary glands, and the clustering of PGM in the duct could be related to particles secreted into the duct by a mechanism including Myosin VI. However the necessity of Myosin VI for proteins secretion should be verified.

The concentration of PGMH in the cell nucleus is a phenomenon that appeared in the columnar follicle cells and the salivary glands secretory cells. The salivary glands cells contain microvilli in the membrane facing to the lumen (Riparbelli et al., 1993). Therefore, the organization of the actin filaments should be similar to those observed in other epithelial cells having a microvillar structure at the cell membrane: in these cells the plus-end of the actin filaments face the cell membrane and the minus ends face the cell interior (Mooseker, 1985). The concentration of PGMH in the cell nucleus is therefore consistent with the tendency of Myosin VI to move to the minus end of the actin filaments, especially when the head and the neck domains of Myosin VI are sufficient for a movement directed to the minus end of the actin filament (Homma et al., 2001; Wells et al., 1999). The concentration of PGMH in the cell nucleus of the columnar follicle cells, and the similar distribution of the actin filaments (a high concentration of actin filaments in the cell cortex and a net of actin filaments spread within the cells) suggest that in these cells the minus-end of the actin filaments is oriented was to the cell interior.

The change in the actin cytoskeleton can be related to the change in the cell shape as they become immobile: PGMH was concentrated at the nucleus of the columnar follicle cells, as they completed migration, but not in the migrating centripetal cells. The organization of the actin filaments in the basal part of in immobile follicle cells was shown to have a different pattern from the one of migrating follicle cells (Gutzeit, 1990). Change in the organization of the filaments in the migrating cells would change the localisation of PGMH since it binds to the filaments.

In the individualization complex, the head domain was localised throughout the actin cone and did not concentrate at the top of the actin cone, where the minus ends of actin are located. Thus PGMH does not move to the regions of the minus-end actin

filaments in all the organs. The orientation of PGMH and actin filaments in the cell nucleus suggest that the head and neck domains affect the polymerisation of actin filaments, either by triggering actin polymerisation or inhibiting de-polymerisation. If the orientation of the head domain triggers actin polymerisation or stabilizes actin filaments at their ends, then the recruitment of the head domain to the base of the actin cone in the individualization complex could be necessary for stabilizing the actin cone and for actin dynamics (Rogat and Miller, 2002).

In the border cells at the leading edge and in the individualization complex, the concentration of the head and the tail domains is different, and in both cases the tail domain seems to be most similar to the localisation of the whole Myosin VI molecule. It seems likely that in systems there are proteins that interact with the tail domain and thus recruit the whole myosin to a specific location.

In the columnar follicle cells and during dorsal closure the tail domain was expressed in the cell cytoplasm in aggregates. When comparing the tail expression with proteins that were found to interact genetically with Myosin VI, the tail aggregates co-localised with vesicles containing Ankyrin, Armadillo, Bazooka and PS2α-integrin, suggesting that the aggregates of the tail domain are formed by attaching to molecules that interact with Myosin VI. These aggregates are not formed when PGM is expressed and this is probably because the head domain pulls the tail to the actin filaments. This shows that both the head and the tail domains affect the localization of Myosin VI, and in different cells and tissues the relative importance of the two domains could change.

In the columnar follicle cells, the movement of the head domains towards the minus-end directed actin filaments, and the co-localization of the tail domain with genetically interacting membrane proteins produces evidence for the role of Myosin VI as a connector between the actin cytoskeleton and membrane proteins during oogenesis.

The localisation of the whole Myosin VI molecule and its separate domains was also studied in normal rat kidney cells, expressing the chicken brush border Myosin VI (Buss et al., 2001). The whole Myosin VI-GFP tagged molecule was concentrated in the Golgi complex, in the ruffles at the leading edge and in a punctate pattern at the plasma membrane, with a partial do-localisation with Clathrin coated pits/vesicles.

The globular tail domain was necessary for targeting the molecule to the Golgi complex and to Clathrin coated pits and the motor domain was found to be necessary for targeting the molecule to the membrane ruffles. In the absence of the globular tail domain (leaving only the coiled-coil region in the tail) the tagged protein was localised in the cytosol and concentrated in the membrane ruffles, but excluded from the nucleus. It would be interesting to investigate the location of the head and the neck in these cells. If the head and neck domains tend to move towards the cell interior, as it was observed in our experiments, then the anchoring of the whole molecule away from the nucleus could be dependent on the coiled-coil region in the tail.

Chapter 5:

The role of Myosin VI in embryogenesis

This work was undertaken in collaboration with Kevin Leaper and Vasiliki Lazou.

5.1 Introduction

This chapter describes recent studies on the function of Myosin VI in dorsal closure and germ band retraction.

Kevin Leaper created four Myosin VI mutant fly lines which fail to complete dorsal closure: jar^{R23}, jar^{R39}, jar^{R70} and jar^{R235}. Many of the mutant embryos die during embryogenesis and a few die in first larval instar. Close inspection reveals that the mutants have loose cells in the amnioserosa and the haemolymph. In several cases the embryos fail to complete germ band retraction, prior to dorsal closure. Protein analysis of the mutants at late stages of embryogenesis revealed that the Myosin VI level is significantly reduced, in the mutants jar^{R39} and jar^{R235}.

In this chapter I describe the molecular analysis of the mutations in the fly lines: jar^{R39} and jar^{R235}. I also mention the mutant rescue tests described in chapter four- these tests prove that the embryonic lethal phenotype observed in the homozygous mutant embryos is connected to the lack of Myosin VI.

The mechanism by which Myosin VI functions during dorsal closure is tested in the Myosin VI mutants and in embryos expressing a Myosin VI dominant negative molecule. In these embryos I examined the expression of myosin II, which is needed for the migration of the cells during dorsal closure; DE-cadherin and Armadillo, which are needed for cell adhesion; and the expression of Dlg and Crumbs, two proteins which play a role in epithelial cells polarity. I also examined the shape of the actin filaments at the cell membrane in order to determine if Myosin VI plays a role in the organisation of actin cytoskeleton during dorsal closure. In a search for factors that control the expression of Myosin VI during dorsal closure, I examined the effect of RhoA on the expression of Myosin VI.

In the final section, I test the effect of Myosin VI on the expression of CLIP-190 in the development of the central nervous system.

5.2 Description of the genetic analysis made previously to mutants: jar^{R23}, jar^{R39}, jar^{R70} and jar^{R235}

Two mutants for Myosin VI had been generated previously: jar^{1} (Castrillon et al., 1993), and jar^{mmw14} mutant, which was created in our laboratory by Wu-Min Deng (Hicks et al., 1999). jar^{1} was created by insertion of a P element, *P[lacZ, ry1]*, into exon 2 of *jaguar*, 4.5 kb from the initiator methionine , and the phenotype of the homozygous mutant jar^{1}/jar^{1} is male sterility (Hicks et al., 1999). jar^{mmw14} was created by a deletion of the non-coding exon 1 (See Fig. 5.2C). Genetic analysis showed that the two mutants fail to complement each other, and the heterozygous mutant jar^{1}/jar^{mmw14} is also male sterile. When jar^{mmw14} is crossed with *Df87-5*, a deficiency line for the *jar* region, the heterozygous line *Df87-5/* jar^{mmw14} is male sterile, and Western analysis shows that there is no expression of Myosin VI in the testes, however, Myosin VI is still expressed in the fly carcass (Hicks et al., 1999).

Figure 5.2: The organisation of the wild type and mutated *jar* genes.
A: The transcript which encodes the EM3 isoform of *jar* (the isoform that contains all the exons (Kellerman and Miller, 1992). **B** *C865* contains a single *P[GawB]* element inserted at bp 306 in exon 1. It is located in the 5′ UTR and causes no observable phenotype. The number of *P[GawB]* elements was determined by Southern blots, and the position of the insertion by plasmid rescue (made by Kevin Leaper). **C** jar^{mmw14} was created by imprecise excision of *P[GawB]*, removing the whole first exon along with 485 bp flanking the 5′ end and 47 bp flanking the 3′ end (total deletion of 862 bp). This allele is homozygous viable but male sterile due to absence of a male specific transcript (Hicks et al., 1999). The location of the primers used for the identification and sequencing of the deletion (C865For, C865 Rev, EXC2For and EXC2Rev) are shown. The gel shows PCR products generated from *jar* genomic DNA from $jar^{mmw14}/TM3$ heterozygous flies: 1) when the PCR was made with the primers C865 For + Exc2Rev, two bands appeared, one corresponding to the predicted size obtained from amplification of *jar* genomic DNA from the balancer chromosome, *TM3* (1.5 kb), and one smaller band (~0.7 kb), corresponding to the size obtained by amplification of the deleted *jar* genomic DNA from jar^{mmw14} chromosome (see arrow). This band was sequenced and the precise location of the deletion was found. 2) When PCR was made with the primers: Exc2For + C865Rev, only one band appeared, which correspond to the predicted size obtained by amplification of *jar* genomic DNA from the balancer chromosome, *TM3* (2.3 kb). The other band was not amplified since the primer Exc2For is located within the deletion region of jar^{mmw14} mutant. **D** After finding the precise location of the deletion in jar^{mmw14}, a pair of primers was designed to replicate the whole deletion region. In that way, only the mutant genomic DNA was amplified by PCR, and the specific mutation (marked by a red asterisk) was located in this region by sequencing. **E** The mutation found in jar^{R39}/jar^{mmw14}: the sequence marked by a dashed line was deleted and the sequence marked in the box was duplicated. **F** The mutation found in jar^{R235}/jar^{mmw14}: the sequence GTATAC was changed to GTTTTC, the nucleotide A, 438 bp upstream to the first exon was deleted, and the nucleotide G (38 bp upstream to the first exon) was replaced with an A.

Figure 5.2

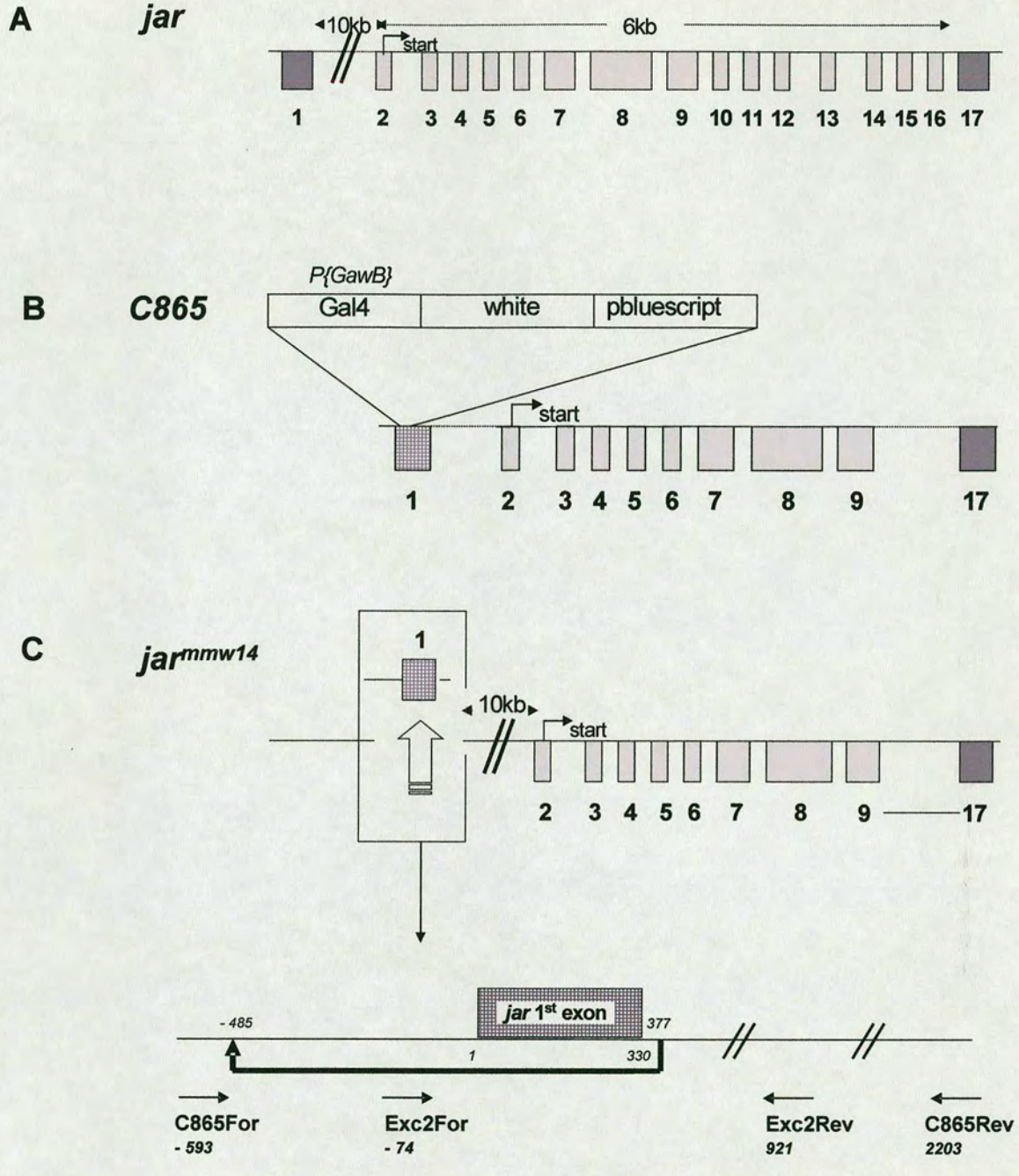
A
jar
10kb
6kb
start
1 2 3 4 5 6 7 8 9 10 11 12 13 14 15 16 17
B
C865
P{GawB}
Gal4
white
pbluescript
start
1 2 3 4 5 6 7 8 9 17
C
jarmmw14
1
10kb
start
2 3 4 5 6 7 8 9 17
jar 1st exon
-485
377
1
330
C865For
- 593
Exc2For
- 74
Exc2Rev
921
C865Rev
2203

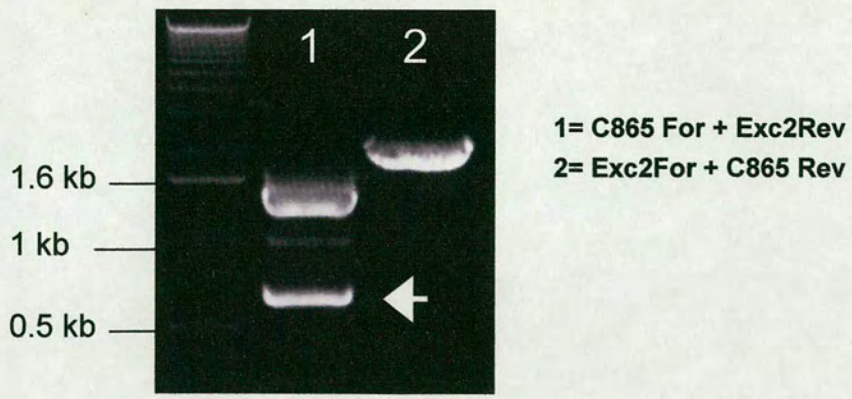
1
2
1.6 kb
1 kb
0.5 kb
1= C865 For + Exc2Rev
2= Exc2For + C865 Rev

Figure 5.2-cont

jar^{mmw14}/ jar^{R39} and jar^{mmw14}/ jar^{R235}

D

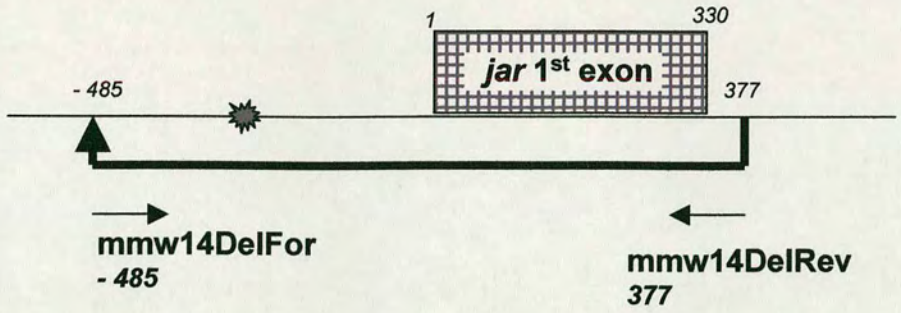

E jar^{R39}

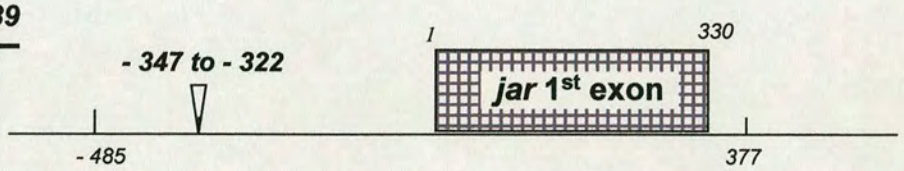

Wild Type

GAAGAGTATAC TGTTTATATATACTGATATGCGGTGC

jar^{R39}

GAAGATTTATATATACTGATATGTTTATATATACTGATATGCGGTG

F jar^{R235}

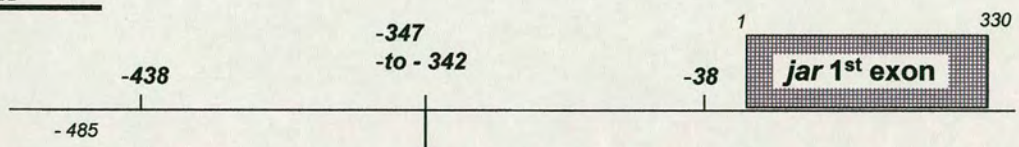

Wild Type: TTAACCC AGAGTATAC TGT GAAGTCG

jar^{R235}: TTACCC AGAGTTTTC TGT GAAATCG

In previous antisense experiments it was shown that Myosin VI is necessary in many other organs as well, like the ovaries and the imaginal discs (Deng et al., 1999), therefore it was necessary to generate more mutants with additional phenotypes.

The mutants were generated by Kevin Leaper, by remobilising a *Gal4* insertion in the *jar* gene.

Figure 5.2A shows the intron-exon organisation of *jar*, which was determined in our lab by sequence analysis and by using the published *Drosophila* genome sequence (Adams et al., 2000.). Figure 5.2.B describes the location of the *P[GawB]* insertion containing the *Gal4* gene in line *C865,* as it was found by Kevin Leaper through plasmid rescue of the *P[GawB]* insertion and sequencing. The insert was found to be located at bp 306 in the first exon (Millo et al., 2004). This is in an untranslated 5' UTR and the insertion causes no observable abnormal phenotype and produces normal levels of Myosin VI transcripts and proteins. Four Myosin VI mutants have been established by Kevin Leaper: jar^{R23}, jar^{R39}, jar^{R70} and jar^{R235}. All of them are homozygous lethal during embryogenesis. When crossed to each other and with *Df87-5* and jar^{mmw14} lines, they fell into two complementation groups: jar^{R23}, jar^{R70} and *Df87-5* were in one group; jar^{R39}, jar^{R235} and jar^{mmw14} were in another group. jar^{R23} and jar^{R70} failed to complement the *Df* line (which is deficient for *jar* region), and the crosses led to lethality in the following progeny; jar^{R39} *and* jar^{R235} did not complement with jar^{mmw14} (which disrupts a specific transcript of *jar* in the testes), and the cross produced male sterile progeny. Therefore the mutants were suggested to be in the *jar* gene.

When a Western blot analysis was made in embryos in late stages of embryogenesis, it was shown that wild type *OrR* and jar^{mmw14} embryos have high levels of several isoforms of Myosin VI. jar^{R23} has slightly reduced Myosin VI, jar^{R70} has much reduced Myosin VI and in jar^{R39} and jar^{R235} no Myosin VI could be detected (Millo et al., 2004). In situ antibody staining revealed that by the time dorsal closure starts there is no detectable Myosin VI and this loss of Myosin VI continues into the fully formed larvae (Millo et al., 2004).

5.3 Molecular analysis of jar^{R39} and jar^{R235} mutants

In order to have a better characterisation of the mutants it was necessary locate the mutations in *jar* gene and to further investigate the effects of Myosin VI depletion in the mutants.

The P element in the *C865* line which was used for the P hop mutagenesis is located in the 5′ UTR of *jar* mRNA (Fig. 5.2B). When we undertook PCR with primers flanking the location of the original P element location, we found that the P element was excised from the 5′ UTR region in all the mutants, jar^{R23}, jar^{R39}, jar^{R70} and jar^{R235} (Fig. 5.3). jar^{R39} and jar^{R235} were the mutants that showed the most severe phenotypes, therefore we decided to determine the molecular basis of the mutations in these lines. The RTPCR results (see following section) suggest the mutations should be in the 5′ region. Since these lines fail to complement jar^{mmw14} (jar^{mmw14}/jar^{R39} and jar^{mmw14}/jar^{R235} heterozygotes are male sterile) the mutations should affect some of the same transcripts that are affected in jar^{mmw14}. In jar^{mmw14}, imprecise excision of the P element caused a deletion of about 1 kb around the 5′ UTR (Hicks et al., 1999). It is therefore possible that in the jar^{R39} and jar^{R235} lines the mutation could have been caused by an imprecise excision event, as in jar^{mmw14}. A restriction analysis was made of the amplified PCR products, however, unlike jar^{mmw14}, any potential deletions in the mutants jar^{R39} and jar^{R235} were not big enough to be visualised on a gel (data not shown).

Figure 5.3: A search for the p element in the 5′ UTR region in the mutant genomic DNA.
The genomic region where the p element was originally located in line *C865* (5′ UTR) was amplified by PCR, in the heterozygous mutant lines: $jar^{R23}/TM3$, $jar^{R39}/TM3$, $jar^{R70}/TM3$, $jar^{R235}/TM3$, in *C865* and in *OrR*, using primers flanking the insert region: C865For and C865Rev. In *C865* two bands appeared: the upper band (arrow) corresponds to the p element, 14 kb, and the lower band corresponds to the same region in the chromosome that does not contain the p element (as in *OrR*). In all the mutants, the p element band does not exist, indicating that the p element was excised from the 5′ UTR.

Figure 5.3

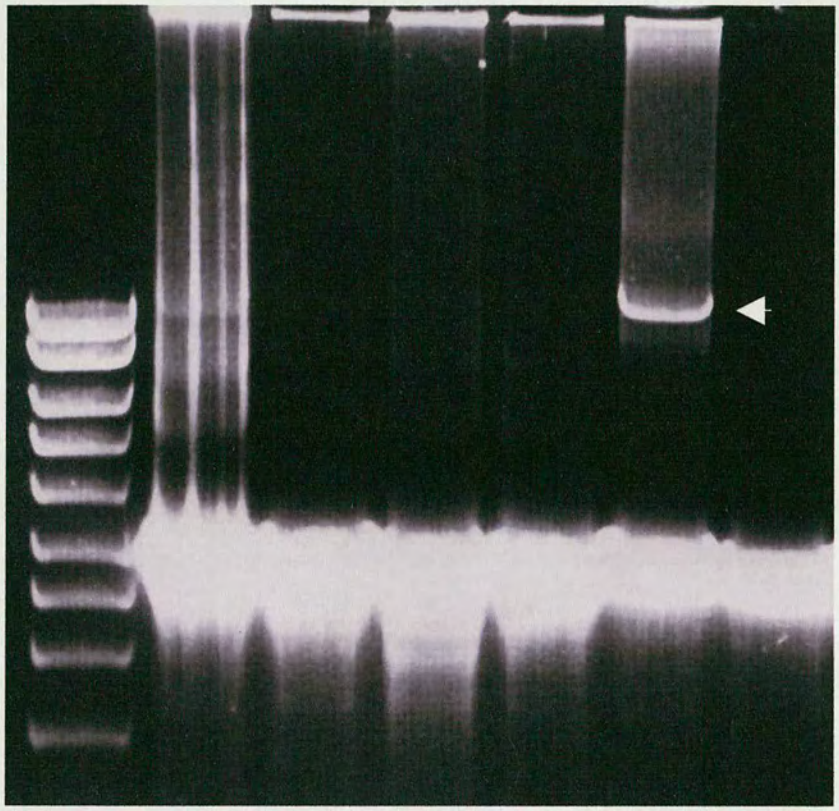

R23 *R39* *R70* *R235* *C865* *OrR*

The mutant flies jar^{R39}, jar^{R235} and jar^{mmw14} are homozygous lethal, therefore they are balanced over a chromosome TM3, which contains the marker stubble (Sb). When $jar^{R39}/TM3$ and $jar^{R235}/TM3$ are crossed with $jar^{mmw14}/TM3$, the heterozygous mutants jar^{R39}/jar^{mmw14} and jar^{R235}/jar^{mmw14} can be visualised since they do not contain the balancer chromosome TM3, therefore they are not Stubble. These heterozygous flies are male sterile. In these heteroallelic lines, one chromosome will contain the genomic DNA of jar^{mmw14}, with the 1 kb deletion in the 5′ UTR, and the other chromosome will contain the genomic DNA of either mutant with its specific mutation. We know any changes at this location are too small to be detected on gels, but any new mutations could well be located within the 1 kb deletion created in jar^{mmw14} (Fig. 5.2D). Therefore, heterozygous flies will have only one copy of the jar^{R235} or jar^{R39} mutant genomic DNA in this region. To establish if there was a mutation caused by excision we needed to sequence this single copy of the DNA. To do this the precise location of the deletion in jar^{mmw14} had to be established. When a PCR was made using DNA from $jar^{mmw14}/TM3$ heterozygous flies with primers located 593 bp upstream and 921 bp downstream of the beginning of the first exon, two bands appeared, one corresponding to the product resulting from amplification of *TM3* genomic DNA, and one smaller band, corresponding to the amplification of the jar^{mmw14} chromosome (Fig. 5.2C on gel, lane 1). Sequencing of the lower band revealed that the deletion in jar^{mmw14} was from 485 bp upstream of the first exon to 47 bp downstream of the first exon (Fig. 5.2C) making an excision of 862 bp, which includes the whole first exon. When this region was amplified and sequenced in the jar^{R39}/jar^{mmw14} heterozygotes and jar^{R235}/jar^{mmw14} it was found that indeed mutations were detected.

In the jar^{R39}/jar^{mmw14} heterozygotes the sequence: GTATACTG (347-340 bp upstream of the first exon) was deleted, while the sequence: TTTATATATACTGATATG (341-322 bp upstream of the first exon) was duplicated (Fig. 5.2E). In jar^{R235}/jar^{mmw14} the sequence: GTATAC (347-342 bp upstream to the first exon) was changed to: GTTTTC, possibly by deletion of the sequence: ATA and duplication of the sequence: TTT (341-339 bp upstream of the first exon, see Figure 5.2F). This mutation is located in the same region as the mutation in jar^{R39} and this explains the similar truncation of the mRNA transcripts that was found at the 5' end

in both mutants.

Both mutations have disrupted the sequence: AGTATACT. In jar^{R235} this sequence has been changed and in jar^{R39} the sequence is deleted. This is a palindromic sequence and as such could potentially regulate the transcription of *jar*. In *Drosophila* palindromic sequences located within the promoter region are often necessary for accurate transcription (Cho et al., 1998; Oh et al., 1999). DNA replication elements are composed of the common palindromic sequence: TATCGATA (Hirose et al., 1993) The transcription of the gene *Timeless* requires the palindromic sequence CACGTG for correct transcription (Okada et al., 2001), and the palindromic sequence: CTTTT-GAAAAG is necessary for proper function of the promoter in the *transcription binding protein* (*TBP*) gene (Oh et al., 1999). The palindromic region might be a specific binding site for transcription factors (Hirose et al., 1993).

jar^{R235} also has a missing nucleotide, A, 438 bp upstream of the first exon (Fig. 5.2F), and the nucleotide G (38 bp upstream of the first exon) was replaced by A (Fig. 5.2F). In spite of the excision of the P element from the 5′ UTR in the two mutants, the flies are red-eyed, therefore a P element must have been inserted into a different region of the genome. Inverse PCR revealed that in jar^{R39} a P element has inserted into the third chromosome, within the region of the hypothetical gene CG5991, which is located upstream of the *jar* gene. The P element in jar^{R235} was also re-inserted into the third chromosome, upstream of the *jar* gene, in a region between the hypothetical genes: CG6164 and CG 6173.

There was therefore a mobilisation of the P element to different genes in each case. The two new *jar* mutants fail to complement each other and the deletion mutant jar^{mmw14} , but we needed to be sure that the lethality associated with jar^{R39}/jar^{R235} transheterozygous embryos and larvae are due to the mutations in Myosin VI and not in the other genes where the P element has inserted. We investigated the expression of Myosin VI and analysed the phenotype of the transheterozygous mutant jar^{R39}/jar^{R235}. Because the insertion sites of the P element in jar^{R39} and jar^{R235} are different, the cross of the two mutants will complement the mutations caused as a result of the P element insertion in different genes, allowing us to test the phenotype

of the mutations within *jaguar* only. The transheterozygous mutants had a similar phenotype to the homozygous mutants: i.e. Myosin VI was absent late in embryogenesis and many embryos failed to complete dorsal closure (Fig. 5.5E, 5.8.3 D-E). Those which completed dorsal closure died during the first larval instar. Thus we can relate the phenotype to a deficiency in Myosin VI late in embryogenesis.

5.4 The transcription of the 5' end mRNA is disrupted in homozygous mutants

Previously it was shown that jar^{mmw14} mRNA is disrupted at its 5′ region: up to 517 nucleotides are not transcribed at the 5′ end of the mRNA (Hicks et al., 1999). Since jar^{mmw14} does not complement with jar^{R39} and jar^{R235} we wanted to test if the transcription at the 5′ end of *jar* mRNA is also disrupted in these mutants. RTPCR was undertaken, using RNA templates from homozygous mutant and *OrR* larvae (1st instar), for two regions at the 5′ end of the *jar* mRNA: the first 1027 nucleotides and the region between nucleotides 517 and 1027 were investigated (Fig. 3A). An additional RTPCR was made for a region located further downstream, 2850–4100 bp from the 5′ end. The RTPCR of the two 5′ regions was very weak in the homozygous mutant larvae, compared to *OrR* larvae (Fig. 3B). It seems that as in jar^{mmw14}, there is reduced transcription of *jar* mRNA at the 5′ end in jar^{R39} and jar^{R235} mutants. When RTPCR was made to transcripts at the 3′ end (Fig. 3C), a high level of product was observed, although not to the same extent as in *OrR*. This is to be expected since transcripts initiated at the 5′ end of the gene are absent. This suggests that only some of the transcripts are affected. When RTPCR was made for mRNA of ribosomal protein (Fig. 3D) and myosin 29D (Fig. 3E) as a control, the expression level in the homozygous mutants was similar to the expression in *OrR*, therefore the disruption in mRNA expression is unique to *jar*.

When RTPCR was made with homozygous young mutant embryos of jar^{R39} and jar^{R235}, all the RNA transcripts appeared at a similar intensity to *OrR* embryos (data not shown). The 5′ transcripts in homozygous mutant embryos are from maternal *jar* mRNA, these maternal transcripts allow the embryos to survive until late stages of embryogenesis and a few even survive to become first instar larvae.

Given that there are at least some transcripts present in larvae in the jar^{R39} and jar^{R235} it seems unlikely either are nulls.

The disruption in the transcription of Myosin VI is consistent with the depletion of Myosin VI protein in the mutants, during late stages of embryogenesis.

5.5 Myosin VI is necessary for dorsal closure and germ band retraction

Most homozygous mutant embryos developed into late embryos which failed to hatch. A few hatched into larvae, but soon died. The anterior/posterior and dorsal/ventral polarity and segment number was normal. A number of embryos failed to complete dorsal closure and thus there was exposed yolk and free floating yolk between the cuticle and the vitelline membrane and many embryos had loose cells inside the vitelline membrane. The cells in the amnioserosa were detached. The leading edge of the epithelial sheets loose their tight and organised shape (Fig. 5.5E compared to 5.5 A-D in wild type embryos, and Fig. 8E), and the tissue was folded inside. Some of the mutant embryos also failed to complete germ band retraction (Fig. 5.8.3D, E), having the tissue folded in and separated from the amnioserosa.

Many of the mutant embryos that died and larvae that hatched had completed dorsal closure but had loose cells floating in the haemolymph in the dorsal aorta (Millo et al., 2004).

Figure 5.4: RTPCR analysis of jar^{R39}, jar^{R235} homozygous mutant and *OrR* larvae. **A:** A diagram of the primers used for the RTPCR analysis of *jar* mRNA. **B** RTPCR for the 5′ region of *jar* mRNA, using the primers p1 + p1027, and p517 + p1027. In jar^{R39} and jar^{R235} the PCR gave a signal which is much weaker compared to *OrR*, suggesting that these transcripts are not synthesized in the larvae and the weak signal obtained was probably from remaining maternal transcripts. **C** RTPCR of the *jar* tail encoding domain (located downstream, see 3A). The 3′ transcripts in the mutants exist, although not to the same extent as in *OrR*. The transcription of a fragment in ribosomal protein, L32 (**D**) and of Myosin 29D mRNA (**E**) was used as a control.

Figure 5.5: Phenotypes of mutant embryos. **A-D**: Dorsal closure in OrR flies (the embryos are stained with antibodies raised against nonmuscle Myosin II). The leading edges of the lateral epidermis are connected along the anterior and the posterior sides, towards the centre (arrows), to cover the amnioserosa. **E:** Failure of dorsal closure in jar^{R39} mutant embryos, the cells in the amnioserosa are detached (arrows), leaving loose yolk. Note that the cells in the leading edge of the epithelium are loose or abnormally shaped. AS = amnioserosa LE = leading edge

Figure 5.4

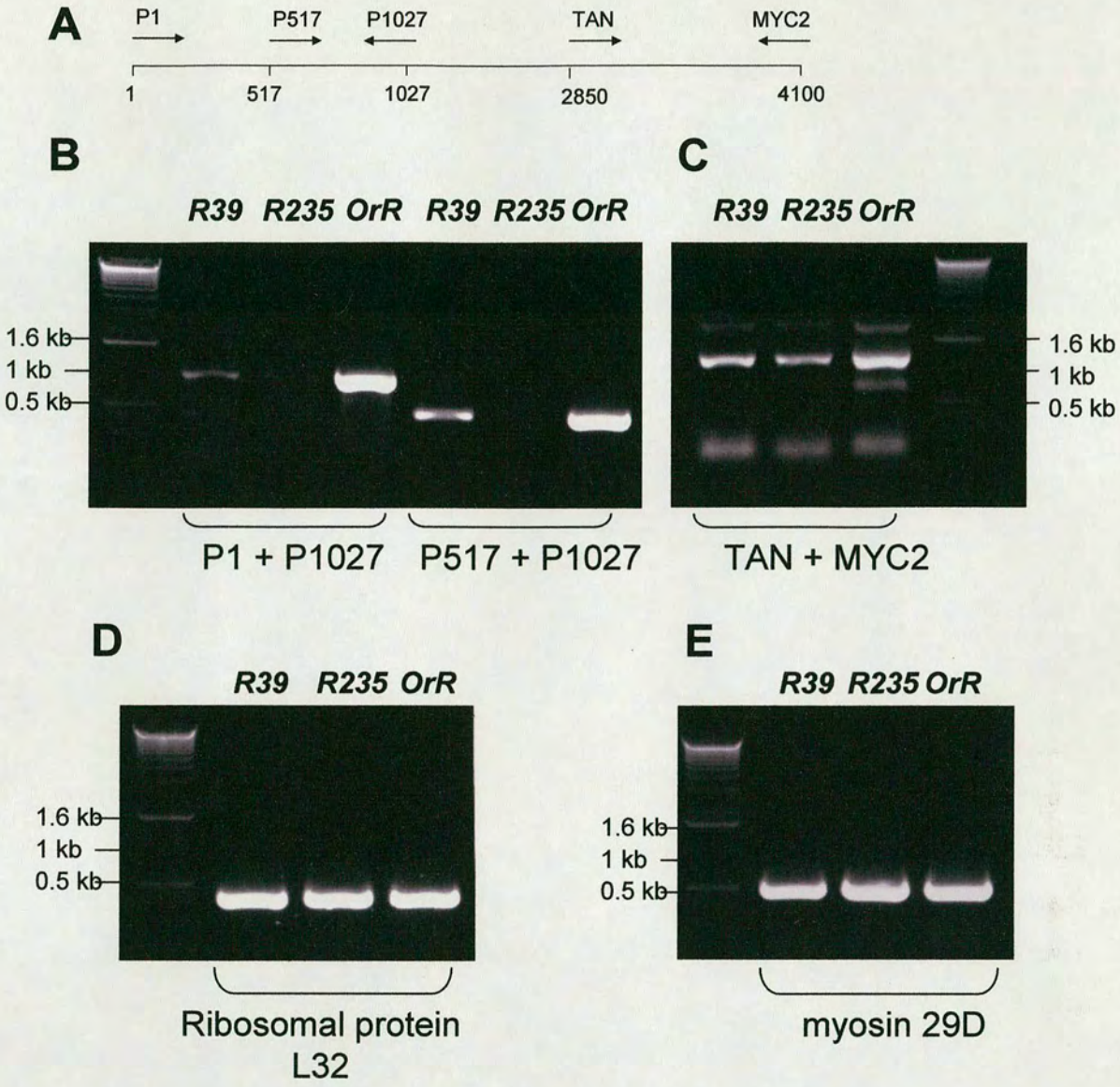
A
P1
P517
P1027
TAN
MYC2
1
517
1027
2850
4100
B
R39 R235 OrR R39 R235 OrR
1.6 kb
1 kb
0.5 kb
P1 + P1027
P517 + P1027
C
R39 R235 OrR
1.6 kb
1 kb
0.5 kb
TAN + MYC2
D
R39 R235 OrR
1.6 kb
1 kb
0.5 kb
Ribosomal protein L32
E
R39 R235 OrR
1.6 kb
1 kb
0.5 kb
myosin 29D

Figure 5.5

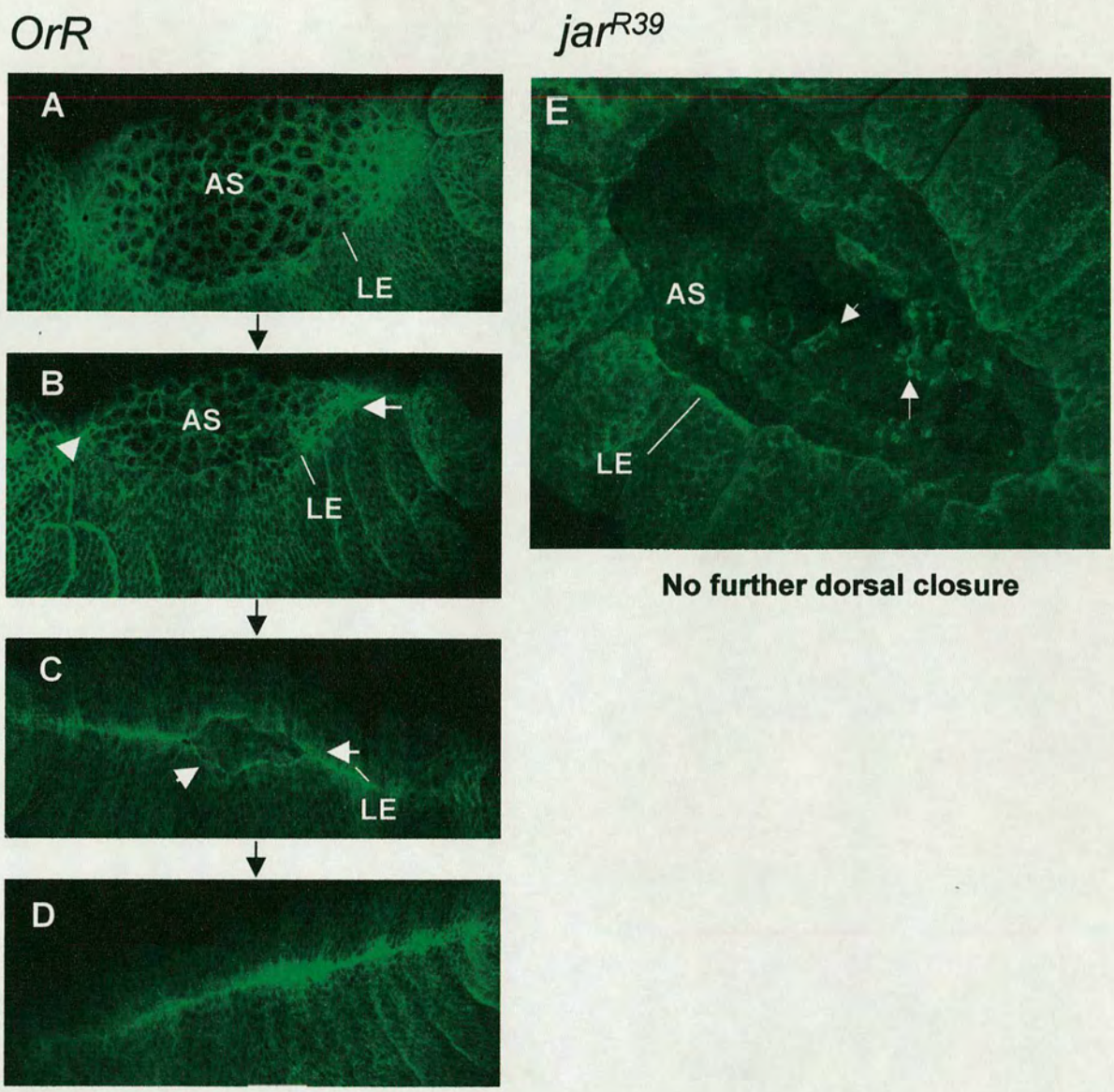
OrR
jarR39
A
AS
LE
B
AS
LE
C
LE
D
E
AS
LE
No further dorsal closure

5.6 Myosin VI cDNA rescues the lethal phenotype of jar^{R39} and jar^{R235} mutant embryos.

As described in the two mutant rescue experiments in chapter 4, the expression of Myosin VI-GFP tagged protein (PGM) rescued the embryonic lethal phenotype of the homozygous mutants: jar^{R39} and jar^{R235} by increasing the viability of the mutant embryos. These results prove that the embryonic lethal phenotype results from to the disruption in Myosin VI expression.

In the adult flies, PGM expression also rescued the male sterile phenotype of the heteroallelic mutants: jar^{R39}/ jar^{mmw14} and jar^{R235}/ jar^{mmw14} by recovering their fertility, showing that the male sterility phenotype of the transheterozygous mutants is also caused by the disruption of Myosin VI expression in the testes.

5.7 Dominant negative expression of Myosin VI leads to cell adhesion defects and failure in germ band retraction

An alternative way to interfere with the function of Myosin VI during dorsal closure is to express a truncated form of Myosin VI, which lacks the ATP binding domain (ΔATP-jar, Petritsch et al. 2003). This dominant-negative Myosin VI was driven by *engrailed-Gal4* (*en-Gal4*). This causes alternating stripes of cells to misexpress Myosin VI so normal cells and potential cell defects can be observed in the same embryo. This caused rupture of the tissue at the leading edge and the amnioserosa (Fig. 5.7 A, 5.9B), leaving loose cells. Furthermore, the detachment of the cells appears only in the stripes of cells expressing ΔATP-jar. The cells at the leading edge tend to separate from the amnioserosa (Fig. 5.7A, 5.9B).

These results suggest that Myosin VI is necessary for cell adhesion during dorsal closure. Embryos that reached the final stages of dorsal closure had holes at the dorsal midline, suggesting that Myosin VI is also necessary for the adhesion of the two edges of the leading edge along the dorsal midline, during the final "zipping" of the epidermis (Fig. 5.7C). As observed in the homozygous mutant embryos, apart from the change in the adhesion properties, the cells also loose their normal

morphology. In many cases, cells expressing ΔATP-jar tend to fold inside, at the lateral epidermis and the leading edge (Fig. 5.7E). Figure 5.7D shows an embryo expressing ΔATP-jar, stained with Myosin VI antibody. The stripes expressing ΔATP-jar have a stronger antibody stain. These are also the specific regions where the tissue is folding in, indicating that it is the ΔATP-jar that causes the folding of the tissue. It could be that the strong expression of Myosin VI in the band of 4-5 cells at the leading edge and the amnioserosa, along with the low expression in the lateral epidermis are necessary for keeping the cells rigid as they migrate. The change in the shape of the actin filaments in stripes expressing the dominant-negative Myosin VI indicates a change in the actin cytoskeleton in these cells, and this could reduce the cells rigidity. However, the loose tissue at the leading edge could also appear as a result of the detachment from the amnioserosa, as appeared when germ band retraction failed.

Embryos expressing ΔATP-jar failed to complete germ band retraction. The germ band tissue appeared loose and separated from the amnioserosa (Fig. 5.7F), and in severe cases germ band retraction did not occur at all (Fig. 5.7G). These results along with the strong expression of Myosin VI observed at the inner edge of the posterior segments during germ band extension (results of Kevin Leaper, (Millo et al., 2004) suggests that Myosin VI is necessary for germ band retraction, either for the migration of the tissue or for the connection with the amnioserosa.

Figure 5.7: The effect of dominant-negative Myosin VI expression. ΔATP-jar was controlled by en-Gal4, at the posterior of every segment. Figures **A-C** and **E** are stained with phalloidin to view the actin filaments and the cell shape. **A**: The disruption of Myosin VI function caused detachment of the cells at the leading edge and the amnioserosa. The actin cable at the leading edge is disrupted in all the areas where ΔATP-jar was expressed. **B**: In some embryos, cells expressing ΔATP-jar in the lateral epidermis changed their shape and the actin filaments lost their tight organization at the cells cortex. **C**: In the final stage of dorsal closure, when Myosin VI is disrupted, dorsal closure is not completed, and holes are left. **D-E**: Some embryos show "folding-in" of the lateral epidermis in the stripes expressing the dominant-negative. **D**: staining with Myosin VI antibody: the stripes expressing the dominant negative Myosin VI have stronger stain of Myosin VI (arrows), and tend to fold inside the embryo. **E**: In severe cases the actin cable disappears and filament aggregates are formed (see arrows). A milder version of this phenotype appeared in the mutants (see figure 5.11). **F-G**: In many cases germ band retraction is not completed, the germ band tissue is loose and folded, and the posterior spiracles are not formed. In **F**, the process of dorsal closure was progressed in spite of the incomplete process of germ band retraction (DE-cadherin stain). In **G** germ band retraction ceased in very early stage: the embryo is totally folded, and the germ band tissue is disconnected from the amnioserosa.

Figure 5.7

ΔATP-jar/ en-gal4

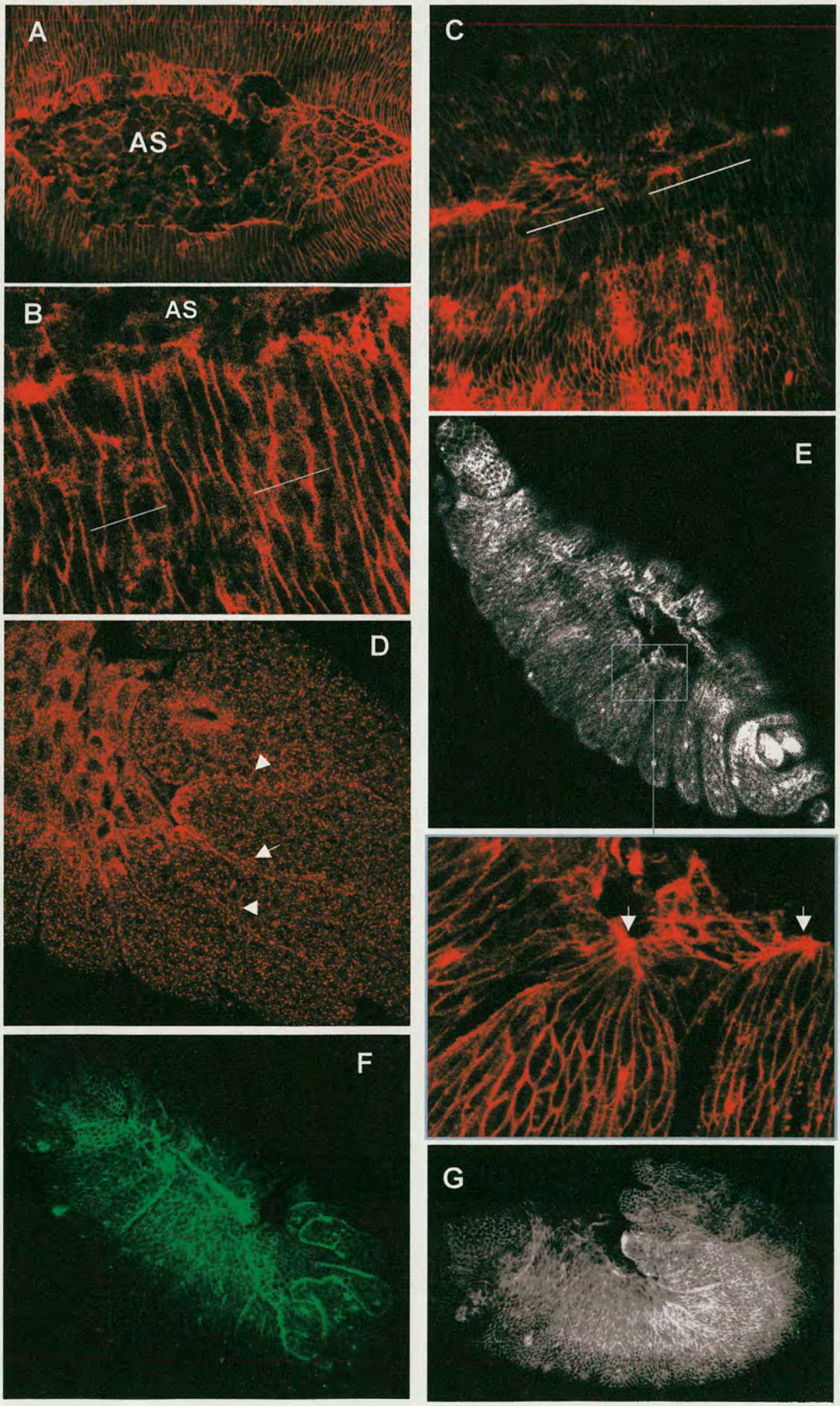

5.8 The affect of Myosin VI depletion on nonmuscle Myosin II expression

Nonmuscle Myosin II is also essential for dorsal closure. Myosin II creates the acto-myosin contractile ring, termed the purse string, at the leading edge. The purse string provides the force to promote dorsal closure. Myosin II also preserves cell shape during the morphogenic changes of the tissue (Young et al., 1993). Previous studies showed expression of Myosin VI (Kellerman and Miller, 1992) and nonmuscle Myosin II (Young et al., 1993) in the amnioserosa and in the surrounding epithelial sheet, but co-localisation of the two proteins during dorsal closure has not been investigated. We were interested to compare the expression of the two myosins in the embryo and to investigate the effect of Myosin VI depletion on Myosin II localisation. For this purpose we used jar^{R39} and jar^{R235} mutant embryos, which lacked any expression of Myosin VI protein during the late stages of embryogenesis. We also used the transheterozygous mutant jar^{R39}/jar^{R235} to ensure that the results are caused by the mutations in *jaguar* gene and not due to the insertion of the P elements on the third chromosome.

In *OrR* flies, we found that Myosin VI and nonmuscle Myosin II show similar localisation in the amnioserosa, and the lateral epidermis (Fig. 5.8.1 A-D), however, Myosin VI shows a stronger expression in the cells surrounding the leading edge compared to Myosin II which is strongly concentrated at the acto-myosin cable. This might suggest that Myosin VI plays a role in keeping the cells connected as dorsal closure progresses. Figure 5.8.1D shows Myosin VI is strongly expressed all over the apical surface of the cells. In the jar^{R39} and jar^{R235} mutants, Myosin VI expression was very weak, while the expression and organisation of nonmuscle Myosin II was similar to that observed in *OrR* (Fig. 5.8.2). In the transheterozygous mutant jar^{R39}/jar^{R235} Myosin II is expressed in the leading edge, the "zipper" region and in the plasma membrane of the cells in the lateral epidermis, although when the embryos fail to complete dorsal closure – the uniform structure of the purse string and the cable at the leading edge disappear and so does the strong expression of Myosin II at the leading edge (Fig. 5.5E, 5.8.3D, E).

The figures in the following pages:

Figure 5.8.1: Expression of Myosin VI and Myosin II in *OrR* embryos during dorsal closure.
A-C show an embryo as the process of dorsal closure is progressing. Myosin VI (**A**) has a strong expression in a layer of four to five cells surrounding the leading edge, while Myosin II (**B**) has a strong expression at the acto-myosin cable, at the leading edge (see magnification). Note the strong expression of Myosin II at the "purse string" and the expression of Myosin VI in the cells surrounding the purse string in the overlay figure (**C**). **D:** observation of the apical surface of the cells at the leading edge shows that Myosin VI is spread all over the cell surface with a very strong intensity. When checking the inner layers Myosin VI appears to be localised in the cytoplasm.

Figure 5.8.2: Expression of Myosin VI and Myosin II in jar^{R39} and jar^{R235} homozygous mutants.
Myosin VI expression is absent in jar^{R39} and jar^{R235} mutants (**A** and **D** respectively). The expression and localisation of Myosin II in these mutant embryos and larvae is not effected (**B** and **E** respectively, and overlay in **C** and **F**).

Figure 5.8.3: Expression of Myosin VI and Myosin II in the heteroallelic mutant jar^{R39} /jar^{R235} and in *ΔATP-jar/ en-Gal4* embryos**.** Figures **A-C** show embryos in the process of dorsal closure. Myosin II is present in the leading edge, in the "zipper" region, and in the plasma membrane of the cells of the lateral epidermis suggesting that the localisation of Myosin II in the heteroallelic mutant is not affected. However, Myosin VI is absent in the cells adjacent to the leading edge (see as comparison the expression in OrR flies). When a heteroallelic mutant embryos fail to complete dorsal closure (**D, E**), the 'purse string' around the amnioserosa is absent and the expression of Myosin II at the leading edge is absent as well, although Myosin II is present in the cells at the lateral epidermis and the amnioserosa. The amnioserosa sheet has lost its organised uniform sheet, having loose cells with a changed shape and holes (arrow). The holes appear also in the area connecting the epidermis and the amnioserosa (**E**, arrow). It seems that the cells at the leading edge have been folded inside so it is impossible to observe the actin-myosin cable. **F:** Myosin II expression is not reduced when ΔATP-jar is expressed in the posterior compartment of the segments, however in some regions myosin II is mislocalised from the membrane (asterisks). The concentration of myosin II is also reduced in the leading edge (arrows), possibly due to the rupture of the acto-myosin cable.

Figure 5.8.1

OrR

Myosin VI (jar)

Nonmuscle Myosin II (zip)

Overlay

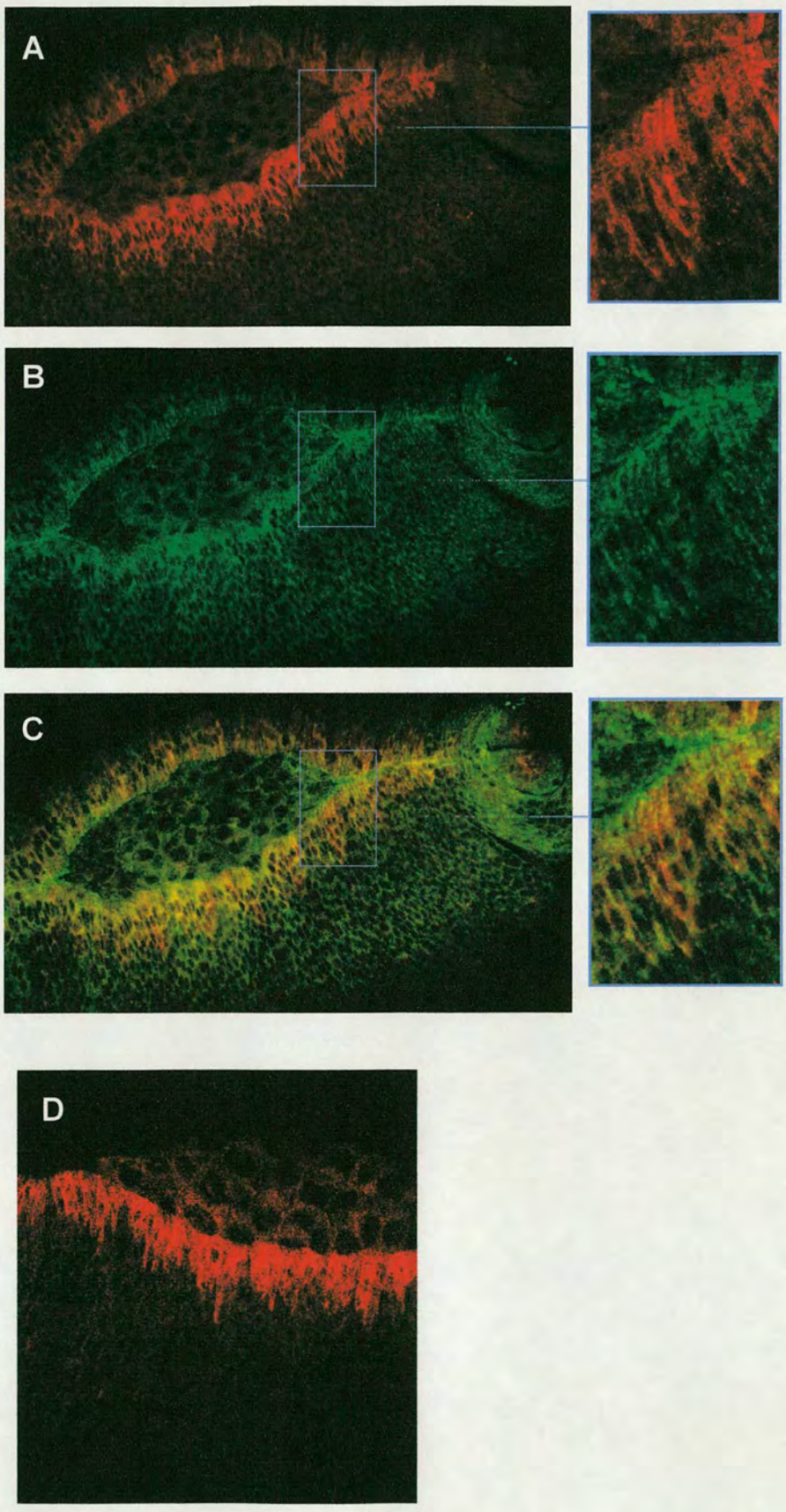

Figure 5.8.2

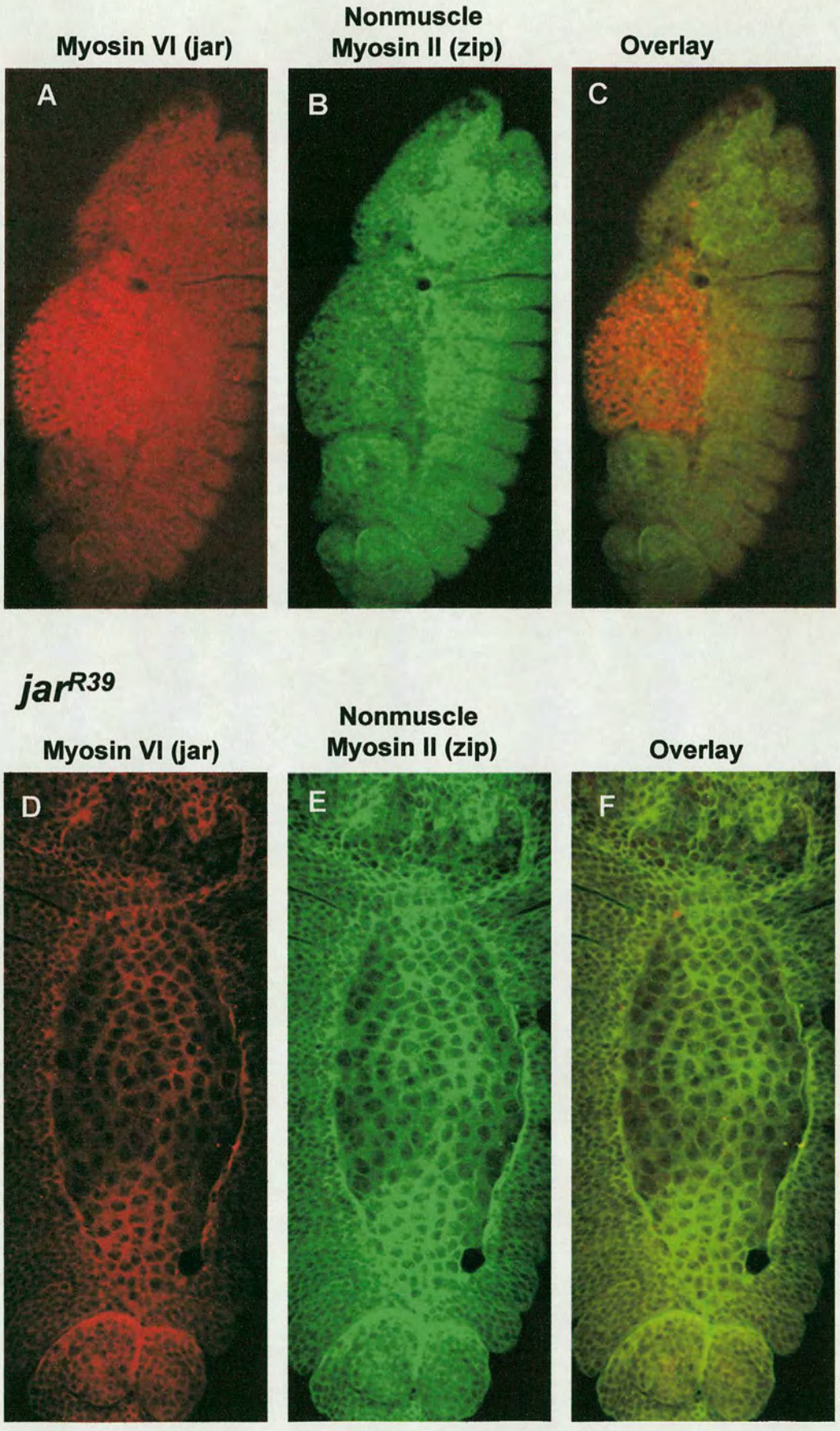
jar R235
Myosin VI (jar)
Nonmuscle Myosin II (zip)
Overlay
A
B
C
jar R39
Myosin VI (jar)
Nonmuscle Myosin II (zip)
Overlay
D
E
F

Figure 5.8.3

jar$^{R39/R235}$

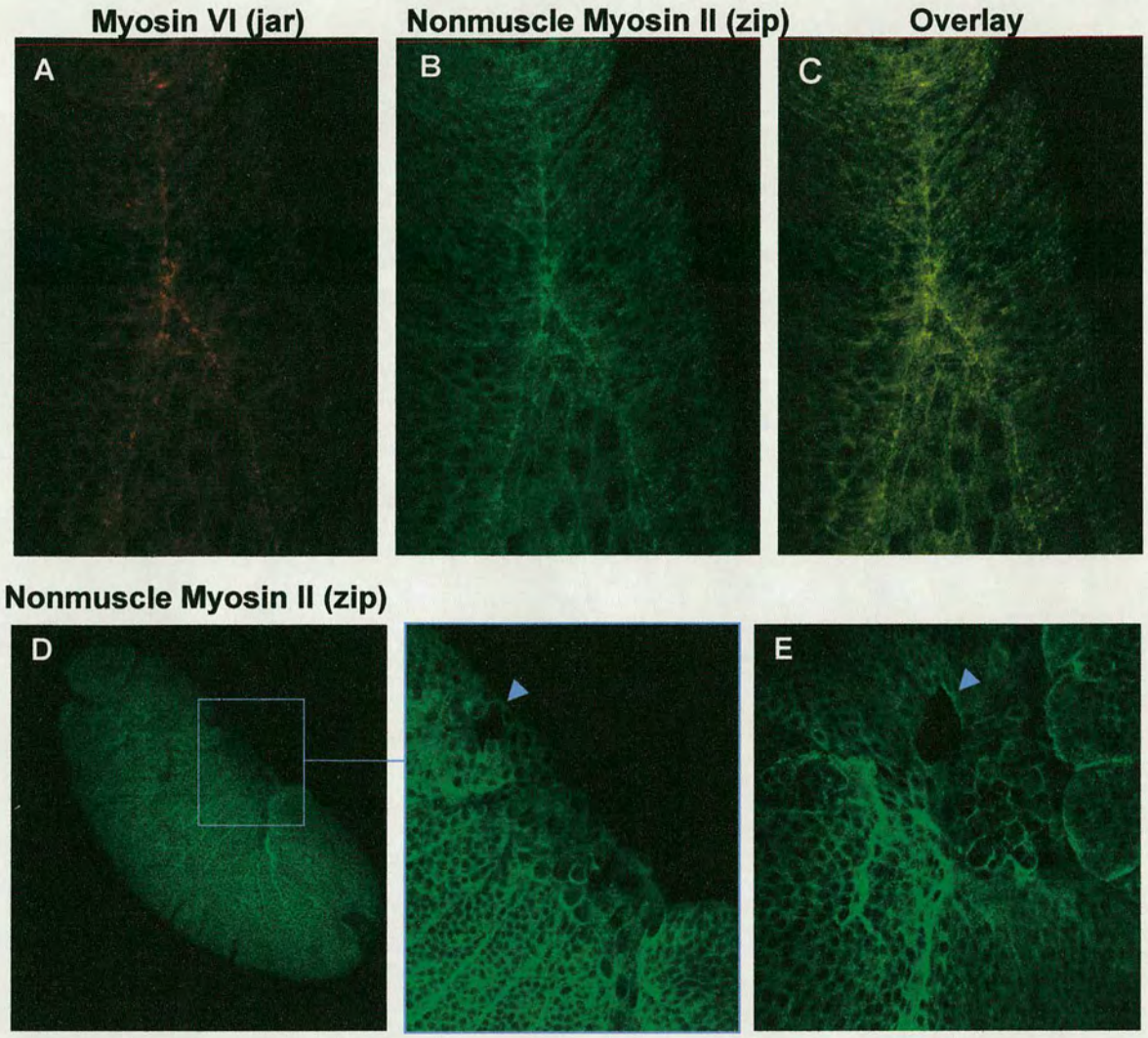

ΔATP-jar/ en-gal4 -Nonmuscle Myosin II (zip)

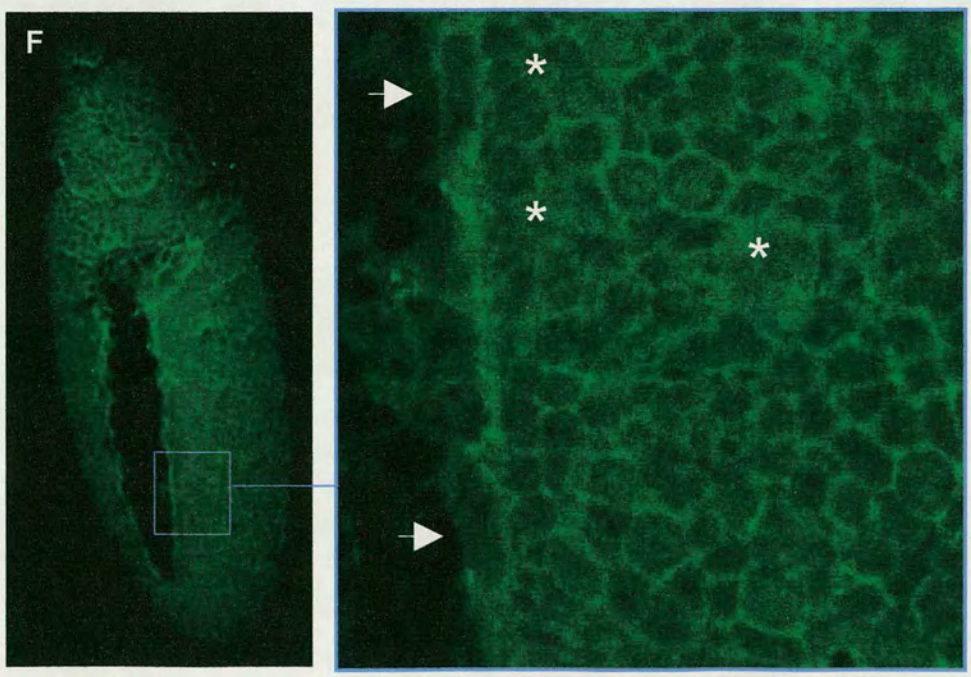

In these embryos the tissue is folded inside the leading edge and is not visible. Considering the strong expression of Myosin VI at the leading edge (Fig. 5.8.1D) we suggest that Myosin VI might be necessary for maintaining the structure of the tissue at the leading edge and preventing it from folding inside during dorsal closure.

To verify these results, the expression of myosin II was also tested when the function of Myosin VI was disrupted by expressing the dominant negative ΔATP-jar (a Myosin VI molecule that lacks the ATP binding domain). This experiment was undertaken my Vasiliki Lazou. At the posterior part of every segment, driven by an *en-Gal4* construct. When looking at the lateral epidermis, the expression of myosin II was not reduced in the posterior stripes and myosin II is localised to the cell membrane, although in some areas localisation was slightly reduced (Fig. 5.8.3, F, asterisks). The mislocalisation of myosin II appeared in isolated groups of cells, therefore it is not clear whether or not it is directly related to the disruption in Myosin VI function. In the leading edge, the expression of myosin II was reduced at the acto-myosin cable, probably due to the rupture of the cable (arrows). Possibly, the mislocalisation of myosin II at the cell membrane could be related to the changes in the actin cytoskeleton in the cell cortex. Previous evidence showed that Myosin II does not co-immunoprecipitate with Myosin VI in embryo extracts (Petritsch et al., 2003). The change in the localisation of myosin II does not seem to be directly related to the function of Myosin VI.

5.9 Disruption of Myosin VI function affects epidermal cell adhesion molecules

Epidermal cells expressing of ΔATP-jar had altered cell adhesion properties. Cell-cell adhesion in the *Drosophila* embryonic epidermis is mediated by DE-cadherin. Myosin VI was found to interact with DE-cadherin during the migration of border cells during oogenesis (Geisbrecht and Montell, 2002). This raises the possibility that Myosin VI interacts with cadherin during embryogenesis and that the loss of cell-cell adhesion in the disruption of Myosin VI function could lead to changes in DE-cadherin expression or localisation.

To test this hypothesis, embryos expressing ΔATP-jar via en-Gal4 expression during dorsal closure were stained with DE-cadherin antibody (Fig. 5.9 A- C). In some of the embryos, DE-cadherin levels were significantly reduced in cells expressing ΔATP-jar (Fig. 5.9 A). In other embryos the localisation of DE-cadherin was disrupted and the protein appeared in the cell cytoplasm and not in the cell membrane as in the wild-type cells (Fig. 5.9B).

In the mutant embryos, the localisation of DE-cadherin in the lateral epidermis, the leading edge and the amnioserosa cells was not altered (Fig. 5.9C). It is possible that the maternal Myosin VI leads to the correct localisation of cadherin. Similar results were observed when the expression of DE-cadherin was examined in *RhoA* homozygous mutant embryos and in embryos expressing the dominant-negative of RhoA, RhoN19: In the homozygous mutant *RhoA* embryos, no defect was observed in the localisation of DE-cadherin, while the in cells expressing RhoN19 the expression of DE-cadherin was significantly reduced (Bloor and Kiehart, 2002).

Figure 5.9: Expression of jar dominant negative molecules disrupts the expression and localization of DE-cadherin and Armadillo within the cells. **A**: some of the areas expressing ΔATP-jar, DE-cadherin is absent from the cell membrane (see arrow in the magnified picture in A), in other areas the localisation of DE-cadherin to the cell membrane is disrupted and DE-cadherin is present in the cell cytoplasm (**B**, arrow). In some areas of the lateral epidermis the tissue is "folding in" (**A**, asterisk). **C**: In homozygous jar^{R235} embryos, no disruption in DE-cadherin expression was observed. **D**: The expression of jar dominant negative also reduced the expression of Armadillo at the cell membrane (arrows).

Figure 5.9

DE-cadherin

ΔATP-jar/ en-gal4

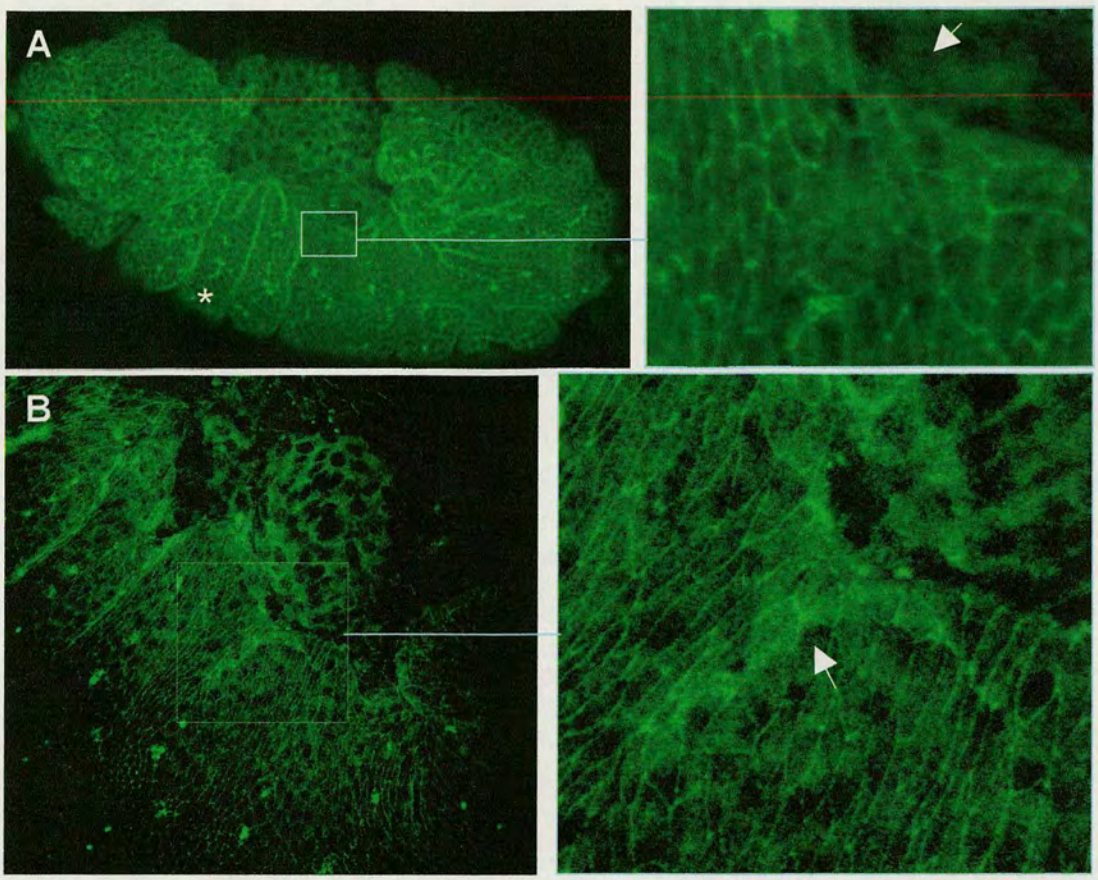

jar^{R235}/ jar^{R235}

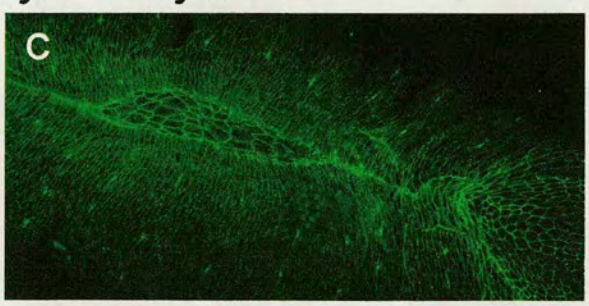

Armadillo

ΔATP-jar/ en-gal4

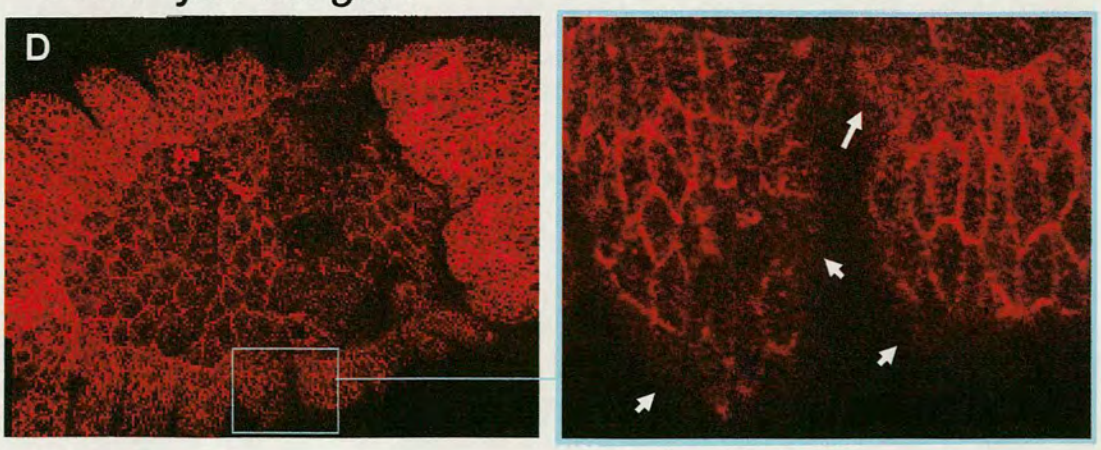

In addition, in embryos expressing ΔATP-jar, the defects observed in the epidermal cells were more severe than the ones observed in the homozygous mutants (possibly due to the maternal contribution of Myosin VI in the mutant embryos).

In *Drosophila* embryogenesis, DE-cadherin interacts with Armadillo, the *Drosophila* homologue of β-catenin. Armadillo binds to Cadherin in cell-cell adhesion complexes, which are necessary for actin co-ordinated movement of cells during epithelial morphogenesis (McCrea et al., 1991; Oda et al., 1994). In the ovary, *Drosophila* Myosin VI interacts with

DE-cadherin and Armadillo (Geisbrecht and Montell, 2002). Since ΔATP-jar expression affects the localisation of DE-cadherin it might also affect the localisation of Armadillo. To test this possibility, *ΔATP-jar/ en-Gal4* embryos were stained with an antibody specific for Armadillo. However, because of the folding- in of the tissue in the stripes expressing ΔATP-jar it was difficult to observe the effects on Armadillo.

In some segments it was possible to see a reduction in Armadillo expression at the lateral epidermis (Fig. 5.9D, arrows), therefore the expression pattern of Armadillo is also changed when Myosin VI function is interfered with.

5.10 The effect of Myosin VI depletion on actin organisation in the amnioserosa and in the leading edge cells

Mutations in the nonmuscle Myosin II gene (*zipper*) have been shown to disrupt actin filaments organisation, causing aberrations of cell shape in the amnioserosa and in the leading edge cells during dorsal closure (Young et al., 1993). Since Myosin VI and nonmuscle Myosin II have a similar pattern of expression, we wanted to check if the depletion of Myosin VI would effect the organisation of actin filaments in the amnioserosa cells in the actin cable and the cells at the leading edge.

In *OrR* flies, Myosin VI and actin have a similar localisation; however, in the leading edge the actin cable is concentrated mainly around the amnioserosa, where Myosin VI is concentrated in a layer of cells between the actin cable and the epithelial sheet (Fig. 5.10A-C). In the leading edge the cells are elongated (Fig. 5.10D), and connected to the actin cable, surrounding the amnioserosa at a uniform width. Not all the mutant embryos showed defects in actin organisation within the cells,

however in some of the mutant embryos that failed to complete dorsal closure, the actin filaments in the amnioserosa are disassociated (Fig. 5.10E). In the leading edge, some of the regions in the actin cable are destroyed, many of the cells are not elongated and the organisation of the cells as a row at the front is disrupted (Fig. 5.10E, increased frame). An aberrant shape is also observed in the border regions between the segments, suggesting that the disruption in the cell shape and movement occurs in other epithelial cells in the lateral epidermis.

When ΔATP-jar was expressed, the loss in cell shape and actin cable organisation was even more dramatic (Fig. 5.7 A-C, E). In severe cases the actin cable disappears, and the cells at the leading edge connect remnants of actin cables that appear as aggregates of filaments (Fig. 7E, arrows). It appears that cell shape in the leading edge and in the amnioserosa changed significantly as a consequence of loss of cell adhesion. In some embryos the cells changed their shape and the tight organisation of the actin filaments at the cell membrane was disrupted (Fig. 5.7 B). The change in the cytoskeletal organisation could be the reason why the cells expressing ΔATP-jar lose their rigidity and fold in. These results suggest that during dorsal closure Myosin VI plays a role not only in the adhesion of the cells, but also in the arrangement of the actin cytoskeleton.

Figure 5.10: Cell shape and actin organisation in the amnioserosa and the leading edge of *OrR* and jar^{R39} mutants. **A-C:** Localisation of actin (**A**) and Myosin VI (**B**) in the embryo prior to dorsal closure. Actin is localised at the leading edge of the migrating epithelial sheet (**C**, white arrowhead), while Myosin VI is localised in a basal layer of cells surrounding actin cables (**C**, yellow arrowhead). Note the strong expression of actin and Myosin VI in the posterior spiracle (arrow). **D** In *OrR*, the cells in the leading edge are elongated, the actin cable is intact and the cells in the amnioserosa are intact and form a uniform layer. **E** a mutant embryo jar^{R39}. The cells in the amnioserosa lose their organised shape, in the leading edge the actin cable is broken in several places (asterisk), and some of the cells still have a polygonal shape and do not elongate. Note the abnormalities in segment organisation, near the asterisk.

Figure 5.10

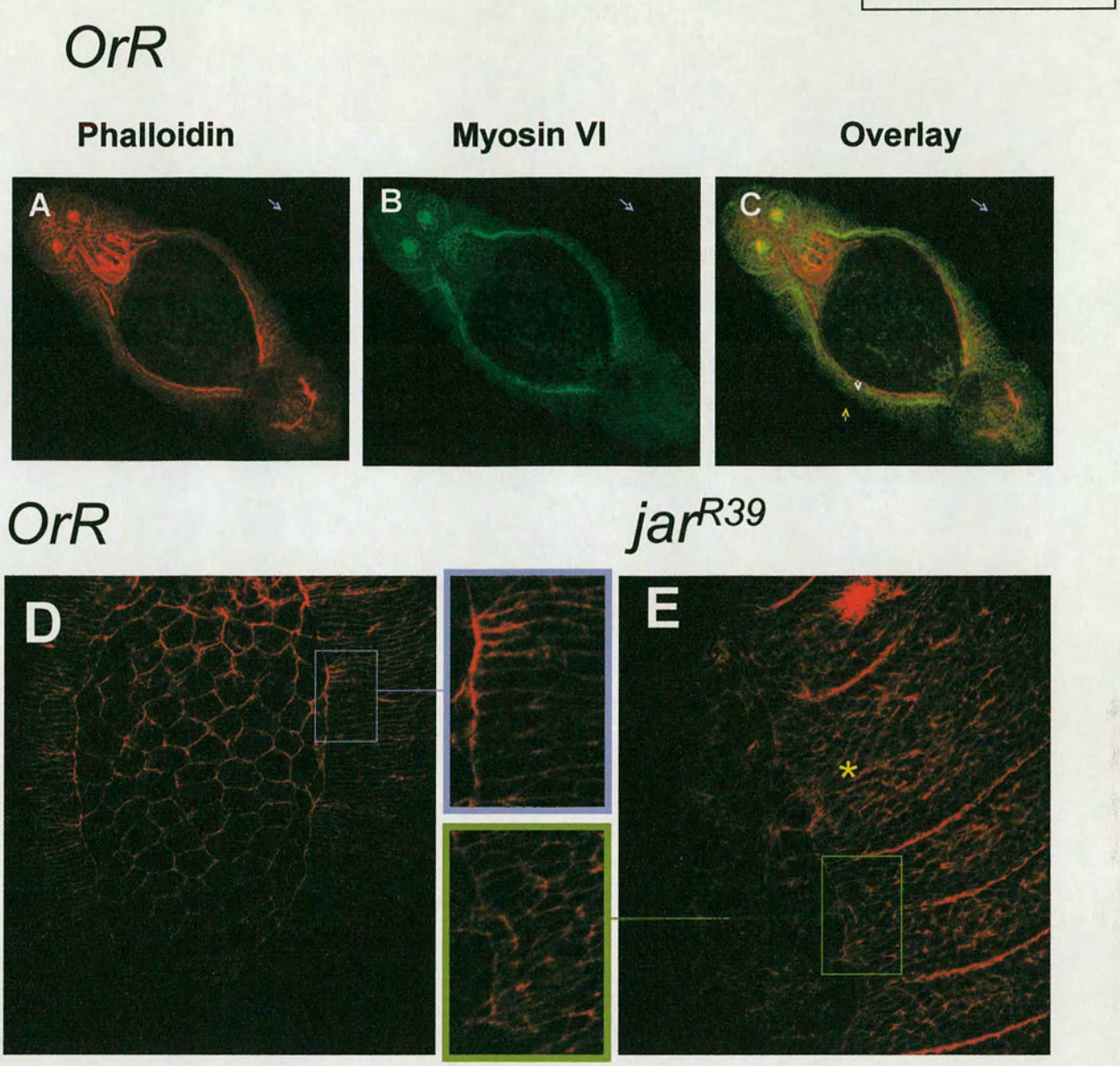

5.11 The expression of Dlg and Crumbs during dorsal closure

In a search for additional proteins that might interact with Myosin VI, Dlg was selected since the mammalian homologue (SAP97) was found to interact with Myosin VI in rat nerve cells. In addition, like Myosin VI, Dlg is necessary for epithelial morphogenesis of the follicle cells during oogenesis, and the epidermis during dorsal closure (Goode and Perrimon, 1997; Perrimon, 1988).

The expression of Dlg was examined in embryos expressing ΔATP-jar in the posterior compartment of every stripe by *en-Gal4*. In cells expressing ΔATP-jar, the expression of Dlg was not changed, and Dlg was localised to the cell membrane, as in wild-type cells (Figs. 5.11A-C).

Crumbs is another protein that is necessary both for the process of dorsal closure and the formation and maintenance of the follicular cells epithelium (Harden et al., 2002; Tanentzapf et al., 2000; Tanentzapf et al., 2003). Crumbs is an integral membrane protein which determines the basal-apical polarity in epithelia (Wodarz et al., 1993). Hypomorphic mutations in the *crumbs* gene cause a failure in germ band retraction, and rupture of the amnioserosa, similar characteristics are observed when the function of Myosin VI is disrupted (Harden et al., 2002). In embryos homozygous for amorphic alleles of *crumbs*, the epidermal cells are disorganised and die (Tepass et al., 1990).

In spite of the similarity in the phenotype of Crumbs mutants and Myosin VI mutants, the expression of Crumbs was hardly changed in cells expressing ΔATP-jar (Fig. 5.11D-E). In several placed the localisation of Crumbs was slightly reduced in the cell membrane however, these areas are relatively small.

Taken together, the disruption in Myosin VI function does not seem to affect the localisation of Dlg and Crumbs during dorsal closure. These proteins are necessary for regulating cell polarity in epithelial cells (Bilder et al., 2000; Wodarz et al., 1993). Perhaps there results indicate that Myosin VI does not play a role in maintaining cell polarity during dorsal closure.

Figure 5.11: The expression of Dlg and Crumbs in *ΔATP-jar/en-Gal4* embryos.**A-C:** Dlg is localised at the cell membrane in wild type cells as well as in cells expressing ΔATP-jar (in the magnification of figure **C**, the stripes of cells expressing ΔATP-jar are marked). **D-E**: The localisation of Crumbs to the cell membrane is found in most of the tissue. Only in several points Crumbs was absent from the cell membrane (marked in asterisks).

5.12 The effect of RhoA on Myosin VI expression during dorsal closure

As shown in this chapter and in previous experiments, Myosin VI and myosin II have a similar pattern of expression during dorsal closure and oogenesis (Deng et al., 1999). The two myosins appear to be necessary in other epithelial tissues: Mutation of the myosin II regulatory light chain, *spaghetti squash (sqh)*, causes malformations of the legs during imaginal disc evagination (Jordan and Karess, 1997). Similar phenotypes appear when the expression of Myosin VI is disrupted, suggesting that the two myosins have similar roles in the evagination of the leg discs (Deng et al., 1999; Edwards and Kiehart, 1996). It is interesting to note that mutations in the signal protein RhoA, cause similar malformations in the legs (Halsell et al., 2000). Genetic studies showed that RhoA signal transduction regulates the activity of Myosin II (Halsell et al., 2000). It is possible that also Myosin VI is also regulated by RhoA, since disruption in the expression of RhoA by using dominant-negative techniques causes similar, but more severe, phenotypes in the embryos, to those we found in Myosin VI mutants (Bloor and Kiehart, 2002).

Previously, the expression of RhoA dominant negative, RhoAN19, interfered with actin filaments organisation, disrupted the localisation of myosin II and reduced the expression of DE-cadherin in the leading edge and the lateral epidermis (Bloor and Kiehart, 2002). To test if Myosin VI expression is controlled by RhoA, the expression pattern of Myosin VI was tested in *UAS-RhoAN19/en-Gal4* embryos. These embryos express RhoA dominant negative protein in a posterior stripe in every segment (Fig. 5.12). The cell shape and the actin filaments were stained with phalloidin. The cells expressing RhoAN19 change their shape and appear larger and rounder than the wild type cells. In addition, the actin cable in the leading edge is present but loses its uniform shape, since the organisation of the actin filaments is disrupted (Fig. 5.12 B, E in the marked stripes). These results are similar to these

jar$^{\Delta ATP}$ X en

Figure 5.11

Dlg

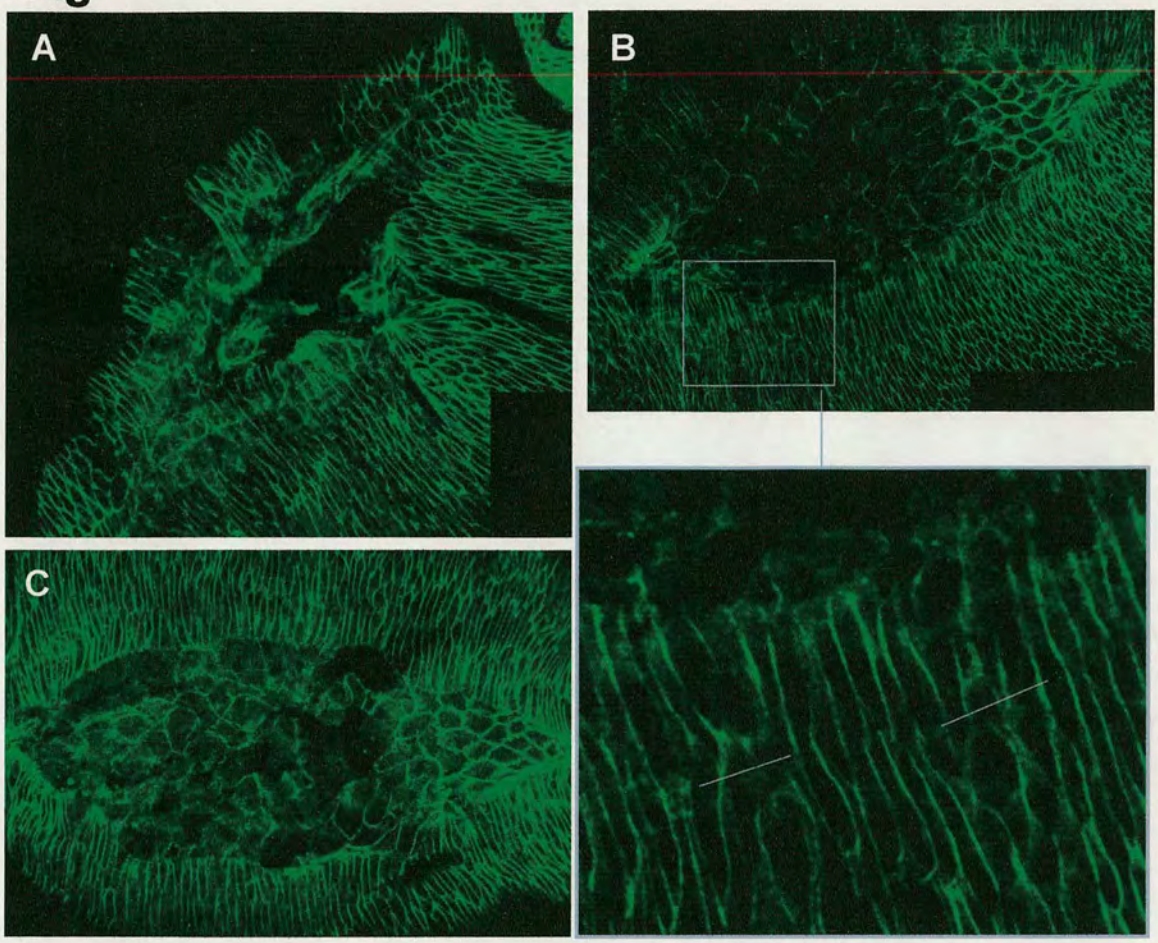

Crumbs

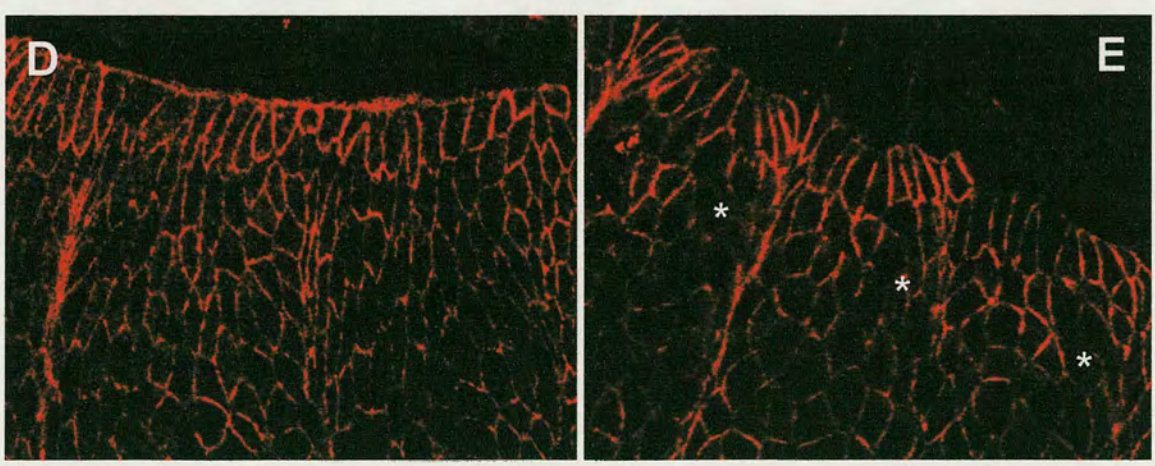

observed previously (Bloor and Kiehart, 2002). When looking at the expression of Myosin VI in wild-type cells, the expression is spread equally in a layer of 4-5 cells at the leading edge, while in

the stripes of cells expressing RhoAN19 Myosin VI is concentrated at the very front line of cells at the leading edge (Fig. 5.12 A, D, arrows). The changes in the localisation could be related to the change in cell size and shape; nevertheless, the results might indicate that RhoA regulates the expression level and the localisation of Myosin VI in the leading edge.

As mentioned previously, the disruption of Myosin VI, myosin II and RhoA lead to abnormal leg morphogenesis. In a genetic screen for genes interacting with myosin II, it was found that the RhoA mutant $RhoA^{E3.10}$ fails to complement the myosin II mutant zip^{Ebr} (Halsell et al., 2000). In this double heterozygous mutant ($RhoA^{E3.10}$ $+/+$ zip^{Ebr}), the adult flies had malformed legs, having a twisted femur and shortened tibia. These results show a genetic interaction between myosin II and RhoA. To test a genetic interaction between Myosin VI and RhoA, a cross was made to create the double mutants: $RhoA^{E3.10}$; +/+; jar^{R39} and $RhoA^{E3.10}$; +/+; jar^{R235}. These flies were originally created from the balanced lines: $RhoA^{E3.10}$ /*Cyo* (balanced at the second chromosome) having curly wings phenotype, jar^{R39}/*TM3, Sb* and jar^{R235}/*TM3, Sb* (balanced on the third chromosome) having stubble bristles on the back.

When crossed together, the double mutant flies lose their balanced chromosomes, and they have straight wings and non-stubble bristles. When the legs were examined in those flies, some of them had malformed legs, however this phenotype was also observed in heterozygous flies that were not double mutants (i.e. $RhoA^{E3.10}$ $+/+$ *TM3)*. In addition, no reduced viability was observed in the double mutant flies.

Therefore, unlike myosin II, Myosin VI and RhoA do complement each other in the double mutant. Perhaps RhoA affects the localisation of Myosin VI during dorsal closure but not during the morphogenesis of imaginal discs.

Figure 5.12: The effect of the disruption in RhoA function on the expression of Myosin VI. Figures **D-F** are magnifications of figures **A-C. A, D**: Myosin VI staining. In stripes expressing RhoAN19 (marked in lines) Myosin VI is concentrated at the very front line of cells in the leading edge, while in the wild type cells the increase in the expression of Myosin VI at the leading edge is less obvious. B, E: Stain of the actin filaments with phalloidin. The cells expressing RhoAN19 are bigger and lost the tight organized shape. Although the actin cable still exists, it lost its uniform shape.

The genetic interactions between Myosin VI and RhoA should be further tested. The two mutations are homozygous lethal at the embryonic stage. The creation of double mutant homozygous mutants for one of the genes could aggravate the phenotype of the embryos. However it might be difficult to observe it since the severity of the phenotypes during embryogenesis is also dependent in the amount of maternal proteins that remain at the late stages of embryogenesis. A double mutant could be created with homozygous alleles that have a weaker phenotype, and survive beyond embryogenesis. For example, the homozygous mutant jar^{322} lives until early stages of the second larval instar. If the double homozygous mutant: $RhoA^{E3.10}$ +/ jar^{322} jar^{322} died during embryogenesis, then it could be concluded that RhoA and Myosin VI genetically interact.

5.13 The effect of Myosin VI on the localisation of CLIP-190 in the central nervous cells.

Although this chapter discusses the role of Myosin VI in dorsal closure, I add this section that deals with the affect of Myosin VI in the localisation of CLIP- 190 (cytoplasmic linker protein 190) in the central nervous system, since the two processes occur during embryogenesis.

Previous studies showed that Myosin VI co-immunoprecipitate with CLIP-190, and that the two proteins co-localise in the connectives and the commissures fibres, which compose the ventral nerve cord (Lantz and Miller, 1998). We were interested to test if reduced expression or disrupted function of Myosin VI would change the localisation of CLIP-190 in the central nerve system.

Figure 5.13: The effect of Myosin VI on the localisation of CLIP-190 in the central nervous cells. **A-C:** In OrR embryos, Myosin VI and CLIP-190 are expressed in the connectives (CN), the commissures (CO) fibres, and the midline glial cells (MGC). **D-F**: Expression of Myosin VI and CLIP-190 in the heteroallelic mutant embryos jar^{R39}/jar^{R235}. **G-L**: Expression of Myosin VI and CLIP-190 in jarΔATP/en-Gal4 embryos. Figures **J-L** are magnifications of figures **G-I**.

Figure 5.12

en-gal4/UAS-RhoN19

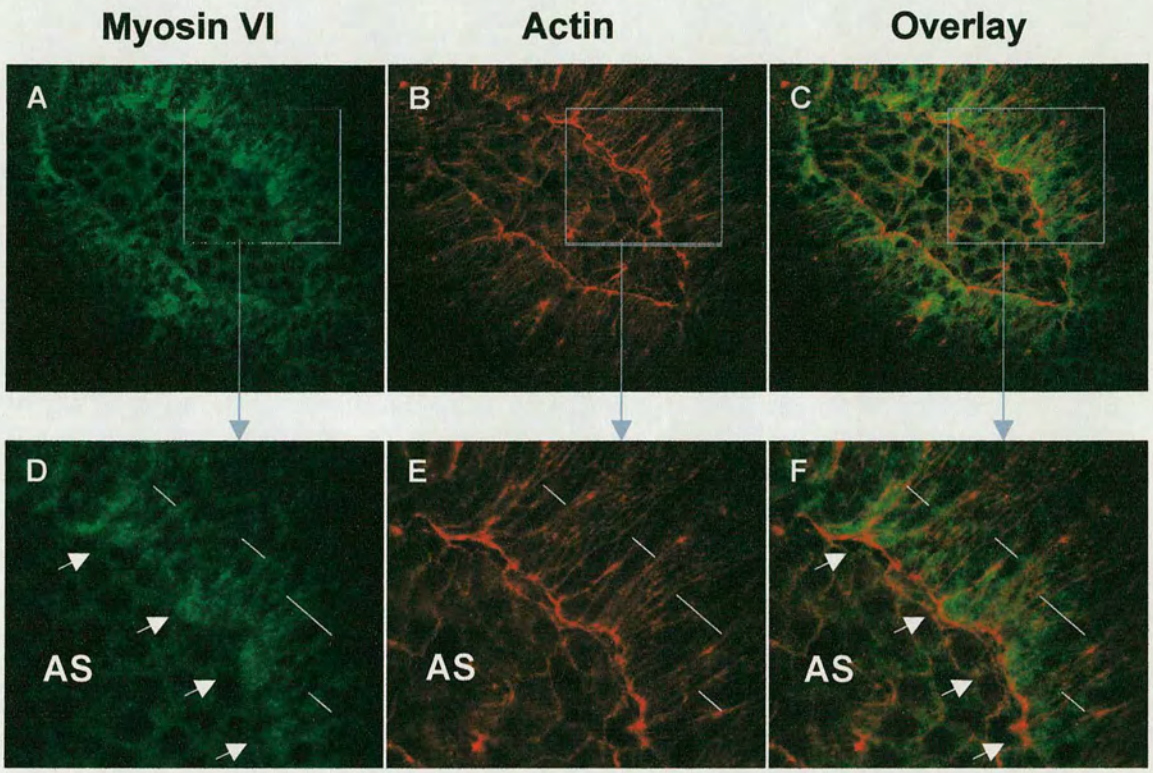

Figure 5.13

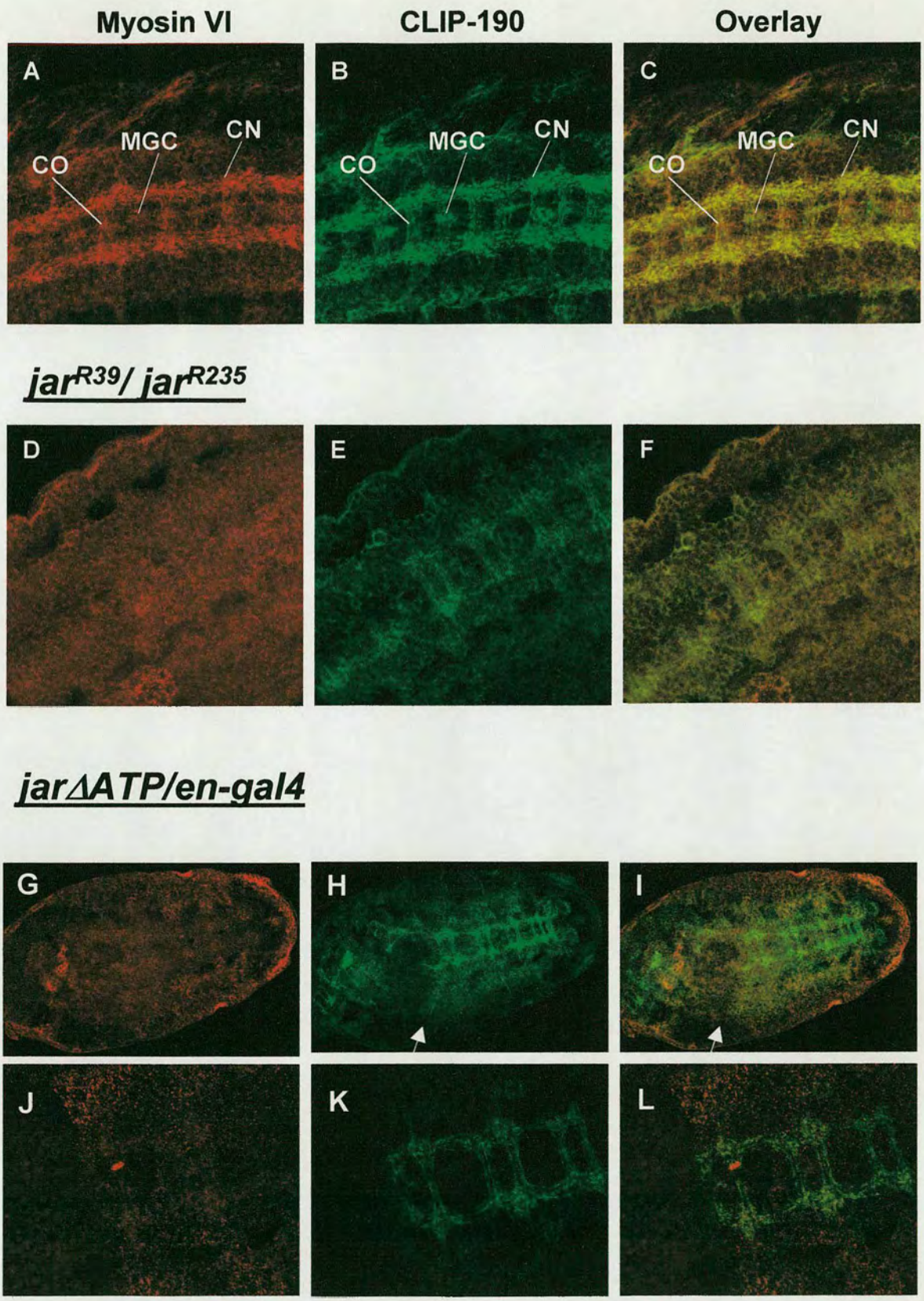
OrR
Myosin VI
CLIP-190
Overlay
A
B
C
CO
MGC
CN
jarR39/ jarR235
D
E
F
jarΔATP/en-gal4
G
H
I
J
K
L

The expression of Myosin VI and CLIP-190 was examined in heteroallelic mutant jar^{R39}/jar^{R235} that has a reduced expression of Myosin VI (Fig. 5.14 D-F), and compared to OrR flies (Fig. 5.14 A-C). In the wild-type embryos, Myosin VI and CLIP-190 were co-localised in the connective (CN) and the commissure (CO) fibres. Co-localisation of the two proteins was also observed in and midline glial cells (MGC), previously Myosin VI was shown to be expressed in the MGC, but CLIP-190 was not observed (Lantz and Miller, 1998). The difference in the expression pattern could be related to the fact that in our experiment the embryos stained were at stage 15, while in the previous experiment the embryos were at stage 16.

In the mutant embryos jar^{R39}/jar^{R235}, the expression of Myosin VI was significantly reduced (Fig. 5.14 D). CLIP-190 was still present in the connective and the commissure fibres, although its expression was slightly reduced. In the midline glial cells, the expression of CLIP-190 was absent.

The expression pattern of CLIP-190 and Myosin VI was also examined when the function of Myosin VI was disrupted at the posterior compartment of every segment by using in *jarΔATP/en-Gal4*. Engrailed was found to be expressed in the central nervous system, during stage 16, in a posterior stripe within every segment (Menne et al., 1997). Although the dominant negative Myosin VI was expressed in the posterior compartments, the expression of Myosin VI was significantly reduced in the entire central nervous system (Fig. 5.14 G, J). Nevertheless,

CLIP-190 was still expressed in the connective and the commissure fibres. The central nerve cord seems to be torn at the anterior (Fig. 5.14 H, I arrow). Presumably, it is related to the destruction of the tissues due to the detachment of the cells, due to the expression of dominant negative Myosin VI.

Taken together, these results show that in spite of the physical interaction between Myosin VI and CLIP-190 in embryos, Myosin VI does not affect the expression or the localisation of CLIP-190 in the central nervous system.

5.14 Conclusions

In this study we provide evidence that Myosin VI is necessary for cell-cell adhesion and maintaining cell rigidity during dorsal closure. Disruption in Myosin VI function caused folding-in of the migrating epithelial tissue and rupture of the tissue, which suggests that Myosin VI is necessary not only for the cell-cell adhesion but also for keeping the cells rigid as they migrate.

5.14.1 Identification of novel Myosin VI mutants

Kevin Leaper has isolated lethal mutants in the *jar* gene of *Drosophila* which encodes Myosin VI (Leaper, 2003). The resulting embryos die late in embryogenesis failing to complete dorsal closure or as early larvae. The expression of fluorescent tagged Myosin VI in the mutant embryos rescued the lethal phenotype of embryos. This indicates that the lethality of the embryos is caused by the mutation within the Myosin VI gene, *jaguar*.

Not all the embryos failed to complete dorsal closure and some hatched as larvae. RTPCR results show that in homozygous mutant embryos (stage 14 onwards) Myosin VI transcripts are still observed. However, in the homozygous mutant larvae, the expression level of Myosin VI transcripts is lower than *OrR* (these results are consistent with the Western Blot and antibody localization results). These results suggest that survival throughout embryogenesis is due largely to the use of maternal Myosin VI.

Genetic and molecular analysis revealed that the two mutants have disruptions in a palindromic sequence 339 – 348 bp upstream of *jar* mRNA. The two mutants jar^{R39} and jar^{R235} had imprecise excision of the P element and a new insertion on the third chromosome. Analysis of the transheterozygous mutant jar^{R39}/jar^{R235} revealed that it is the imprecise excision of the P elements from the *jar* gene and not the re-insertion of the P element elsewhere in the chromosome that caused the observed phenotypes and the disruption in Myosin VI expression. Since there is no disruption in the coding sequence, but there is interference with the expression of *jar* transcripts that initiate at the 5′ end of Myosin VI, it seems likely that the *jar* gene has been

disrupted in its promoter/enhancer sequences. It is surprising to find that the deletion of this palindromic region and the whole first exon in *jar*^{mmw14} does not disturb the development of the flies until adolescence, causing only a disruption in the expression of *jar* transcripts and protein in the testes, while the smaller deletions and duplications in *jar*^{R39} and *jar*^{R235} disrupt significantly the expression of *jar* transcripts and protein from embryogenesis, causing late embryonic and early larval lethality. It is possible that the mutations in *jar*^{R39} and *jar*^{R235} not only interfere in the transcription initiation of specific transcripts in this region, but also interfere with the synthesis of other transcripts, driven by other upstream enhancers, while in *jar*^{mmw14} this interference does not exist.

In the three mutants: *jar*^{mmw14}, *jar*^{R39} and *jar*^{R235} the 5' end of the mRNA was truncated, however the truncated region in *jar*^{R39} and *jar*^{R235} is bigger than that observed in *jar*^{mmw14} (1027 bp compared with 517 bp). When comparing with the results of the protein expression in late embryos, it seems possible that the truncation of mRNA in *jar*^{mmw14} disrupts the expression of a specific isoform of Myosin VI in the testes, allowing the rest of the isoforms to be expressed and survive until adolescence, while in the mutants *jar*^{R39} and *jar*^{R235} the bigger truncation disrupts the translation of all the protein isoforms in the larvae, causing lethality in the late embryonic and early larval stages. In contrast to the disruption in the protein expression, some transcripts covering 3′ end of the gene in *jar*^{R39} and *jar*^{R235} were detected. The antibody used for the testing the expression of Myosin VI was raised against the whole tail domain, so if the transcripts covering the 3′ region were translated, the resulting proteins should be detected. It is possible therefore that these mRNAs are not translated.

Analysis of the null mutant *jar*^{322} , published after completion of our experiments (Petritsch et al., 2003), showed that it affected the embryonic neuroblasts and there is no mention of any defects in cell shape in the lateral epidermis, or of some embryos failing in dorsal closure. However, we have shown that the same dominant negative Myosin VI that caused mislocalisation of Miranda and misorientation of the spindle in neuroblasts is shown to disrupt cell attachment in the amnioserosa and the

leading edge epidermis during dorsal closure. Therefore, Myosin VI is necessary for both neuroblast morphogenesis and dorsal closure during embryogenesis. It is surprising to find that the null mutant jar^{322} lives until the early stages of second instar, while the homozygous mutants jar^{R39} and jar^{R235} die during embryogenesis and during first instar. Since no protein was observed in the mutants jar^{R39} and jar^{R235}, the severe effect of the mutants might be expected to be the same as in a null mutant.

5.14.2 The function of Myosin VI during dorsal closure

Depletion and disruption in Myosin VI function caused detachment of cells and folding-in of the migrating epidermis, during dorsal closure. In *en/ΔATP-jar* embryos these affects were dramatic; if the cells expressing ΔATP-jar are not as robust as the wild type cells, they might not be able to bear the multiple forces applied on them during dorsal closure, and as a result the cells will detach from each other, causing a rupture of the tissue.

The rupture of the tissue in the amnioserosa and the epidermis seem to be related to the changes in the adhesion properties of the cells in the absence of Myosin VI function. This assumption is supported by the reduced expression and disruption in the localisation of DE-cadherin and Armadillo in the expression of ΔATP-jar. During oogenesis, DE-cadherin, as well as Myosin VI is necessary for border cell migration and the proteins are co-expressed in the columnar follicle cells, as the epithelium forms around the oocyte (Geisbrecht and Montell, 2002). Indeed, egg chambers expressing Myosin VI antisense RNA show a similar phenotype when comparing them embryos failing to complete dorsal closure: the follicle cells fail to migrate; the cells loose their shape and separate from the epithelium (Deng et al., 1999). In both cases Myosin VI is needed for the correct movement of a sheet or tight cluster of follicle cells.

The reduction of Armadillo expression observed in ΔATP-jar expressing cells suggests that Myosin VI is necessary for the localization of Armadillo, as well as DE-cadherin, to the cell membrane. Interestingly, as in Myosin VI mutants, mutations in *Armadillo* (arm^{XP33}) cause detachment of cells in the amnioserosa. The

amnioserosa rips from the leading edge and as a result the cells at the leading edge remain polygonal in shape (McEwen et al., 2000). This could suggest the two proteins interact to maintain cell-cell interactions during dorsal closure.

In many mutant embryos that failed to complete dorsal closure the leading edge folded inwards. We suggest that the strong expression of Myosin VI at the apical surface of the leading edge cells might be necessary as a physical support for the leading edge during its migration over the amnioserosa. The reduction in the rigidity of the cells could also be related to the change in the organisation of the actin cytoskeleton. In several cases, cells that express ΔATP-jar and mutant cells had an aberrant organisation of the actin filaments in the cell cortex at the leading edge, and the cells lost their elongated shape. This is the area that was found to fold-in in many embryos. The connection between the change in cell shape and the disorganization of the cytoskeleton could suggest that the cytoskeleton is necessary for maintaining cell rigidity. This suggests that Myosin VI preserves cell shape by participating in the synthesis or the patterning of the actin filaments during the migration of the epithelial cells. This is consistent with previous studies showing the role of Myosin VI in actin dynamics in the individualization complex in the testes, via interactions Cortactin, Arp 2/3 and Dynamin (Rogat and Miller, 2002).

Kiehart et al. (Kiehart et al., 2000) showed that the leading edge created a purse-string–like structure that promotes forces required for dorsal closure. As dorsal closure progresses, these cells become elongated and robust. The cells change their shape by the contraction of the acto-myosin cable; however their shape is dependent upon other factors including the adhesion between the cells in the leading edge and in the amnioserosa, and the connection between the leading edge and the amnioserosa. All these properties could contribute to the forces on a cell at the leading edge during dorsal closure and all these parameters change when the function of Myosin VI is disrupted.

The creation of multiple wounds by laser beams in embryos did not prevent their quick recovery (Kiehart et al., 2000). Disruption caused by Myosin VI prevents or does not enable recovery of the ripped tissues, probably due to the loss of cell

adhesion properties. This suggests a potentially important role for Myosin VI in wound healing. Myosin VI and myosin II localise at the leading edge during dorsal closure although Myosin VI seems to have a very little affect on the localisation of myosin II at the cell membrane. Myosin II was found previously to be expressed at the leading edge of wounds in chick embryos and at the wound borders in *Xenopus* oocytes, creating the purse string during the wound closure (Bement et al., 1999; Brock et al., 1996). In the chick bud wounds, antibody staining revealed localisation of cadherins in cell junction clusters at the wound margins. It would be interesting to test whether or not Myosin VI is expressed and necessary for wound healing in mammals.

Many mutant and dominant-negative embryos failed to complete germ band retraction during stages 12-13. The direction of movement of the germ band is opposite to the leading edge in which the germ band moves away from the amnioserosa, leaving it exposed, while the leading edge covers the amnioserosa, therefore the forces applied on every tissue would be different. In spite of the different directions of migration both tissues fail to migrate properly following the disruption of Myosin VI and in both cases the tissues become detached from the amnioserosa, and was loose and disorganized. Myosin VI could maintain the contacts between cells and the extracellular matrix. Mutation in the genes encoding βPS-integrin and αPS3-integrin, which compose PS3, a member of the position-specific integrin family that are necessary for the connection of cells to the extracellular matrix during the *Drosophila* development, caused failure in dorsal closure and germ band retraction (Brown et al., 2000; Narasimha and Brown, 2004). Interestingly, mutations in αPS3-integrin cause the same u-shaped phenotype observed in jar mutants that failed to complete germ band retraction (Schock and Perrimon, 2003). Mutations in βPS αPS1 and αPS2-integrins also cause rupture in the amnioserosa (Roote and Zusman, 1995). In wild type embryos, βPS- integrin is expressed in many areas at the interface between the yolk and the surrounding mesoderm (Leptin et al., 1989), and αPS2-integrin is expressed in the mesoderm which composes the germ band (Bogaert et al., 1987), however PS integrins are not expressed at the leading edge or the amnioserosa. As described in chapter 6, Myosin

VI affects the expression of βPS and αPS2-integrins in the follicle cells. It would be interesting to test the expression of these proteins in the mesoderm in Myosin VI mutants during germ band retraction.

In spite of the necessity for Myosin VI in cell shape organisation and cell movement, depletion of Myosin VI did not significantly change the expression of Myosin II. However, when the function of Myosin VI was disrupted by ΔATP-jar, the localisation of myosin II to the cell membrane was slightly reduced in several regions at the lateral epidermis. Myosin VI and Myosin II also showed similar patterns of expression in the egg chambers during mid and late stages of oogenesis (Deng et al., 1999), however, disruption of Myosin VI expression did not reduce the expression of nonmuscle Myosin II.

5.14.3 Results obtained recently by Vasiliki Lazou: Myosin VI is present at the filopodia and lamellipodia during dorsal closure

As the epidermis covers the amnioserosa during dorsal closure, the epithelial cells at the leading edge shows an extensive activity of filopodia and lamellipodia, which are crucial for zipping together the epithelial sheets and for the precise matching of the cells in the zipping process (Jacinto et al., 2000). The filopodia (and subsequently the lamellipodia) are necessary for bringing together the epithelial cells from opposing edges. Initially, filopodia sent from both edges meet and create a weak adhesion. A regression of the filopodia brings the cells closer and allows a stronger adhesion between the cells along the attached cell membranes (Martin and Wood, 2002). In order to observe the location of Myosin VI during the closure of the dorsal midline, PGM was expressed during dorsal closure, using an *en-Gal4* line, and filopodia and lamellipodia were observed in live embryos. There is strong expression of PGM in the cell membrane at the edge of epithelial cells facing the opposite edge (Millo et al., 2004). PGM was also present in filopodia and lamellipodia. As the cells from opposite tissues meet, PGM expression increased in the adhesion area. When the adhesion between the cells is completed, the expression of PGM between the joined cells is reduced. The expression of PGM in the filopodia and lamellipodia suggests that Myosin VI is necessary for the migration of the cells as well as for cell adhesion;

however the expression in lamellipodia could be necessary for the initial attachment of the cells.

SEM images of embryos expressing of Myosin VI dominant negative revealed that the filopodia was loose and did not connect the two leading edges. The tight organisation of the leading edge was lost and contained membrane protrusions that were not observed in previous studies. These results should be verified with images of wild-type embryos produced in Edinburgh (in order to ensure that there are no artefacts in the way the embryos were treated in this experiment). However if the results are genuine then it is possible the expression of Myosin VI in the lamellipodia is necessary for the attachment of the opposite cells, and that Myosin VI plays a role in membrane ruffling during dorsal closure.

During spermatogenesis in *Drosophila* male sterile *jar* mutants fail in sperm individualization, (Hicks et al., 1999) an event which requires separation of sperm by membranes. It is possible that Myosin VI also plays a role in the remodelling of cell membranes at the leading edge, that this is crucial for the adhesive properties of the cells during dorsal closure. The presence of Myosin VI in filopodia and lamellipodia indicates that Myosin VI functions within those cell extensions. Myosin VI could either be needed for the adhesion of the filopodia to the opposite cells. The presence of Myosin VI could also be necessary for the organisation of the actin filaments or for the synthesis of the cell membrane.

In this chapter two Myosin VI mutants, jar^{R39} and jar^{R235} were characterized, by defining their molecular structure and their mRNA transcription pattern. In a mutant rescue experiment it was shown that the embryonic lethal phenotype of the mutants is related to the lack of Myosin VI. Disruption of Myosin VI function by the expression of Myosin VI dominant negative caused similar abnormalities to the mutants: the embryos failed to complete dorsal closure and sometimes germ band retraction; the cells in the amnioserosa and the epidermis were detached and lost their stringency, causing rupture of the tissues. Myosin VI seems to play a role in the localisation of DE-cadherin and Armadillo to the cell membrane, and in the organisation of actin filaments in the cells membranes. These results suggest that Myosin VI is necessary for mediating the adhesion properties and contributes to the maintenance of the actin cytoskeleton during dorsal closure.

Chapter 6:

The genetic interactions between Myosin VI and other proteins during oogenesis

This work was undertaken in collaboration with Vasiliki Lazou.

6.1 Introduction

Previous research showed that Myosin VI is necessary for the migration of all the follicle cells during oogenesis (Deng et al., 1999; Geisbrecht and Montell, 2002) and that disruption of the expression of Myosin VI causes abnormal organisation of the follicle cell epithelium and deformation of the cells. We asked what the function of Myosin VI is in maintaining the organisation of the follicle cell epithelium. Does it play a role in the adhesion of the cells as they move or does it participate in the actual movement of every single cell?

In order to answer these questions, it was necessary to examine the genetical interaction of Myosin VI with several proteins. Initially the interaction of Myosin VI with proteins that were found to contact with *Drosophila* Myosin VI during other stages of development, or in other species was tested. We investigated the expression of CLIP-190 (cytoplasmic linker protein-190), Clathrin, α-adaptin, and Dlg (Discs Large) (Buss et al., 2001; Lantz and Miller, 1998; Wu et al., 2002). After finding an interaction between Dlg and Myosin VI, the interaction of Myosin VI was tested with a protein that functions downstream to Dlg in the follicle cells, Bazooka.

Another approach was to test the interaction of Myosin VI with proteins that participate in cell adhesion. This approach relates to previous experiments that showed that during oogenesis Myosin VI interacts genetically with DE-cadherin and Armadillo – two proteins that are implicated in cell-cell adhesion (Geisbrecht and Montell, 2002). The interaction of Myosin VI with other cell adhesion proteins was tested, and with proteins interacting with DE-cadherin and Armadillo namely α-spectrin and Ankyrin.

And finally, the effect of Myosin VI function was also tested on proteins necessary for the adhesion of cells to extracellular matrix: the position-specific (PS) integrins 2α-integrin and β-integrin comprising the PS2 integrins (Brown, 2000).

The result for each of the proteins selected is described, followed by a discussion about the possible roles of Myosin VI in epithelial morphogenesis in view of the results obtained.

6.2 Disruption of Myosin VI expression in groups of follicle cells during oogenesis.

The expression of Myosin VI was disrupted in groups of columnar follicle cells using a site-directed gene silencing technique (Deng et al., 1999). Then, a comparison was made between the expression pattern of proteins that were suspected to interact with Myosin VI in the Myosin VI knock-out cells and in wild-type follicle cells. If the expression pattern of a protein changed in the Myosin VI knock-out cells, then it is possible that this protein interacts genetically with Myosin VI.

In previous experiments, the induction of Myosin VI antisense was generated in most of the follicle cells (apart from the border cells), using *C532-Gal4* line (Deng et al., 1999). A more accurate way to examine the effect of Myosin VI is by comparing groups of cells depleted for Myosin VI to wild-type follicle cells within the same egg chamber. In order to induce the knock-out of Myosin VI in a small population of columnar follicle cells, a Myosin VI antisense line, Am 8-2 was crossed with the *E4-Gal4* line. The plasmid insert in the line Am 8-2 contains a UAS target sequence upstream of the Myosin VI antisense sequence. The binding of Gal4 protein with the UAS target sequence triggers the transcription of Myosin VI antisense and the knock-out of Myosin VI in the specific groups of cells that express Gal4.

In all the figures in the following pages, cells with disrupted Myosin VI expression were marked with an asterisk.

Figure 6.2.1: The expression pattern of the *E4-Gal4* line, as shown after crossing with *UAS-PGM* line, 17-1. E4 is expressed in patches of follicle cells: Figure A shows an egg at approximately stage 7-8, and figure B shows an egg at later stage of development, approximately stage 10. Frequently, expression is in groups of cells at the posterior part of the egg chamber (**B**), although PGM also appeared in groups of cells in the whole egg chamber (**A**).

Figure 6.2.2: The antibodies *Drosophila* Myosin VI (**A**) and porcine Myosin VI (**B**) are equally specific. The two antibodies have a weak expression only in cells where Myosin VI is knocked-out (asterisk).

Figure 6.2.3: In some mature eggs, the knock-out of Myosin VI in a group of cells disrupts the creation of the egg shell in this area.

Figure 6.2.1

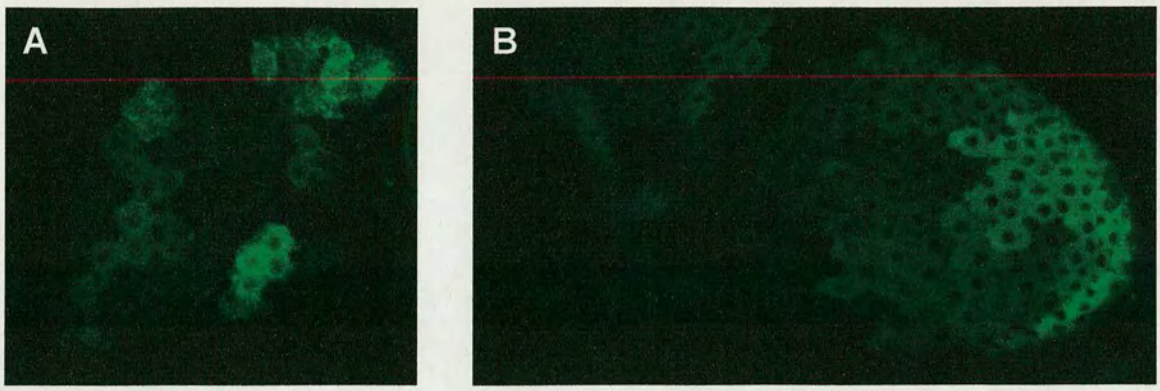

E4 X PGM 17-1

Figure 6.2.2

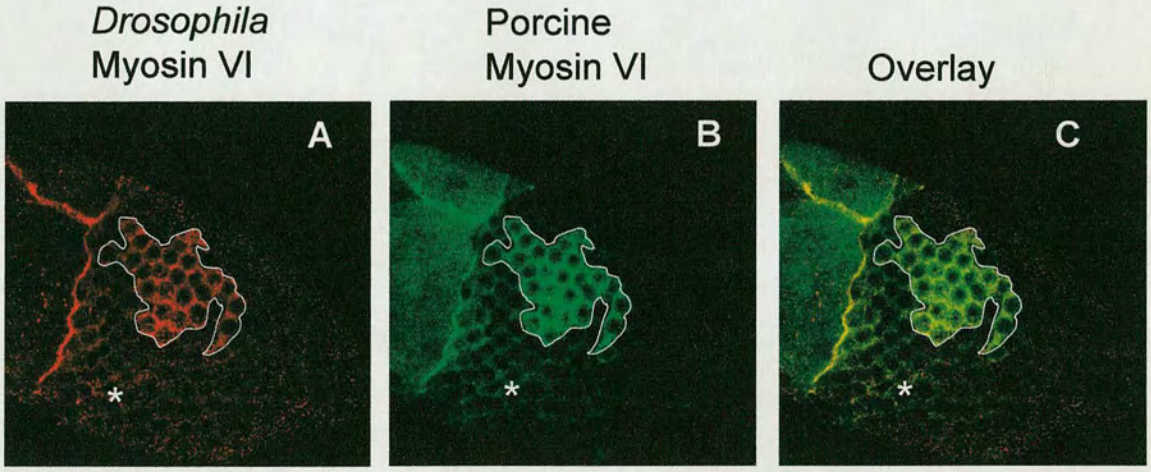

Figure 6.2.3

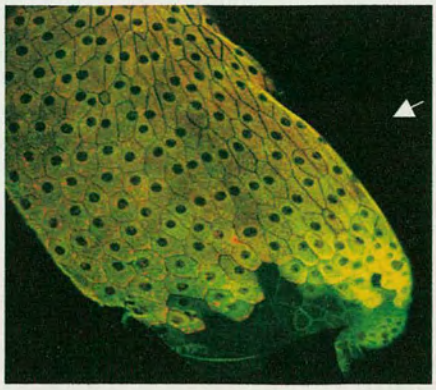

At late stages of oogenesis, E4 expresses Gal4 in patches of follicle cells, mainly at the posterior part of the egg, but during early staged eggs (stage 8 approximately), Gal4 is also expressed in more anterior regions (Fig.6.2.1).

In many cases, the induction of Myosin VI antisense by *E4-Gal4* disrupted the expression of Myosin VI in follicle cells in the anterior part of the oocyte rather then in the posterior region. It seems that there is a time delay between the expression of Myosin VI antisense and the total depletion of the protein. Therefore, the expression of Gal4 in the posterior part of the egg chamber affects the expression of Myosin VI only in later stages, while the disruption of Myosin VI expression in cells located anteriorly could be derived from the induction of Myosin VI antisense in groups of follicle cells located in anterior regions, during earlier stages (stages 8-9). The misexpression of Myosin VI in *Am 8-2; E4-Gal4* flies did not interfere with the organisation of the follicle cell epithelium. However, since the chorion layer was not created at this area (Fig. 6.2.3), in several cases the posterior part of the egg remained open .This can be possibly explained by the fact that the disruption of Myosin VI prevented the proper migration of the follicle cells to this area and for that reason the chorion could not be secreted there properly. Another possibility is that the disruption of Myosin VI interfered with the secretion of the chorion by the follicle cells.

The antibody used to detect *Drosophila* Myosin VI was raised in mice. Some of the antibodies that were tested were also raised in mice. In order to make double staining of Myosin VI with other proteins, it is necessary to use antibodies that were raised in two different host species. For this reason a Myosin VI antibody was needed that would be specific for *Drosophila* Myosin VI but who not raised in mouse. The porcine Myosin VI antibody was raised in rabbit. This antibody was raised against the whole Myosin VI tail, having 61% identity with *Drosophila* Myosin VI tail. In order to test its specific binding to *Drosophila* Myosin VI, a double staining was made with anti-*Drosophila* and anti-porcine Myosin VI, in *Am8-2; E4-Gal4* egg chambers (Fig. 6.2.2). The expression of the two antibodies appeared in wild-type cells, while the expression in Myosin VI knocked-out cells was significantly reduced.

Therefore the porcine Myosin VI antibody is specific for *Drosophila* Myosin VI and could be used as a substitute for the experiments.

6.3 The effect of Myosin VI knock-out on the expression of CLIP-190, α-adaptin, Clathrin and Dlg

As discussed in the previous section, the first approach used in the experiments was to examine the interaction of Myosin VI during oogenesis with proteins that were found to interact with Myosin VI at different stages of development or in other species.

Previous experiments show that CLIP-190 (cytoplasmic linker protein-190) was found to interact with Myosin VI and co-localise in the central nerve system and in the posterior pole, in *Drosophila* embryos (Lantz and Miller, 1998). In the follicle cells, CLIP-190 is expressed in the cytoplasm. The results of the co-localisation experiments show that the knock-out of Myosin VI does not affect the expression or the localisation of CLIP-190 (Fig. 6.3.1).

Myosin VI interacts physically α-adaptin and Clathrin with and was found to be associated with Clathrin coated pits in polarized cells containing microvilli (Buss et al., 2001). During oogenesis, these proteins had already been found to be expressed in follicle cells, mainly at the interface between the follicle cells and the oocyte (Dollar et al., 2002; Richard et al., 2001). Clathrin is expressed in the cell cytoplasm, and excluded from the nucleus (Fig. 6.3.2). When the expression of Myosin VI is disrupted, the organisation of Clathrin around the nucleus is not as clear as in the wild-type follicle cells (Fig. 6.3.2). This could suggest that Myosin VI plays a role in the localisation of Clathrin. However, because the change in the localisation of Clathrin is very small, the slight change in Clathrin localisation could be related to a physiological change in cell shape in the absence of Myosin VI.

The disruption in Myosin VI expression had a more significant effect on the expression of α-adaptin (Fig. 6.3.3). In figures 6.3.3. A-C, three groups of follicle cells that show a reduced expression of Myosin VI are marked with asterisks.

In figures 6.3.3. D-F, the upper left group of cells are magnified, and viewed on a focus level closer to the basal side of the cells.

On the lateral surface of the cells the expression of α-adaptin in the cell membrane is reduced significantly. The disruption of Myosin VI expression also reduced the expression of α-adaptin in the area between the follicle cells and the region facing the oocyte (Fig. 6.3.6. J-K). These results seem to suggest that Myosin VI and α-adaptin co-localise in the cell membrane and in the follicle cell-oocyte interphase, and that Myosin VI plays a role in the localisation of α-adaptin to the cell membrane. The reduction of Myosin VI expression did not always affect the expression of α-adaptin (Fig. 6.3.3 G-I). This result may indicate that the interaction of Myosin VI with α-adaptin is not direct, but rather is mediated by other proteins.

Myosin VI was found to interact with SAP97 (synapse-associated protein) in rat nerve cells and to form a complex with GluR1 (Wu et al., 2002). The *Drosophila* homologue of SAP97 is Discs Large (Dlg). Dlg is a tumour suppressor protein that is necessary to block follicle cell invasion and to maintain cell polarity (Goode and Perrimon, 1997). Loss of Dlg function causes invasion of follicle cells (which are not border cells) to the nurse cells cluster as a result of abnormal cell proliferation and migration (Goode and Perrimon, 1997). The invasive follicle cells were also found to lose their polarity. It was tested if Myosin VI and Dlg have related functions during the formation of the follicle cell epithelium. In columnar follicle cells, Myosin VI and Dlg co-localise to the cell membrane (Fig. 6.3.4.1 and 6.3.4.2 A-C). In migrating cells, the expression of the two proteins increases and Dlg is also expressed in the cytoplasm (Fig. 6.3.4.1, arrows). When the expression of Myosin VI is disrupted (Fig. 6.3.4.2 A-F, area marked in asterisk), Dlg is mislocalised to the cytoplasm and, in severe cases, the expression of Dlg is reduced noticeably (Fig. 6.3.4.2 G-I, area marked in asterisk). These results show that Myosin VI is crucial for the expression and the localisation of Dlg to the follicle cell membrane.

In addition, Myosin VI plays a role in the localisation of the endocytic proteins: Clathrin and α-adaptin, although the affect of Myosin VI knock-out on the expression pattern of these proteins is less significant. The disruption of Myosin VI did not seem to affect the expression of CLIP-190.

In all the figures in the following pages, cells with disrupted Myosin VI expression were marked with an asterisk.

Figure 6.3.1: The expression of Myosin VI and CLIP-190 in ovaries expressing Myosin VI antisense directed by E4-Gal4. Myosin VI (**A**) and CLIP-190 (**B**) co-localise in the follicle cell cytoplasm (**C**), however disruption in Myosin VI expression does not affect the expression of CLIP-190 (area marked with asterisk). Figures **D-F** are magnification of figures **A-C**.

Figure 6.3.2: The expression of Myosin VI (**A, D**) and Clathrin (**B, E**) in ovaries expressing Myosin VI antisense directed by E4-Gal4. Myosin VI and Clathrin co-localise in the cell membrane and cytoplasm (**C, F**), segregated from the nucleus. In cells where Myosin VI expression is disrupted, the exclusion of Clathrin from the nucleus is less obvious.

Figure 6.3.3: The expression of Myosin VI (**A, D, G**) and α-adaptin (**B, E, H**) in ovaries expressing Myosin VI antisense directed by E4-Gal4. Myosin VI and α-adaptin co-localise mainly at the cell membrane (**C, F, I**). In many cases, the disruption in Myosin VI expression had only a slight effect on α-adaptin expression (**B, H**). However, in some cells the knock-out of Myosin VI significantly reduced the expression of α-adaptin at the lateral cell membrane (**E**), and at the apical side of the follicle cells (**J, K**, arrows).

Figure 6.3.4.1: Myosin VI (**A**) and Dlg (**B**) show a strong expression in the migrating dorsal-anterior follicle cells during stage 11. Dlg is localised to the cell membrane in most of the follicle cells, and in the migrating cells. Dlg is also expressed in the cytoplasm (arrow).

Figure 6.3.4.2: The expression of Myosin VI (**A, D, G**) and Dlg (**B, E, H**) in ovaries expressing Myosin VI antisense by E4-Gal4. Myosin VI and Dlg co-localise at the cell membrane (**C, F, I**). Cells in which Myosin VI expression is disrupted, Dlg is mislocalised to the cytoplasm (**E**, asterisk) or not expressed at all (**H**).

Figure 6.3.1

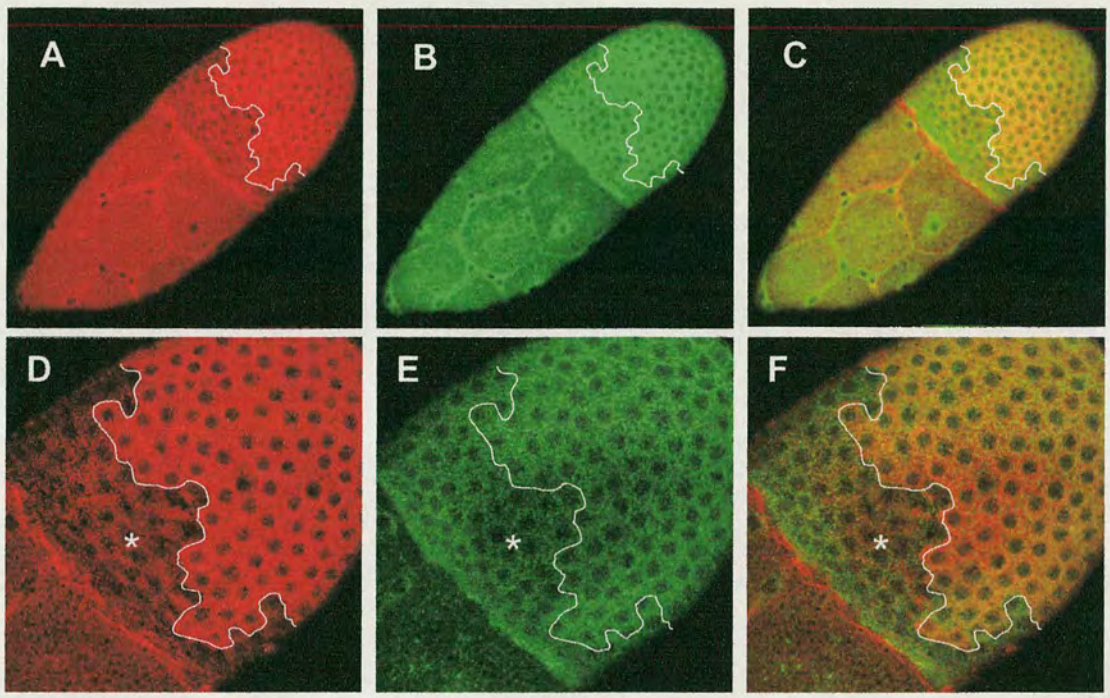

Figure 6.3.2

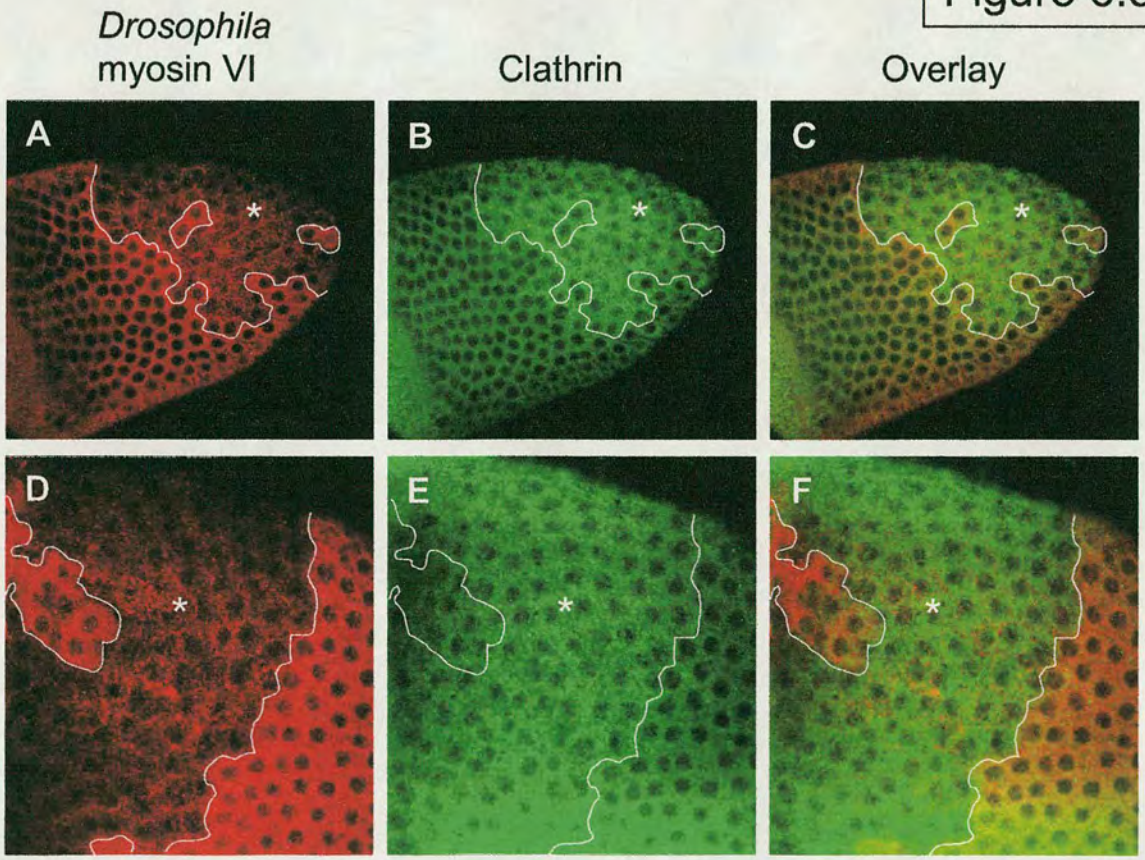

Figure 6.3.3

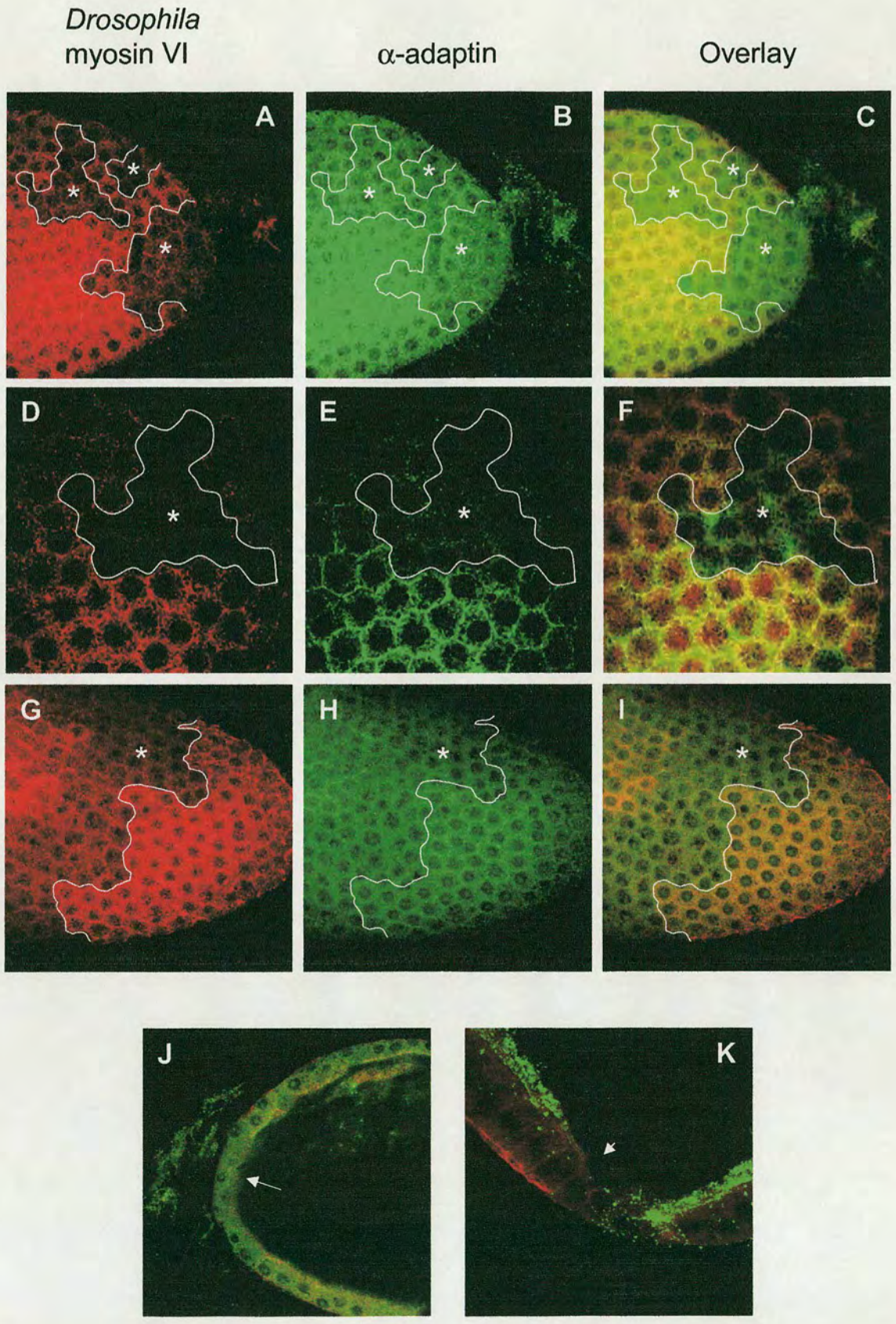

Figure 6.3.4.1

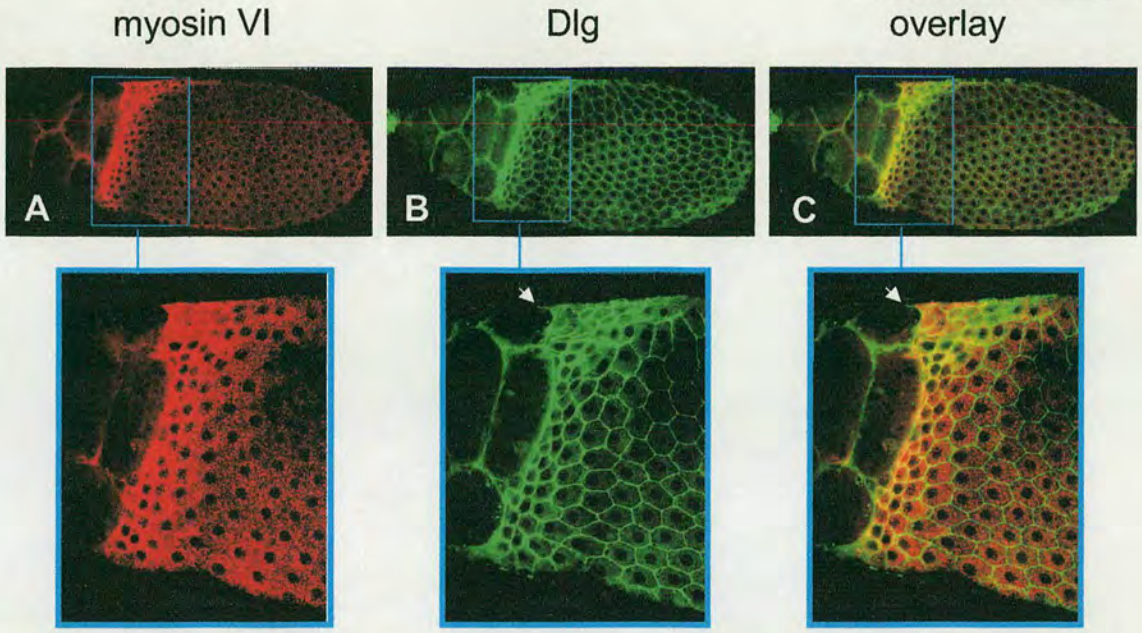

Figure 6.3.4.2

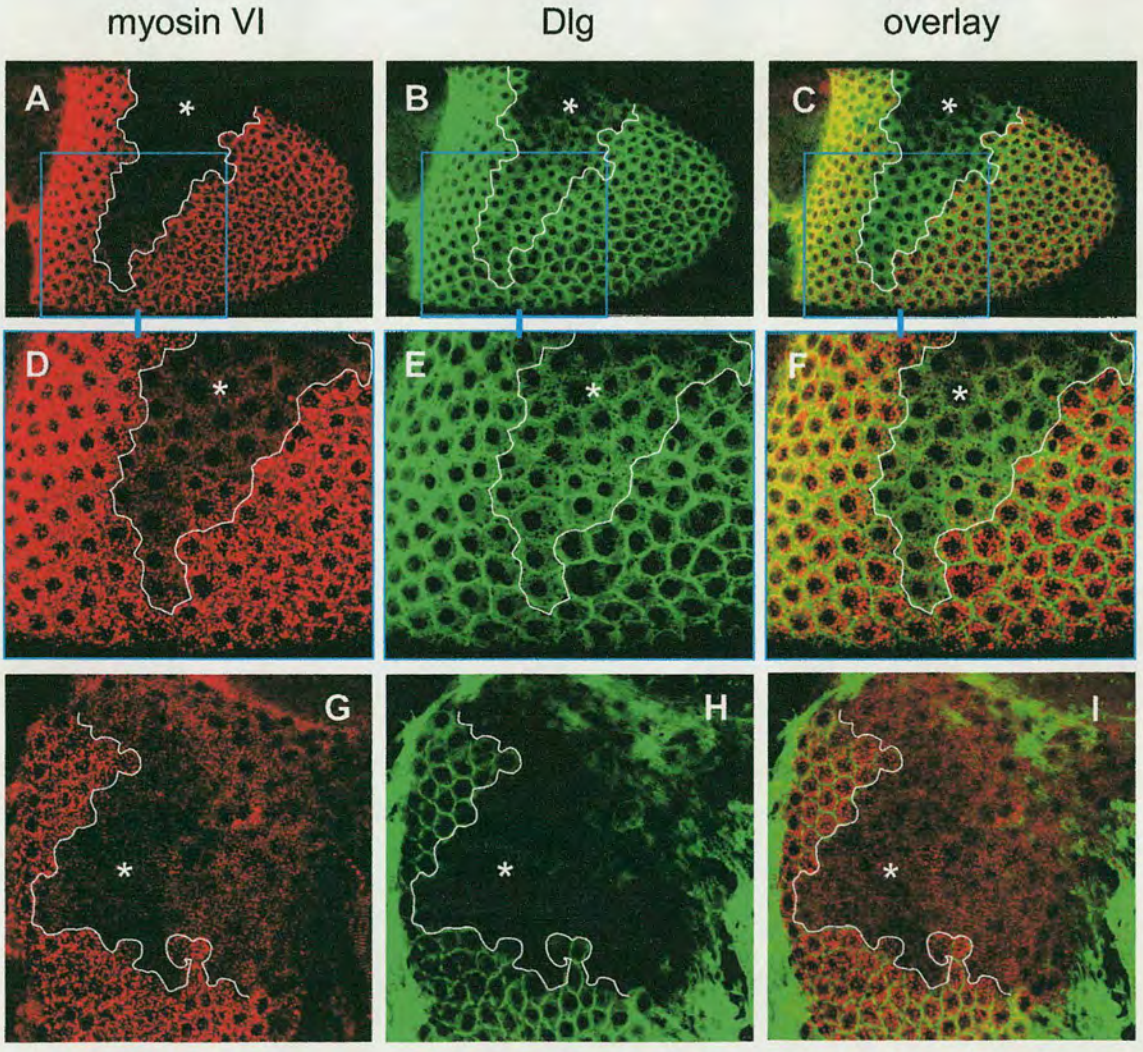

6.4 The genetic interaction of Myosin VI with Bazooka

After finding the affect of Myosin VI on Dlg expression, possible interactions of Myosin VI with proteins that interact with Dlg were investigated. Dlg interacts genetically with Bazooka in the follicle cells (Abdelilah-Seyfried et al., 2003). In *dlg* mutants, Bazooka loses its apical polarity. In the double mutant for the *dlg* and *bazooka* genes, the invasion of the follicle cells is prevented, suggesting that Bazooka acts as a permissive factor in invasive follicle cells created in *dlg* mutants, possibly by stabilising the adhesion between the follicle cells and the nurse cells (Abdelilah-Seyfried et al., 2003). Mutation in the *bazooka* gene increases the proliferation of the follicle cells (Huynh et al., 2001). In the border cells, Bazooka does not play a permissive role, but rather regulates the adherence of cells within the cluster.

When examining the basal surface in wild-type follicle cells, Bazooka is expressed strongly in a punctate form, possibly attached to cytoplasmic vesicles that co-localise with Myosin VI (Fig. 6.4.1 A-F). A strong expression of Bazooka also appears in the cell membrane and around the nucleus. In Myosin VI knock-out follicle cells, the strong expression of Bazooka in vesicles at the cell cytoplasm is reduced significantly (Fig. 6.4.1 A-F, area marked in asterisk).

These results suggest that a genetic interaction between Myosin VI and Bazooka takes place. Because Dlg was shown to function upstream of Bazooka in the follicle cells, and the affect of Myosin VI on the expression and localisation of Dlg, it is possible that the reduced expression of Bazooka in Myosin VI knock-out cells is related to the mislocalisation of Dlg.

Figure 6.4.1: The expression of Myosin VI (**A, D**) and Bazooka (**B, E**) in ovaries, expressing Myosin VI antisense directed by E4-Gal4. Figures **D-E** are magnifications of figures **A-C**. Myosin VI and Bazooka are expressed at the cell cytoplasm in a punctuated manner (**C, F**). Disruption of Myosin VI expression reduces the strong punctate expression of Bazooka in the cell cytoplasm (**E**, asterisk).

6.5 The effect of Myosin VI depletion on the expression of α-spectrin, Ankyrin, PS2α-integrin and PSβ-integrin

It was investigated if Myosin VI could interact with proteins implicated on the organisation of follicle cell monolayer by mediating adhesion or polarity properties of the cells. Previous experiments have shown that during oogenesis, Myosin VI interacts in the follicle cells (border and columnar cells) with the adhesion proteins DE-cadherin and Armadillo (Geisbrecht and Montell, 2002). It is also known that Myosin VI is necessary for the adhesion of the cells during dorsal closure (chapter 5, (Millo et al., 2004). These results seem to suggest that during oogenesis, Myosin VI maintains the cells attached to each other as they migrate. Alternatively, it may be that Myosin VI is necessary for maintaining cell polarity.

α-spectrin is an actin binding protein located in the follicle cells that creates a network of αβ heterodimers (attachment of α and β spectrin subunits) to the lateral plasma membrane, and heterodimers with a larger β-spectrin subunit (β_H) at the apical surface (Lee et al., 1997). The formation of the network appears to be essential for the maintenance of the follicle cell monolayer (Deng et al., 1995). When the expression of α-spectrin is disrupted in follicle cell clones, the organisation of the follicle cell monolayer is disturbed from stage 9 onwards, causing overlap of cells in certain areas and absence of cells in other areas (Deng et al., 1995; Lee et al., 1997). In the areas where follicle cell organisation is disrupted, the cells lose their shape and their polarity, which suggests that α-spectrin is necessary for determining the orientation of the follicle cells in the monolayer (Lee et al., 1997).

Figure 6.5.1: The expression of Myosin VI (**A**) and α-spectrin (**B**) in ovaries, expressing Myosin VI antisense directed by E4-Gal4. Myosin VI and α-spectrin co-localise at the lateral membrane (**C**). Knock-out of Myosin VI does not seem to affect on the expression of α-spectrin (**B**, asterisk).

Figure 6.4.1

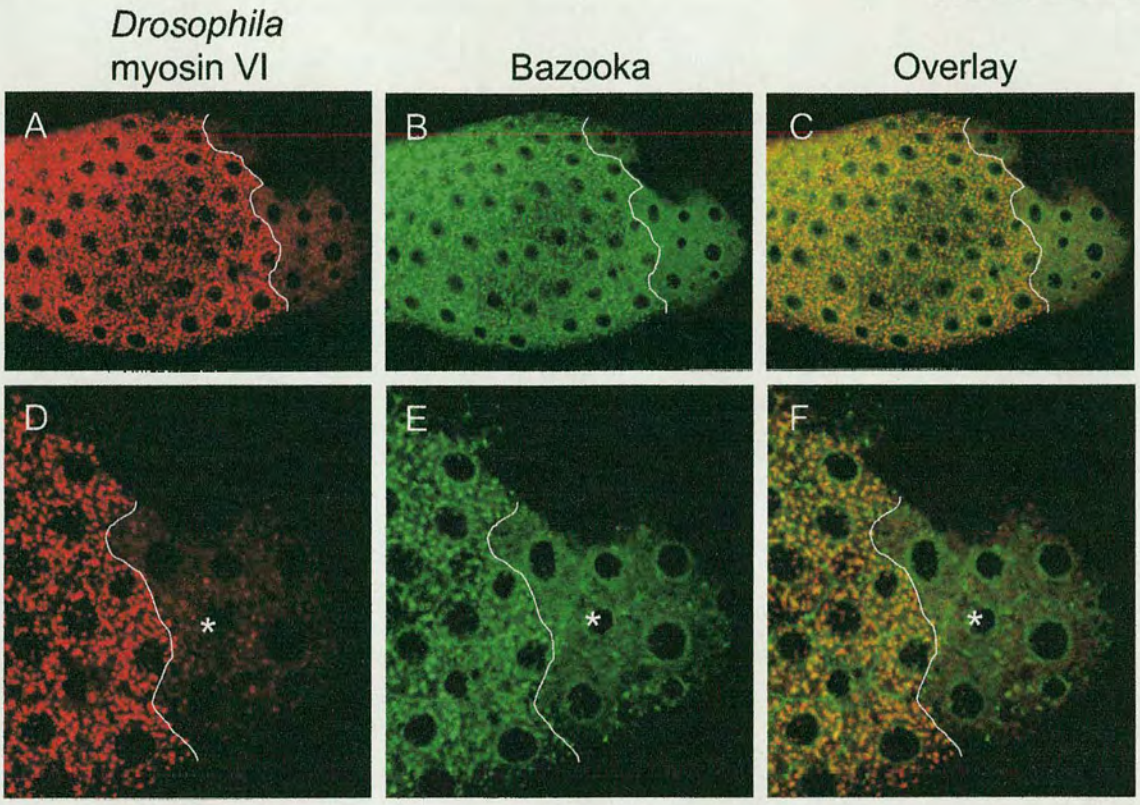

Figure 6.5.1

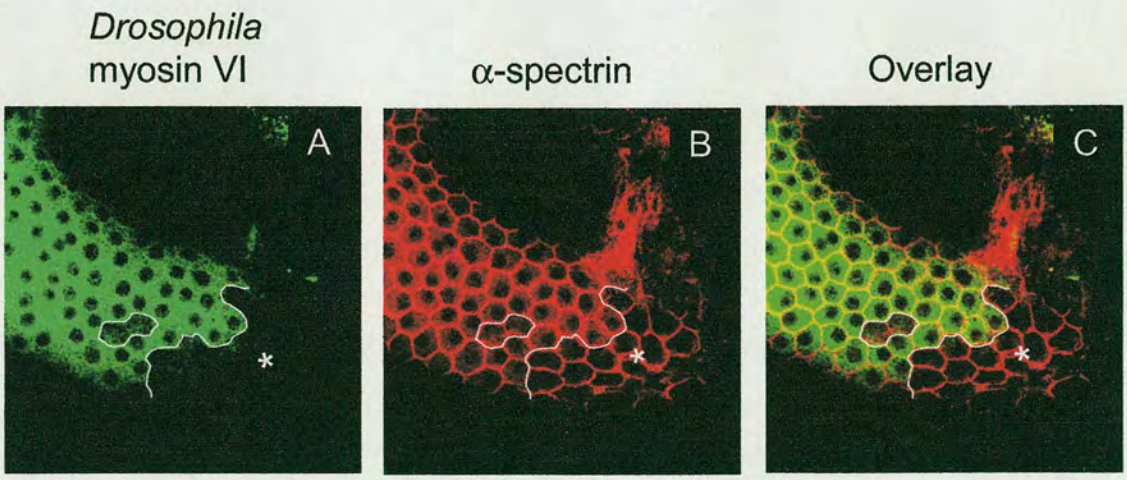

In *Armadillo* mutants follicle cells that lost the organisation of the adherens junctions, the expression of α-spectrin in the lateral membrane was reduced (Tanentzapf et al., 2000). The upstream effect of Myosin VI on Armadillo expression in the follicle cells could also affect the expression of spectrin (Geisbrecht and Montell, 2002). In order to examine whether Myosin VI participates in the polarisation of the follicle cells, during the follicle cell epithelium formation, the expression of α-spectrin in the absence of Myosin VI was tested.

In Madin-Darby canine kidney (MDCK) cells, during the assembly of the cells to an epithelial tissue, a complex containing E-cadherin, Ankyrin, Na, K-ATPase and Fodrin was formed (Nelson et al., 1990). In *Drosophila* S2 cells, Ankyrin and β-spectrin were recruited to sites of cell-cell adhesion, when the cells expressed the homophilic adhesion molecule neuroglian, however DE-cadherin did not affect the recruitment of Ankyrin (Dubreuil and Grushko, 1999). Taken together, the localisation of Ankyrin at cell-cell adhesion sites might suggest that Ankyrin plays a role in cell-cell adhesion.

Previous experiments showed that Ankyrin functions as a peripheral membrane protein that connects the spectrin network with the plasma membrane in red blood cells (Bennett and Baines, 2001). In *Drosophila* embryos, an αβ-spectrin complex was found to co-immunoprecipitate when using Ankyrin antiserum, although in the *α-spectrin* mutant larvae, the expression levels of Ankyrin and β-spectrin was not affected (Dubreuil and Yu, 1994). In the follicle cells, Ankyrin was found in the lateral plasma membrane of the follicle cells, where it co-localises with αβ-spectrin (Lee et al., 1997). The disruption in the expression of α-spectrin in the follicle cells affected the expression and localisation of Ankyrin in two ways: in stage 7, the expression of Ankyrin in posterior follicle cells that lost their organisation was shifted from the lateral membrane to the entire cell surface, and at stage 10, the expression of Ankyrin was reduced (Lee et al., 1997). In the light of these results, if the disruption of Myosin VI affects α-spectrin expression, then the expression of Ankyrin could be affected as well.

The figures in the following pages:

Figure 6.5.2: The expression of Myosin VI (**A, D**) and Ankyrin (**B, E**) in ovaries, expressing Myosin VI antisense directed by E4-Gal4. Myosin VI and Ankyrin co-localise at the cell membrane (**C, F**). In cells where Myosin VI expression is disrupted, Ankyrin expression is reduced (**B**) or absent from the cell membrane (**E**, asterisk).

Figure 6.5.3: The expression of Myosin VI (**A**) and PS2α-integrin (**B**) in ovaries expressing Myosin VI antisense directed by E4-Gal4. Myosin VI and PS2α-integrin co-localise at the cell cytoplasm (**C**). Disruption of Myosin VI expression reduces the expression of PS2α-integrin in the cell cytoplasm (**B**, asterisk).

Figure 6.5.4: The expression of Myosin VI (**A, D**) and PSβ-integrin (**B, E**) in ovaries expressing Myosin VI antisense directed by E4-Gal4. Myosin VI and PSβ-integrin co-localise at the cell cytoplasm (**C, E**). Disruption of Myosin VI expression reduces the expression of PSβ-integrin in the cell cytoplasm (**B**, asterisk).

Figure 6.5.2

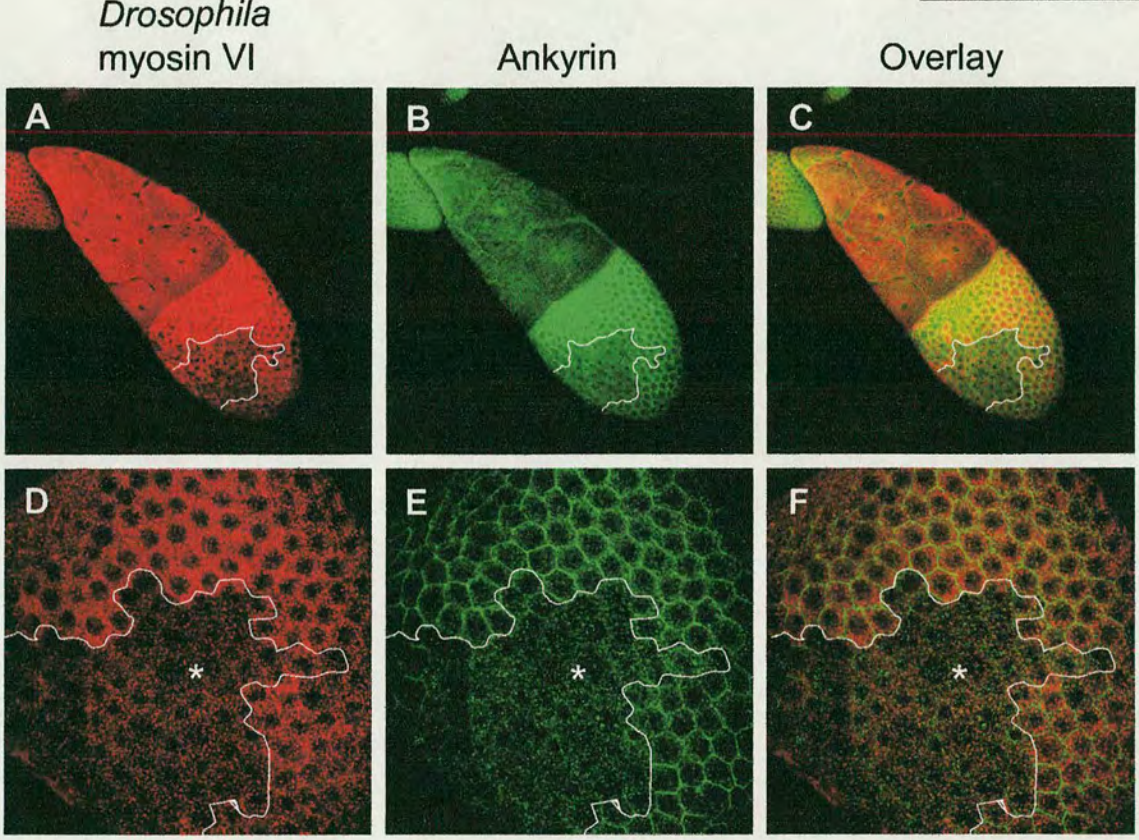

Figure 6.5.3

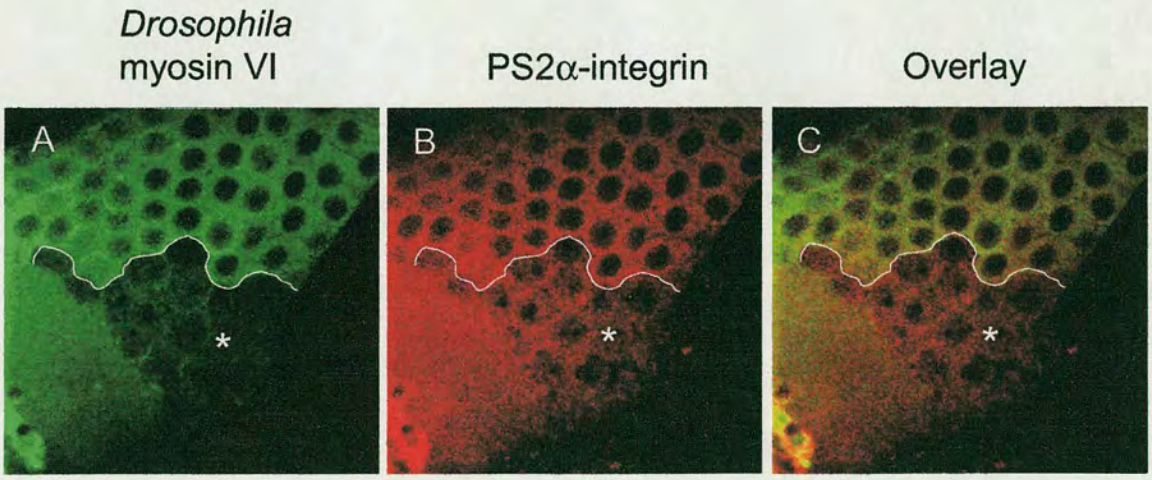

Figure 6.5.4

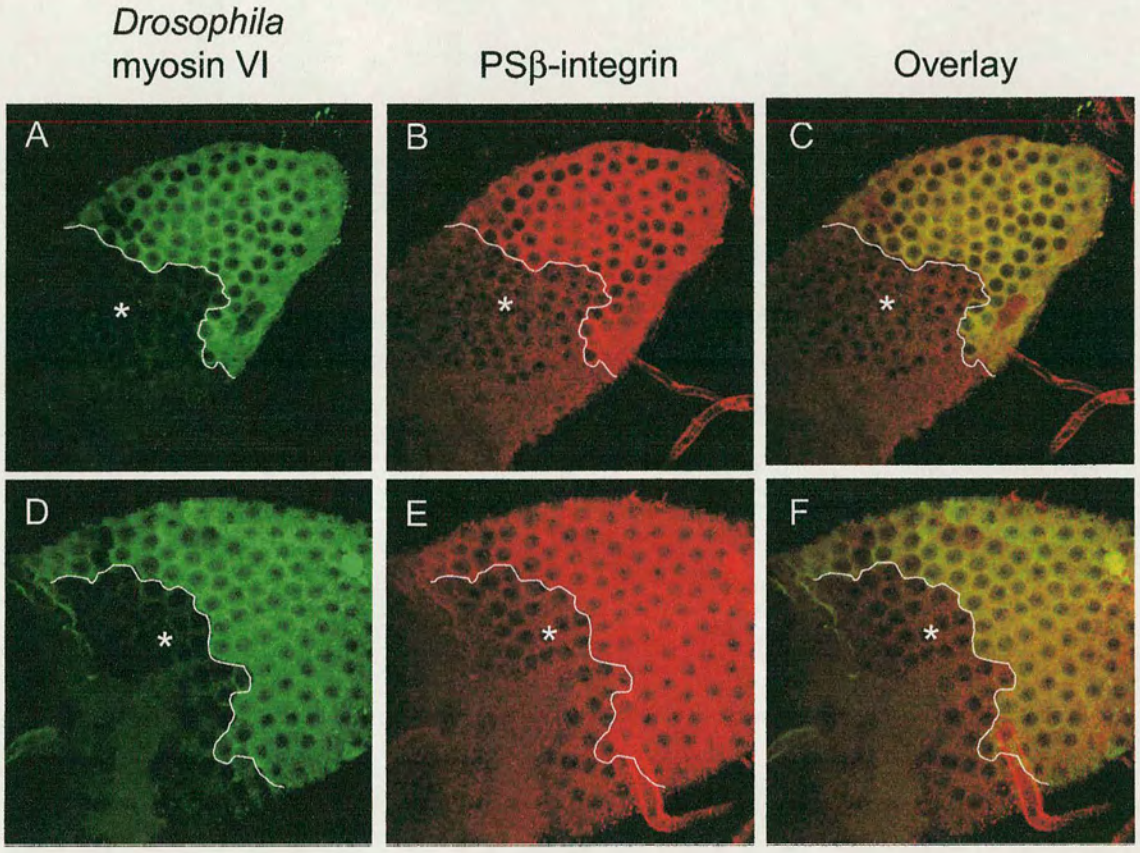

Disrupting the expression Myosin VI did not affect the expression of α-spectrin at the cell membrane (Fig. 6.5.1). However, misexpression of Myosin VI reduced the expression of Ankyrin significantly, at the lateral membrane (Fig. 6.5.2).

In addition, the interaction of Myosin VI was tested with the position-specific integrins. Integrins are membrane proteins that participate in cell-cell adhesion by binding to the extracellular membrane (ECM). PS2 integrin is a heterodimer composed of an α subunit and a β subunit (PS2α-integrin and PSβ-integrin). PS2 integrins belong to one of three groups of integrins found in *Drosophila melanogaster*: PS1, PS2 and PS3. Each of these proteins interacts with actin filaments (Brakebusch and Fassler, 2003). PS-β integrin was found to be associated with basal actin filaments in the follicle cell epithelium, mainly in areas of cell-cell contact and where actin filaments terminate. When follicle cell clones are created, containing mutations in the gene encoding PS-β integrin (*mysopheroid*), the organisation of the basal actin filaments is disrupted, as found in stage 8 and stage 12 egg chambers (Bateman et al., 2001). PS-β integrin was found to function in coordination with the receptor tyrosine phosphatase Dlar, where a double mutation in the genes encoding the two proteins caused failure in oocyte elongation. This phenomenon is correlated to the loss in actin cytoskeleton organisation. Similar results were obtained in mutant follicle clones that were made for the genes encoding α integrin subunits: PS1α-integrin and with PS2α-integrin. The proper organisation of the cytoskeleton is a crucial factor for maintaining the integrity of the follicle cell monolayer. In the *Drosophila* individualization complex, Myosin VI was shown to interact with proteins necessary for actin dynamics. Following these findings the interaction of Myosin VI with PSβ-integrin and with PS2α-integrin was tested. Originally it was intended to test the expression of PS1α-integrin as well, but it was impossible to obtain the antibody for this protein.

The expression of PS2α-integrin and PSβ-integrin at the cell membrane and cell cytoplasm was reduced substantially when Myosin VI was absent from the follicle cells (Fig. 6.5.3-6.5.4). Therefore, we can conclude that Myosin VI regulates the expression of PS2α and PSβ-integrin.

6.6 Conclusions

In this chapter, a search was conducted for proteins that are necessary for the morphogenesis of the follicle cell epithelium, and that have an expression that is dependent on Myosin VI.

The results show that Myosin VI was necessary for the expression and localisation of Dlg and Bazooka, two proteins necessary for controlling the follicle cells invasion and polarisation, during the early stages of oogenesis. Myosin VI was found to interact with PS2α-integrin and PSβ-integrin, which are implicated in actin filament organisation on the basal side of the follicle epithelium. When interaction of Myosin VI with α-spectrin was tested the, it was revealed that the depletion of Myosin VI does not affect the localisation of α-spectrin to the cell membrane. In spite of the interaction between α-spectrin and Ankyrin during embryogenesis, the depletion of Myosin VI reduced significantly the expression of Ankyrin at the lateral membrane. The experiments also showed that Myosin VI affected the expression of the endocytic proteins Clathrin and α-adaptin, although the connection between those proteins and Myosin VI seems to be indirect. Finally, the depletion of Myosin VI did not affect CLIP-190 expression in the follicle cells.

When Myosin VI antisense was expressed under the *C532* driver, the organisation of the follicle cell epithelium was disrupted completely (Deng et al., 1999), while the silencing of Myosin VI in follicle cells patches by *E4-Gal4* did not affect the organisation maintaining of the follicle cells. It is possible that the expression of Myosin VI in the follicle cells surrounding the antisense targeted cells prevented the total disorganization of the follicle cell epithelium.

In stage 9, the follicle cells that migrate posteriorly to cover the oocyte are interconnected. The cells move in relation to their positions in the egg chamber, but not in relation to the adjacent follicle cells (Spradling, 1993). When the expression of Myosin VI was disrupted in the whole follicle cell epithelium from stage 9, the epithelium lost its uniform monolayer shape - the follicle cells gathered in groups and changed their shape. In severe cases, several follicle cells invaded the nurse cluster (Deng et al., 1999).

The invasion of the follicle cells in severe cases of Myosin VI silencing could be related to the interaction of Myosin VI with Dlg and Bazooka discovered in this

study. Bazooka and Dlg function in concert to allow the follicle cells to migrate without invasion. Perhaps the strong expression of Myosin VI that appears in migrating follicle cells is necessary for regulating the migration of the cells while preventing their invasion by controlling the expression and localisation of Dlg and Bazooka. This assumption is consistent with the strong expression and the co-localisation of Myosin VI and Dlg in migrating follicle cells. It must be stated, however, that Dlg and Bazooka were found to mediate the invasion of the follicle cells before the migration of the follicle cells around the oocyte (Abdelilah-Seyfried et al., 2003; Goode and Perrimon, 1997). Furthermore, the disruption of Dlg expression did not affect the migration of the follicle along the egg chamber at stage 9. Nevertheless, the expression of these proteins in the follicle cell membranes after stage 9, combined with the strong expression during the cells migration may indicate that Dlg and Bazooka are still necessary for maintaining the epithelium.

In *Drosophila*, Dlg is necessary for blocking cell invasion and for maintaining cell polarity and cell adhesion in embryonic and adult epithelial tissues (De Lorenzo et al., 1999a; Humbert et al., 2003). In the imaginal discs, mutations in Dlg cause loss of septate junctions and formation of ectopic adherens junctions, suggesting that Dlg is necessary for cell adhesion and polarity (Woods et al., 1996). The loss of Dlg also changes the distribution of Fasciclin III and Neuroglian (two proteins involved in cell adhesion) (Woods et al., 1996), and DE-cadherin, while the expression of Armadillo in Dlg mutants significantly decreased (Woods et al., 1997). This may indicate that the upstream function of Myosin VI on Dlg in the follicle cells mediates the adhesive properties of the follicle cells.

Previously it was shown that Dlg does not have a physical interaction with Myosin VI in *Drosophila* ovaries (Geisbrecht and Montell, 2002). In addition, the mammalian homologue of Dlg, SAP97 showed to interact physically with Myosin VI in nerve cells but not in colonic epithelial cells (Wu et al., 2002). It seems that the interaction between Dlg and Myosin VI is indirect and the upstream effect of Myosin VI on Dlg is mediated via additional proteins.

The reduced expression of Bazooka could also explain the disruption in follicle cell adhesion and migration in the absence of Myosin VI. It was suggested that Bazooka permits invasion in wild-type follicle cells by stabilising the adhesion between the

invading follicle cells and the germ cells, or by mediating the migration of the follicle cells (Abdelilah-Seyfried et al., 2003). Further tests are necessary to establish the role of Bazooka in the migration or adhesion of the follicle cells, and the necessity of the interaction between Bazooka and Myosin VI in the follicle cells.

The interaction of Myosin VI with PS2α-integrin and PSβ-integrin suggests that Myosin VI participates in maintaining the integrity of an epithelial tissue through the adhesion of the epithelial cells at their basal side to the extracellular matrix. The adhesion of the cells to the extracellular matrix contributes to cell movement and provides an additional dimension to maintain the integrity of follicle cells monolayer (Brown, 2000).

The findings seem to indicate that the Myosin VI connects between DE-cadherin and PS-integrins, hence connecting between the adhesion of cells to adjacent cells and the adhesion of cells to other tissues through the extracellular matrix. Any molecule that is proposed to mediate a strong adhesion between cadherins and integrins should have to bind not only to these molecules, but also to the cytoskeleton (Brown et al., 2000). Myosin VI, which directly interacts with actin filaments, is an ideal molecule for such a role.

The role of PS integrins in the organisation of the basal actin filaments in the follicle cells could help maintain the integrity of the epithelium and the adhesion of the follicle cells. This suggests the possibility that the maintenance of a uniform epithelium by Myosin VI is made by the control of actin dynamics. In order to examine this possibility, the actin filaments in the follicle cell cortex should be tested.

In *Drosophila*, PS integrins were found to be necessary for the connection between epithelial sheets in the wing (Bateman et al., 2001; Brown, 2000). PS1 and PS2 integrins are expressed at the dorsal and the ventral epithelia, respectively, where they mediate the adhesion between the epithelia. Mutations in PS1 and PS2 integrin cause a separation of the epithelial sheets and blistering of the wing (Brabant et al., 1998; Brabant et al., 1996). The expression of Myosin VI in the basal part of the epithelial cells in the wings, the connection area between the epithelial sheets, and the similar function that was found in this study for Myosin VI raises the possibility that the interaction of Myosin VI and integrins could be crucial in wings. When

Myosin VI antisense was induced by *C532-Gal4* line, the wings in the adult flies were unfolded and malformed although no blistering was observed. It seems that in this case Myosin VI antisense was induced after the adhesion of the wing sheets was completed (30 hours after pupariation (Brabant et al., 1996). PS integrins are also required for the development of the trachea and for dorsal closure (Brown, 2000), two processes during which Myosin VI was found to be expressed (and in dorsal closure Myosin VI is essential).

Although Myosin VI did not affect the expression of α-spectrin, the expression of Ankyrin was significantly reduced in the absence of Myosin VI. This finding might be related to previous evidence showing that the accumulation of Ankyrin is not affected in α-spectrin mutant larvae. In addition, the reduced expression of α-spectrin in the anterior columnar follicle cells did not affect the localisation of Ankyrin in the lateral membrane (Lee et al., 1997). These results indicate that in spite of a possible physical interaction between α-spectrin and Ankyrin during embryogenesis, the expression of the two proteins is controlled separately, and that the interaction between the proteins is probably not direct.

In the *Drosophila* S2 cells, the cell adhesion molecule Neuroglian recruits Ankyrin to cell-cell contact sites. In the follicle cells and the salivary gland cells, Ankyrin was found to co-localise with Neuroglian in the lateral membrane (Dubreuil et al., 1997). This seems to suggest that the signalling by Neuroglian is dependent on extracellular adhesion and that the binding of Ankyrin plays a role in stabilising the adhesion between the cells (Hortsch et al., 1998). It would be interesting to test the relationship between Myosin VI and Neuroglian.

The expression of Neuroglian and the assembly of Ankyrin and αβ-spectrin were found to concentrate Na, K-ATPase at sites of cell-cell contact (Dubreuil et al., 1997). Previous studies showed that Ankyrin interacts directly with Na, K-ATPase (Nelson and Veshnock, 1987). The presumed interaction between the two proteins could suggest that a connection exists between cell adhesion and cell polarity mediated by Ankyrin. The interaction of Myosin VI with Ankyrin suggests that during the creation or the maintenance of the follicle epithelium Myosin VI mediates the contact between the cells and perhaps their polarity as well. Even if Ankyrin does not directly affect the cell polarity, the reduced expression of Ankyrin at the lateral

membrane in the absence of Myosin VI could indicate that Myosin VI plays a role in cell polarity.

E-cadherin, integrins and the human homologue of Dlg are all necessary for mediating the organisation of epithelial tissues in mammals. Interestingly, in ovarian carcinomas the expression levels of integrins and E-cadherin in the surface of the epithelial cells increase. These proteins are proposed increase the cells invasiveness (Skubitz, 2002; Sundfeldt et al., 1997). The homologue of *Drosophila* Dlg, *Ne-Dlg* was also found to be up-regulated in ovarian carcinomas (Tapper et al., 2001). It was also found that Myosin VI was expressed at elevated levels in ovarian cancer cells (Montell, 2003). This may indicate that Myosin VI is also involved in tumour spreading. In collaboration with Leanne McGurk in our group, Myosin VI was shown to be expressed strongly in the granulosa cells of the mouse ovary (data not shown). Following these findings, it would be interesting to test the interaction of Myosin VI with these proteins during the organisation of the granulosa cells around the oocyte in mammalian ovaries.

Clathrin and α-adaptin are expressed at the boundary between the follicle cells and the developing oocyte at the early stages of vitellogenesis (stages 8-9) (Richard et al., 2001). Richard et al. claimed that when the development of the ovaries is arrested at the pre-vitellogenic stage, the expression of Clathrin, α-adaptin and yolk protein receptors in the follicle cells are reduced. It should be noted, however, that the data for these results are not shown in the article. In the results shown here, the expression of α-adaptin at the boundary between the follicle cells and the oocyte is reduced in the absence of Myosin VI. When the function of Myosin VI was inhibited in normal kidney cells, by over-expression of the tail domain, the endocytosis of Transferrin (a protein that undergoes endocytosis in mammalian cells) was reduced by approximately 70% (Buss et al., 2001). In *Drosophila*, α-adaptin also plays a role in the recycling of pre-synaptic vesicles in the nervous system through Clathrin-mediated endocytosis (Gonzalez-Gaitan and Jackle, 1997). It would be interesting to test whether Myosin VI is also necessary for the transport of yolk proteins from the follicle cells to the oocyte via Clathrin mediated endocytosis.

Previous experiments showed that the migration of the border cells is not established through endocytosis (Geisbrecht and Montell, 2002). Therefore the connection of

Myosin VI with the endocytic proteins would probably related to the transport of proteins to the oocyte and not to the migration of the follicle cells.

Finally, an attempt was made to test the interaction between Myosin VI and Disabled. In mammals, Myosin VI was found to interact with Dab-2 (Inoue et al., 2002), the mammalian homologue of *Drosophila* Disabled. Dab-2 is a tumour suppressor linked to cell signalling and endocytosis. The expression pattern of Disabled in the follicle cells could not be tested since the antibody for *Drosophila* Disabled was not available. I therefore tested the genetic interaction between Myosin VI and Disabled, by crossing the Myosin VI mutant flies: jar^{R39}*/TM3, Sb,* and jar^{R235}*/TM3, Sb* with a Disabled mutant: dab^{M54}*/ TM3, Sb.* In this cross, 66% of the flies were suspected to be heterozygous with Stubble phenotype, and 33% of the flies would be suspected to be non-Stubble, containing the Disabled and Myosin VI mutants on the two copies of the third chromosome (jar^{R39}*/* dab^{M54} and jar^{R235}*/* dab^{M54}). If the combination of the two mutants would be lethal, then non-Stubble flies would not survive. The results of the cross showed no significant change between the observed and the expected ratios, suggesting that the two mutants did not significantly affect the viability of the flies. The morphology of the legs and wings looked normal, however the morphology of the ovaries and the fertility in the double mutant should be further tested. Interestingly, when the double mutant of Abelson and disabled (*abl* $dab^{22.1}$*/ TM3, Sb*) was crossed with Myosin VI mutants, all the flies were stubble, and non-stubble flies did not survive. The interaction of Myosin VI and Abelson should be further tested.

In this study, the absence of Myosin VI was shown in to disrupt the creation of the chorion. This could suggest that Myosin VI is necessary for the transport of the chorion proteins, although it would probably interact with different proteins since the expression of Clathrin and α-adaptin in the follicle cells decreases by stage 10 (Richard et al., 2001) and the secretion of the chorion starts at stage 12a (Papassideri and Margaritis, 1996).

The results shown here propose several potential ways in which Myosin VI could function in the migration of the follicle cells epithelium while preserving epithelial integrity:

1. Myosin VI could maintain the adhesion between the cells via Ankyrin, Dlg, Bazooka, and the proteins that were previously found to interact with Myosin VI: DE-Cadherin and Armadillo.
2. Myosin VI could play a role in binding the follicle cells to the basal extracellular matrix (ECM) via PS2α-Integrin and PSβ-Integrin. The interaction with the ECM could be necessary for maintaining the follicle cells as a monolayer, and for the migration of the whole epithelium while maintaining epithelial integrity. The interaction of Myosin VI with PS2 integrins could also affect the integrity of the actin cytoskeleton in the ECM.
3. Myosin VI could mediate the migration of the follicle cells while preventing their invasion into the germ line derived cells via an interaction with Bazooka and Dlg.
4. Myosin VI might affect the polarity of the follicle cells either directly or via Ankyrin and Dlg.

Chapter 7:

Discussion and summary

This thesis has explored the role of Myosin VI in the patterning of epithelial tissues. The main results are mostly discussed in each chapter and we only briefly summerised here, considering options for future research.

7.1 The molecular function of Myosin VI

Myosins are motor proteins that move along actin filaments. Myosins are composed of a head domain (termed the motor domain), a neck domain (which serves as a lever arm), and a tail domain (which binds to the cargo). Myosin VI is unique as it moves to the minus end of the actin filament which is the opposite direction to the other myosins. In order to examine the function of the whole Myosin VI molecule in epithelial tissues, the whole Myosin VI molecule or its separate domains (the head+ neck domains or the tail domain) tagged to GFP were expressed in somatic cells under the control of Gal4 protein and their localisation in the cells was observed. Previous experiments showed that the head and the tail domain are sufficient to drive the movement of Myosin VI towards the minus end (Homma et al., 2001; Wells et al., 1999). Consistent with these results, the head + neck domains were found in the nucleus of salivary gland and columnar follicle cells, where the minus end is localised.

In spite of the tendency of Myosin VI towards the cell interior, the localisation of the molecule was found to be determined by the tail domain. In all the cells examined, Myosin VI was anchored away from the cell nucleus, by the tail domain. These results suggest that Myosin VI tends to move towards the cell interior, but at least in some regions in the cell, the localisation of the molecule is determined by the tail domain, probably via interaction with other proteins. In the border cells, the anchoring of Myosin VI to the leading edge of cells by the tail domain could be one of the ways to control the direction of cell migration.

Prior to the observation of Myosin VI-GFP tagged protein (PGM) in the cells, it was crucial to test whether this protein preserved the normal function of the native Myosin VI. This was established by two mutant rescue tests, as described in chapter 4, which proved that the tagging of Myosin VI to GFP did not disrupt its function. It also proved that the male sterility and embryonic lethal phenotypes of the Myosin VI

mutants were due to defects in Myosin VI gene, *jaguar*. The rescue of Myosin VI mutants by the expression of PGM will be a useful tool to verify existence of a mutation in the *jaguar* gene, in novel mutations, or to test upstream factors that control Myosin VI expression.

When the tail domain-GFP tagged protein (PGMT) was expressed, it appeared in all the tissues in a punctate pattern. In the ovaries it was found that the PGMT clusters were co-localised with proteins that interact with Myosin VI during oogenesis: Ankyrin, armadillo, Bazooka and PS2-integrin. This suggests that the tail domain gathers around proteins that interact with Myosin VI. However, the physical interactions need to be investigated by immunoprecipitation.

The tail domain of Myosin VI contains no recognizable motifs and it is a globular tail domain. Also, the binding sites of Myosin VI in Dab2 and SAP97 did not have any common features. The Dab2 binding site is serine and proline rich, and the binding site in SAP97 at the N domain of the molecule in a region which targets the molecule to cell adhesion sites in epithelial cells, (Hasson, 2003), though it does not contain any specific amino acid at a high concentration. Finding the specific site of Myosin VI binding in additional proteins will enable us to build a better picture about the nature of interactions between Myosin VI and other proteins.

7.2 The maintenance of epithelial tissue integrity by Myosin VI during migration

During oogenesis and dorsal closure, the epithelial tissues migrate while maintaining their uniform structure. The cells remain inter-connected without changing their location in comparison to their neighbouring cells. The maintenance of the integrity of the tissues is essential for the completion of morphogenic changes and indeed the loss of the cell adhesion or shape change arrests dorsal closure and the migration of the follicular epithelium.

In the light of the results obtained in this thesis and previous results it seems that Myosin VI maintains tissue integrity by preserving the adhesion between the epithelial cells and by mediating the adhesion between the epithelial cells and the extracellular matrix. Myosin VI, by being a molecule that moves along the actin

cytoskeleton and connects the cytoskeleton and membrane proteins, could serve as a good mediator for cell-cell and cell-matrix adhesion.

The requirement for Myosin VI for cell-cell adhesion is shown during dorsal closure when the absence of Myosin VI and the expression of a Myosin VI dominant negative caused detachment of the cells in the leading edge and the amnioserosa (Millo et al., 2004). Also during oogenesis the follicle cells lost their monolayer arrangement and tended to separate from each other in the absence of Myosin VI (Deng et al., 1999). In both morphogenic events DE-cadherin and Armadillo expression and localisation was disrupted in the absence of Myosin VI, and during oogenesis Armadillo was found to interact physically with Myosin VI (Geisbrecht and Montell, 2002).

In this thesis we show evidence that Myosin VI plays a role in the connection of the epithelial cells to the extracellular matrix. In Myosin VI mutant embryos, the leading edge is often separated from the amnioserosa and appears loose and folded (Millo et al., 2004). The separation of the germ band from the amnioserosa gives additional evidence that Myosin VI is essential for the connection of epithelial cells to an extracellular matrix.

During oogenesis the depletion of Myosin VI reduced the expression of PS2 integrins. These integrins were found to be crucial for the maintenance of the actin cytoskeleton in the basal extracellular matrix. The upstream affect of Myosin VI on PS2 integrins could have an indirect role in the organization of actin filaments in the basal lamina. The interaction of Myosin VI with the PS integrins as well as with proteins implicated in cell adhesion (DE-cadherin, Ankyrin, Armadillo, Dlg and Bazooka) makes Myosin VI a potential mediator between cell-cell adhesion and cell-matrix adhesion. As discussed in chapter 5, PS integrins are necessary for dorsal closure and germ band retraction (Brown et al., 2000; Narasimha and Brown, 2004). The possible interaction between PS integrins during embryogenesis and Myosin VI should be investigated.

The expression of Myosin VI in the cell membranes connecting the wing epithelial sheets and the creation of wing blisters in the absence of Myosin VI provides additional evidence for the function of Myosin VI in the connection of epithelial cells

to the extracellular matrix. This is an additional developmental stage that requires PS integrins for holding together the two epithelial cell layers that form the adult wing.

Apart from maintaining the epithelial sheets intact, Myosin VI seems to be necessary for maintaining cell shape and rigidity. During oogenesis the absence of Myosin VI changes the cell shape (Deng et al., 1999). During dorsal closure the changes were even more obvious when the expression of a Myosin VI dominant negative caused a folding-in of the tissue at the lateral epidermis (Millo et al., 2004). The changes in the cells shape and strength indicate that Myosin VI preserves cell shape as cells migrate. The strong expression of Myosin VI at the apical surface of the cells in the leading edge could serve as a shield that protects the cells from folding-in. The abnormal organization of the actin filaments in cortex of cells that tend to fold-in at the lateral epidermis may also suggest that Myosin VI preserves cell rigidity by maintaining the cytoskeleton.

The migration of the border cells during oogenesis is arrested in the absence of Myosin VI, indicating that Myosin VI is also necessary for the migration itself. Moreover, the increase of DE-cadherin expression in Myosin VI depleted ovaries restored the migration of the cells. Therefore Myosin VI seems to control the migration of the cells through the interaction with the adhesion molecules DE-cadherin and Armadillo (Geisbrecht and Montell, 2002). Ankyrin is localised at sites of cell adhesion and the interaction of Myosin VI with it could also be necessary for the cells migration (Dubreuil et al., 1997). The interaction of Myosin VI with Dlg and Bazooka, as described in chapter 6, could suggest additional roles for Myosin VI in controlling cell invasion and polarity (Lee et al., 1997). As previous studies showed, Myosin VI is not involved in endocytosis during the migration of the follicle cells (Geisbrecht and Montell, 2002).

Interestingly, as the migration of the border cells is arrested at the nurse cell-oocyte border, the Myosin VI molecule was found to be anchored to the leading edge, by the tail domain. The arrest of Myosin VI movement in the cells by anchoring the Myosin VI seems to be one of the ways of controlling the migration of the cells.

7.3 Myosin VI and actin dynamics

The expression of the Myosin VI head domain in salivary gland cells not only showed that the head domain tends to concentrate in the cell nucleus, but also showed that in the same regions where the head domain was concentrated, actin filaments were synthesized. The accumulation of the actin filaments in the cell nucleus did not appear when the tail domain or the whole Myosin VI was expressed, although in these cases actin filaments were co-localised with the tagged molecules. These results led to the conclusion that the head domain participates in the synthesis of actin filaments, perhaps by stabilizing the synthesized filaments. The co-localisation of actin filaments with the tail clusters around the nucleus shows that this domain also affects filament polymerisation.

Previous results showed that Myosin VI is necessary for the organization of actin filaments in the individualization complex (IC), of the testes (Hicks et al., 1999). While the mutant Myosin VI jar^{mmw14} exhibited abnormal organization of the actin filaments in the IC, no actin filaments could be observed in the heteroallelic male flies jar^{mmw14}/jar^{R39} and jar^{mmw14}/jar^{R235}. Possibly, the presence of the two alleles significantly reduced the stability of the filaments in the IC. The expression of Myosin VI tagged to GFP restored fertility and the formation of the actin filaments in the IC of male flies, indicating that Myosin VI is necessary for the organization and stability of the filaments.

A recent study suggests that the actin cone contains long filaments at the cone cortex, while in the centre of the cortex the filaments are short and cross-linked (Noguchi and Miller, 2003). Two roles were proposed for the actin filaments at the cone cortex. First the filaments are thought to push the cystic bulge foreword, through actin polymerisation. Second, the filaments must attach the cell membrane around them and shape it into a tubular structure (Noguchi and Miller, 2003). The organization of Myosin VI as a ring at the base of the cone indicates that Myosin VI would normally interact with the cortical actin filaments, which are adjacent to the formed membrane. This is also the initial contact region between the cell membrane of the spermatids and the actin filaments. Inhibition of ATPase did not prevent the movement of the cystic bulge; therefore it is likely that Myosin VI participates only

in the association of the cell membrane to the sites of actin filaments. This assumption is also supported by the interaction of Myosin VI with Cortactin and Dynamin, two proteins that associate with actin at sites of membrane assembly (Rogat and Miller, 2002).

Our results show that when the head + neck domains are expressed, they are localised along the whole actin cone. However the whole Myosin VI molecule is anchored to the base of the cone (the plus end) by the tail domain, probably due a specific cargo binding to the tail domain. The anchoring of Myosin VI to the base of the cone is possibly necessary for the organization and stabilization of the cortical actin filaments at the site of interaction with the membrane. The possible role of the head domain in actin polymerisation as described above suggests that the head domain of Myosin VI may stabilize actin filaments. Accordingly, the tail domain would anchor the whole molecule to the base of the cone in order to allow the head domain to bind to the actin filaments and mediate their polymerisation. Alternatively, the attachment of the head domain to the plus end of the actin filaments could bring the filament end in contact with other proteins involved in actin polymerisation that are attached or located in close proximity to the tail domain.

The recovery of fluorescent actin filaments from bleaching in the whole cone indicates that the synthesis of new actin filaments occurs in the entire cone, and no flow of actin filament was observed towards the minus end (Noguchi and Miller, 2003). Therefore Myosin VI might be necessary for the stabilization of actin filaments rather than the synthesis itself.

The involvement of Myosin VI in the organization of actin filaments was also observed in embryos during dorsal closure. As described in chapter 5, in the jar^{R39} and jar^{R235} mutant embryos, the tight organization of the actin cable at the leading edge was disrupted. In several places along the cable aggregates of actin filaments were formed. These aberrations were even more obvious in embryos that expressed a Myosin VI dominant negative. Very often, cell stripes expressing Myosin VI dominant negative tended to fold-in. In these cells the organization of the actin filaments in the cell cortex was aberrant: the filaments were spread and lost their tight organization. These results suggested that the folding-in of the cells might be connected to the abnormal organization of the cytoskeleton.

During oogenesis, staining of egg chambers lacking Myosin VI with α-spectrin, which binds to actin filaments, revealed that the shape of the cells was changed (Deng et al., 1999).

7.4 Myosin VI and secretion

Disruption of Myosin VI in the columnar follicle cells interfered with the creation of the chorion layer. The depletion of Myosin VI also reduced the expression of *a*-adaptin, a protein participating in endocytosis, at the interface between the follicle cells and the oocyte. These results suggest a possible role for Myosin VI in chorion secretion. This could be verified by examining the effect of Myosin VI depletion on the transport of choriogenic proteins to the oocyte. Vitelline membrane proteins and choriogenic proteins were found to be localised in the same vesicles that secrete yolk proteins, therefore, Myosin VI could be needed for the secretion of yolk proteins as well (Butterworth et al., 1999; Trougakos et al., 2001).

When PGM was expressed under the control of a *Myosin VI-Gal4* line (*C865*), strong expression of Myosin VI was observed in the salivary gland. The expression gradually increased in the area close to the salivary ducts, and it was often possible to observe PGM clusters within the duct of the salivary gland. The salivary gland is the largest secretory tissue in the larvae, and many genes involved in the secretory pathways such as vesicular transport from the ER to the Golgi, are highly expressed. In mammalian cells, Myosin VI is localised in the Golgi complex as a peripheral membrane protein and is necessary for secretion from the Golgi complex, and for preserving its proper morphology (Buss et al., 1998; Warner et al., 2003). The strong expression of PGM in the salivary gland, mainly in the salivary duct could suggest a role of Myosin VI in secretion from the salivary glands, and the clustering of PGM in the duct could be related to particles secreted into the duct by a mechanism including Myosin VI. When the expression of Myosin VI is disrupted in the salivary glands by targeted expression of Myosin VI antisense, the size of the salivary glands significantly decreases (data not shown); therefore Myosin VI is needed for the proper development of the salivary glands. It would be interesting to test the effect of Myosin VI depletion on the release of secretory vesicles at the apical surface of the

salivary glands. The transport of membrane vesicles by Myosin VI could also be observed *in vivo*, by using membrane markers such as FM1-43 in live salivary glands expressing PGM (Noguchi and Miller, 2003).

7.5 Future research

Dlg, Bazooka, PS2 integrin, Ankyrin Clathrin and α-adaptin were found to function downstream of Myosin VI during dorsal closure and oogenesis. In order to test the mutual effect of these proteins on Myosin VI, the expression of Myosin VI could be examined in the egg chambers and embryos lacking these proteins. For example, in the heteroallelic *dlg* mutant dlg^{hf321}/dlg^{lv55}, the expression of Myosin VI could be tested and compared, especially in follicle cells that become invasive (Goode and Perrimon, 1997). The morphology of the tissues could also be tested in heterozygous mutants containing a mutation in *jaguar* and in the gene encoding one the other proteins.

The cooperative function of Myosin VI and the interacting proteins could also be observed in live cells expressing PGM and the examined proteins tagged to a different fluorophore. The physical interaction of these proteins with Myosin VI should be tested by immunoprecipitation and two-hybrid screens.

The proteins that were found to be affected by Myosin VI depletion are localised to different regions in the cell. DE-cadherin and Armadillo are localised in the adherens junction, while Dlg is localised in the septate junction. The disruption in the expression of proteins localised at different sites could be established if the whole structure of the junctions in the lateral membrane is changed. This could also explain how the expression of Dlg is disrupted by Myosin VI in the absence of a physical connection between the two proteins (Geisbrecht and Montell, 2002). In order to verify this possibility, the structure of the junctions and the organization of the cytoskeleton in the lateral membrane should be examined.

A search for additional proteins that could interact with Myosin VI could clarify the cascade in which Myosin VI functions (i.e. the proteins that function upstream and downstream of Myosin VI). The search could be made for proteins that interact with the proteins found here, and that are expressed in the follicle cells during oogenesis

or in the amnioserosa and the epidermis during dorsal closure. For example, one candidate is Scribble, which interacts with Dlg, and it is expressed in the follicle cells (Mathew et al., 2002).

The screen for proteins that could interact with Myosin VI could be done according to genes that were found to have a similar phenotype to Myosin VI mutants. One of the genes that could be examined is *Dcdc-42*. During dorsal closure the expression of the *Drosophila* cdc42 dominant negative, Dcdc42N17 creates similar abnormalities in tissues shape and actin filament organisation to those observed when Myosin VI dominant negative is expressed (folding-in of the tissue and disorganization of actin filaments) (Ricos et al., 1999). During germ band retraction, there are several mutants which have similar phenotypes to Myosin VI mutants, including: *scab* (encoding αPS3-integrin), *mysopheroid* (encoding βPS-integrin), *wing blister*, *u-shaped*, and *tail-up* (Frank and Rushlow, 1996; Schock and Perrimon, 2003). A complementation test of Myosin VI with these genes and expression analysis could indicate if some of these genes function in cooperation with Myosin VI.

In the experiments described in the thesis, the expression of PGMT and PGMH was established in wild-type flies that express myosin, the native Myosin VI. Because the function of Myosin VI is normal in these cells, the tail domain could be localised at its final destination (where the cargo was transferred by the normal Myosin VI). The observation of PGMT in mutant cells lacking Myosin VI and the comparison with the results obtained here could give additional information about the localisation of the cargo prior to its transport by Myosin VI, and the region in the cell where the cargo is transported.

The observation of Myosin VI and its domains tagged to GFP in live images could provide a better understanding of the function of Myosin VI in different organs. During dorsal closure Myosin VI is expressed in filopodia and lamellipodia in the leading edge cells, examination *in vivo* of how the expression of Myosin VI dominant negative affects the adhesion of the filopodia to opposite epithelial cells, and the adhesion of adjacent cells in the lateral epidermis and the amnioserosa could be of a value. This could be done by expressing Myosin VI dominant negative and actin-GFP simultaneously. This experiment could also enable us to test the change in the organization of actin filaments at the leading edge.

The expression of the tagged proteins under the control of a *Myosin VI-Gal4* line allowed us to observe all the organs and tissues that express Myosin VI during the life cycle. In some of the organs, the expression of Myosin VI was not previously known, such as the trachea, the brain, and eye-antenna imaginal disc and the salivary gland. This opens the possibilities of a new research on the role of Myosin VI in the development of these organs.

In *Drosophila melanogaster* 8 myosins have been identified previously and five new myosins have been identified and classified by our group when the *Drosophila* genome was published. Chapter 3 describes the characterization of the new myosins. Apart from Myosin VI, there are other myosins that are expressed in oogenesis, including myosin I, II, and V. Their role in oogenesis is described in the Introduction. In situ hybridisation experiments showed that the new myosins, Myo10A, Myo29 and Myo95E are also expressed during oogenesis. Their function in oogenesis could be further examined, and it would also be interesting to test their expression and function in other epithelial tissues. Each myosin has a unique structure that fits a specific function. It would be interesting to test the separate function of each myosin and their interacted functions and expression *in vivo*.

Finally, the results obtained in this thesis could be investigated in other species, for example the role of Myosin VI in wound healing. Dorsal closure serves as a model to study wound healing. Previous studies showed that myosin II, which is crucial for the process of dorsal closure, is strongly expressed at the leading edge of wounds in chick embryos and at the wound borders in *Xenopus* oocytes, creating the purse string during the wound closure (Bement et al., 1999; Brock et al., 1996). Myosin II was also expressed in wounds created in *Drosophila* embryos with a laser (Wood et al., 2002). The localisation of Myosin VI and myosin II at the leading edge of the lateral epidermis, and the interaction of Myosin VI with cell adhesion molecules could make Myosin VI crucial for the healing process of wounds.

The elevation of Myosin VI expression levels in ovarian cancer cells (Montell, 2003) indicates that Myosin VI is necessary for the development of epithelial tissues in humans. The publication of the human and mouse genome enabled to find the genes responsible for various diseases. Several mutations in Myosin VI were already found to be connected with hearing loss. One of the mutations in Myosin VI that was found

recently was associated with sensorineural deafness and hypertrophic cardiomyopathy (cardio-auditory syndrome) (Mohiddin et al., 2004). Antibody staining of mice ovaries revealed that Myosin VI is present in the granulosa cells, prior to ovulation (the experiment was established in our lab by Leeanne McGurk). This could indicate a role for Myosin VI in the morphogenesis of the granulosa epithelium. It is planned to investigate if Myosin VI is also expressed after ovulation and if it is necessary for the healing process of the ovarian follicle.

Bibliography

Abdelilah-Seyfried, S., Cox, D. N. and Jan, Y. N. (2003). Bazooka is a permissive factor for the invasive behavior of discs large tumour cells in *Drosophila* ovarian follicular epithelia. *Development* **130**, 1927-35.

Adams, M. D., Clinker, S. E., Gibbs, R. A. and Rubin, G. M. (2000.). The genome sequence of *Drosophila melanogaster. Science* **287**, 2185-2195.

Agrawal, V. and Kishan, K. V. (2002). Promiscuous binding nature of SH3 domains to their target proteins. *Protein Pept Lett* **9**, 185-93.

Ahmed, Z. M., Morell, R. J., Riazuddin, S., Gropman, A., Shaukat, S., Ahmad, M. M., Mohiddin, S. A., Fananapazir, L., Caruso, R. C., Husnain, T. et al. (2003). Mutations of MYO6 are associated with recessive deafness, DFNB37. *Am J Hum Genet* **72**, 1315-22. Epub 2003 Apr 8.

Altman, D., Sweeney, H. L. and Spudich, J. A. (2004). The mechanism of Myosin VI translocation and its load-induced anchoring. *Cell* **116**, 737-49.

Aschenbrenner, L., Lee, T. and Hasson, T. (2003). Myo6 facilitates the translocation of endocytic vesicles from cell peripheries. *Mol Biol Cell* **14**, 2728-43. Epub 2003 Mar 20.

Aschenbrenner, L., Naccache, S. N. and Hasson, T. (2004). Uncoated endocytic vesicles require the unconventional myosin, myo6, for rapid transport through actin barriers. *Mol Biol Cell* **5**, 5.

Avraham, K. B., Hasson, T., Steel, K. P., Kingsley, D. M., Russell, L. B., Mooseker, M. S., Copeland, N. G. and Jenkins, N. A. (1995). The mouse Snell's waltzer deafness gene encodes an unconventional myosin required for structural integrity of inner ear hair cells. *Nat Genet* **11**, 369-75.

Bahler, M. (2000). Are class III and class IX myosins motorized signalling molecules? *Biochim Biophys Acta* **1496**, 52-9.

Bahloul, A., Chevreux, G., Wells, A. L., Martin, D., Nolt, J., Yang, Z., Chen, L. Q., Potier, N., Van Dorsselaer, A., Rosenfeld, S. et al. (2004). The unique insert in Myosin VI is a structural calcium-calmodulin binding site. *Proc Natl Acad Sci U S A* **101**, 4787-92. Epub 2004 Mar 22.

Baker, J. P. and Titus, M. A. (1998). Myosins: matching functions with motors. *Curr. Opin. Cell. Biol.* **10**, 80 - 86.

Barros, C. S., Phelps, C. B. and Brand, A. H. (2003). *Drosophila* nonmuscle myosin II promotes the asymmetric segregation of cell fate determinants by cortical exclusion rather than active transport. *Dev Cell* **5**, 829-40.

Bateman, J., Reddy, R. S., Saito, H. and Van Vactor, D. (2001). The receptor tyrosine phosphatase Dlar and integrins organize actin filaments in the *Drosophila* follicular epithelium. *Curr Biol* **11**, 1317-27.

Bates, M. and Martines-Arias, A. (1993). The Development of *Drosophila Melanogaster*. Cold Spring Harbor, New York: Cold spring Harbor Laboratory Press.

Bement, W. M., Mandato, C. A. and Kirsch, M. N. (1999). Wound-induced assembly and closure of an actomyosin purse string in Xenopus oocytes. *Curr Biol* **9**, 579-87.

Bennett, V. and Baines, A. J. (2001). Spectrin and Ankyrin-based pathways: metazoan inventions for integrating cells into tissues. *Physiol Rev* **81**, 1353-92.

Berger, B., Wilson, D. B., Wolf, E., Tonchev, T., Milla, M. and Kim, P. S. (1995). Predicting coiled coils by use of pairwise residue correlations. *Proc Natl Acad Sci U S A* **92**, 8259-63.

Biemesderfer, D., Mentone, S. A., Mooseker, M. and Hasson, T. (2002). Expression of Myosin VI within the early endocytic pathway in adult and developing proximal tubules. *Am J Physiol Renal Physiol* **282**, F785-94.

Bilder, D., Li, M. and Perrimon, N. (2000). Cooperative regulation of cell polarity and growth by *Drosophila* tumour suppressors. *Science* **289**, 113-6.

Biru, W. G. T., Attila Jozsef University, Szeged,. (1999). *Drosophila melanogaster* mRNA for myosin heavy chain, partial., (ed. Szeged, Hungary.: Attila Jozsef University.

Bloor, J. W. and Kiehart, D. P. (2002). *Drosophila* RhoA regulates the cytoskeleton and cell-cell adhesion in the developing epidermis. *Development* **129**, 3173-83.

Bogaert, T., Brown, N. and Wilcox, M. (1987). The *Drosophila* PS2 antigen is an invertebrate integrin that, like the fibronectin receptor, becomes localized to muscle attachments. *Cell* **51**, 929-40.

Bohrmann, J. (1997). *Drosophila* unconventional Myosin VI is involved in intra- and intercellular transport during oogenesis. *Cellular and molecular life sciences* **53**, 652-62.

Bonafe, N. and Sellers, J. R. (1998). Molecular characterization of myosin V from *Drosophila melanogaster*. *Journal of Muscle Research and Cell Motility* **19**, 129 - 141.

Bownes, M. (1975). A photographic study of development in the living embryo of *Drosophila melanogaster*. *J Embryol Exp Morphol* **33**, 789-801.

Brabant, M. C., Fristrom, D., Bunch, T. A., Baker, S. E. and Brower, D. L. (1998). The PS integrins are required for a regulatory event during *Drosophila* wing morphogenesis

Distinct spatial and temporal functions for PS integrins during *Drosophila* wing morphogenesis. *Ann N Y Acad Sci* **857**, 99-109.

Brabant, M. C., Fristrom, D., Bunch, T. A. and Brower, D. L. (1996). Distinct spatial and temporal functions for PS integrins during *Drosophila* wing morphogenesis. *Development* **122**, 3307-17.

Brakebusch, C. and Fassler, R. (2003). The integrin-actin connection, an eternal love affair. *Embo J* **22**, 2324-33.

Brand, A. H. and Perrimon, N. (1993). Targeted gene expression as a means of altering cell fates and generating dominant phenotypes. *Development* **118**, 401-15.

Breckler, J., Au, K., Cheng, J., Hasson, T. and Burnside, B. (2000). Novel Myosin VI isoform is abundantly expressed in retina. *Exp Eye Res* **70**, 121-34.

Brock, J., Midwinter, K., Lewis, J. and Martin, P. (1996). Healing of incisional wounds in the embryonic chick wing bud: characterization of the actin purse-string and demonstration of a requirement for Rho activation. *J Cell Biol* **135**, 1097-107.

Brown, N. H. (2000). Cell-cell adhesion via the ECM: integrin genetics in fly and worm. *Matrix Biol* **19**, 191-201.

Brown, N. H., Gregory, S. L. and Martin-Bermudo, M. D. (2000). Integrins as mediators of morphogenesis in *Drosophila*. *Dev Biol* **223**, 1-16.

Bunn, R. C., Jensen, M. A. and Reed, B. C. (1999). Protein interactions with the glucose transporter binding protein GLUT1CBP that provide a link between GLUT1 and the cytoskeleton. *Mol Biol Cell* **10**, 819-32.

Buss, F., Arden, S. D., Lindsay, M., Luzio, J. P. and Kendrick-Jones, J. (2001). Myosin VI isoform localized to Clathrin-coated vesicles with a role in Clathrin-mediated endocytosis. *Embo J* **20**, 3676-84.

Buss, F., Kendrick-Jones, J., Lionne, C., Knight, A., Cote, G. and Paul Luzio, J. (1998). The localization of Myosin VI at the golgi complex and leading edge of fibroblasts and its phosphorylation and recruitment into membrane ruffles of A431 cells after growth factor stimulation. *Journal of Cell Biology* **143**, 1535-45.

Butterworth, F. M., Burde, V. S., Mauchline, D. and Bownes, M. (1999). A yolk protein mutant leads to defects in the secretion machinery of *Drosophila melanogaster*. *Tissue Cell* **31**, 212-22.

Campos-Ortega, J. A., Hartenstein, V. (1985). The Embryonic development of *Drosophila melanogaster*. Berlin, Heidelberg: Springer Verlag.

Castrillon, D. H., Gonczy, P., Alexander, S., Rawson, R., Eberhart, C. G., Viswanathan, S., DiNardo, S. and Wasserman, S. A. (1993). Toward a molecular genetic analysis of spermatogenesis in *Drosophila melanogaster*: characterization of male-sterile mutants generated by single P element mutagenesis. *Genetics* **135**, 489-505.

Chen, T.-I., Edwards, K. A., Lin, R. C., Coates, L. W. and Kiehart, D. P. (1998). *Drosophila* myosin heavy chain at 35B,C. *J. Cell Biol.* **115**, 330a.

Chen, Z. Y., Hasson, T., Kelley, P. M., Schwender, B. J., Schwartz, M. F., Ramakrishnan, M., Kimberling, W. J., Mooseker, M. S. and Corey, D. P. (1996). Molecular cloning and domain structure of human myosin-VIIa, the gene product defective in Usher syndrome 1B. *Genomics* **36**, 440-8.

Cheney, R. E., Riley, M. A. and Mooseker, M. S. (1993). Phylogenetic analysis of the myosin superfamily. *Cell Motil Cytoskeleton* **24**, 215-23.

Cho, N., Oh, Y., Hwang, S. Y., Han, D., Park, S. P., Yoon, J., Han, K. and Baek, K. (1998). Promoter analysis of the *Drosophila* genes encoding TFIIB and TATA box-binding protein. *Mol Cells* **8**, 770-6.

Cope, M. J., Whisstock, J., Rayment, I. and Kendrick-Jones, J. (1996). Conservation within the myosin motor domain: implications for structure and function. *Structure* **4**, 969-87.

De Lorenzo, C., Mechler, B. M. and Bryant, P. J. (1999a). What is *Drosophila* telling us about cancer? *Cancer Metastasis Rev* **18**, 295-311.

De Lorenzo, C., Strand, D. and Mechler, B. M. (1999b). Requirement of *Drosophila* I(2)gl function for survival of the germline cells and organization of the follicle cells in a columnar epithelium during oogenesis. *Int J Dev Biol* **43**, 207-17.

Deng, H., Lee, J. K., Goldstein, L. S. and Branton, D. (1995). *Drosophila* development requires spectrin network formation. *J Cell Biol* **128**, 71-9.

Deng, W. M. and Bownes, M. (1998). Patterning and morphogenesis of the follicle cell epithelium during *Drosophila* oogenesis. *Int J Dev Biol* **42**, 541-52.

Deng, W.-M., Leaper, K. and Bownes, M. (1999). A targeted gene silencing technique shows that *Drosophila* Myosin VI is required for egg chamber and imaginal disc morphogenesis. *Journal of Cell Science.* **112**, 3677-90.

Deng, W.-M., Zhao, D., Rothwell, K. and Bownes, M. (1997). Analysis of P[Gal4] insertion lines of *Drosophila melanogaster* as a route to identifying genes important in the follicle cells during oogenesis. *Molecular Human Reproduction* **3**, 853-62.

Dollar, G., Struckhoff, E., Michaud, J. and Cohen, R. S. (2002). *Rab11* polarization of the *Drosophila* oocyte: a novel link between membrane trafficking, microtubule organization, and oskar mRNA localization and translation. *Development* **129**, 517-26.

Dubreuil, R. R. and Grushko, T. (1999). Neuroglian and DE-cadherin activate independent cytoskeleton assembly pathways in *Drosophila* S2 cells. *Biochem Biophys Res Commun* **265**, 372-5.

Dubreuil, R. R., Maddux, P. B., Grushko, T. A. and MacVicar, G. R. (1997). Segregation of two spectrin isoforms: polarized membrane-binding sites direct polarized membrane skeleton assembly. *Mol Biol Cell* **8**, 1933-42.

Dubreuil, R. R. and Yu, J. (1994). Ankyrin and beta-spectrin accumulate independently of alpha-spectrin in *Drosophila*. *Proc Natl Acad Sci U S A* **91**, 10285-9.

Edwards, K. A. and Kiehart, D. P. (1996). *Drosophila* nonmuscle myosin II has multiple essential roles in imaginal disc and egg chamber morphogenesis. *Development* **122**, 1499-511.

Frank, L. H. and Rushlow, C. (1996). A group of genes required for maintenance of the amnioserosa tissue in *Drosophila*. *Development* **122**, 1343-52.

Fristrom, D. and Fristrom, J. W. (1993). The metamorphic development of the adult epidermis. In *The Development of Drosophila melanogaster*, vol. 2 (ed. M. Bate and A. M. Arias), pp. 843-897. New York: Cold Spring Harbor Laboratory Press.

Fulga, T. A. and Rorth, P. (2002). Invasive cell migration is initiated by guided growth of long cellular extensions. *Nat Cell Biol* **4**, 715-9.

Geeves, M. A. (2002). Stretching the lever-arm theory. *Nature* **415**, 129-31.

Geisbrecht, E. and Montell, D. (2002). Myosin VI is required for E-cadherin-mediated border cell migration. *Nature Cell Biology* **4**, 616-20.

Geli, M. I., Lombardi, R., Schmelzl, B. and Riezman, H. (2000). An intact SH3 domain is required for myosin I-induced actin polymerisation. *Embo J* **19**, 4281-91.

Gonzalez-Gaitan, M. and Jackle, H. (1997). Role of *Drosophila* alpha-adaptin in presynaptic vesicle recycling. *Cell* **88**, 767-76.

Goode, S. and Perrimon, N. (1997). Inhibition of patterned cell shape change and cell invasion by Discs large during *Drosophila* oogenesis. *Genes Dev* **11**, 2532-44.

Gustafson, K. and Boulianne, G. L. (1996). Distinct expression patterns detected within individual tissues by the GAL4 enhancer trap technique. *Genome* **39**, 174-82.

Gutzeit, H. O. (1990). The microfilament pattern in the somatic follicle cells of mid-vitellogenic ovarian follicles of *Drosophila*. *Eur J Cell Biol* **53**, 349-56.

Halsell, S. R., Chu, B. I. and Kiehart, D. P. (2000). Genetic analysis demonstrates a direct link between rho signalling and nonmuscle myosin function during *Drosophila* morphogenesis. *Genetics* **155**, 1253-65.

Harden, N., Loh, H. Y., Chia, W. and Lim, L. (1995). A dominant inhibitory version of the small GTP-binding protein Rac disrupts cytoskeletal structures and inhibits developmental cell shape changes in *Drosophila*. *Development* **121**, 903-14.

Harden, N., Ricos, M., Yee, K., Sanny, J., Langmann, C., Yu, H., Chia, W. and Lim, L. (2002). Drac1 and Crumbs participate in amnioserosa morphogenesis during dorsal closure in *Drosophila*. *J Cell Sci* **115**, 2119-29.

Hasson, T. (2003). Myosin VI: two distinct roles in endocytosis. *J Cell Sci* **116**, 3453-61.

Hasson, T., Gillespie, P. G., Garcia, J. A., MacDonald, R. B., Zhao, Y., Yee, A. G., Mooseker, M. S. and Corey, D. P. (1997). Unconventional myosins in inner-ear sensory epithelia. *J Cell Biol* **137**, 1287-307.

Hasson, T. and Mooseker, M. S. (1994). Porcine myosin-VI: characterization of a new mammalian unconventional myosin. *J Cell Biol* **127**, 425-40.

He, B. and Adler, P. N. (2002). The genetic control of arista lateral morphogenesis in *Drosophila*. *Dev Genes Evol* **212**, 218-29. Epub 2002 Apr 12.

Heintzelman, M. B., Hasson, T. and Mooseker, M. S. (1994). Multiple unconventional myosin domains of the intestinal brush border cytoskeleton. *J Cell Sci* **107**, 3535-43.

Hicks, J., Deng, W.-M., Rogat, A., Miller, K. and Bownes, M. (1999). Class VI unconventional myosin is required for spermatogenesis in *Drosophila*. *Molecular Biology of the Cell* **10**, 4341-53.

Hirose, F., Yamaguchi, M., Handa, H., Inomata, Y. and Matsukage, A. (1993). Novel 8-base pair sequence (*Drosophila* DNA replication-related element) and specific binding factor involved in the expression of *Drosophila* genes for DNA polymerase alpha and proliferating cell nuclear antigen. *J Biol Chem* **268**, 2092-9.

Homma, K., Yoshimura, M., Saito, J., Ikebe, R. and Ikebe, M. (2001). The core of the motor domain determines the direction of myosin movement. *Nature* **412**, 831-4.

Hortsch, M., Homer, D., Malhotra, J. D., Chang, S., Frankel, J., Jefford, G. and Dubreuil, R. R. (1998). Structural requirements for outside-in and inside-out signalling by *Drosophila* neuroglian, a member of the L1 family of cell adhesion molecules. *J Cell Biol* **142**, 251-61.

Houdusse, A. and Sweeney, H. L. (2001). Myosin motors: missing structures and hidden springs. *Curr Opin Struct Biol* **11**, 182-94.

Humbert, P., Russell, S., Richardson, H., De Lorenzo, C., Mechler, B. M. and Bryant, P. J. (2003). *Dlg, Scribble* and *Lgl* in cell polarity, cell proliferation and cancer. *Bioessays* **25**, 542-53.

Huynh, J. R., Petronczki, M., Knoblich, J. A. and St Johnston, D. (2001). *Bazooka* and *PAR-6* are required with *PAR-1* for the maintenance of oocyte fate in *Drosophila*. *Curr Biol* **11**, 901-6.

Inoue, A., Sato, O., Homma, K. and Ikebe, M. (2002). DOC-2/DAB2 is the binding partner of Myosin VI. *Biochem Biophys Res Commun* **292**, 300-7.

Jacinto, A., Wood, W., Balayo, T., Turmaine, M., Martinez-Arias, A. and Martin, P. (2000). Dynamic actin-based epithelial adhesion and cell matching during *Drosophila* dorsal closure. *Curr Biol* **10**, 1420-6.

Jordan, P. and Karess, R. (1997). Myosin light chain-activating phosphorylation sites are required for oogenesis in *Drosophila*. *J Cell Biol* **139**, 1805-19.

Jung, G., Remmert, K., Wu, X., Volosky, J. M. and Hammer, J. A., 3rd. (2001). The Dictyostelium CARMIL protein links capping protein and the Arp2/3 complex to type I myosins through their SH3 domains. *J Cell Biol* **153**, 1479-97.

Kalhammer, G. and Bahler, M. (2000). Unconventional myosins. *Essays Biochem* **35**, 33-42.

Kalinichenko, V. V., Gusarova, G. A., Kim, I. M., Shin, B., Yoder, H. M., Clark, J., Sapozhnikov, A. M., Whitsett, J. A. and Costa, R. H. (2004). Foxf1 haploinsufficiency reduces Notch-2 signalling during mouse lung development. *Am J Physiol Lung Cell Mol Physiol* **286**, L521-30. Epub 2003 Nov 7.

Karess, R. E., Chang, X. J., Edwards, K. A., Kulkarni, S., Aguilera, I. and Kiehart, D. P. (1991). The regulatory light chain of nonmuscle myosin is encoded by spaghetti-squash, a gene required for cytokinesis in *Drosophila*. *Cell* **65**, 1177-89.

Kelleher, J. F., Mandell, M. A., Moulder, G., Hill, K. L., L'Hernault, S. W., Barstead, R. and Titus, M. A. (2000). Myosin VI is required for asymmetric segregation of cellular components during C. elegans spermatogenesis. *Curr Biol* **10**, 1489-96.

Kellerman, K. A. and Miller, K. G. (1992). An unconventional myosin heavy chain gene from *Drosophila melanogaster*. *J Cell Biol* **119**, 823-34.

Kiehart, D. P., Galbraith, C. G., Edwards, K. A., Rickoll, W. L. and Montague, R. A. (2000). Multiple forces contribute to cell sheet morphogenesis for dorsal closure in *Drosophila*. *J Cell Biol* **149**, 471-90.

Kiehart, D. P., Lutz, M. S., Chan, D., Ketchum, A. S., Laymon, R. A., Nguyen, B. and Goldstein, L. S. (1989). Identification of the gene for fly non-muscle myosin heavy chain: *Drosophila* myosin heavy chains are encoded by a gene family. *Embo J* **8**, 913-22.

Kiehart, D. P., Montague, R. A., Roote, J. and Ashburner, M. (1998). Evidence that *crinckled*, mutation in which cause numerous defects in *Drosophila* morphogenesis, encodes a Myosin VII. *Mol. Biol. Cell.* **9**, 388a.

King, R. C. (1970). Ovarian development of *Drosophila* melongaster. New York: Academic Press.

Lamka, M. L. and Lipshitz, H. D. (1999). Role of the amnioserosa in germ band retraction of the *Drosophila* melanogaster embryo. *Dev Biol* **214**, 102-12.

Langford, G. M. (2002). Myosin-V, a versatile motor for short-range vesicle transport. *Traffic* **3**, 859-65.

Lantz, V. A. and Miller, K. G. (1998). A class VI unconventional myosin is associated with a homologue of a microtubule-binding protein, cytoplasmic linker protein-170, in neurons and at the posterior pole of *Drosophila* embryos. *J Cell Biol* **140**, 897-910.

Leaper, K. (2003). Myosin VI - Its role in epithelial cell migration during *Drosophila* oogenesis. In *Institure of Cell and Molecular Biology*, (ed. Edinburgh: University of Edinburgh.

Lee, J. K., Brandin, E., Branton, D. and Goldstein, L. S. (1997). alpha-Spectrin is required for ovarian follicle monolayer integrity in *Drosophila melanogaster*. *Development* **124**, 353-62.

Lee, W. L., Ostap, E. M., Zot, H. G. and Pollard, T. D. (1999). Organization and ligand binding properties of the tail of Acanthamoeba myosin-IA. Identification of an actin-binding site in the basic (tail homology-1) domain. *J Biol Chem* **274**, 35159-71.

Leptin, M., Bogaert, T., Lehmann, R. and Wilcox, M. (1989). The function of PS integrins during *Drosophila* embryogenesis. *Cell* **56**, 401-8.

Lister, I., Schmitz, S., Walker, M., Trinick, J., Buss, F., Veigel, C. and Kendrick-Jones, J. (2004). A monomeric Myosin VI with a large working stroke. *Embo J* **23**, 1729-38. Epub 2004 Mar 25.

Macias, M. J., Wiesner, S. and Sudol, M. (2002). WW and SH3 domains, two different scaffolds to recognize proline-rich ligands. *FEBS Lett* **513**, 30-7.

MacIver, B., McCormac, A., Slee, R. and Bownes, M. (1998). Identification of an essential gene encoding a class - V inconventional myosin in *Drosophila* melongaster. *Eur. J. Biochem* **257**, 529 - 537.

Maniak, M. (2001). Cell adhesion: ushering in a new understanding of Myosin VII. *Curr Biol* **11**, R315-7.

Mansfield, S. G., al-Shirawi, D. Y., Ketchum, A. S., Newbern, E. C. and Kiehart, D. P. (1996). Molecular organization and alternative splicing in zipper, the gene that encodes the *Drosophila* non-muscle myosin II heavy chain. *J Mol Biol* **255**, 98-109.

Martin, P. and Wood, W. (2002). Epithelial fusions in the embryo. *Curr Opin Cell Biol* **14**, 569-74.

Martines-Arias, A. (1993). Development and patterning of the larval epidermis of *Drosophila*. In *The Development of Drosophila Melanogaster.*, vol. 1 (ed. M. Bates and A. Martines-Arias), pp. 517-607. Cold Spring Harbor, New York: Cold spring Harbor Laboratory Press.

Mathew, D., Gramates, L. S., Packard, M., Thomas, U., Bilder, D., Perrimon, N., Gorczyca, M. and Budnik, V. (2002). Recruitment of scribble to the synaptic scaffolding complex requires GUK-holder, a novel DLG binding protein. *Curr Biol* **12**, 531-9.

McCrea, P. D., Turck, C. W. and Gumbiner, B. (1991). A homolog of the armadillo protein in *Drosophila* (plakoglobin) associated with E-cadherin. *Science* **254**, 1359-61.

McEwen, D. G., Cox, R. T. and Peifer, M. (2000). The canonical Wg and JNK signalling cascades collaborate to promote both dorsal closure and ventral patterning. *Development* **127**, 3607-17.

Melchionda, S., Ahituv, N., Bisceglia, L., Sobe, T., Glaser, F., Rabionet, R., Arbones, M. L., Notarangelo, A., Di Iorio, E., Carella, M. et al. (2001). MYO6, the human homologue of the gene responsible for deafness in Snell's waltzer mice, is

mutated in autosomal dominant nonsyndromic hearing loss. *Am J Hum Genet* **69**, 635-40. Epub 2001 Jul 20.

Menne, T. V., Luer, K., Technau, G. M. and Klambt, C. (1997). CNS midline cells in *Drosophila* induce the differentiation of lateral neural cells. *Development* **124**, 4949-58.

Mermall, V., McNally, J. G. and Miller, K. G. (1994). Transport of cytoplasmic particles catalysed by an unconventional myosin in living *Drosophila* embryos. *Nature* **369**, 560-2.

Mermall, V. and Miller, G. M. (1995). The 95F unconventional myosin is required for proper organization of the *Drosophila* syncytial blastoderm. *J. Cell Biol.* **129**, 1575 - 1588.

Millo, H., Leaper, K. and Bownes, M. (2004). Myosin VI plays a role in cell-cell adhesion during epithelial morphogenesis. *Mechanisms of Development* **121**, 1335-51.

Mizuno, T., Tsutsui, K. and Nishida, Y. (2002). *Drosophila* Myosin phosphatase and its role in dorsal closure. *Development* **129**, 1215-23.

Mohiddin, S. A., Ahmed, Z. M., Griffith, A. J., Tripodi, D., Friedman, T. B., Fananapazir, L. and Morell, R. J. (2004). Novel association of hypertrophic cardiomyopathy, sensorineural deafness, and a mutation in unconventional Myosin VI (MYO6). *J Med Genet* **41**, 309-14.

Montell, C. and Rubin, G. M. (1988). The *Drosophila* ninaC locus encodes two photoreceptor cell specific proteins with domains homologous to protein kinases and the myosin heavy chain head. *Cell* **52**, 757-72.

Montell, D. J. (2003). Border-cell migration: the race is on. *Nat Rev Mol Cell Biol* **4**, 13-24.

Mooseker, M. S. (1985). Organization, chemistry, and assembly of the cytoskeletal apparatus of the intestinal brush border. *Annu Rev Cell Biol* **1**, 209-41.

Mooseker, M. S. and Cheney, R. E. (1995). Unconventional myosins. *Annu Rev Cell Dev Biol* **11**, 633-75.

Morgan, N. S., Heintzelman, M. B. and Mooseker, M. S. (1995). Characterization of myosin Ia and myosin Ib, two unconventional myosin associated with the *Drosophila* brush border cytoskeleton. *Dev. Biol.* **172**, 51 - 71.

Morgan, N. S., Skovronsky, D. M., Artavanis-Tsakonas, S. and Mooseker, M. S. (1994). The molecular cloning and characterization of *Drosophila melanogaster* myosin-IA and myosin-IB. *J Mol Biol* **239**, 347-56.

Morris, C. A., Wells, A. L., Yang, Z., Chen, L. Q., Baldacchino, C. V. and Sweeney, H. L. (2003). Calcium functionally uncouples the heads of Myosin VI. *J Biol Chem* **278**, 23324-30. Epub 2003 Apr 6.

Morris, S. M., Arden, S. D., Roberts, R. C., Kendrick-Jones, J., Cooper, J. A., Luzio, J. P., Buss, F., Inoue, A., Sato, O., Homma, K. et al. (2002). Myosin VI binds to and localises with Dab2, potentially linking receptor-mediated endocytosis and the actin cytoskeleton

DOC-2/DAB2 is the binding partner of Myosin VI. *Traffic* **3**, 331-41.

Muller, H. A. (2000). Genetic control of epithelial cell polarity: lessons from *Drosophila*. *Dev Dyn* **218**, 52-67.

Muller, H. A. and Bossinger, O. (2003). Molecular networks controlling epithelial cell polarity in development. *Mech Dev* **120**, 1231-56.

Narasimha, M. and Brown, N. H. (2004). Novel functions for integrins in epithelial morphogenesis. *Curr Biol* **14**, 381-5.

Nelson, W. J. (2003). Tube morphogenesis: closure, but many openings remain. *Trends Cell Biol* **13**, 615-21.

Nelson, W. J., Shore, E. M., Wang, A. Z. and Hammerton, R. W. (1990). Identification of a membrane-cytoskeletal complex containing the cell adhesion molecule uvomorulin (E-cadherin), Ankyrin, and Fodrin in Madin-Darby canine kidney epithelial cells. *J Cell Biol* **110**, 349-57.

Nelson, W. J. and Veshnock, P. J. (1987). Ankyrin binding to (Na+ + K+)ATPase and implications for the organization of membrane domains in polarized cells. *Nature* **328**, 533-6.

Noguchi, T. and Miller, K. G. (2003). A role for actin dynamics in individualization during spermatogenesis in *Drosophila melanogaster*. *Development* **130**, 1805-16.

Oda, H., Uemura, T., Harada, Y., Iwai, Y. and Takeichi, M. (1994). A *Drosophila* homolog of cadherin associated with armadillo and essential for embryonic cell-cell adhesion. *Dev Biol* **165**, 716-26.

Oh, Y., Lee, C., Baek, K., Kim, W., Yoon, J., Han, K. and Cho, N. (1999). An element with palindromic structure is required for the expression of TBP (TATA box-binding protein) gene in *Drosophila melanogaster*. *Mol Cells* **9**, 673-7.

Okada, T., Sakai, T., Murata, T., Kako, K., Sakamoto, K., Ohtomi, M., Katsura, T. and Ishida, N. (2001). Promoter analysis for daily expression of *Drosophila* timeless gene. *Biochem Biophys Res Commun* **283**, 577-82.

Oliver, N. T., Berg, J. S. and Cheney, R. E. (1999). Tails of unconventional myosins. *Cell Mol. Life Sci.* **56**, 243 - 257.

Papassideri, I. S. and Margaritis, L. H. (1996). The eggshell of *Drosophila melanogaster*: IX. Synthesis and morphogenesis of the innermost chorionic layer. *Tissue Cell* **28**, 401-9.

Parsons, J. T. (2003). Focal adhesion kinase: the first ten years. *J Cell Sci* **116**, 1409-16.

Perrimon, N. (1988). The maternal effect of lethal(1)discs-large-1: a recessive oncogene of *Drosophila melanogaster*. *Dev Biol* **127**, 392-407.

Petritsch, C., Tavosanis, G., Turck, C., Jan, L. and Jan, Y. (2003). The *Drosophila* Myosin VI *Jaguar* is required for basal protein targeting and correct spindle orientation in mitotic neuroblasts. *Developmental Cell* **4**, 273-81.

Rayment, I., Holden, H. M., Whittaker, M., Yohn, C. B., Lorenz, M., Holmes, K. C. and Milligan, R. A. (1993). Structure of the actin - myosin complex and its inplications for muscle contrction. *Science* **261**, 58 - 65.

Richard, D. S., Gilbert, M., Crum, B., Hollinshead, D. M., Schelble, S. and Scheswohl, D. (2001). Yolk protein endocytosis by oocytes in *Drosophila melanogaster*: immunofluorescent localization of Clathrin, adaptin and the yolk protein receptor. *J Insect Physiol* **47**, 715-723.

Ricos, M. G., Harden, N., Sem, K. P., Lim, L. and Chia, W. (1999). Dcdc42 acts in TGF-beta signalling during *Drosophila* morphogenesis: distinct roles for the Drac1/JNK and Dcdc42/TGF-beta cascades in cytoskeletal regulation. *J Cell Sci* **112**, 1225-35.

Riparbelli, M. G., Callaini, G. and Dallai, R. (1993). Spatial organization of microtubules and microfilaments in larval and adult salivary glands of *Drosophila melanogaster*. *Tissue Cell* **25**, 751-62.

Rock, R. S., Rice, S. E., Wells, A. L., Purcell, T. J., Spudich, J. A. and Sweeney, H. L. (2001). Myosin VI is a processive motor with a large step size. *Proc Natl Acad Sci U S A* **98**, 13655-9. Epub 2001 Nov 13.

Rodriguez, O. C. and Cheney, R. E. (2000). A new direction for myosin. *Trends Cell Biol* **10**, 307-11.

Rogat, A. and Miller, K. (2002). A role for Myosin VI in actin dynamics at sites of membrane remodelling during *Drosophila* spermatogenesis. *Journal of Cell Science* **115**, 4855-65.

Roote, C. E. and Zusman, S. (1995). Functions for PS integrins in tissue adhesion, migration, and shape changes during early embryonic development in *Drosophila*. *Dev Biol* **169**, 322-36.

Royou, A., Field, C., Sisson, J. C., Sullivan, W. and Karess, R. (2004). Reassessing the role and dynamics of nonmuscle myosin II during furrow formation in early *Drosophila* embryos. *Mol Biol Cell* **15**, 838-50. Epub 2003 Dec 2.

Royou, A., Sullivan, W. and Karess, R. (2002). Cortical recruitment of nonmuscle myosin II in early syncytial *Drosophila* embryos: its role in nuclear axial expansion and its regulation by Cdc2 activity. *J Cell Biol* **158**, 127-37. Epub 2002 Jul 8.

Rubin, G. M. and Spradling, A. C. (1982). Genetic transformation of *Drosophila* with transposable element vectors. *Science* **218**, 348-353.

Schober, M. and Perrimon, N. (2002). Unconventional ways to travel. *Nat Cell Biol* **4**, E211-2.

Schock, F. and Perrimon, N. (2002). Cellular processes associated with germ band retraction in *Drosophila*. *Dev Biol* **248**, 29-39.

Schock, F. and Perrimon, N. (2003). Retraction of the *Drosophila* germ band requires cell-matrix interaction. *Genes Dev* **17**, 597-602.

Schultz, J., Milpetz, F., Bork, P. and Ponting, C. P. (1998). SMART, a simple modular architecture research tool: identification of signalling domains. *Proc Natl Acad Sci U S A* **95**, 5857-64.

Self, T., Sobe, T., Copeland, N. G., Jenkins, N. A., Avraham, K. B. and Steel, K. P. (1999). Role of Myosin VI in the differentiation of cochlear hair cells. *Dev Biol* **214**, 331-41.

Sellers, J. R. (2000). Myosins: a diverse superfamily. *Biochim Biophys Acta* **1496**, 3-22.

Sirotkin, V., Seipel, S., Krendel, M. and Bonder, E. M. (2000). Characterization of sea urchin unconventional myosins and analysis of their patterns of expression during early embryogenesis. *Mol Reprod Dev* **57**, 111-26.

Skubitz, A. P. (2002). Adhesion molecules. *Cancer Treat Res* **107**, 305-29.

Soldati, T. (2003). Unconventional myosins, actin dynamics and endocytosis: a menage a trois? *Traffic* **4**, 358-66.

Spradling, A. C. (1993). Developmental genetics of oogenesis. In *The development of Drosophila melanogaster*, vol. 1 (ed. M. Bates and A. Martines-Arias), pp. 1-70. Cold Spring Harbor, New York: Cold spring Harbor Laboratory Press.

Sun, C. X., Robb, V. A. and Gutmann, D. H. (2002). Protein 4.1 tumour suppressors: getting a FERM grip on growth regulation. *J Cell Sci* **115**, 3991-4000.

Sundfeldt, K., Piontkewitz, Y., Ivarsson, K., Nilsson, O., Hellberg, P., Brannstrom, M., Janson, P. O., Enerback, S. and Hedin, L. (1997). E-cadherin expression in human epithelial ovarian cancer and normal ovary. *Int J Cancer* **74**, 275-80.

Suter, D. M., Espindola, F. S., Lin, C. H., Forscher, P. and Mooseker, M. S. (2000). Localization of unconventional myosins V and VI in neuronal growth cones. *J Neurobiol* **42**, 370-82.

Tan, C., Stronach, B., Perrimon, N., De Lorenzo, C., Strand, D., Mechler, B. M., Halsell, S. R., Kiehart, D. P., Jordan, P., Karess, R. et al. (2003). Roles of myosin phosphatase during *Drosophila* development. *Development* **130**, 671-81.

Tanentzapf, G., Smith, C., McGlade, J. and Tepass, U. (2000). Apical, lateral, and basal polarization cues contribute to the development of the follicular epithelium during *Drosophila* oogenesis. *J Cell Biol* **151**, 891-904.

Tanentzapf, G., Tepass, U., Smith, C. and McGlade, J. (2003). Interactions between the crumbs, lethal giant larvae and Bazooka pathways in epithelial polarization

Apical, lateral, and basal polarization cues contribute to the development of the follicular epithelium during *Drosophila* oogenesis. *Nat Cell Biol* **5**, 46-52.

Tang, N., Lin, T., Ostap, E. M., Lee, W. L., Zot, H. G. and Pollard, T. D. (2002). Dynamics of myo1c (myosin-ibeta) lipid binding and dissociation
Organization and ligand binding properties of the tail of Acanthamoeba myosin-IA. Identification of an actin-binding site in the basic (tail homology-1) domain. *J Biol Chem* **277**, 42763-8. Epub 2002 Sep 6.

Tapper, J., Kettunen, E., El-Rifai, W., Seppala, M., Andersson, L. C. and Knuutila, S. (2001). Changes in gene expression during progression of ovarian carcinoma. *Cancer Genet Cytogenet* **128**, 1-6.

Tepass, U., Theres, C. and Knust, E. (1990). crumbs encodes an EGF-like protein expressed on apical membranes of *Drosophila* epithelial cells and required for organization of epithelia. *Cell* **61**, 787-99.

Titus, M. A. (2000). Getting to the point with Myosin VI. *Curr Biol* **10**, R294-7.

Trougakos, I. P., Papassideri, I. S., Waring, G. L. and Margaritis, L. H. (2001). Differential sorting of constitutively co-secreted proteins in the ovarian follicle cells of *Drosophila*. *Eur J Cell Biol* **80**, 271-84.

Tuxworth, R. I., Weber, I., Wessels, D., Addicks, G. C., Soll, D. R., Gerisch, G. and Titus, M. A. (2001). A role for Myosin VII in dynamic cell adhesion. *Curr Biol* **11**, 318-29.

Tzolovsky, G., Millo, H., Pathirana, S., Wood, T. and Bownes, M. (2002). Identification and phylogenetic analysis of *Drosophila melanogaster* myosins. *Mol Biol Evol* **19**, 1041-52.

Vale, R. D. and Milligan, R. A. (2000). The way things move: looking under the hood of molecular motor proteins. *Science* **288**, 88 - 95.

Volkman, N. and Hanein, D. (2000). Actomyosin: law and order in motility. *Curr. Opin. Cell. Biol.* **12**, 26 - 34.

Walsh, T., Walsh, V., Vreugde, S., Hertzano, R., Shahin, H., Haika, S., Lee, M. K., Kanaan, M., King, M. C. and Avraham, K. B. (2002). From flies' eyes to our ears: mutations in a human class III myosin cause progressive nonsyndromic hearing loss DFNB30. *Proc Natl Acad Sci U S A* **99**, 7518-23.

Warner, C., Stewart, A., Luzio, J., Steel, K., Libby, R., Kendrick-Jones, J. and Buss, F. (2003). Loss of Myosin VI reduces secretion and the size of the Golgi in fibroblasts from Snell's waltzer mice. *EMBO Journal* **22**, 569-79.

Wells, A. L., Lin, A. W., Chen, L. Q., Safer, D., Cain, S. M., Hasson, T., Carragher, B. O., Milligan, R. A. and Sweeney, H. L. (1999). Myosin VI is an actin-based motor that moves backwards. *Nature* **401**, 505-8.

Wheatley, S., Kulkarni, S. and Karess, R. (1995). *Drosophila* nonmuscle myosin II is required for rapid cytoplasmic transport during oogenesis and for axial nuclear migration in early embryos. *Development* **121**, 1937-46.

Wodarz, A., Grawe, F. and Knust, E. (1993). CRUMBS is involved in the control of apical protein targeting during *Drosophila* epithelial development. *Mech Dev* **44**, 175-87.

Wolenski, J. S. (1995). Regulation of calmodulin - binding myosins. *Trends in Cell Biology* **5**, 310 - 316.

Wood, W., Jacinto, A., Grose, R., Woolner, S., Gale, J., Wilson, C. and Martin, P. (2002). Wound healing recapitulates morphogenesis in *Drosophila* embryos. *Nat Cell Biol* **4**, 907-12.

Woods, D. F., Hough, C., Peel, D., Callaini, G. and Bryant, P. J. (1996). Dlg protein is required for junction structure, cell polarity, and proliferation control in *Drosophila* epithelia. *J Cell Biol* **134**, 1469-82.

Woods, D. F., Wu, J. W., Bryant, P. J., Hough, C., Peel, D. and Callaini, G. (1997). Localization of proteins to the apico-lateral junctions of *Drosophila* epithelia Dlg protein is required for junction structure, cell polarity, and proliferation control in *Drosophila* epithelia. *Dev Genet* **20**, 111-8.

Wu, H., Nash, J. E., Zamorano, P. and Garner, C. C. (2002). Interaction of SAP97 with minus-end-directed actin motor Myosin VI. Implications for AMPA receptor trafficking. *J Biol Chem* **277**, 30928-34.

Wu, X., Jung, G. and Hammer, J. A., 3rd. (2000). Functions of unconventional myosins. *Curr Opin Cell Biol* **12**, 42-51.

Yamashita, R. A., Sellers, J. R. and Anderson, J. B. (2000). Identification and analysis of the myosin superfamily in *Drosophila*: a database approach. *J Muscle Res Cell Motil* **21**, 491-505.

Yoshimura, M., Homma, K., Saito, J., Inoue, A., Ikebe, R. and Ikebe, M. (2001). Dual regulation of mammalian Myosin VI motor function. *J Biol Chem* **276**, 39600-7. Epub 2001 Aug 21.

Young, P. E., Pesacreta, T. C. and Kiehart, D. P. (1991). Dynamic changes in the distribution of cytoplasmic myosin during *Drosophila* embryogenesis. *Development* **111**, 1-14.

Young, P. E., Richman, A. M., Ketchum, A. S. and Kiehart, D. P. (1993). Morphogenesis in *Drosophila* requires nonmuscle myosin heavy chain function. *Genes Dev* **7**, 29-41.

Zhang, S. and Bernstein, S. I. (2001). Spatially and temporally regulated expression of myosin heavy chain alternative exons during *Drosophila* embryogenesis. *Mech Dev* **101**, 35-45.

Appendix

Identification and Phylogenetic Analysis of *Drosophila melanogaster* Myosins

George Tzolovsky, Hadas Millo, Stephen Pathirana, Timothy Wood, and Mary Bownes
Institute of Cell and Molecular Biology, University of Edinburgh

Myosins constitute a superfamily of motor proteins that convert energy from ATP hydrolysis into mechanical movement along the actin filaments. Phylogenetic analysis currently places myosins into 17 classes based on class-specific features of their conserved motor domain. Traditionally, the myosins have been divided into two classes depending on whether they form monomers or dimers. The conventional myosin of muscle and nonmuscle cells forms class II myosins. They are complex molecules of four light chains bound to two heavy chains that form bipolar filaments via interactions between their coiled-coil tails (type II). Class I myosins are smaller monomeric myosins referred to as unconventional myosins. Now, at least 15 other classes of unconventional myosins are known. How many myosins are needed to ensure the proper development and function of eukaryotic organisms? Thus far, three types of myosins were found in budding yeast, six in the nematode *Caenorhabditis elegans*, and at least 12 in human. Here, we report on the identification and classification of *Drosophila melanogaster* myosins. Analysis of the *Drosophila* genome sequence identified 13 myosin genes. Phylogenetic analysis based on the sequence comparison of the myosin motor domains, as well as the presence of the class-specific domains, suggests that *Drosophila* myosins can be divided into nine major classes. Myosins belonging to previously described classes I, II, III, V, VI, and VII are present. Molecular and phylogenetic analysis indicates that the fruitfly genome contains at least five new myosins. Three of them fall into previously described myosin classes I, VII, and XV. Another myosin is a homolog of the mouse and human PDZ-containing myosins, forming the recently defined class XVIII myosins. PDZ domains are named after the postsynaptic density, disc-large, ZO-1 proteins in which they were first described. The fifth myosin shows a unique domain composition and a low homology to any of the existing classes. We propose that this is classified when similar myosins are identified in other species.

Introduction

The past decade has seen a significant increase in research on myosins. A major effort has been put into finding novel members of this family of actin-based motor proteins. More than 16 classes of myosins have been discovered and characterized, and this number is still rising (Hodge and Cope 2000; Sellers 2000). These myosins are often referred to as unconventional (Mooseker and Cheney 1995). The total number of known myosins is 17 if the conventional two-headed filament forming myosin II is included in the classification. Myosins have been identified in a wide variety of eukaryotic organisms. Some myosin classes are found in phylogenetically diverse organisms, whereas others, which have arisen later in evolution, have been found in only a single organism (Hodge and Cope 2000).

Current research concentrates on the functional analysis of these new types of myosins. A number of studies suggest that these motors play important roles in a variety of cellular functions, including organelle, RNA and protein transport, maintenance of the cell architecture, cell movements, and signal transduction (table 1).

All known myosins comprise an N-terminal head domain, a neck regulatory domain, and a specific carboxy-terminal tail domain (fig. 1) (Mooseker and Cheney 1995). The head or motor domain contains ATP- and actin-binding sites and is responsible for the mechanochemical properties of the protein (Gilbert and Mackey 2000). Myosins show an actin-stimulated Mg^{2+} ATPase activity, thus converting the energy stored in ATP into mechanical force (Volkmann and Hanein 2000). The latter is used to move the myosin molecules along the actin filaments or to translocate other molecules (Hasson and Mooseker 1995; Langford 1995).

The neck domain contains regulatory sites, composed of IQ (isoleucine-glutamine) motifs, repeats of 23–30 aa (Mercer et al. 1991; Rhoads and Friedberg 1997). Each IQ motif provides a binding site for a calmodulin or a related protein of the EF-hand family (Kawasaki, Nakayma, and Kretsinger 1998). EF proteins have helix-loop-helix motifs in which the loop contains highly conserved residues that bind Ca^{2+} ions. The size of the neck domain varies from one to seven IQ tandem repeats. In addition, the neck is often the site of alternative splicing. This produces necks with variable lengths (variable number of IQ repeats), which are associated with the regulatory function. In general, calmodulin activates a diverse group of target cellular proteins when bound to Ca^{2+}. Interestingly, most of the unconventional myosins carry IQ motifs that bind calmodulin with higher affinity in the absence of Ca^{2+}.

After the neck domain, each myosin has a highly divergent tail domain. A subset of myosin tails has predicted coil-coil α-helical domains, which promote the formation of dimmers, a typical example being the two-headed conventional myosin II. Some other myosins lack coiled-coil domains but contain structural domains found in other proteins (table 1).

The classification of myosins is based on the sequence comparison of their core motor domains (myosin head), equivalent to amino acids 88–780 of chicken skeletal myosin II (Cope et al. 1996). The motor domain is highly conserved among all myosins, reflecting the high conservation of its function. However, they have a number of class-specific features (characteristic inserts

Key words: unconventional myosins, evolution, genome project.

Address for correspondence and reprints: Mary Bownes, Institute of Cell and Molecular Biology, University of Edinburgh, King's Buildings, Edinburgh EH9 3JR, United Kingdom.
E-mail: mary.bownes@ed.ac.uk.

Mol. Biol. Evol. 19(7):1041–1052. 2002

Table 1
Domain Structure and Function of Myosin Classes

Class Myosins	Number of IQ Motifs	Number of Heavy Chains	Other (N- and C-terminal) Domains	Function
I				
Subclass 1	One or two IQ	1 (monomer)	TH1, GPA or GPQ, and SH3	Vesicle transport, cell growth, and cell motility
Subclass 2	Three to six IQ	1 (monomer)	TH1	Function in the microvilli of the brush border
Subclass 3	Three IQ	1 (monomer)	TH1	Epithelial morphogenesis and hair cells function
Subclass 4	Two IQ	1 (monomer)	TH1	Epithelial morphogenesis
II				
Muscle	Two IQ	2 (dimer)	CC	Smooth or skeletal muscle contraction
Nonmuscle	Two IQ	2 (dimer)	CC	Maintainance of the cell architecture, cell motility, and phagocytosis
III	One or two IQ	1 (monomer)	N-terminal protein kinase	Role in prototransduction
IV	One IQ	1 (monomer)	MyTH4 and SH3	? (Only in *Acanthamoeba* species)
V	Six IQ	2 (dimer)	CC, transmembrane, specific C-terminal globular domain	Membrane trafficking, polarized cell growth, vesicle, protein and/or mRNA transport
VI	One IQ	2 (dimer) ?	CC, reverse gear, specific C-terminal globular domain	Vesicle transport, epithelial morphogenesis, and stereocilia function. Spermatid individualization. Moves toward the "-" end of actin filaments
VII	Four or five IQ	2 (dimer) ?	CC, MyTH4, FERM, and SH3	Membrane trafficking, hair and photoreceptor cells function
VIII	Three or four IQ	2 (dimer) ?	CC, serine rich domain, specific C-terminal domain	Cell wall function in plants, intracellular transport
IX	Four to six IQ	1 (monomer)	N-terminal extension, zinc binding, and Rho-GAP domains	Signaling (GTPase activating)
X	Three IQ	2 (dimer) ?	CC, PH, MyTH4, FERM	Localized to regions of dynamic actin. Signal transduction
XI	Five to six IQ	2 (dimer) ?	CC	Vesicular transport in plants
XII	IQ ?	2 (dimer) ?	CC, N-terminal extension, and MyTH4 domains	? (In *C. elegans* only)
XIII	Four to seven IQ	1 (monomer)		? (In plants only).
XIV	IQ ?	1 (monomer)		? (In *Toxoplasma* and *Plasmodium* species)
XV	Two to three IQ	1 (monomer)	N-terminal extension MyTH4, FERM, and SH3	Hair cell function
XVI	Two IQ	1 (monomer)	Ankyrin repeats	Neuronal cell migration
XVII	IQ ?	1 (monomer)	Chitin synthase domain	? (In *Pyricularia* and *Emiricella* species)
XVIII	One or two IQ	2 (dimer) ?	CC, KE, and PDZ domain	? Maintenance of the stromal cell architecture

NOTE.—The number of heavy chains reflects their ability to dimerize (based on coiled-coil predictions). Key to domain abbreviations: TH1, Tail Homology Basic 1 domain; GPA, glycine-proline-alanine–rich domain; GPQ, glycine-proline-glutamine–rich domain; SH3, Tail Homology 3 domain (binds to proline-rich motifs); CC, coiled-coil; MyTH4, Myosin Tail Homology 4 domain; Rho-GAP domain (activates small GTPases of the Rho family); PH, Pleckstrin Homology domain; KE, lysine-glutamate–rich domain; PDZ or DHR (Dlg homologous region). For recent reviews on the structure and properties of the unconventional myosins see Wu, Jung, and Hammer (2000), Oliver, Berg, and Cheney (1999), Baker and Titus (1998), and Mermall, Post, and Mooseker (1998). In the construction of this table, data were used from these reviews, the myosin home page, and Cope et al. (1996).

or substitutions), which might be important in defining the precise function of a given myosin. For further information see the Myosin home page at http://www.mrc-lmb.cam.ac.uk/myosin/myosin.html (Hodge and Cope 2000). Phylogenetic analysis of the tail domain sequences produces similar results, indicating that heads and tails have coevolved (Korn 2000).

Five myosin genes have been identified in yeast (*Saccharomyces cerevisiae*), falling into three classes: two class I myosins, one class II myosin, and two class V myosins (Brown 1997). It was suggested that the whole yeast genome had undergone a duplication in ancient times, followed by a number of modifications. As a result, a small fraction of the genes were retained in duplicate (most of them being deleted), thus explaining the loss of the second myosin II gene (Wolfe and Shields 1997). *Saccharomyces cerevisiae* is the organism with the lowest known number of myosin genes. This demonstrates that a eukaryote can function with a set of only three types of myosins.

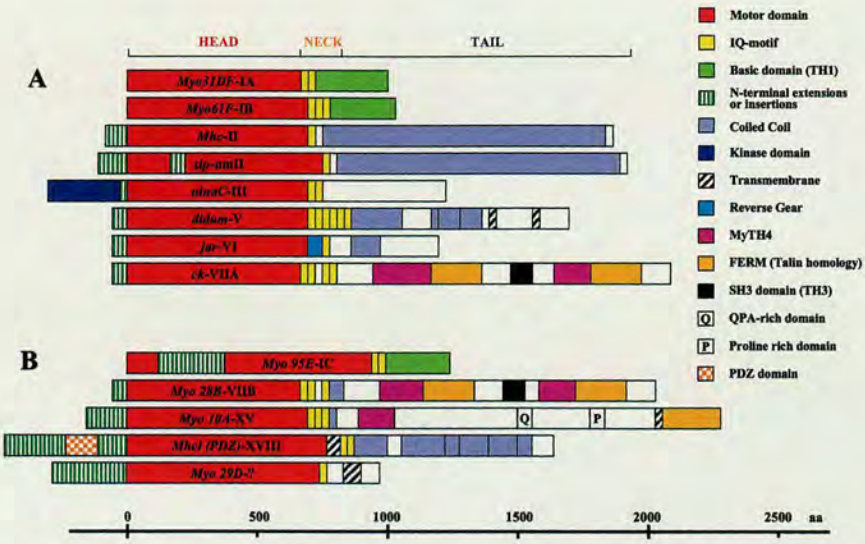

FIG. 1.—Schematic diagram of the domain structure of *Drosophila* myosins. (*A*) The previously described *Drosophila* myosins. Their sequence and structure have been studied and confirmed. For DNA and protein accession numbers see table 2. (*B*) The five new or previously uncharacterized *Drosophila* myosins. Their domain structure is based on the predicted cDNAs for these myosins (see table 2). The presence of some domains (e.g., the PDZ domain in Mhcl myosin) was verified with RT-PCR. A color key to the domain names is given on the left. Some of the names are abbreviated: MyTH4, Myosin Tail Homology 4 domain; FERM, Band 4.1, ezrin, radixin, moesin-homology domain; QPA, glutamine-proline-alanine–rich domain; PDZ, a domain with potential for targeting membrane sites.

Multicellular organisms have the ability to express some 10–40 myosin genes encoding at least six types of myosins. It seems that multicellular organisms require a multitude of specialized myosins. This has raised the question of what is the degree of functional redundancy between the classes and between the members of a given myosin class.

So far, 11 myosin genes have been identified in the slime mould *Dictyostelium discoideum*. Despite the fact that this is one of the simplest multicellular organisms, it expresses a diverse set of myosin genes (Soldati, Geissler, and Schwarz 1999). They encode at least six different classes of highly specific myosins. There are six class I myosins (MyoA, B, C, D, E, K, and probably MyoF) and one member each of class II (MhcA), class VII (MyoI) (Titus 1999), and class XI (MyoJ) (Hammer and Jung 1996). The highly divergent MyoM is still to be classified (Schwarz, Geissler, and Soldati 1999).

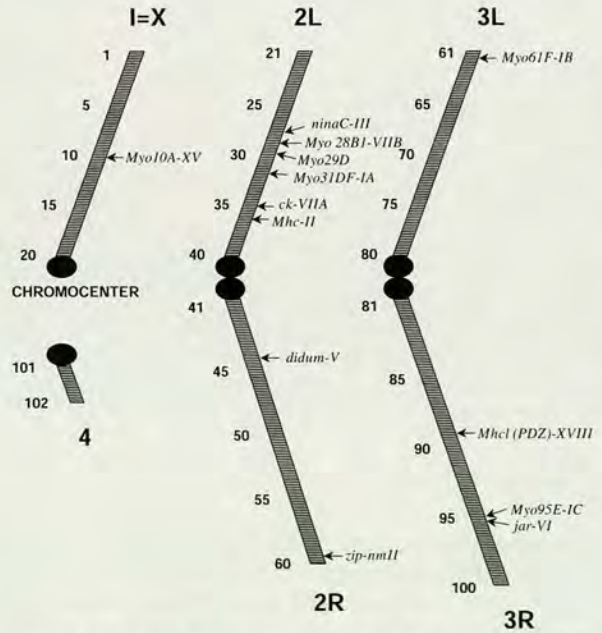

FIG. 2.—Polytene chromosome position of *D. melanogaster* myosin genes (based on the data provided by the Berkeley Drosophila Genome Project). The figure presents all myosin genes, new and previously identified, in relation to their chromosomal locations. So far, no myosin genes have been found on the fourth chromosome.

Fourteen myosin genes have been identified in the nematode *Caenorhabditis elegans* (Baker and Titus 1997). They encode two structurally distinct class I, six class II, one class V, two class VI, one class VII, and one class IX myosins. It was found that *C. elegans* has a highly divergent type of myosin, which is the founding and only member of class XII myosins.

The situation with vertebrates appears even more complex. They express some 40 myosin genes grouped into 12 classes. In humans, there are 8 class I, 16 class II, 2 class III, 3 class V, 1 class VI, 2 class VII, 2 class IX, 1 class X, 2 class XV, and 1 class XVI myosins (Hasson et al. 1996; Berg et al. 2000; Berg, Powell, and Cheney 2001). Recent studies have discovered two PDZ-containing myosins (Furusawa et al. 2000), as well as a novel unclassified myosin (Berg, Powell, and Cheney 2001). PDZ domains are named after the postsynaptic, disc-large, ZO-1 proteins in which they were first described.

In *Drosophila* eight different myosin genes have been described thus far (figs. 1*A*, 2, and table 2). There are two class I myosins, members of subclass 3 (myosin IB) and subclass 4 (myosin IA) (Morgan et al. 1994; Mooseker and Cheney 1995; Morgan, Heinzelman, and Mooseker 1995). Only a single muscle myosin II gene was found in *Drosophila* (Hastings and Emerson 1991; Bernstein and Milligan 1997). It encodes more than 13 protein isoforms with complex temporal and spatial ex-

Table 2
A List of *Drosophila melanogaster* Myosins

Gene–Protein	Class	Chromosome Position	Genomic DNA Length (bp)	mRNA Length (bp)	Protein Length (aa)	EST
Myo31DF (CG7438)* Myosin IA	I	2L (31E3-6)	AE003628 (15,084)	U07595 (3,886)	AAA19590, AAF52966 (1,011)	LP03284.5, LP04189.5
Myo61F (CG9155)* Myosin IB	I	3L (61F6-7)	AE003471, AC005847 (5,057)	U07596 (3,382)	AAA19591 (1,026)	GH13657.5, GH13670.5, GH25605.5, LP08690.5, LP05759.5, CK01057.5, GH23689.5
Myo95E (CG5501) Myosin IC	I	3R (95E1-4)	AE003746 (4,604)	AF454350 (5,285), AF454351 (5,225), AF454352 (5,301)	AF454350 (1,278), AF454351 (1,258)	GH25580.5, GH25580.3, HL05373.5
zip (zipper) (CG15792)* Nonmuscle myosin-II	II	2R (60E7-8)	AE003465 (21,711)	U35816 (6,734)	AAF47311, AAB09048 (2,056)	GM04963.5, SD07905.5, GH27070.5
Myo (CG17927)* Myosin heavy chain	II	2L (36A8-9)	M61229, AE003652, AC005119 (22,663)	M61229 (5,889)	AAA28686, AAA28687 (1,962)	GH21445.5, GH06021.5, GH02291.5, LP07131.3, LD16079.5, HL04385.5, GH11211.5, LD35610.3, HL03720.5, GM03715.5, GM03876.5
ninaC (CG5125)* (Nina C protein)	III	2L (27F5-6)	AE003617, J03131 (7,220)	M20230 (4,809), M20230 (3,643)	AAA28718 (1,501), AAA28719 (1,135)	LP02603.5, LP02603.3
didum (CG2146)* Myosin V	V	2R (43D1-3)	AC004280, AE003841 (8,217)	AF003826 (6,214)	AAF59241, AC99496 (1,792)	GH04445.5, GH04445.3
jar (jaguar) (CG5695)* Myosin VI	VI	3R (95F1-2)	AE003747 (6,312)	X67077 (4,280)	AAF56269, CAA47462 (1,253)	HL03149.5, GH09735.5
ck (crinkled) (CG7595)* Myosin VIIA	VII	2L (35C1)	AE003646 (12,392)	AE003646 (7,030)	AAF53435, AAF44915 (2,167)	LD14917.5, LD14917.3
Myo28B1 (CG6976) Myosin VIIB	VII	2L (28B3-C1)	AE003618, AC005834 (10,519)	AF233269 (6,590)	AAF52536, AAF34810 (2,129)	GH25551.5, GH25551.3
Myo10A (CG2174) Myosin XV	XV	X (10A1)	AE003484 (10,235)	AE003484, AF454346 (7,275)	AAF47980, Q9VZ48, (2,424) (2,333)	LP03318.5
Mhcl (CG10218) Myosin heavy chain–like (PDZ) Myosin	XVIII	3R (89B7)	AE003711 (21,620)	AE003711, AF454347, AY051503	AAK92927, AF454347, AAF55271, AAF55272 (6,603) (6,603) (6,420)	GH03004.5, GM10420.5, GH04935.5, LP04491.5, GH15471.5, GH15471.3
Myo29D (CG10595) Myosin	?	2L (29D1)	AE003621 (5,732)	AF454348 (4,402), AF454349 (2,530)	AF454348 (1,313), AF454349 (689), AAF52683, Q9VLK6, AF405293, AAK97502	LD47348.5, LD47348.3, LP07160.5, AI124339

NOTE.—Myosins denoted with * have been previously identified and characterized. The others resulted from the analysis of published genomic sequence for *Drosophila melanogaster* and molecular studies undertaken in this study. The classification is based on domain and phylogenetic analysis of the predicted mRNAs for these myosins. In several cases the presence or absence of certain motifs was verified by RT-PCR (for detailed explanation of this, see text). The accession numbers show the most recent and complete sequence reports on the presented myosins. ESTs for all of the predicted genes have been identified and partially sequenced. In the case of *Mhcl* the presented mRNA sequences were combined and the three longest transcripts shown.

pression patterns (Bernstein and Milligan 1997; Zhang and Bernstein 2001). *Drosophila* has a second myosin II gene that encodes a cytoplasmic nonmuscle myosin (Kiehart and Feghali 1986; Mansfield et al. 1996). The founding member of class III myosins was discovered in *Drosophila* (Montell and Rubin 1988). The *ninaC-III* gene encodes two isoforms resulting from alternative RNA splicing. These differ in the composition of their C-terminal tails and show differential expression patterns (Porter et al. 1992; Li, Porter, and Montell 1998). A single myosin V gene, with at least two different splice forms, was identified in *Drosophila* (Bonafe and Sellers 1998; MacIver et al. 1998). Kellerman and Miller (1992) cloned a novel unconventional myosin from *Drosophila*—the first member of class VI myosins. The gene produces multiple protein isoforms, which are present throughout

Drosophila development (Kellerman and Miller 1992; Mermall and Miller 1995; Deng, Leaper, and Bownes 1999; Hicks et al. 1999). *Drosophila* myosin VIIA was the first member of this class to be described (Cheney, Riley, and Mooseker 1993; Kiehart et al. 1998).

While this manuscript was in preparation, another paper dealing with *Drosophila* myosins was published (Yamashita, Sellers, and Anderson 2000). The data from both research groups is complementary, with our manuscript focusing in detail on the molecular analysis and domain structure of the myosins.

Materials and Methods

Analysis of the *Drosophila* Genome—Analysis and Manipulation of Sequences

We have used the completed *D. melanogaster* Genome Project to determine the number of myosin-encoding genes in this species and to classify them. The new myosin genes were identified by comparing the *Drosophila* genome sequence with the conserved head (equivalent to amino acids 88–780) of the chicken skeletal myosin II. Comparison with the GenBank Data Base was done using the BLASTP algorithm of the National Center for Biotechnology Information (NCBI) (http://www.ncbi.nlm.nih.gov/BLAST/), the Pôle Bio-Informatique Lyonnaism server (http://pbil.univ-lyon1.fr/BLAST/blast.html), and The Berkeley Drosophila Genome Project BLAST (http://www.fruitfly.org/blast/). This search retrieved the eight previously described myosin genes as well as three new genes: *Myo 28B1* (AAF52536), *Myo10A* (AAF47980), and *Mhcl* (or *Myo89B*) (AAF55271). Subsequent detailed analysis was done using the conserved head or specific tails from all known classes of myosins to search the translated *Drosophila* genome sequence (TBLASTN on the NCBI server). These searches identified two other sequences highly similar to myosins: *Myo29D* (AAF52683, AF454348) and *Myo95E* (AAF56246, AF454350).

Domain Analysis—Multiple Sequence Alignment

The domain structure was predicted with the Simple Modular Architecture Research Tool (SMART) server at http://smart.embl-heidelberg.de/ (Schultz et al. 1998), the Pfam HMM database at http://pfam.wustl.edu/hmmsearch.shtml or http://www.sanger.ac.uk/Software/Pfam/search.shtml (The Sanger Centre), and the ProFile Scan Server of ISREC (Swiss Institute for Experimental Cancer Research) at http://www.isrec.isbsib.ch/software/PFSCAN_form.html. Alignments of the detected domains were performed with CLUSTAL W (Thompson, Higgins, and Gibson 1994) available from the Gene Jockey II software package distributed by Biosoft or from the WEB-based package at http://www2.ebi.ac.uk/clustalw/. Subsequently, the sequences were run on WEB-based BoxShade Server (http://ludwig-sun1.unil.ch:8080/software/BOX_form.html) and manually adjusted in Microsoft Word 98.

Coiled-coil regions were predicted with the Paircoil program developed by Berger and coworkers (Berger et al. 1995) at http://nightingale.lcs.mit.edu/cgi-bin/score.

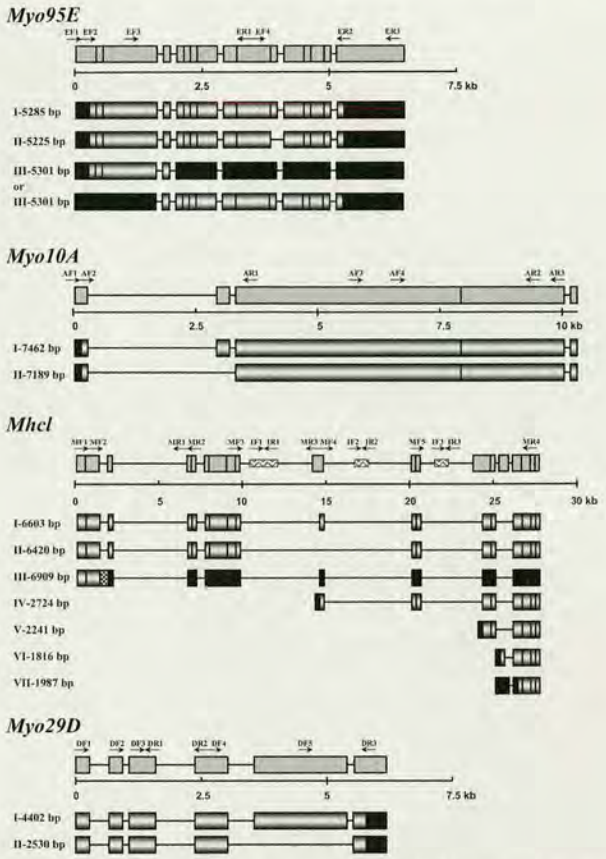

FIG. 3.—Molecular organization of *Myo95E, Myo10A, Mhcl,* and *Myo29D* myosin genes. The exon structure of the myosin genes is represented by gray boxes. Arrows indicate the primers used in the RT-PCR analysis of the gene structure. The length of the predicted mRNAs is noted on the left side of the transcript maps. Shaded boxes represent ORFs; solid boxes represent untranslated sequences (5′UTR or 3′UTR); dotted boxes represent the intron sequence in the spliced mRNA; wave pattern boxes represent exons from genes located within the myosin gene. The gene depicted by IF1 and IR1 primers is at least a three-exon gene, but for simplicity it is presented with a single box here (for more information see text).

RNA Extraction and RT-PCR

Total RNA from larvae and adult flies was isolated using RNAeasy-Total RNA Kit (QIAGEN, Cat #: 74104). The RNA (4 μg) was primed with Oligo-p(dT)$_{18}$ and reverse transcribed by Superscript™ II (GIBCO BRL), following the supplier's protocol. For subsequent DNA amplification, 2 μl out of 20 μl of the first-strand reaction mix was used. The PCRs were carried out with appropriate pairs of forward and reverse primers. The position of the primers is indicated in figure 3. Primers for *Myo95E:* EF1 (TGT TGC TCG CCA GCA CAT G), EF2 (ATG GAG CAG GAA ATC GGC AC), EF3 (CAT CAG CGG CCT TCC TGA AT), EF4 (GAA GTA CAT AAG CGC TGC CT), ER1 (AGG CAG CGC TTA TGT ACT TC), ER2 (ACA ATT ATC TCC ATG CGG TTC G), ER3 (ACG TAG ATG CCT GAA CTA TC). Primers for *Myo10A:* AF1 (GCA GCA ATG AAT CAA CCG GT), AF2 (TGA TCT GGT CTG GTT CGA TC), AF3 (TCA GTG TCC AGA GGC ATG TG), AF4 (TGG AGT GGC GTG CCT GGA), AR1 (CAT CTT GTA CGG ATT CAC

CG), AR2 (TCC GCA CGC GCA ACT TCC A), AR3 (CTT GCG GAA CTC CTG GAC A). Primers for *Mhcl:* MF1 (CAA CTT TAT GAA GAA GAG CGC), MF2 (AAG GCA GCT AGT GAT CAG GC), MF3 (TCG CAT AGG ACC CAG CCA G), MF4 (ATG TGG TCG GAT AAA AGT GCA), MF5 (GCT CTC AGA TCG CAT TAT ACA G), MR1 (AGC TCG CAG ATG TCC TCG A), MR2 (ACA TGG AGA CAA CCT TCT CG), MR3 (TAT ACG GAC GCA GGC GAT AG), MR4 (TCT TCC AGA TCA CTG ATA GAG). Primers for *Myo29D:* DF1 (ATC CGC ACA ACA TTC TGC AC), DF2 (ATG CAT CTT CAT CCA ACG AG), DF3 (AAT CAC AGC TTC AGC CAC AC), DF4 (GAG ACT GAT GCC TTC AAG CAC), DF5 (ACT TTG TGC GCT GCA TCC G), DR1 (GTC CCG ACA AGT GGA TCA G), DR2 (GTG CTT GAA GGC ATC AGT CTC), DR3 (AGG AAG AGT TGA ACA GAT GGA). Primers for genes in the *Mhcl* gene: IF1 (TTA CCT CCA TAA ACC TGC GG), IF2 (GTC GCC GAG CCC GAA GAG), IF3 (AAC GTC GCG TTC GCA AGA GG), IR1 (AAC GAT TCG GAG GTG CAC G), IR2 (CTA GCT CTG CGA AGA TCT CA), IR3 (CGT TCA TGG CTG CTA GTA CG). QIAGEN Taq and Stratagene Pfu Turbo® Polymerase in a 3:1 ratio were used in the PCR reactions. The QIAGEN PCR protocol designed to work with Q-Solution was followed. The PCR reactions were carried out as follows: one cycle at 94°C for 4 min; 35 cycles, step one—94°C for 40 s, step two—60°C for 40 s, step three—72°C for 1.8 min per expected kilobase pair of the PCR product; and one cycle at 72°C for 10 min. The obtained PCR products were isolated from Tris-acetate/Ethylenediaminetetra-acetate (TAE) gels, purified, and sequenced on a 373A automated DNA sequencer (ABI).

Results

The BLASTP and BLASTN searches with the conservative chicken skeletal myosin II head, against the completed *Drosophila* genome sequence, retrieved the previously identified genes and five new myosin genes (fig. 1). We selected a limit of 30%–40% identity for a myosin to fall into a given myosin class, and 25%–30% was considered as the lower threshold for a protein to be classified as a myosin. The new myosins (fig. 1*B*) were named according to their chromosome position (fig. 2). Interestingly, half of the myosin genes are located between polytene bands 27F–36A, thus forming a myosin hot spot on the left arm of the second chromosome.

In the cases of *Myo 95E, Myo10A, Mhcl,* and *Myo29D,* we did a detailed analysis of the molecular structure of the genes and the transcripts they produced. The main reason for this was that the predicted sequences for these genes encode proteins that produced low homology scores to other myosins. They were obviously myosins, containing all the conserved sequences and structural parts defining them as myosins and at the same time showing no more than 15%–29% identity to other myosins. This implied either incorrectly predicted genes or incorrectly predicted splicing of the transcripts. Open reading frames (ORF), 5′untranslated regions (UTRs), 3′UTRs, and the presence or absence of given motifs were tested by RT-PCR and subsequent sequencing of the products obtained. In these experiments we employed an ovarian Uni-ZAP XR® library produced in our lab, along with cDNAs produced by reverse transcription of RNAs from larvae and adult flies (see *Materials and Methods*). As a result, we determined a number of new myosin sequences and submitted them to the MEDLINE Database. The accession numbers for these are—*Myo95E:* AF454350, AF454351, and AF454352; *Myo10A:* AF454346 (presents a part of the first three exons including the 5′UTR); *Mhcl:* AF454347 (presents a part of the first four exons including the sequence encoding the PDZ domain); *Myo29D:* AF454348 and AF454349. *Myo28B* was not subjected to detailed analysis because it was found to be almost identical to the other myosin VII (crinkled) from *Drosophila* at both the DNA and protein levels.

To examine the evolutionary relationships between members of the myosin family in *Drosophila* and other phylogenetically diverse species, we used two different phylogenetic methods. We applied Distant-matrix and Maximum-Parsimony methods (PROTDIST and PROTPARS from the PHYLIP package) to compare the conserved head domains. These methods were chosen because they tend to outperform other methods (i.e., lower variance), such as the Maximum Likelihood, when dealing with large data sets. The two programs produced trees with similar topology (see the unrooted consensus tree in fig. 4). Multiple sequence alignments were performed with CLUSTAL W without corrections for gaps or multiple substitutions. Excluding the positions with gaps would have omitted a significant proportion of the data, a problem that occurs when large amounts of input sequences are dealt with. CLUSTAL W (GCG software package) is provided by the Human Genome Mapping Project Resource Centre, Cambridge, at http://www.hgmp.mrc.ac.uk/ (Thompson, Higgins, and Gibson 1994). The reliability of the tree structure was checked by bootstrapping (1,000 trials) and reordering the alignments randomly (bootstrapping was performed with SEQBOOT from the PHYLIP package). The tests produced trees with similar branching order. A consensus tree was produced by the CONSENSE program of the PHYLIP package and graphically drawn with the TREEVIEW program (Page 1996), and was then transferred to and manipulated with PowerPoint.

The protein sequences for the new *Drosophila* myosins are theoretical predictions. Myosins are large multiexon genes and are difficult to assemble with 100% accuracy from sequence data. There are also various isoforms of some myosins, which can lead to some misalignments; hence, it is unlikely that the tree shown perfectly reflects the evolution of the *Drosophila* myosins.

It is possible that some of the new *Drosophila* myosins could be pseudogenes. However, we found that the probability for this was low. Pseudogenes generally lack introns and are not transcribed into mRNA. We identified expressed sequence tags (ESTs) for all the myosin genes we predicted (the accession numbers for these are given in table 2), which confirmed their in vivo expression. The new myosins are described in detail subsequently.

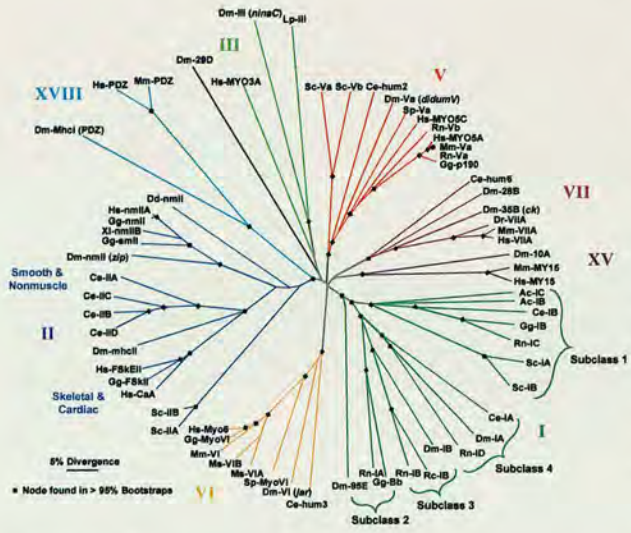

Abbrevation full terms:

Ac	*Acanthamoeba castellanii*	Lp	*Limulus polyphemus*	Bb	Brush border myosin I
Ce	*Caenorhabdites elegans*	Mm	*Mus musculus*	Ca	Cardiac alpha myosin II
Dd	*Dictyostelium discoideum*	Ms	*Morone saxatilis*	FSk	Fast skeletal muscle myosin II
Dm	*Drosophila melanogaster*	Rc	*Rana catesbeiana*	mhc	Myosin heavy chain
Gg	*Gallus gallus*	Rn	*Rattus norvegicus*	nm	Non-muscle myosin II
Hs	*Homo sapiens*	Sc	*Saccharomyces cerevisiae*	PDZ	PDZ containing myosin XVIII
		Xl	*Xenopus laevis*	sm	Smooth muscle myosin II

FIG. 4.—Phylogenetic analysis of the myosin superfamily in *D. melanogaster*. The head domains of *Drosophila* myosins (equivalent to amino acids 88–780 of chicken skeletal myosin) were compared with selected myosins representing phylogenetically diverse organisms. The alignment of 67 myosins (performed with the CLUSTAL W package) was used to generate data for an unrooted tree to scale based on sequence divergence (for details see text). Each myosin class is defined by the first node represented in >95% of the bootstrap trials (starting from the tree center) and is color coded. The accession numbers for the myosins used in the alignment are given subsequently. These are produced for the protein sequences, except in the case of Dm95E (*Myo95E* gene) and Dm29D (*Myo29D* gene), where the cDNA accession numbers are given. Myosin class I: Ac-IB (AAA27708), Ac-ICy (AAA27707), ScMyo3-IA (AAB34124), ScMyo5-IB (CAA89745), Cehum5-IA (CAA53244), CehumI-IB,1 Dm31D- IA (AAA19590), Dm61F-IB (AAA19591), Dm95E (AF454350), Rc-IB (AAA57192), Gg-Bb (AAB38373), Gg-IB (CAA49850), Rnmyr1-IA (CAA48287), Rnmyr2-IB (CAA52807), Rnmyr3-IC (CAA52815), Rnmyr4-ID (CAA50871). Myosin class II: ScMYO1-IIA (CAA37894), ScMYS1-IIB (P08964), Dd-nmII (AAA33227), Ce myo3-IIA (CAA30856), Cemyo4-IIB (AAA28124), Cemyo2-IIC (CAA30855), Cemyo1-IID (CAA30854), Dm-mhcII (AAA28686), Dmzip-nmII (AAF47311), Xl-nmIIb (AAA49915), Gg-FSkII (P13538), Gg-nmII (AAA48974), Gg-smII (CAA29793), Hs-FSkEII (CAA32167), Hs-CaA (BAA00791), Hs nmIIA (AAA59888). Myosin class III: Lp-III (AAC16332), Dm-NinaC-III (AAA28718), HsMYO3A (AAF70861). Myosin class V: ScMyo2p-Va (AAA34810), ScMyo4p-Vb (AAC37409), Cehum2 (AAA97926), SpMyo-Va (AAF78910), Dmdidum-Va (AAC99496), Ggp190-Va (CAA77782), Mmdilute-Va (CAA40651), Rnmyo5-Va (BAA88350), Rnmyr6-Vb (AAB38840), HsMYO5A (AAD00702), HsMYO5C (AAF78783). Myosin class VI: SpMyo-VI (AAF72176), Cehum3 (AAC67447), Dmjar-VI (CAA47462), Ms-VIA (AAD52005), Ms-VIB (AAD52006), GgMyoVI (CAB96536), MmWaltzerVI (AAB00194), HsMYO6 (AAC51654). Myosin class VII: Cehum6-VII (AAB37988), Dmck-IIA (AAF53435), Dm28B-VIIB (AAF52536), DrMyo-VIIA (CAC05418), Mmshaker-VIIA (AAB40708), HsUsherIb-VIIA (AAB03679). Myosin class XV: Dm10A-XV (AAF47980), Mm-Myo15 (AAF05904), HsMYO15 (AAF05903). Myosin class XVIII: Dm89B-PDZ (AAF55271), Mm-PDZ (BAA93660), Hs-PDZ (BAA13206).2 Myosin class ?: Dm29D (AF454348).

Myo95E (Myosin IC)

This myosin was not found during the initial searches of the fly genome. It was subsequently identified in the AE003746 genome scaffolding. The predicted sequence for this gene is unusually short, resulting in only a 59-aa protein (accession number AAF56246). Detailed analysis showed that the gene was not predicted correctly by the Genome Project. The sequence for *Myo95E* was manually assembled, taking into account the reported sequence for this gene along with the identified ESTs (table 2), as well as the homology of the translated genomic DNA to other myosins (preserving the exon-intron spacing). To test our theoretical predictions, we used two splice-site prediction programs: The Neural Network at http://www.fruitfly.org/seq_tools/splice.html and the GENSCAN Server at MIT—http://genes.mit.edu/GENSCAN.html. Using the artificially assembled sequence, we were able to design primers, amplify a PCR product, and hence sequence the cDNA for *Myo95E* (see *Materials and Methods*). The resulting sequence differed from the predicted sequence, showing the presence of an unusually long exon 3 and variations in exon 4. RT-PCR analysis showed that the gene produces at least three different transcripts expressed during oogenesis, and larval and adult stages (fig. 3). Two of the transcripts (I-AF454350 and II-AF454351), which represent 5%–10% of the total amount of *Myo95E* transcripts, translate into two protein isoforms of 1,278 and 1,258 aa, respectively. Transcript I (5,285 bp) comprises all 16 exons of the gene. Transcript II (5,225 bp) lacks exon 12. The major third transcript (III-AF454352) has a longer exon 4 (a downstream extension of 16 bp, GTG CAC ATT ACC CAT T). This shifts the ORF and produces a stop codon TGA in exon 5. The third transcript (5301 bp) encodes two putative truncated proteins. The first is a 464 aa sequence containing only the GESGAGKT conserved region from the P-loop of the myosin head domain. It does not contain the Switch-1 (NxxSSR) and Switch-2 (DxxGxE) regions which together with the P-loop have been implicated as having a role in the hydrolysis of ATP. The second is an 864 aa protein containing a large part of the head domain, two IQ motifs and a myosin tail domain. The head of this myosin form contains only the Switch-2 (DFYGFE) conserved sequence, which prevents it from converting ATP, probably rendering the form inactive. Homology searches with the protein sequence for the head domain showed 33% identity (53% similarity) to vertebrate brush border class I myosins. Three ESTs were found for *Myo95E*. A search with them revealed up to 37% identity to vertebrate brush border myosins and less to other myosin classes. Analysis of Myosin 95E with domain-scanning programs confirmed its structural similarity to class I myosins (fig. 1*B*). It was found to contain two IQ domains (928–974 aa), the second being poorly conserved (fig. 5),

←

[1] This is a joint sequence from the first 72 amino acids of T21544 and from the 11th amino acid to the end of AAA97925.

[2] The sequence for the human PDZ-containing myosin is truncated. This does not seem to affect its evolutionary position in the phylogenetic tree.

FIG. 5.—Alignment of the IQ motifs for the five newly identified myosins from *D. melanogaster*: Myosin IC (*Myo95E*), Myosin VIIB (*Myo28B*), Myosin XV (*Myo10A*), Myosin 89B (*Mhcl*), and Myosin 29D (*Myo29D*). The consensus sequence is shown below the alignment, and the highly conservative positions are shaded. Residues in bold indicate similarity to the consensus sequence. Myosin IC has two different variants (A and B) of its second IQ motif, a result of alternative splicing.

and a Basic Tail domain (974–1,278 aa for isoform I and 974–1,258 aa for isoform II) (fig. 1*B* and table 1). The latter is thought to be involved in membrane binding. Recent studies have shown that it can also bind to actin filaments (Lee et al. 1999; Liu, Brzeska, and Korn 2000). This changes the number of class I myosins in *Drosophila* to three, hence Myosin 95E was renamed Myosin IC. The *Drosophila* Myosin IC does differ from other myosins of class I. The unusually long exon 3 results in a 281-aa insertion into the head domain. This insertion contains a partial AAA domain, a conserved region that contains an ATP-binding site. So far, no other myosins from class I have been identified which contain such an insertion.

Myo28B (Myosin VIIB)

The amino acid sequence of the Myosin 28B head showed 61% identity (74% similarity) to *ck-Drosophila* myosin VIIA. It also exhibited a very high identity of 58% (72% similarity) to Myosin VIIA from zebrafish and to other class VII myosins. Analysis of Myosin 28B revealed that it has four IQ motifs (753–845 aa), the third being poorly conserved (figs. 1*B* and 5). Two Myosin Tail Homology 4 (MyTH4) (1,070–1,246 and 1,681–1,826 aa), two FERM (1,246–1,454 and 1,826–2,039 aa), and one SH3 (Src homology 3) (1,561–1,626 aa) domains were identified (fig. 6*A* and *B*). The function of the MyTH4 domains is unknown. The FERM domain (the name stands for Band 4.1, ezrin, radixin, moesin-homology) is believed to be involved in linking cytoskeletal proteins to the membrane as well as in dimerization. Talin, merlin, and philopodin are other major members of the FERM superfamily. These deserve mentioning, especially the Talin, because the FERM domain exhibits the highest homology to the FERM domain in Talins (fig. 7) and less homology to FERM domains from other members of the FERM family. The SH3 domain has been identified in many proteins involved in signal transduction. It is believed that the SH3 domains mediate protein-protein interactions by binding to proline-rich domains. Other myosins, such as IV, X, and XV, also contain this

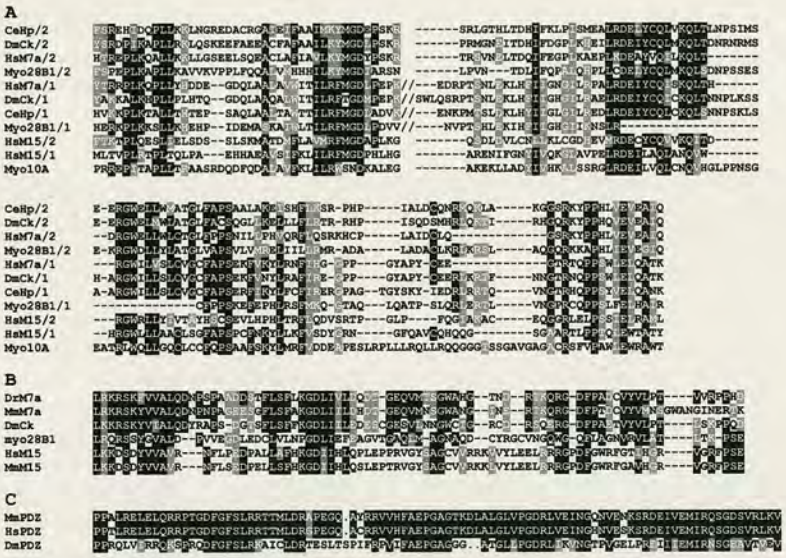

FIG. 6.—CLUSTAL W alignment of the predicted (*A*) MyTH4, (*B*) SH3, and (*C*) PDZ domains in the tails of the newly identified *Drosophila* myosins. The sequences were shaded on the BoxShade server and manipulated with Microsoft Word 98. The parameters set on BoxShade are as follows—output format: RTF New; fraction of sequences: 0.5; input sequence format: MSF or multisequence format (this is the output format of CLUSTAL W). Identical amino acids are shaded in black, similar residues are shaded in gray. Myosin VII has two MyTH4 domains. The first MyTH4 domain in HsM7a, DmCk, CeHp, and Myo28B1 contain an insert of 61–88 aa (regions 1057–1144, 1048–1135, 971–1055, and 1107–1168, respectively) that was not included in the alignment. Accession numbers and abbreviation full terms: Ce, *Caenorhabditis elegans* (Myosin VII, T25888); Hp, hypothetical protein; Dm, *Drosophila melanogaster* (ck, VIIA, AAF44915; Myo28B, AAF52536; PDZ-Myosin, AE003711); ck, crinkled; Hs, *Homo sapiens* (M7A, Q13402; Myosin XV, A59266; PDZ-Myosin, AL080245 and Z98949); Dr, *Danio rerio* (Myosin VIIA, CAC05418); Mm, *Mus musculus* (Myosin VIIA, P97479; Myosin XV, A59295; PDZ-Myosin, BAA93660).

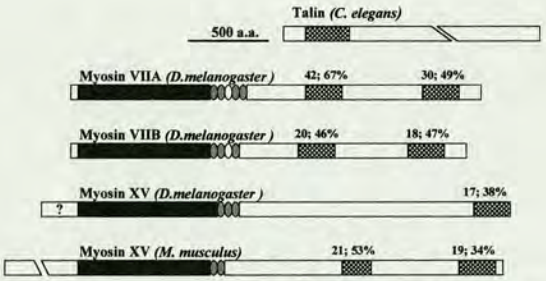

FIG. 7.—Sequence comparison of the FERM domains found in *Drosophila* Myosin VII and XV. These were aligned separately to the Talin domain from *C. elegans* Talin protein. Multiple alignment was not appropriate in this case because the similarity between FERM 1 and FERM 2 to the Talin domain (from the Talin protein) is very low and results in unordered alignment. The comparison was performed by CLUSTAL W (http://www2.ebi.ac.uk/clustalw/). In addition, the FERM domains from *Mus musculus* Myosin XV were included in the diagram. In general, FERM1 motifs from Myosin VII show ~12%–21% similarity to proteins from the FERM family and ~16% to the band 4.1 protein. FERM2 domains (Myosin VII) show a higher similarity of ~17%–18% to band 4.1 protein and ~18%–20% to proteins from the FERM family. FERM domains from Myosin XV show less similarity of 9%–17% to FERM proteins and ~14% to the band 4.1 protein. Accession numbers are—*C. elegans* (Talin): AAA74747; *D. melanogaster* (Myosin VIIA): CAC05418, (Myosin VIIB): AAF52536, (Myosin 10A-XV): AAF47980; *M. musculus* (myosin XV): AAF05904.

motif. A short coiled-coil domain (849–908 aa) was predicted by the Paircoil program (fig. 8).

Myo10A (Myosin XV)

An RT-PCR analysis was used to verify the exon composition and the exon length of *Myo10A* transcripts. It was found that there are at least two transcripts, which are expressed from the larval stage onward (fig. 3). The longer transcript (7,462 bp) consists of all the previously known five exons and represents no more than 5% of the total amount of mRNA for this myosin. The shorter transcript (7,189 bp) lacks exon 2 and is expressed abundantly. The two transcripts translate into two protein isoforms of 2,424 and 2,333 aa, respectively. A BLAST search with the conserved head domain showed significant 47% identity (64% similarity) to mouse and human myosin XV. *Myo10A* is also related to human and mouse myosin VIIA with an identity of 42% (59% similarity). A specific N-terminal domain was identified in Myosin 10A (1–149 aa). The latter showed no similarity to the characteristic N-terminal domain found in other class XV myosins. The shorter protein isoform lacks this N-terminal domain. In the neck region three IQ domains (841–910 aa) were identified (fig. 5). Immediately after the IQ motifs there is a short coiled-coil region (919–946 aa) (fig. 8). Analysis of the tail revealed the presence of one MyTH4 domain (1,014–1,173 aa) (fig. 6), a glutamine-proline-alanine (QPA)-rich domain, a proline-rich domain (the borders of QPA and the proline-rich domain were not clearly defined), a short transmembrane motif (2,194 aa) (fig. 1*B*), and an FERM domain (2,220–2,424 aa). The latter showed a very high identity of 40% (59% similarity) to the first and 13% identity (30% similarity) to the second FERM domain from mouse myosin XV and a limited similarity of 38% (17% identity) to Talin itself (fig. 7).

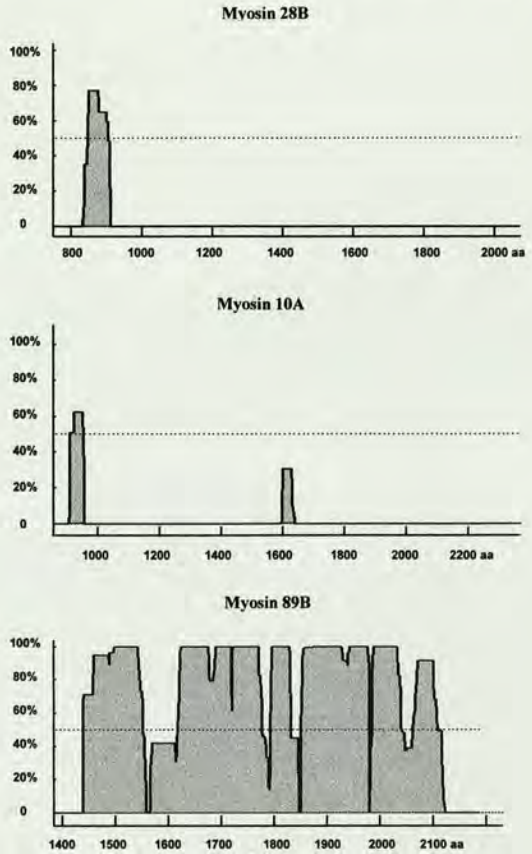

FIG. 8.—Predicted coiled-coil structures in the tails of the newly identified *Drosophila* myosins. Only three of the five myosins are likely to form coiled-coils, these being myosin 28B-VIIB, myosin 10A-XV, and Mhcl-PDZ. Both myosin 28B-VIIB and 10A-XV produced scores close to the lower threshold. Whether they form coiled-coils or not can only be determined experimentally.

Mhcl (Myosin XVIII)

A partial sequence of this gene has been submitted to the GenBank Data Base by Biru (1999). It shows high similarity to the Mhc type II of myosins and was termed Myosin heavy chain–like. Subsequently, the full length for this myosin was published by Celera (Adams et al. 2000). The RT-PCR analysis we have undertaken shows that *Mhcl* has a very complex structure and expresses multiple transcripts throughout the *Drosophila* life cycle (fig. 3). Data from the available ESTs for *Mhcl,* PCR analysis, and a Promoter-predicting program (http://www.fruitfly.org/seq_tools/promoter.html) suggest that the seven identified transcripts are transcribed from four putative promoters. Transcripts I (6,603 bp) and III (6,909 bp) are highly expressed. The other five identified transcripts are expressed at comparatively lower levels. Transcripts I and III are composed of 18 exons (the gene comprises 19 exons), lacking exon 15. The difference between them is that transcript III has the second intron spliced out, which introduces a stop codon in the ORF. One unusual feature of *Mhcl* is the fact that it contains three other genes within it (fig. 3). The exons of these genes are not found in combination with any of the exons of the myosin gene. Importantly, there are ESTs for each of the three genes. One of the genes has been previously

identified as phosphatidylserine-specific phospholipase A1 (CG4979). It is located in intron 9, and its reading frame is in the opposite direction to that of the *Mhcl* reading frame (EST: GH15759). The other two genes have ORFs in the same direction as the main (*Mhcl*) gene. The gene in intron 10 (ESTs: RE41368, RE44374) is a novel gene and does not show any significant homology to previously characterized genes. The gene in intron 12 (ESTs: LP08646, LP05315) shows a limited identity of 35% (46% similarity) to bovine synaptojanine 1 protein (synaptic inositol-1,4,5-trisphosphate 5-phosphatase 1). The *Mhcl* transcripts translate into a set of protein isoforms—I: 2,200 aa; II: 2,139 aa; III: 439 aa; IV: 899 aa; V: 730 aa; VI: 512 aa; and VII: 479 aa. Only the isoforms produced by transcripts I and II contain the conserved motor domain. BLAST analysis showed that Myosin heavy chain–like is most closely related to mouse PDZ-Myosin (41% identity) and human PDZ-Myosin (40% identity). It showed a limited identity of 28%–29% to smooth muscle and nonmuscle myosins and less than 25% to skeletal muscle myosin. BLAST searches revealed that the tail domain shows the highest similarity, 32%, to PDZ-containing myosins and less than 25% similarity to other types of myosins. Interestingly, this myosin was not predicted to contain a PDZ domain. We used the DNA sequence encoding the mouse PDZ domain to search the genomic sequence (AE003711) surrounding *Mhcl* (approximately 10 kb in each direction). This detected a PDZ domain 4,810 bp upstream of the predicted start for the *Mhcl* mRNA (the domain was found in the borders of the predicted genomic DNA for this gene but has not been previously included in its ORF). The presence of the PDZ domain was verified by RT-PCR, and the sequence was submitted to the NCBI database (AF454347). A sequence alignment of the PDZ domains from Drosophila, mouse, and human is given in figure 6. Interestingly, transcript III translates into a truncated protein containing only this PDZ domain (349–429 aa). PDZ domains are known to bind C-terminal or internal (non–C-terminal) polypeptides. Two IQ domains were found in Mhcl (1,379–1,428 aa) (figs. 1*B* and 5), although the second differed slightly from the consensus sequence. The Paircoil program predicted two coiled-coil domains at 1,439–1,549 and 1,616–2,121 aa (fig. 8).

Myo29D

Database searches suggested that the first three exons of *Myo29D* are probably part of a gene adjacent to the myosin. Subsequent RT-PCR showed that they splice together with the other three myosin exons to produce at least two different transcripts. Transcript I (4,402 bp) contains all the six exons, whereas transcript II (2,530 bp) lacks exon 5. Transcripts I and II are present during all the stages of *Drosophila* development, with transcript I being expressed at the higher levels. Transcript II produces a truncated form of the protein, lacking most of the motor head domain. Analysis of the conserved head domain revealed that Myosin 29D is not similar to any of the known classes of myosins. It showed 29% identity (45% similarity) to myosin VII, X, and V from different species, which is sufficient for it to be considered as a myosin but not enough to be related to a given class. A search with the available ESTs for this myosin showed 36%–39% identity to myosin V from different species and 31%–36% to vertebrate Myosin heavy chains (myosin II). Motif search programs detected in Myosin 29D a specific N-terminal extension (1–338 aa), two IQ motifs (1,089–1,136 aa), the second being poorly conserved, and a short transmembrane motif in the tail (1,144–1,279 aa) (fig. 1*B*).

The detailed search of the translated *Drosophila* genome sequence produced several low-score hits. Close analysis of these (searches up and downstream of the respective sequences) revealed that they are not true myosins. Despite exhibiting certain similarities to given parts of the myosins, none of them showed high homology to a larger part of the head domain. AE003112 showed similarity to the highly conserved region (GESGAGKT) from the P-loop of the head domain. Its polytene chromosome location remains undetermined. AE003614 (CG11199) showed homology to the myosin tail, containing coiled-coil and FERM domains. It is located on the chromosome arm 2L (27E), next to the *ninaC* gene. AE003495 (CG12047) also showed similarity to the myosin tail, containing coiled-coil and FERM domains. This is located on the X chromosome (12E1), close to the newly identified *Myo10A*.

The BLAST search retrieved one more myosin-like gene *CG15831* in the AE002795 genome scaffolding. This is a single-exon gene, 219 bp long. The chromosome position of AE002795 has not been determined previously. The program showed similarity to a highly conservative part of the myosin head domain (**LGV LDIFGF**ENFSH**NSFEQ**LC**INYTNEKLHKFFN**H). We found that the DNA surrounding the gene shows no similarity to the myosin genes (at the DNA or protein level). This suggests that AE002795 is either incorrectly assembled in the genome or that the gene *CG15831* is a partial duplication of a myosin gene (this might be either a part of *Mhc* [muscle myosin II] or *didum* [Myosin V], which produced the highest score for this sequence, 59% and 54% identity, respectively).

Discussion

The myosin family has grown significantly in the past decade to encompass more than 177 myosins these days. All these myosins, with a few exceptions, fall into 18 classes. Myosins are expressed in both prokaryotes (though these have not been well studied) and eukaryotes.

The annotation of the genome sequences for *S. cerevisiae*, *Dictyostelium discoideum*, *Arabidopsis thaliana*, *C. elegans*, *Drosophila melanogaster*, and *Homo sapiens* made it possible to identify the complete sets of myosin genes in these organisms. It appears that all eukaryotes have an essential set of three myosin genes, these being from classes I, II, and V, as well as a number of species-specific myosins. In *Drosophila* 13 different myosin genes were identified. The fruitfly has three I, two II (one encoding for muscle and one for nonmuscle myosins), one III, one V, one VI, two VII, one XV, and one XVIII myosin

genes, and one yet to be classified myosin gene. These classes of myosins have been found in a wide range of invertebrate and vertebrate animals. It has been shown that they have a role in a variety of cell functions, including membrane trafficking, signal transduction, and maintenance of the cell architecture. Several new myosin genes were identified in the fruitfly. The genome data provided cDNA sequences for four of them (*Myo28B, Myo10A, Mhcl,* and *Myo29D*). The sequences and the ORF for these myosins were verified by RT-PCR and sequencing. In addition, a fifth myosin was found (*Myo95E*). Using the fruitfly genomic sequence, we were able to predict and subsequently isolate and sequence this gene.

Only two of the five newly identified genes in *Drosophila* fell directly into previously known classes, these being Myosin VIIB (*Myo28B*) and Myosin heavy chain–like (*Mhcl*). Myosin VIIB is from the well-studied class VII myosins with a role in the membrane trafficking and stereocilia function.

Mhcl is a member of the recently defined class XVIII of myosins, which consists of only two other members, mouse and human PDZ-containing myosins. The PDZ domain, also called DHR (Dlg homologous region), is known to bind either C-terminal or internal (non–C-terminal) polypeptides. These domains have been identified in a broad range of signaling proteins from bacteria, yeast, plants, insects, and vertebrates. PDZ domains have been implicated in targeting signaling molecules to submembranous sites.

Myosin IC (*Myo95E*) is the third member of class I myosins in *Drosophila*. It contains the Basic Tail domain (TH1) specific to all class I myosins. It is thought that TH1 binds to acidic phospholipids and actin filaments. Interestingly, this myosin contains an additional N-terminal insertion, which is similar to the AAA motif, a conserved region of about 220 aa that contains an ATP-binding site. This domain is inserted in the region of the loop 1 of the motor domain, the other region associated with the hydrolysis site for ATP, and probably modulates its activity.

Myo10A is closely related to class XV myosins. This myosin has a short N-terminal extension, which differs from the N-terminal domain characteristic for vertebrate myosins of class XV. It also lacks the SH3 and the second MyTH4 domain found in other myosin XV tails. Instead, the *Drosophila* Myosin XV tail contains three addition motifs, a glycine-proline-glutamine–rich domain, a proline-rich domain, and a small transmembrane domain. The proline-rich sequences have been demonstrated to bind to SH3, a small 50-aa motif. SH3 domains have been identified in a wide variety of intracellular and membrane-associated proteins and are implicated in signal transduction, linking signals transmitted from the cell surface by protein tyrosine kinases to effector proteins located downstream on the hierarchical pathways.

Myosin 29D is a highly divergent member of the myosin superfamily. Presently, it forms a class of its own. This myosin contains an unusual N-terminal extension, which shows no homology to other proteins. It also has a small transmembrane domain in its tail rich in proline residues.

Drosophila melanogaster expresses many myosins genes. Apart from the essential myosins (classes I, II, and V), it also has myosins from classes III, VI, VII, XV, and XVIII, as well as a novel type of myosin. This new data should help to design experiments to investigate the roles of these newly identified myosins in the cell histology and development of *Drosophila*.

Acknowledgments

We are grateful to Neville Cobbe for help with the phylogenetic analysis programs, to Gillian Millburn from flybase for comments on the manuscript, and to Sheila Milne for help with the preparation of the manuscript. We are grateful to the Darwin Trust, MRC, BBSRC, and B'nei B'rith Scholarship Committee for their support.

LITERATURE CITED

ADAMS, M. D., S. E. CLINKER, R. A. GIBBS, G. M. RUBIN, and C. J. VENTER. 2000. The genome sequence of Drosophila melanogaster. Science **287**:2185–2195.

BAKER, J. P., and M. A. TITUS. 1997. A family of unconventional myosins from the nematode *Caenorhabditis elegans*. J. Mol. Biol. **272**:523–535.

———. 1998. Myosins: matching functions with motors. Curr. Opin. Cell Biol. **10**:80–86.

BERG, J. S., B. H. DERFLER, C. M. PENNISI, D. P. COREY, and R. E. CHENEY. 2000. Myosin-X, a novel myosin with pleckstrin homology domains, associates with regions of dynamic actin. J. Cell Sci. **113**:3439–3451.

BERG, J. S., B. C. POWELL, and R. E. CHENEY. 2001. A millennial myosin census. Mol. Biol. Cell **12**:780–794.

BERGER, B., D. B. WILSON, E. WOLF, T. TONCHEV, M. MILLA, and P. S. KIM. 1995. Predicting coiled coils by use of pairwise residue correlations. Proc. Natl. Acad. Sci. USA **92**: 8259–8263.

BERNSTEIN, S. I., and R. A. MILLIGAN. 1997. Fine tuning a molecular motor: the location of alternative domains in the *Drosophila* myosin head. J. Mol. Biol. **271**:1–6.

BIRU, W. G. 1999. Thesis, Attila Jozsef University, Szeged, Hungary. *Drosophila melanogaster* mRNA for myosin heavy chain, partial. GenBank/EMBL/DDBJ: AJ132656.

BONAFE, N., and J. R. SELLERS. 1998. Molecular characterization of myosin V from *Drosophila melanogaster*. J. Muscle Res. Cell Motil. **19**:129–141.

BROWN, S. S. 1997. Myosins in yeast. Curr. Opin. Cell Biol. **9**:44–48.

CHENEY, R. E., M. A. RILEY, and M. S. MOOSEKER. 1993. Phylogenetic analysis of the myosin superfamily. Cell Motil. Cytoskelet. **24**:215–223.

COPE, M., T. V. JAMIE, J. WHISSTOCK, I. RAYMENT, and J. KENDRICK-JONES. 1996. Conservation within the myosin motor domain: implications for structure and function. Structure **4**:969–987.

DENG, W.-M., K. LEAPER, and M. BOWNES. 1999. A targeted gene silencing technique shows that *Drosophila* myosin VI is required for egg chamber and imaginal disc morphogenesis. J. Cell Sci. **112**:3677–3690.

FURUSAWA, T., S. IKAWA, N. YANAI, and M. OBINATA. 2000. Isolation of a novel PDZ-containing myosin from hematopoietic supportive bone marrow stromal cell lines. Biochem. Biophys. Res. Commun. **270**:67–75.

GILBERT, S. P., and A. T. MACKEY. 2000. Kinetics: a tool to study molecular motors. Methods **22**:337–354.

HAMMER, J. A., and G. JUNG. 1996. The sequence of the dictyostelium myo J heavy chain gene predicts a novel, dimeric, unconventional myosin with a heavy chain molecular mass of 258 kDa. J. Biol. Chem. **271**:7120–7127.

HASSON, T., and M. S. MOOSEKER. 1995. Molecular motors, membrane movements and physiology: emerging roles for myosins. Curr. Opin. Cell Biol. **7**:587–594.

HASSON, T., J. F. SKOWRON, D. J. GILBERT et al. (15 co-authors). 1996. Mapping of unconventional myosins in mouse and human. Genomics **36**:431–439.

HASTINGS, G. A., and C. P. EMERSON JR. 1991. Myosin functional domains encoded by alternative exons are expressed in specific thoracic muscles of *Drosophila*. J. Cell Biol. **114**:263–276.

HICKS, J. L., W.-M. DENG, A. D. ROGAT, K. G. MILLER, and M. BOWNES. 1999. Class VI unconventional myosin is required for spermatogenesis in *Drosophila*. Mol. Biol. Cell **10**:4341–4353.

HODGE, T., and M. J. T. V. COPE. 2000. A myosin family tree. J. Cell Sci. **113**:3353–3354.

KAWASAKI, H., S. NAKAYAMA, and R. H. KRETSINGER. 1998. Classification and evolution of EF-hand proteins. Biometals **11**:277–295.

KELLERMAN, K. A., and K. G. MILLER. 1992. An unconventional myosin heavy chain gene from *Drosophila melanogaster*. J. Cell Biol. **119**:823–834.

KIEHART, D. P., and R. FEGHALI. 1986. Cytoplasmic myosin from *Drosophila melanogaster*. J. Cell Biol. **103**:1517–1525.

KIEHART, D. P., R. A. MONTAGUE, J. ROOTE, and M. ASHBURNER. 1998. Evidence that crinkled, mutations in which cause numerous defects in *Drosophila* morphogenesis, encodes a myosin VII. Mol. Biol. Cell Suppl. **9**:388a.

KORN, E. D. 2000. Coevolution of head, neck, and tail domains of myosin heavy chains. Proc. Natl. Acad. Sci. USA **97**: 12559–12564.

LANGFORD, G. M. 1995. Actin- and microtubule-dependent organelle motors: interrelationships between the two motility systems. Curr. Opin. Cell Biol. **7**:82–88.

LEE, W. L., E. M. OSTAP, H. G. ZOT, and T. D. POLLARD. 1999. Organization and ligand binding properties of the tail of Acanthamoeba myosin-IA. Identification of an actin-binding site in the basic (tail homology-1) domain. J. Biol. Chem. **274**(49):35159–35171.

LI, H. S., J. A. PORTER, and C. MONTELL. 1998. Requirement for the NINAC kinase/myosin for stable termination of the visual cascade. J. Neurosci. **18**:9601–9606.

LIU, X., H. BRZESKA, and E. D. KORN. 2000. Functional analysis of tail domains of Acanthamoeba myosin IC by characterization of truncation and deletion mutants. J. Biol. Chem. **275**(32):24886–24892.

MACIVER, B., A. MCCORMACK, R. SLEE, and M. BOWNES. 1998. Identification of an essential gene encoding a class-V unconventional myosin in *Drosophila melanogaster*. Eur. J. Biochem. **2573**:529–537.

MANSFIELD, S. G., D. Y. AL-SHIRAWI, A. S. KETCHUM, E. C. NEWBERN, and D. P. KIEHART. 1996. Molecular organization and alternative splicing in zipper, the gene that encodes the *Drosophila* nonmuscle myosin II heavy chain. J. Mol. Biol. **255**:98–109.

MERCER, J. A., P. K. SEPERACK, M. C. STROBEL, N. G. COPELAND, and N. A. JENKINS. 1991. Novel myosin heavy chain encoded by murine dilute coat colour locus. Nature **349**: 709–713.

MERMALL, V., and K. G. MILLER. 1995. The 95F unconventional myosin is required for proper organization of the *Drosophila* syncytial blastoderm. J. Cell Biol. **129**:1575–1588.

MERMALL, V., P. L. POST, and M. S. MOOSEKER. 1998. Unconventional myosins in cell movement, membrane traffic, and signal transduction. Science **279**:527–533.

MONTELL, C., and G. M. RUBIN. 1988. The *Drosophila ninaC* locus encodes two photoreceptor cell specific proteins with domains homologous to protein kinases and the myosin heavy chain head. Cell **52**:757–772.

MOOSEKER, M. S., and R. E. CHENEY. 1995. Unconventional myosins. Annu. Rev. Cell Dev. Biol. **11**:633–675.

MORGAN, N. S., M. B. HEINTZELMAN, and M. S. MOOSEKER. 1995. Characterization of myosin-IA and myosin-IB, two unconventional myosins associated with the *Drosophila* brush border cytoskeleton. Dev. Biol. **172**:51–71.

MORGAN, N. S., D. M. SKOVRONSKY, S. ARTAVANIS-TSAKONAS, and M. S. MOOSEKER. 1994. The molecular cloning and characterization of *Drosophila melanogaster* myosin-IA and myosin-IB. J. Mol. Biol. **239**:347–356.

OLIVER, T. N., J. S. BERG, and R. E. CHENEY. 1999. Tails of unconventional myosins. Cell Mol. Life Sci. **56**:243–257.

PAGE, R. D. M. 1996. TREEVIEW: an application to display phylogenetic trees on personal computers. Comput. Appl. Biosci. **12**:357–358.

PORTER, J. A., J. L. HICKS, D. S. WILLIAMS, and C. MONTELL. 1992. Differential localizations of and requirements for the two *DrosophilaninaC* kinase/myosins in photoreceptor cells. J. Cell Biol. **116**:683–693.

RHOADS, A. R., and F. FRIEDBERG. 1997. Sequence motifs for calmodulin recognition. FASEB J. **11**:331–340.

SCHULTZ, J., F. MILPETZ, P. BORK, and C. P. PONTING. 1998. SMART, a simple modular architecture research tool: identification of signaling domains. Proc. Natl. Acad. Sci. USA **95**:5857–5864.

SCHWARZ, E. C., H. GEISSLER, and T. A. SOLDATI. 1999. Potentially exhaustive screening strategy reveals two novel divergent myosins in Dictyostelium. Cell Biochem. Biophys. **30**:413–435.

SELLERS, J. R. 2000. Myosins: a diverse superfamily. B. B. A.—Mol. Cell Res. **1496**:3–22.

SOLDATI, T., H. GEISSLER, and E. C. SCHWARZ. 1999. How many is enough? Exploring the myosin repertoire in the model eukaryote *Dictyostelium discoideum*. Cell Biochem. Biophys. **30**:389–411.

THOMPSON, J. D., D. G. HIGGINS, and T. J. GIBSON. 1994. CLUSTAL W: improving the sensitivity of progressive multiple sequence alignment through sequence weighting, position-specific gap penalties and weight matrix choice. Nucleic Acids Res. **22**:4673–4680.

TITUS, M. A. 1999. A class VII unconventional myosin is required for phagocytosis. Curr. Biol. **9**:1297–1303.

VOLKMANN, N., and D. HANEIN. 2000. Actomyosin: law and order in motility. Curr. Opin. Cell Biol. **12**:26–34.

WOLFE, K. H., and D. C. SHIELDS. 1997. Molecular evidence for an ancient duplication of the entire yeast genome. Nature **387**:708–713.

WU, X., G. JUNG, and J. A. HAMMER. 2000. Functions of unconventional myosins. Curr. Opin. Cell Biol. **12**:42–51.

YAMASHITA, R. A., J. R. SELLERS, and J. B. ANDERSON. 2000. Identification and analysis of the myosin superfamily in *Drosophila*: a database approach. J. Muscle Res. Cell Motil. **21**:491–505.

ZHANG, S., and S. I. BERNSTEIN. 2001. Spatially and temporally regulated expression of myosin heavy chain alternative exons during *Drosophila* embryogenesis. Mech. Dev. **101**:35–45.

ANTONY DEAN, reviewing editor

Accepted February 7, 2002

ELSEVIER

Mechanisms of Development 121 (2004) 1335–1351

www.elsevier.com/locate/modo

Myosin VI plays a role in cell–cell adhesion during epithelial morphogenesis

Hadas Millo, Kevin Leaper, Vasiliki Lazou, Mary Bownes*

Institute of Cell and Molecular Biology, University of Edinburgh, Edinburgh EH9 3JR, UK

Received 7 April 2004; received in revised form 8 June 2004; accepted 9 June 2004

Available online 10 July 2004

Abstract

Myosin VI is an unconventional Myosin that has been implicated in vesicle transport and membrane trafficking. We isolated lethal mutants of Myosin VI, which lack protein once maternal supplies have been utilised during embryogenesis. Dorsal closure, where there is a ring of Myosin VI at the edge of the migrating epithelial sheet, is often abnormal. The sheet of migrating cells is irregular, rather than a smooth epithelium and cells begin to detach. Some embryos hatch into larvae, containing detached cells loose in the haemolymph. Myosin VI is crucial for correct cell morphology and maintenance of adhesive cellular contacts within epithelial cell layers.

Keywords: Cell migrations; Epithelial morphogenesis; Unconventional Myosins

1. Introduction

Unconventional myosins are motor proteins that move along actin filaments. There are many classes of myosins in this superfamily and they have been identified in a wide variety of organisms. The head domains are well conserved and contain the motor, ATP and actin-binding domains that allow the protein to move. The tails vary dramatically between classes of myosins and often carry cargoes. Myosins play a variety of roles in organelle, RNA and protein transport, cell movements, signal transduction, maintaining the morphology of cells, and membrane trafficking (Wu et al., 2000; Oliver et al., 1999; Baker and Titus, 1998; Mermall et al., 1998).

In mammals Myosin VI is encoded by the mouse *Snell's Waltzer* deafness gene (Hasson and Mooseker, 1994; Avraham et al., 1995, 1997). The protein is thought to be necessary for anchoring the stereocilia membrane into the cuticular plate of the inner ear (Avraham et al., 1995; Hasson et al., 1997). This region is active in transporting vesicles to the apical surface of cells. It would seem that in the mouse, without Myosin VI the structural integrity of hair cells is lost, leading to a loss of hearing. The connection between hearing loss and Myosin VI was found also in humans, where patients suffering from a non-syndromic dominant form of deafness (NSAD), were found to have a missense mutation in the human Myosin VI gene, MYO6 (Melchionda et al., 2001; Ahmed et al., 2003; Mohiddin et al., 2004). In rat brain, Myosin VI interacts with SAP97, a member of the MAGUK (membrane-associated guanylate kinase homologue) family, which plays a role in synaptic localisation and membrane trafficking of GluR1, a subunit of a-amino-3-hydroxy-5-methylsoxazole-4-propionic acid (AMPA)-type glutamate receptors. It seems that Myosin VI translocates AMPA receptors via connection to SAP97 to and from postsynaptic plasma membranes (Wu et al., 2002).

Myosin VI has been shown to be associated with the Golgi complex and the leading edge of the cell. In cultured rat and human cells Myosin VI is specifically phosphorylated and then translocated to the ruffles that form as the cells move (Buss et al., 1998). Furthermore, Myosin VI associates with the adaptin complex on clathrin-coated vesicles (Buss et al., 2001), and with Disabled 2 (DAB2), which connects Myosin VI to clathrin coated pits (Morris et al., 2002). These results suggest that Myosin VI has a key role in membrane trafficking, both in secretion and endocytosis.

Myosin VI (Myosin 95F) is encoded in *Drosophila* by the *jaguar* (*jar*) gene (Hicks et al., 1999). It has been shown to be expressed at a variety of developmental stages and is

* Corresponding author. Tel.: + 44-131-650-5369; fax: + 44-131-650-5371.

E-mail address: mary.bownes@ed.ac.uk (M. Bownes).

0925-4773/$ - see front matter © 2004 Elsevier Ireland Ltd. All rights reserved.
doi:10.1016/j.mod.2004.06.007

essential for several developmental events (Kellerman and Miller, 1992; Kellerman et al., 1992; Lantz and Miller, 1998; Deng et al., 1999). A partial loss of function mutant causing male sterility demonstrated a key role for Myosin VI in sperm individualisation (Hicks et al., 1999). In the testes Myosin VI interacts with Cortactin and the Arp2/3 complex, which is necessary for regulation of actin polymerisation, and also with Dynamin, a protein promoting the transition of clathrin-coated pits into clathrin-coated vesicles (Rogat and Miller, 2002). It is proposed that Myosin VI is important for the assembly of actin filaments in the region where membranes are assembled within the individualization complex, during sperm morphogenesis. Myosin VI is also essential in *C. elegans* spermatogenesis, where it is involved in the unequal distribution of organelles and cytoskeletal components during the formation of the Residual body and the budding spermatids (Kelleher et al., 2000).

During oogenesis Myosin VI is required for all the cell migrations undertaken by the follicle cells. By interfering with Myosin VI expression using an antisense RNA in vivo, the formation of the follicle cell epithelium by the columnar and centripetal cells was disrupted (Deng et al., 1999). Recently it has been shown that the migration of the border cells is disrupted when the expression of Myosin VI is blocked, and that the migration is coordinated with E-cadherin and Armadillo (Geisbrecht et al., 2002). Deng et al. (1999) also showed that Myosin VI was needed for epithelial morphogenesis at a variety of developmental stages. Using inhibition of Myosin VI by antibody injection it was shown that the invaginations of membranes needed for blastoderm cell formation in the embryo required Myosin VI (Mermall et al., 1994; Mermall and Miller, 1995). Using a similar method Myosin VI has been shown to be important for transport of material from the nurse cells to the oocyte during oogenesis (Bohrmann, 1997).

Finally, since the work in this paper was completed Myosin VI was found to interact with Miranda. Myosin VI is necessary for the basal localisation of Miranda, and for spindle orientation in the metaphase neuroblast. In homozygous null mutant embryos, jar^{322}, Miranda is mislocalized to cortical patches and to the cytoplasm rather than the basal crescent of the metaphase neuroblast and the spindle was misorientated (Petritsch et al., 2003).

We demonstrate, using newly isolated mutants, that Myosin VI is crucial for viability and maintenance of cells in epithelial cell layers.

2. Results

We have generated lethal mutants of the *jar* gene encoding Myosin VI. They die as late embryos and larvae. The mutants are shown to lack Myosin VI by antibody staining of embryos and by Western blotting. Mutant embryos survive well into embryogenesis using the supply of maternally stored mRNA but in later stages specific transcripts are depleted. When the epithelial sheets migrate during normal dorsal closure they express a tight Myosin VI band at the moving front. The mutants lack this Myosin VI band and fold inside the embryos, some cells are loose and begin to detach from the epithelium and embryos frequently fail to complete dorsal closure. Similar results were obtained when a Myosin VI dominant negative was expressed.

2.1. Isolation of new *jar* mutants

Previous mutant screens in our laboratory had generated a male sterile mutation in the *jar* gene which encodes Myosin VI. The jar^{mmw14} mutant lacks transcripts in the testis, but generates transcripts in other tissues and at other developmental stages (Hicks et al., 1999), due to a deletion of non-coding exon 1 (Fig. 1C). To generate further mutants we used a similar strategy and remobilised a *gal4* insertion in the *jar* gene (C865). Fig. 1A shows the intron-exon organisation of *jar*, which we determined by sequence analysis and by using the published *Drosophila* genome sequence (Adams et al., 2000).

Mutations were created by remobilising the P element insertion line *C865* and 480 new lines were established. Five red-eyed lines were homozygous lethal. Two of the red-eyed lines jar^{R23} and jar^{R70} failed to complement the deficiency line for the *jar* region, *Df87-5*, resulting in embryonic lethality. Two other red-eyed lines, jar^{R39} and jar^{R235} failed to complement the mutant jar^{mmw14} resulting in male sterility. The complementation tests along with the protein expression analysis (described in the following section) suggests that all the four lines are homozygous lethal due to mutations in the *jar* gene.

2.2. Molecular analysis of jar^{R39} and jar^{R235} mutants

The P element in the *C865* line which was used for the P hop mutagenesis is located in the 5′ UTR of *jar* mRNA (Fig. 1B). When we undertook PCR with primers flanking the location of the original P element location, we found that the P element was excised from the 5′ UTR region in all the mutants, jar^{R23}, jar^{R39}, jar^{R70} and jar^{R235} (Fig. 2). jar^{R39} and jar^{R235} were the mutants that showed the most severe phenotypes, therefore we decided to determine the molecular basis of the mutations in these lines. The details of how this was undertaken are presented in the Materials and Methods. As the alternations were small, they were established by sequencing the mutant DNA in the region deleted in jar^{mmw14} mutants. This revealed that in the jar^{R39}/jar^{mmw14} heterozygotes the sequence: GTA TAC0TG (347–340 bp upstream of the first exon) was deleted, while the sequence: TTTATATATACTGA-TATG (341-322 bp upstream of the first exon) was duplicated (Fig. 1D). In jar^{R235}/jar^{mmw14} the sequence: GTATAC (347–342 bp upstream to the first exon) was

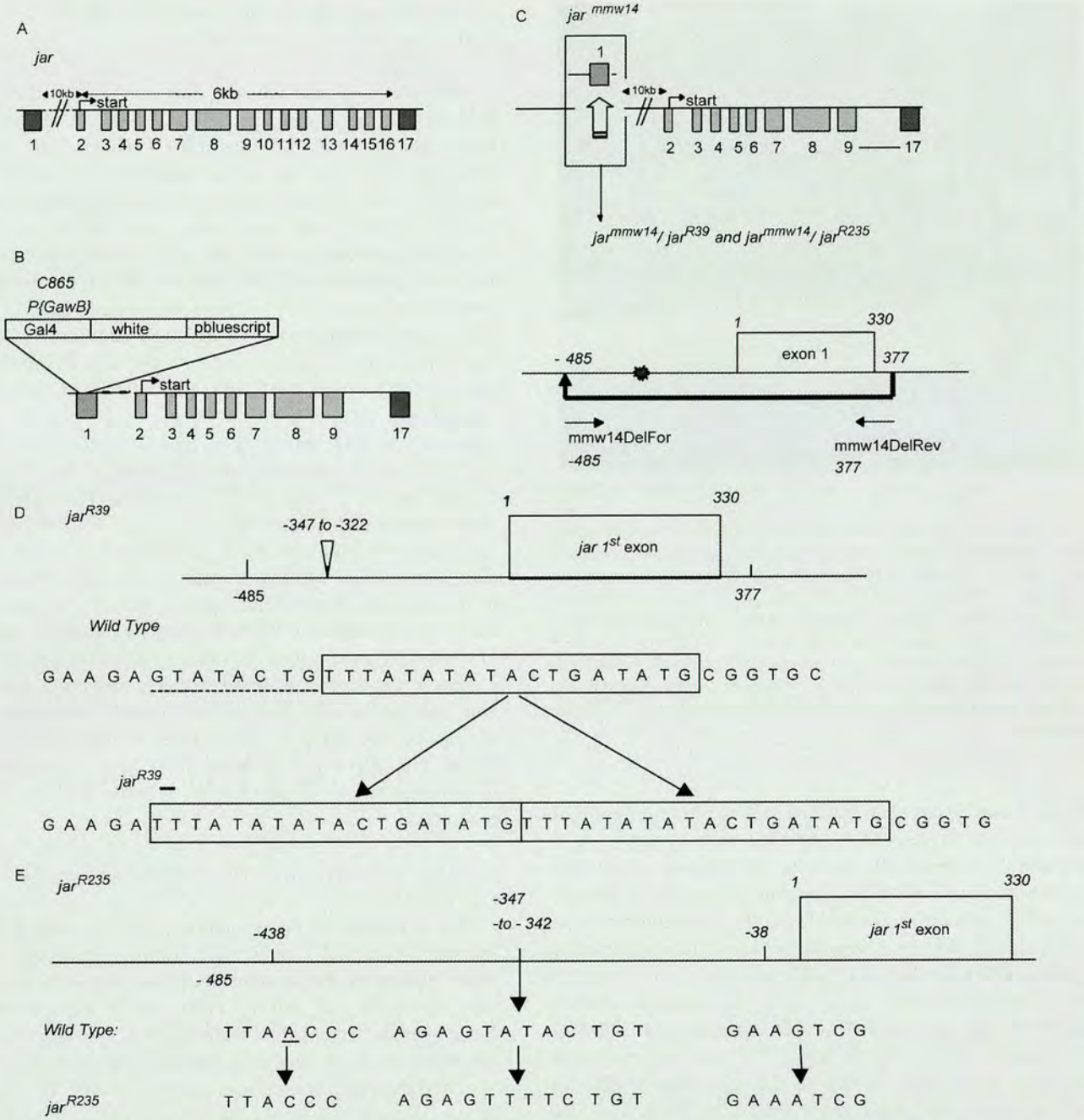

Fig. 1. Organisation of the wild type and mutated *jar* genes. (A): The canonical transcript which encodes the EM3 isoform of *jar*. (B): *C865* contains a single *P[GawB]* element inserted at bp 306 in exon 1. It is located in the 5′ UTR and causes no observable phenotype. The number of *P[GawB]* elements was determined by Southern blots, and the position of the insertion by plasmid rescue. (C): jar^{mmw14} was created by imprecise excision of *P[GawB]*, removing the whole first exon along with 485 bp flanking the 5′ end and 47 bp flanking the 3′ end (total deletion of 862 bp). The primers used to locate the deletion are: C865For, C865 Rev, EXC2For and EXC2Rev (see Materials and Methods). After finding the precise location of the deletion in jar^{mmw14}, a pair of primers were designed to replicate the whole deletion region. In that way, only the mutant genomic DNA was amplified by PCR, and the specific mutation (marked by a red asterisk) was located in this region by sequencing. (D): The mutation found in jar^{R39}/jar^{mmw14}: the sequence marked by a dashed line was deleted and the sequence marked in the box was duplicated. (E): The mutation found in jar^{R235}/jar^{mmw14}: the sequence GTATAC was changed to GTTTTC, the nucleotide A, 438 bp upstream to the first exon was deleted, and the nucleotide G (38 bp upstream to the first exon) was replaced with an A.

changed to: GTTTTC, possibly by deletion of the sequence: ATA and duplication of the sequence: TTT (341–339 bp upstream of the first exon, see Fig. 1E). This mutation is located in the same region as the mutation in jar^{R39} and explains why the two new mutant lines fail to complement each other. jar^{R235} also has a missing nucleotide, A, 438 bp upstream of the first exon (Fig. 1E), and the nucleotide G (38 bp upstream of the first exon) was replaced by A (Fig. 1E).

In spite of the excision of the P element from the 5′ UTR in the two mutants, the flies are red-eyed, therefore a P

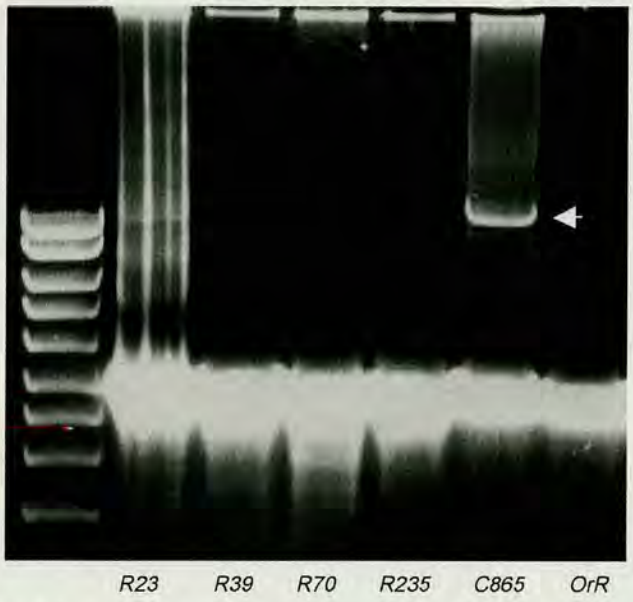

Fig. 2. Search for the P element in the 5′ UTR region in the mutant genomic DNA. The genomic region where the P element was originally located in line *C865* (5′ UTR) was amplified by PCR, in the heterozoygous mutant lines: jar^{R23}/*TM3*, jar^{R39}/*TM3*, jar^{R70}/*TM3*, jar^{R235}/*TM3*, in *C865*and in *OrR*, using primers flanking the insert region: C865For and C865Rev. In *C865* two bands appeared: the upper band (arrow) corresponds to the P element, 14 kb, and the lower band corresponds to the same region in the chromosome that does not contain the P element (as in *OrR*). In all the mutants, the P element band is not detected indicating that the P element was excised from the 5′ UTR.

element must have been inserted into a different region of the genome. Inverse PCR revealed that in jar^{R39} a P element has inserted into the third chromosome, within the hypothetical gene CG5991, upstream of *jar*. The P element in jar^{R235} was also re-inserted into the third chromosome, upstream of *jar*, in a region between the hypothetical genes: CG6164 and CG 6173. The two new *jar* mutants fail to complement each other and the deletion mutant jar^{mmw14} but we needed to be sure that the lethality associated with jar^{R39}/jar^{R235} trans-heterozygous embryos and larvae are due to the mutations in Myosin VI and not in the other genes where the P element has inserted. We investigated the expression of Myosin VI and analysed the phenotype of the trans-heterozygous mutant jar^{R39}/jar^{R235}. Because the insertion sites of the P element in jar^{R39} and jar^{R235} are different, the cross of the two mutants will complement any mutations caused by the re-insertion of chromosome 3, allowing us to test the phenotype of the mutations within *jaguar* only. The trans-heterozygous mutants had a similar phenotype to the homozygous mutants: i.e. Myosin VI was absent late in embryogenesis and many embryos failed to complete dorsal closure (Fig. 5E–I). Those which completed dorsal closure died during the first larval instar. Thus we can attribute the phenotypes to a deficiency in Myosin VI late in embryogenesis.

2.3. The transcription of the 5′ end of the mRNA is disrupted in homozygous mutants

Previously it was shown that jar^{mmw14} mRNA is disrupted in the 5′ region: up to 517 nucleotides are not transcribed at the 5′ end of the mRNA (Hicks et al., 1999). Since jar^{mmw14} does not complement jar^{R39} or jar^{R235} we wanted to test if transcription is also disrupted in these mutants. RTPCR was undertaken, using RNA templates from homozygous mutant and *OrR* larvae (1st instar), for two regions at the 5′ end of the *jar* mRNA: the first 1027 nucleotides and the region between nucleotides 517 and 1027 were investigated (Fig. 3A). An additional RTPCR was made for a region located further downstream, 2850–4100 bp from the 5′ end. The RTPCR of the two 5′ regions was very weak in the homozygous mutant larvae, compared to *OrR* larvae (Fig. 3B). It seems that as in jar^{mmw14}, there is reduced transcription of *jar* mRNA at the 5′ end in jar^{R39} and jar^{R235} mutants. When RTPCR undertaken at the 3′ end (Fig. 3C), a high level of product was observed, although not to the same level as in *OrR*. This is to be expected since transcripts initiated at the 5′ end of the gene are absent. This suggests that only some of the transcripts are affected. When RTPCR was made for mRNA of ribosomal protein (Fig. 3D) and myosin 29D (Fig. 3E) as a control, the expression level in the homozygous mutants was similar to the expression in *OrR*, therefore the disruption in mRNA expression is unique to *jar*. Given that there are at least some transcripts present in larvae in the jar^{R39} and jar^{R235} it seems unlikely either are nulls.

2.4. Mutants lack or have reduced myosin VI protein

We next tested if these mutations led to a reduction or loss of Myosin VI expression during embryogenesis, since studies of the mutants indicated that they died as late embryos and during early larval development. Since there is a supply of maternal mRNA we collected late embryos, and analysed them by Western blotting. We used the yolk proteins as a loading control. The results in Fig. 3F show that wild type *OrR* and jar^{mmw14} embryos have high levels of several isoforms of Myosin VI. jar^{R23} has slightly reduced Myosin VI, jar^{R70} has much reduced Myosin VI and in jar^{R39} and jar^{R235} no Myosin VI could be detected by Western blotting. This demonstrated that two of the mutants we had isolated affected the expression of Myosin VI in late embryogenesis dramatically. Taken together with the complementation analysis and our molecular studies these two mutants are identified as *jar* mutants and have thus been called jar^{R39} and jar^{R235}.

Using Myosin VI antibody the temporal and spatial distribution of Myosin VI protein was analysed in wild type and homozygous mutant embryos. Myosin VI could be seen in the forming blastoderm cells. This was observed in both wild type and mutant embryos and reflects the stored

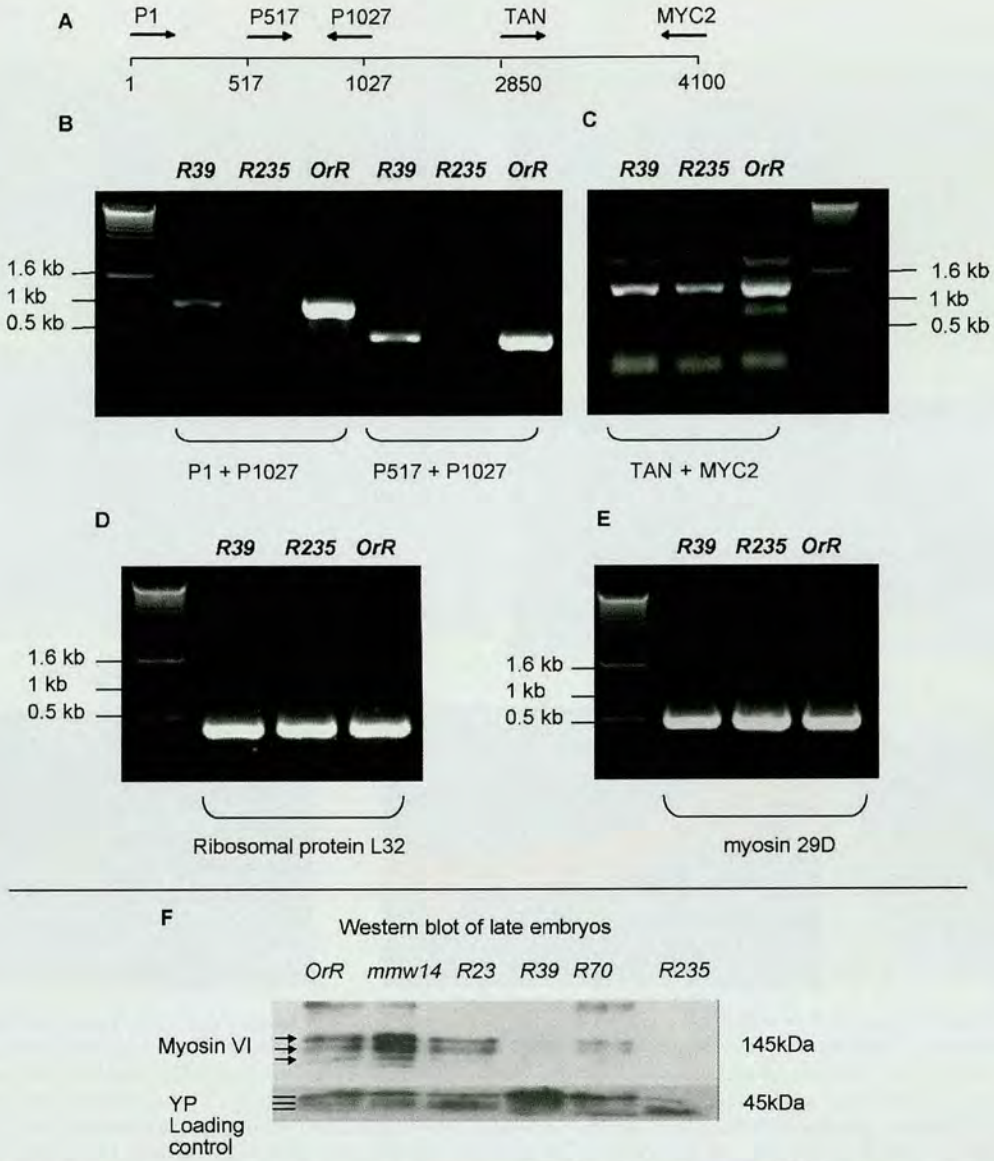

Fig. 3. Analysis of Myosin VI expression in wild type and mutant embryos. (A–D): RTPCR analysis of jar^{R39}, jar^{R235} homozygous mutant and *OrR* larvae. (A): A diagram of the primers used for the RTPCR analysis of *jar* mRNA. (B): RTPCR for the 5′ region of *jar* mRNA, using the primers p1 + p1027, and p517 + p1027. In jar^{R39} and jar^{R235} the PCR gave a signal which is much weaker compared to *OrR*, suggesting that these transcripts are not synthesized in the larvae and the weak signal obtained was probably from remaining maternal transcripts. (C): RTPCR of the *jar* tail encoding domain (located downstream, see 3A). The 3′ transcripts in the mutants exist, although not to the same extent as in *OrR*. The transcription of a fragment in ribosomal protein, L32 (D) and of Myosin 29D mRNA (E) was used as a control. (F): Western blotting wild type and mutant embryos. Lane 1: *OrR*. Lane 2: jar^{mmw14} male sterile allele exhibits higher levels of Myosin VI expression during embryogenesis. Lane 3 and 5: homozygous lethal lines, jar^{R23} and jar^{R70}, that fail to complement *Df87-5*, but do complement jar^{mmw14}.Myosin VI protein expression is detected in both jar^{R23} and jar^{R70}. Lane 4 and 6: homozygous lethal lines, jar^{R39} and jar^{R235}, that do not complement jar^{mmw14}. No Myosin VI protein expression is detected in either jar^{R39} or jar^{R235}. In each case there is yolk protein present to show that similar numbers of embryos were loaded on the tracks. The three bands near Myosin VI correspond to the three isoforms bearing molecular weights of 120, 140 and 145 kDa, and the three lines near the YP correspond to the yolk polypeptides YP1, YP2, and YP3, having a molecular weight of 47, 46 and 45 kDa, respectively.

component of maternal Myosin VI (data not shown). Once the embryo begins to develop Myosin VI is seen in many cells. In *OrR* flies, Myosin VI expression is strong during germ band extension (Fig. 4A) and during dorsal closure there is a very tight ring of expression in the cells migrating to close the gut (Fig. 4B), and a strong expression of myosin VI is observed along the apical side of the cells at the leading edge (Fig. 4D). There are two patches of expression of Myosin VI in the posterior of the larva and late embryo possibly in the posterior spiracle (Fig. 4C). In the mutants, by the time dorsal closure commences there is no detectable Myosin VI (Fig. 4E) and this loss of Myosin VI continues into the fully formed larvae (Fig. 4F). Myosin VI was also below detectable levels in late embryos of heteroallelic mutants jar^{R39}/jar^{R235} (Fig. 4G).

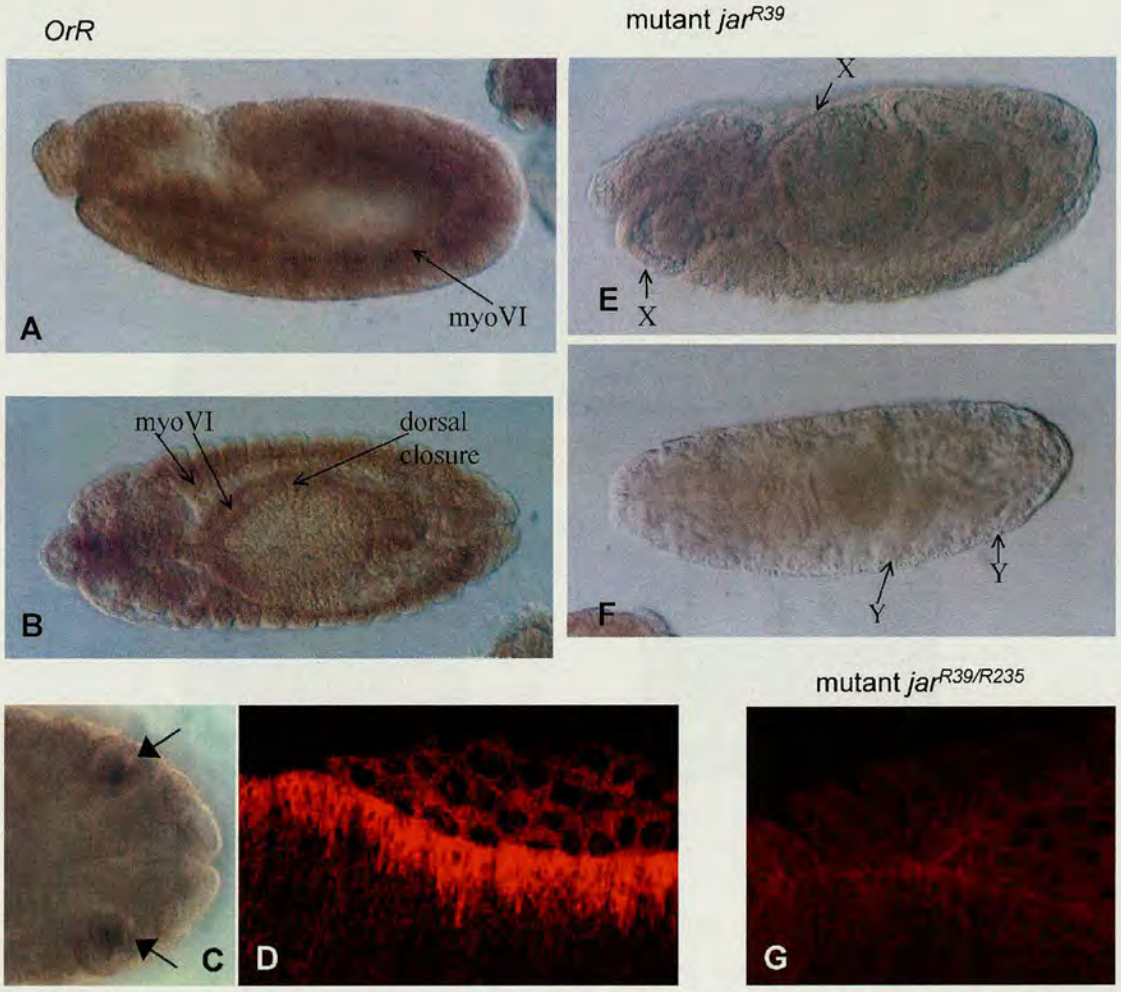

Fig. 4. Analysis of Myosin VI expression in wild type and mutant embryos by antibody staining of tissues. (A–F): Comparison of Myosin VI expression between *OrR* and *jar* mutant at different embryonic stages. (A–D) are *OrR* and (E,F) are *jaguar* mutant jar^{R39} and (G) is the trans-heterozygous mutant jar^{R39}/jar^{R235}. (A): Lateral view of an extended germ band stage embryo. Myosin VI expression is present in the labial, labral and maxillary segments and in all posterior segments on the inner edge. (B): Dorsal view of a contracted germ band stage embryo. Myosin VI is expressed in abdominal segments and in leading edge of epithelial cells during dorsal closure. (C): Notice the two small groups of cells in the posterior spiracle expressing very high levels of Myosin VI. (D): At the leading edge of the lateral epidermis Myosin VI is strongly expressed at the apical side of the cells. Expression of Myosin VI is also observed in the amnioserosa and the lateral epidermis. (E): Lateral view of a jar^{R39} germ band stage embryo. Myosin VI expression is absent and the morphology of the embryo is abnormal at positions marked X. (F): A jar^{R39} embryo when the gut has formed. Note there is no Myosin VI expression in the segment nor in the small groups of cells at the posterior (see C in wild type). (G): Myosin VI is also absent in the heteroallelic mutant jar^{R39}/jar^{R235}. myo VI = Myosin VI protein. X = abnormalities in the organisation of the embryo. Y = note the absence of Myosin VI in these regions.

2.5. Myosin VI is necessary for dorsal closure and germ band retraction

Most homozygous mutant embryos developed into late embryos which failed to hatch. A few hatched into larvae, but soon died. The anterior/posterior and dorsal/ventral polarity and segment number was normal. A number of embryos failed to complete dorsal closure and thus there was exposed yolk and free floating yolk between the cuticle and the vitelline membrane and many embryos had loose cells inside the vitelline membrane. The cells in the amnioserosa were detached. The leading edge of the epithelial sheets lost their tight and organised shape (Figs. 5E–I), and the tissue was folded inside.

In some of embryos the germ band remained elongated and detached from the amnioserosa, indicating that germ band retraction was incomplete (Fig. 5H–I). Many of the mutant embryos that died and larvae that hatched had completed dorsal closure but had loose cells floating in the haemolymph in the dorsal aorta. These were best visualised in living embryos. Fig. 6A–D shows the same larva photographed at 2 s intervals and the different location of a group of the floating cells can be seen. Each larva often contained several clumps of cells and lots of individual loose cells. No such loose cells were ever observed in wild type embryos.

Similar results were obtained when the function of Myosin VI was disrupted by the expression of a Myosin VI

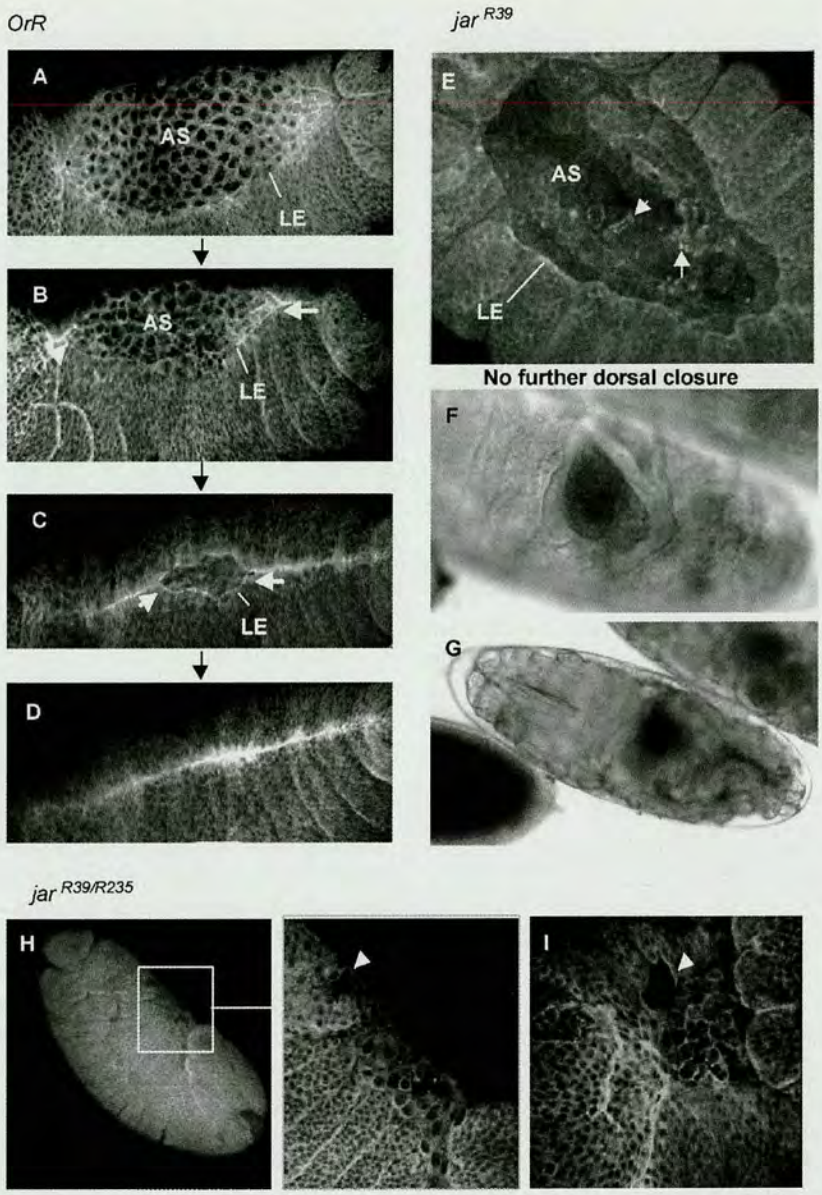

Fig. 5. Phenotypes of mutant embryos and larvae. (A–D): Dorsal closure in *OrR* flies. The leading edges of the lateral epidermis are connected along the anterior and the posterior sides, towards the centre (arrows), to cover the amnioserosa. (E): Failure of dorsal closure in *jar* ^{R39} mutant embryos, the cells in the amnioserosa are detached (arrows), leaving loose yolk. (F) and (G): Two focal planes of a *jar* ^{R39} mutant which has failed in dorsal closure. F shows a view of the dorsal surface. There is still exposed yolk and an abnormal and irregular attempt at dorsal closure and loose cells are escaping. (G): Germ band shortening is complete, the mouthparts are normal and the correct number of segments exists but there is a gap in the epithelium, and segments are incomplete on the dorsal/ventral axis. Figures H and I show trans-heterozygous mutant embryos *jar* ^{R39}/*jar* ^{R35} stained with myosin II antibody. They fail to complete dorsal closure and germ band retraction. In figures E and I the 'purse string' around the amnioserosa is absent and the expression of Myosin II at the leading edge is absent as well, although Myosin II is present in the cells of the lateral epidermis and the amnioserosa. The amnioserosa sheet has lost its organised uniform sheet, having loose cells with a changed shape and holes (arrows). The cells at the leading edge have been folded inside thus it is impossible to observe the actin-myosin cable. The embryos in A-D, H-I are stained with nonmuscle Myosin II. AS = amnioserosa. LE = leading edge.

dominant negative, ΔATP-jar (Fig. 7). When ΔATP-jar was expressed by *engrailed-gal4* (*en-gal4*) at the posterior stripes of each segment, the tissue was ruptured, the cells at the leading edge and in the amnioserosa were detached and in certain areas the two tissues were disconnected (Figs. 7A and 9B). Embryos that reached the final stages of dorsal closure had holes in the dorsal midline, suggesting that Myosin VI is necessary for the adhesion of the cells at the leading edge and in the amnioserosa and for the adhesion of the opposite leading edges along the dorsal midline, during the final 'zipping' of the epidermis (Fig. 7C). The changes in cell shape and the tendency of the cells to fold inside in stripes of cells expressing ΔATP-jar indicates that Myosin VI is involved in maintaining cell shape and rigidity in the lateral epidermis (Fig. 7D,E). Finally, many embryos failed to complete germ band

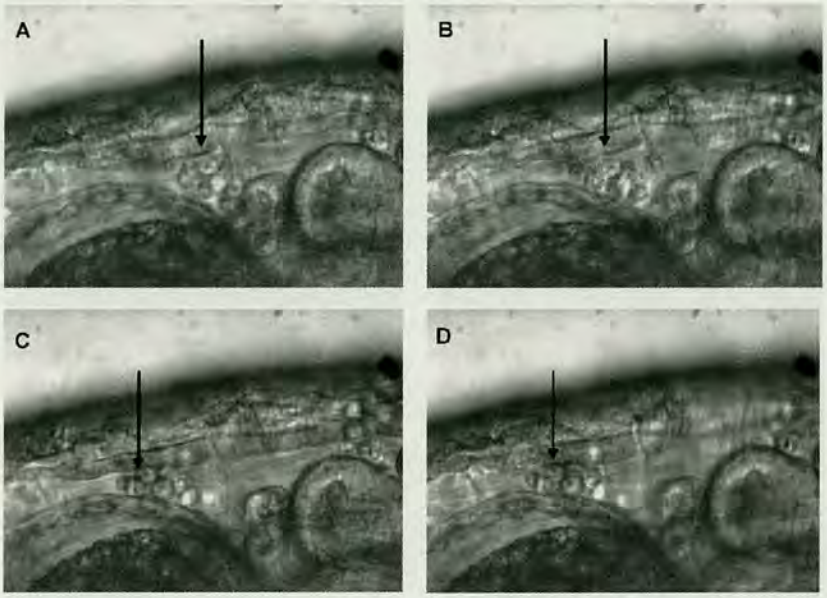

Fig. 6. Phenotypes of mutant larvae. Figures A–D show some of the loose cells in a *jar*^{R39} mutant. Note that they are in a different position in each frame. This is a living embryo photographed at 2-second intervals to show these detached cells moving in the embryo.

retraction, leaving the germ band tissue loose and separated from the amnioserosa (Fig. 7F), and the retraction arrested (Fig. 7G).

2.6. Myosin VI cDNA rescues the lethal phenotype of *jar*^{R39} and *jar*^{R235} mutant embryos

In order to determine whether or not the embryonic lethal phenotype in *jar*^{R39} and *jar*^{R235} mutants was caused by the reduction in Myosin VI expression, we tested the ability of ectopic Myosin VI expression to rescue *jar*^{R39} and *jar*^{R235} embryonic lethality.

In this experiment, a cross was undertaken between heterozygous flies, to create two groups of mutant embryos: the first group express Myosin VI tagged to GFP (PGM) throughout the embryo; therefore the embryos of this group are fluorescent. The second group, which does not express PGM were non-fluorescent. In every group, 25% of the flies are homozygous mutant (the details of the cross and the corresponding progeny genotypes are described in the Materials and Methods, and summarised in Fig. 8D). In the non-fluorescent group, many of the homozygous mutant flies will fail to hatch. However, if the expression of PGM rescues the embryos, the number of fluorescent larvae hatching from the eggs will be higher than the number of non-fluorescent larvae. A reciprocal cross was established to test the effect of maternal PGM. As a control, heterozygous flies were crossed with the balancer line TM3/TM6: this cross is expected to create progeny with a similar survival rate in the fluorescent and the non-fluorescent group.

The results are shown in Fig. 8E. In both the control and the experimental groups the survival of fluorescent embryos was slightly higher, but the *difference* between the survival of fluorescent and non fluorescent embryos in the experimental group was significantly higher, than the control group thus the expression of PGM significantly increased the survival of the mutant embryos. When female fluorescent heterozygous flies were crossed, the embryonic survival was slightly higher than in the reciprocal cross; however, the differences are not significant. The survival rate of all the embryos was lower than the expected presumably due to the manual collection and frequent handling of the embryos, to assess their fluorescence signal. The survival rate of *OrR* embryos with similar handling is 74% (data not shown). Taken together these results show that the expression of PGM rescues the embryonic lethal phenotype of *jar*^{R39} and *jar*^{R235} mutants. Therefore the embryonic lethal phenotype results from the disruption in Myosin VI expression.

2.7. Disruption of Myosin VI function affects DE-cadherin expression

Epidermal cells expressing of ΔATP-jar had altered cell adhesion properties. Cell–cell adhesion in the *Drosophila* embryonic epidermis is mediated by DE-cadherin. Myosin VI was found to interact with DE-cadherin during the migration of border cells during oogenesis (Geisbrecht and Montell, 2002). This raises the possibility that Myosin VI interacts with cadherin during embryogenesis and that the loss of cell–cell adhesion Myosin VI function is disrupted could lead to changes in DE-cadherin expression or localisation.

Embryos expressing ΔATP-jar by *en-gal4* during dorsal closure were stained with DE-cadherin antibody (Fig. 9A,B). In some of the embryos, DE-cadherin levels were significantly reduced in cells expressing ΔATP-jar (Fig. 9A). In other embryos the localisation of DE-cadherin

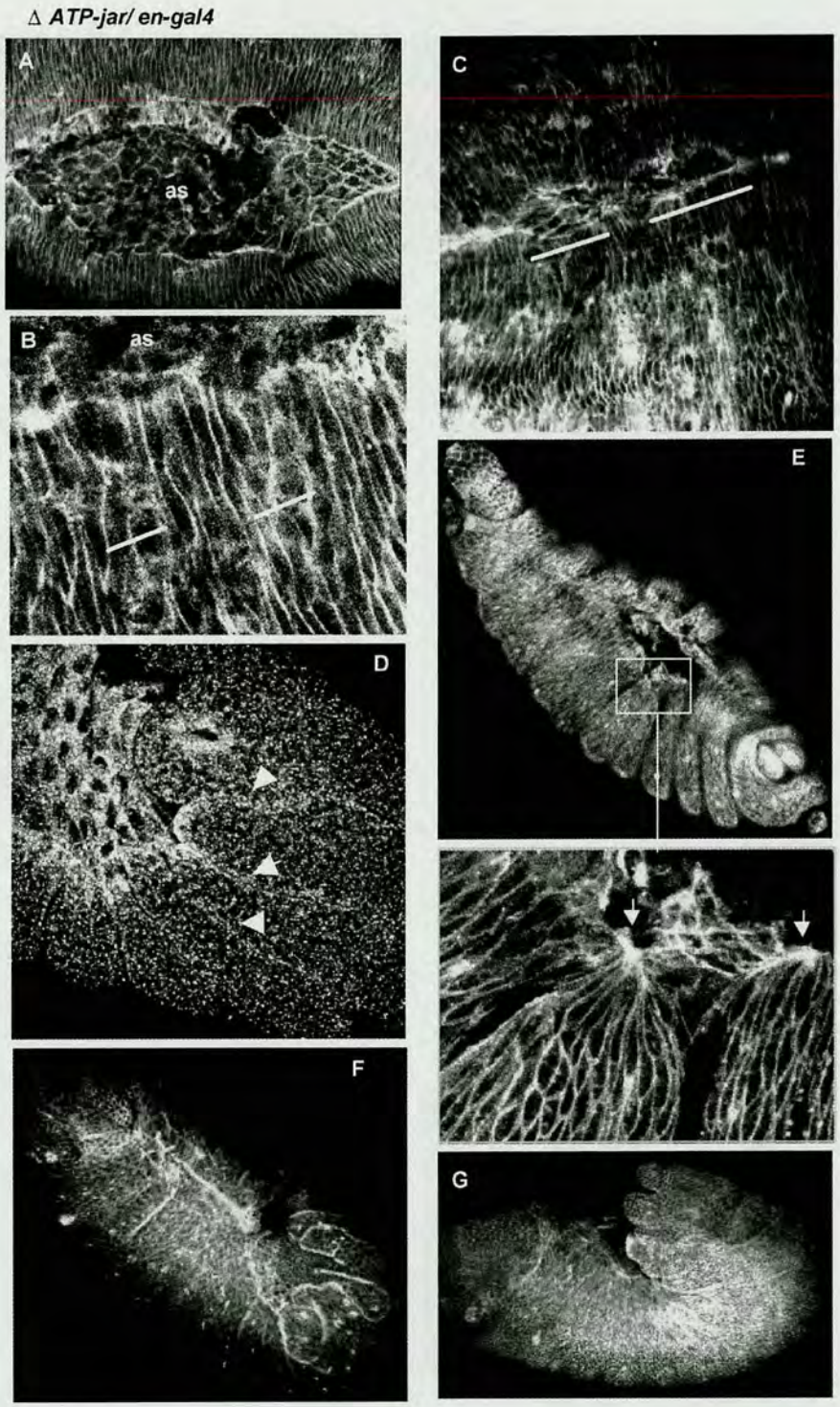

Fig. 7. The effect of dominant-negative Myosin VI expression. ΔATP-jar was controlled by *en-Gal4*, as this expressed at the posterior of every segment. Figs. A-C and E are stained with phalloidin to view the actin filaments and the cell shape. (A): The disruption of Myosin VI function caused detachment of the cells at the leading edge and the amnioserosa. The actin cable at the leading edge is disrupted in all the areas where ΔATP-jar was expressed. (B): In some embryos, cells expressing ΔATP-jar in the lateral epidermis changed their shape and the actin filaments lost their tight organization at the cells cortex. (C): In the final stage of dorsal closure, when Myosin VI is disrupted, dorsal closure is not completed, and holes are left. (D,E): Some embryos show 'folding-in' of the lateral epidermis in the stripes expressing the dominant-negative. (D): staining with Myosin VI antibody: the stripes expressing the dominant negative Myosin VI have stronger stain of Myosin VI (arrows), and tend to fold inside the embryo. (E): In severe cases the actin cable disappears and filament aggregates are formed (see arrows). A milder version of this phenotype appeared in the mutants (see Fig. 11). (F,G): In many cases germ band retraction is not completed, the germ band tissue is loose and folded, and the posterior spiracles are not formed. In (F), the process of dorsal closure was progressed in spite of the incomplete process of germ band retraction (DE-cadherin stain). In (G) germ band retraction ceased in very early stage: the embryo is totally folded, and the germ band tissue is disconnected from the amnioserosa.

A

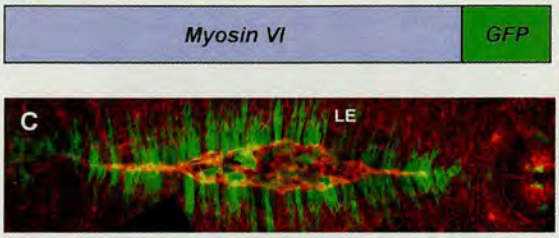

PGM 43-2 X C865: stage 15

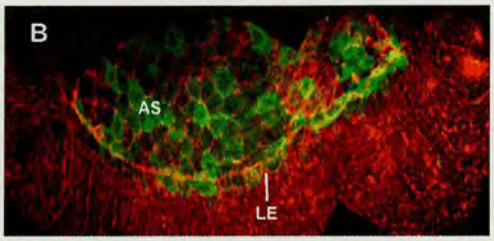

PGM 75-5-2 X C865 stage 14

D

Test (groups 1, 2)			Control (groups 3, 4)		
Fo: +; +; *jar^{R39}/TM3* X *PGM; e22C; jar^{R39}/TM3*			Fo: +; +; *TM3/TM6* X *PGM; e22C; jar^{R39}/TM3*		
F1: Third chromosome genotype:			F1: Third chromosome genotype:		
Genotype	**Probability**	**Viability**	**Genotype**	**Probability**	**Viability**
TM3/TM3	25%	Lethal	*TM3/TM3*	25%	Lethal
jar^{R39}/TM3	50%	Viable	*jar^{R39}/TM3*	25%	Viable
jar^{R39}/jar^{R39}	25%	**Lethal in non-fluorescent embryos.**	*jar^{R39}/TM6*	25%	Viable
			TM3/TM6	25%	Viable
Expected: 50% viability in non-fluorescent flies			**Expected: 75% viability in fluorescent and non-fluorescent flies**		

E

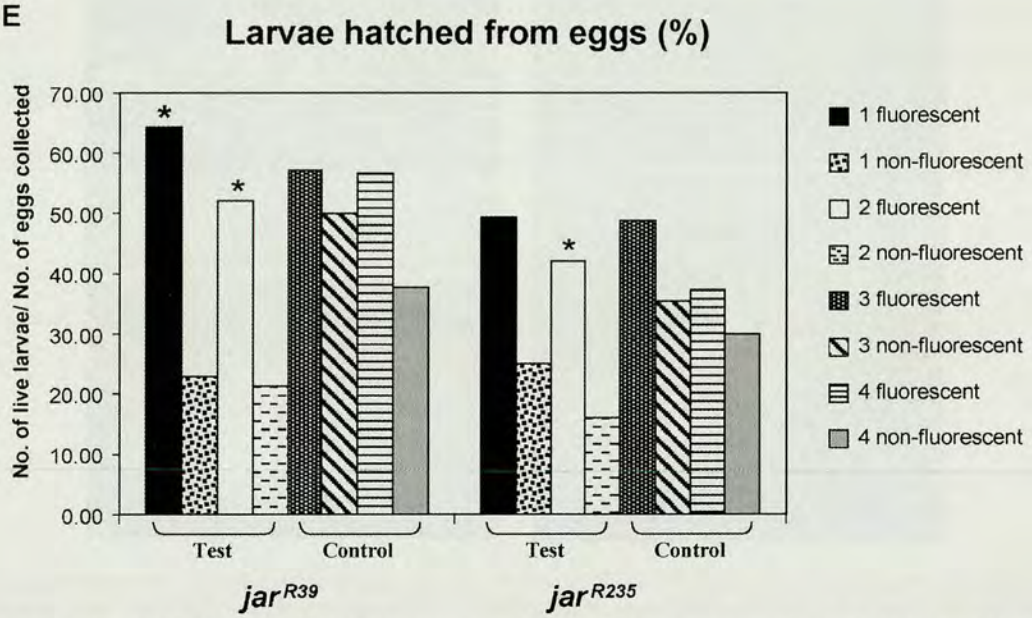

Fig. 8. The expression of Myosin VI-GFP tagged protein in embryos rescues lethality. (A): A diagram representing the fusion protein Myosin VI-GFP (PGM) expressed by the DNA construct created. The whole Myosin VI is fused in-frame at its C terminus to GFP. (B): The cross of PGM lines with Myosin VI gal4 line C865 triggers the expression of PGM fusion protein during dorsal closure at the leading edge (LE) and in the amnioserosa (AS). (C): The expression of Myosin VI as dorsal closure progresses (stage 15). (D): Mutant rescue test: the table describes the crosses undertaken in the test and the control groups, and the expected genotype of the progeny. (E): Mutant rescue analysis of the mutant flies *jar^{R39}* and *jar^{R235}*. Crosses 1 and 2 were the experimental group and crosses 3 and 4 were the control group (see description in the Materials and Methods). Crosses 1 and 3 (the first two columns) were made with heterozygous female mutants expressing PGM protein (fluorescent) and non-fluorescent male. Crosses 2 and 4 were created with fluorescent heterozygous male and non-fluorescent females. The difference between the survival of fluorescent and non-fluorescent embryos was compared between groups 1 and 3, and between groups 2 and 4 and examined statistically with a chi-squared test. The asterisks indicate a significant increase in the survival rate of fluorescent embryos ($P < 0.005$).

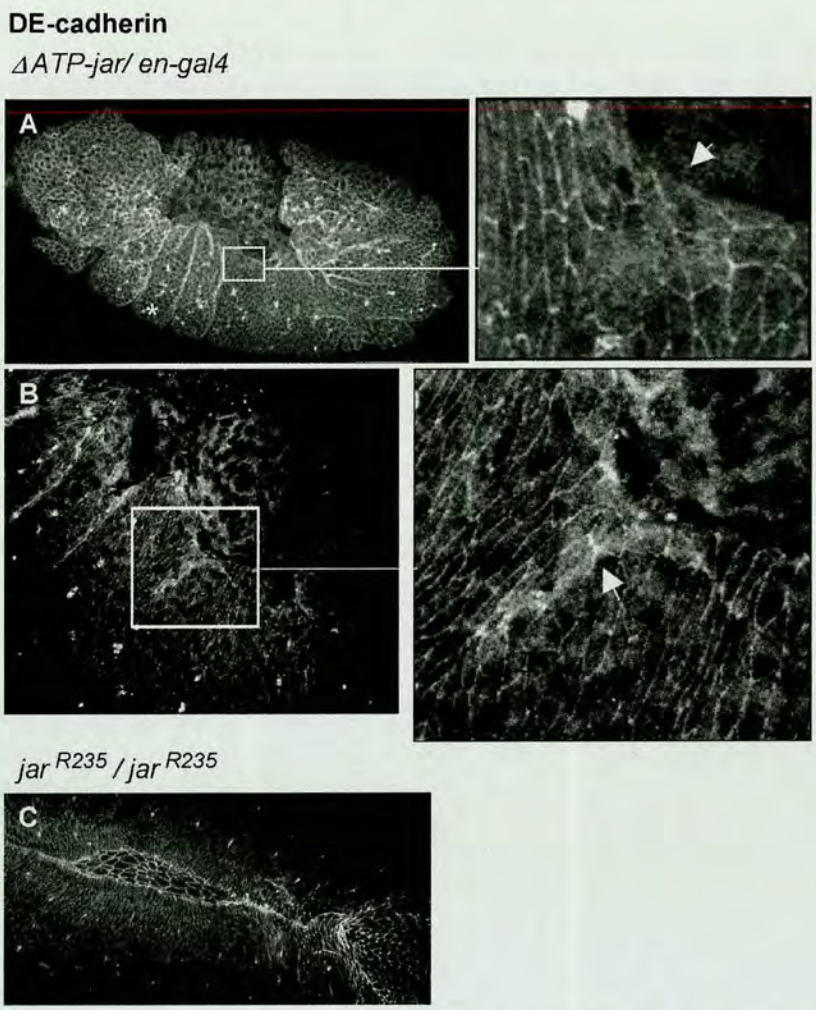

Fig. 9. Expression of jar dominant negative molecules disrupts the expression and localization of DE-cadherin within the cells. (A): In some of the areas expressing ΔATP-jar, DE-cadherin is absent from the cell membrane (see arrow in the magnified picture in A), in other areas the localisation of DE-cadherin to the cell membrane is disrupted and DE-cadherin is present in the cell cytoplasm (B, arrow). In some areas of the lateral epidermis the tissue is "folding in" (A, asterisk). (C): In homozygous *jar*^{R235} embryos, no disruption in DE-cadherin expression was observed.

was disrupted and the protein appeared in the cell cytoplasm and not in the cell membrane as in the wild-type cells (Fig. 9B). In the mutant embryos, the localisation of DE-cadherin in the lateral epidermis, the leading edge and the amnioserosa cells was not altered (Fig. 9C). It is possible that the maternal Myosin VI leads to the correct localisation of cadherin. Similar results were observed when the expression of DE-cadherin was examined in *RhoA* homozygous mutant embryos and in embryos expressing the dominant-negative of RhoA, RhoN19: In the homozygous mutant *RhoA* embryos, no defect was observed in the localisation of DE-cadherin, while the in cells expressing RhoN19 the expression of DE-cadherin was significantly reduced (Bloor and Kiehart, 2002). In the embryos expressing ΔATP-jar, the defects observed in the epidermal cells were more severe than the ones observed in the homozygous mutants (possibly due to the maternal contribution of Myosin VI in the mutant embryos).

To test if Myosin VI is also involved in the maintenance of cell shape we examined the effect of Myosin VI on the expression of Myosin II, which is necessary for preserving cell shape at the leading edge and in the amnioserosa during the morphogenic changes of the tissues during dorsal closure (Young et al., 1993). The expression of Myosin II did not change significantly in the *jar*^{R39} and *jar*^{R235} mutants, nor in embryos expressing Myosin VI dominant negative (Fig. 5E,H, and I and unpublished results). These results are consistent with previous studies showing that Myosin VI and Myosin II do not have a physical interaction during embryogenesis (Petritsch et al., 2003).

2.8. Myosin VI is present in the filopodia and lamellipodia during dorsal closure

As the epidermis covers the amnioserosa during dorsal closure, the epithelial cells at the leading edge show

extensive activity of filopodia and lamellipodia, which are crucial for zipping together the epithelial sheets and for the precise matching of the cells in the zipping process (Jacinto et al., 2000; Martin and Wood, 2002). Filopodia and lamellipodia are created through membrane remodelling. The involvement of Myosin VI in the creation of the pseudocleavage furrows in the cyncitial blastoderm (Mermall and Miller, 1995), and the separating membrane in the stereocilia of the in mice cochlear cells (Avraham et al., 1995; Avraham et al., 1997) raises the possibility that Myosin VI is also involved in the creation of filopodia and lamellipodia at the leading edge. PGM was therefore, expressed during dorsal closure, using an *en-gal4* line, and filopodia and lamellipodia were observed in living embryos. There is strong expression of PGM in the cell membrane at the edge of epithelial cells facing the opposite edge (Fig. 10A–C, yellow arrows). PGM is also present in filopodia (Fig. 10A–C, white arrows) and lamellipodia (Fig. 10D, asterisks). As the cells meet, PGM expression increases in the adhesion area (Fig. 10B,C, yellow arrows). When the adhesion between the cells is completed, the expression of PGM is reduced (Fig. 10E). The expression of PGM in the filopodia and lamellipodia suggests that Myosin VI is necessary for the migration of the cells as well as for cell adhesion; however the expression in lamellipodia could be necessary for the initial attachment of the cells.

2.9. The effect of Myosin VI depletion on actin organisation in the amnioserosa and leading edge cells

Myosin VI was shown to be necessary for the organisation of actin filaments in the individualisation complex in the testes. To test if Myosin VI plays a role in actin dynamics during dorsal closure, actin filaments were stained in mutant embryos with phalloidin. In *OrR* flies, Myosin VI and actin generally have a similar localisation; however, in the leading edge the actin cable is concentrated mainly around the amnioserosa, whereas the strongest expression of Myosin VI is in a layer of cells between the actin cable and the epithelial sheet (Fig. 11A–C).

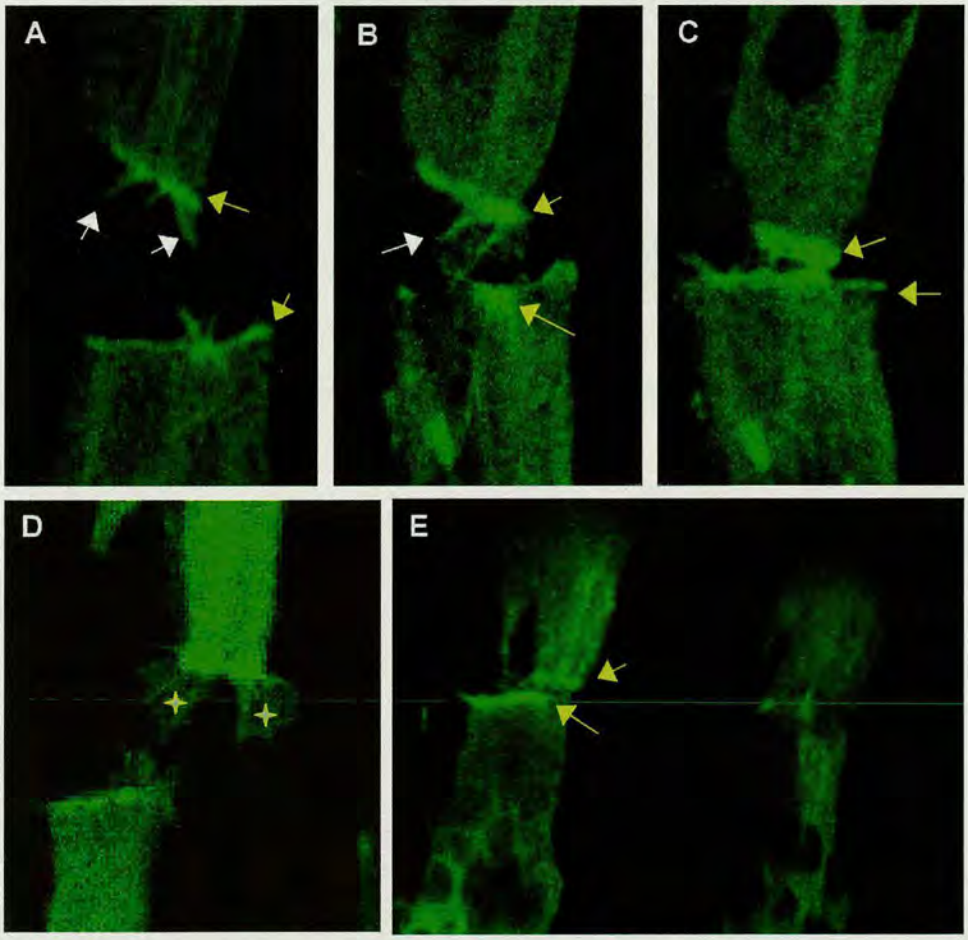

Fig. 10. Expression of Myosin VI-GFP in live embryo during dorsal closure. Myosin VI-GFP (PGM) was expressed in the posterior stripes of the embryo by *en-gal4*. A–C shows the expression of PGM in the leading edge as the opposite tissues meet. (A): When the epithelial tissues migrate, PGM is strongly expressed in the leading edge (yellow arrows) and is also present in the filopodia of the epithelial cells (white arrows). PGM is also expressed in lamellipodia (D, asterisks). (B,C): As the contacts between the opposite cells were created, the presence of PGM in the leading edge increases. (E): Once the adhesion between the cells is complete, the expression of PGM in the connection declines (right stripe of cells).

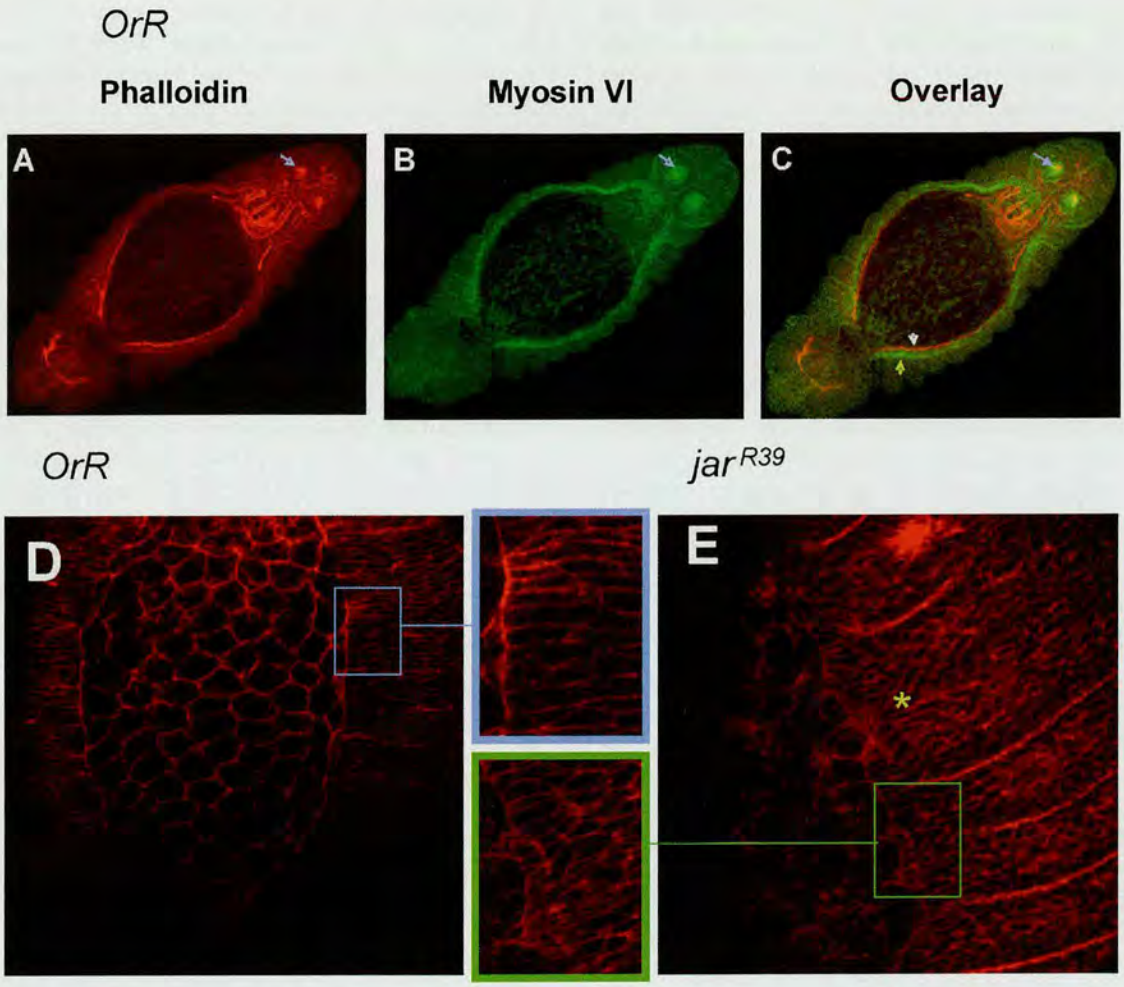

Fig. 11. Cell shape and actin organisation in the amnioserosa and the leading edge of *OrR* and *jar* ^{R39} mutants. (A–C): Localisation of actin (A) and Myosin VI (B) in the embryo prior to dorsal closure. Actin is localised at the leading edge of the migrating epithelial sheet (C, white arrowhead), while Myosin VI is localised in a layer of cells surrounding actin cables (C, yellow arrowhead). Note the strong expression of actin and Myosin VI in the posterior spiracle (arrow). (D): In *OrR*, the cells in the leading edge are elongated, the actin cable is intact and the cells in the amnioserosa are intact and form a uniform layer. (E): A mutant embryo *jar* ^{R39}. The cells in the amnioserosa lose their organised shape, in the leading edge the actin cable is broken in several places (asterisk), and some of the cells still have a polygonal shape and do not elongate. Note the abnormalities in segment organisation, near the asterisk.

In the leading edge the cells are elongated (Fig. 11D), and connected to the actin cable surrounding the amnioserosa at a uniform width. Not all the mutant embryos showed defects in actin organisation, however in some of the mutant embryos that failed to complete dorsal closure, the actin filaments in the amnioserosa are disassociated (Fig. 11E). At the leading edge, some regions of the actin cable are destroyed, many of the cells are not elongated and the organisation of the row of cells at the front is disrupted (Fig. 11E). The aberrant shape of the cells also appears in the border regions between the segments, suggesting that the disruption in cell shape and movement appear not just in the leading edge of the epithelia during dorsal closure, but also in other epithelial cells in the lateral epidermis. When ΔATP-jar is expressed, the loss in cell shape and actin cable organisation was even more dramatic (Fig. 7 A–C,E). In severe cases the actin cable disappears, and the cells at the leading edge connect remnants of actin cables that appear as aggregates of filaments (Fig. 7E, arrows). It seems that cell shape in the leading edge and in the amnioserosa changed significantly as a consequence of loss of cell adhesion. In some embryos the cells at the lateral epidermis changed their shape and the tight organisation of the actin filaments at the cell membrane was disrupted (Fig. 7B). Therefore the change in the cytoskeletal organisation could be the reason why the cells expressing ΔATP-jar lose their rigidity and fold in. These results suggest that during dorsal closure Myosin VI plays a role not only in the adhesion of the cells, but also in the arrangement of the actin cytoskeleton.

3. Discussion

Previous studies showed that in *Drosophila* Myosin VI plays a role in cell migration during oogenesis (Deng et al., 1999; Geisbrecht and Montell, 2002), actin dynamics during

sperm individualisation (Hicks et al., 1999; Rogat and Miller, 2002), membrane synthesis during cellularization (Mermall and Miller, 1995) and spindle orientation in the metaphase neuroblast (Petritsch et al., 2003). In this study we provide evidence that Myosin VI is necessary for cell–cell adhesion and maintaining cell rigidity during dorsal closure. Disruption in Myosin VI function caused folding-in of the migrating epithelial tissue and rupture of the tissue, which suggests that Myosin VI is necessary not only for the cell–cell adhesion but also for keeping the cells rigid as they migrate.

We have isolated lethal mutants in the *jar* gene of *Drosophila* which encodes Myosin VI. The resulting embryos die late in embryogenesis failing to complete dorsal closure or as early larvae. The expression of fluorescent tagged Myosin VI in the mutant embryos rescued the lethal phenotype of embryos indicating that the lethality is caused due to the *jaguar* mutation.

Genetic and molecular analysis revealed that the two mutants have been disrupted in the sequence: AGTATACT. In jar^{R235} this sequence has been changed and in jar^{R39} the sequence is deleted. This is a palindromic sequence and as such could potentially regulate the transcription of *jar*. In *Drosophila* palindromic sequences located within the promoter region are often necessary for accurate transcription (Cho et al., 1998; Oh et al., 1999; Okada et al., 2001).The palindromic region might be a specific binding site for transcription factors (Hirose et al., 1993).

Not all the embryos failed to complete dorsal closure and some hatched as larvae. RTPCR results showed that in homozygous mutant embryos (stage 14 onwards) Myosin VI transcripts are still observed. However, in the homozygous mutant larvae, the expression level of Myosin VI transcripts is lower than *OrR* (these results are consistent with the Western Blot and antibody localization results). These results suggest that survival throughout embryogenesis is due largely to the use of maternal Myosin VI.

In the three mutants: jar^{mmw14}, jar^{R39} and jar^{R235} the 5′ end of the mRNA was truncated, however the truncated region in jar^{R39} and jar^{R235} is bigger than that observed in jar^{mmw14} (1027 bp compared with 517 bp). This could explain why jar^{mmw14} mutants survive until adulthood while the jar^{R39} and jar^{R235} mutants die during embryogenesis and the first larval instar.

Analysis of the null mutant jar^{322}, published after completion of our experiments (Pertrisch et al., 2003), showed that it affected the embryonic neuroblasts but there is no mention of any defects in cell shape in the lateral epidermis, or of some embryos failing in dorsal closure. However, we have shown that the same dominant negative Myosin VI that caused mislocalisation of Miranda and misorientation of the spindle in neuroblasts is shown to disrupt the cell attachment in the amnioserosa and the leading edge epidermis during dorsal closure. Therefore, Myosin VI is necessary for both neuroblasts morphogenesis and dorsal closure during embryogenesis. It is surprising to find that the null mutant jar^{322} lives until the early stages of second instar, while the homozygous mutants jar^{R39} and jar^{R235} die during embryogenesis and during first instar. Since no protein was detected in the mutants jar^{R39} and jar^{R235}, the severe effect of the mutants might be expected to be the same as in a null mutant.

Depletion and disruption in Myosin VI function caused detachment of cells and folding-in of the migrating epidermis during dorsal closure. In *en-Gal4/ΔATP-jar* embryos these affects were dramatic; if the cells expressing ΔATP-jar are not as robust as the wild type they might not be able to bear the multiple forces applied to them during dorsal closure, which could lead to the rupture of the tissue caused initially by the detachment of cells.

Cells that express ΔATP-jar and mutant cells had an aberrant organisation of the actin filaments in the cell cortex at the leading edge, and the cells lost their elongated shape. This is the area that was found to fold-in in many embryos. The connection between the change in cell shape and the disorganisation of the cytoskeleton could suggest that the cytoskeleton is necessary for maintaining cell rigidity. This suggests that Myosin VI preserves cell shape by participating in the synthesis or the patterning of the actin filaments during the migration of the epithelial cells. This is consistent with previous studies showing the role of Myosin VI in actin dynamics in the individualisation complex in the testes (Rogat and Miller, 2002).

The creation of multiple wounds by laser beams in embryos did not prevent their quick recovery (Kiehart et al., 2000). Disruption caused by Myosin VI prevents recovery of the ripped tissues, probably due to the loss of cell adhesion properties. This suggests a potentially important role for Myosin VI in wound healing.

The failure in dorsal closure which we observed corresponds well with our antisense experiments during development which led to failures in all the cell migrations of follicle cells during oogenesis. In each case Myosin VI is needed for the correct movement of a sheet or tight cluster of follicle cells (Deng et al., 1999; K. Leaper and M. Bownes, unpublished), and in each case the cells lost their shape, therefore Myosin VI might also be needed for the preservation of cell shapes as they migrate. We also observed that the follicle cell layer was disorganised and did not remain as a unicellular sheet (Deng et al., 1999). The phenotype is similar in the lethal embryos, where cells detach from sheets and are found loose in the haemolymph and the cells in the leading edge loose their tight organisation. The reduced expression and mislocalisation of DE-cadherin in the follicle cells and the lateral epidermis following the disruption in Myosin VI expression and function support the assumption that Myosin VI might play similar roles in the organisation of the two tissues (Geisbrecht et al., 2002).

During spermatogenesis in *Drosophila* male sterile *jar* mutants fail in sperm individualisation, (Hicks et al., 1999) an event which requires separation of sperm by membranes.

It is possible that Myosin VI also plays a role in the remodelling of cell membranes at the leading edge and that this is crucial for the adhesive properties of the cells during dorsal closure. The presence of Myosin VI in the filopodia and lamellipodia in epithelial cells at the leading edge could be necessary for the remodelling of the cell membrane.

It seems that Myosin VI is crucial for maintaining epithelial sheets and keeping cells in the correct spatial relationship to one another. This could be achieved by Myosin VI anchoring cells to the basement membranes that surround epithelial sheets, or perhaps if Myosin VI is absent from the apical surface of cells, cell polarity is not correctly defined and cell contacts are thus lost.

We need to identify additional potential cargoes carried by the Myosin VI tail by protein–protein interaction experiments in vitro. Although the *jar* mutants are lethal, we can still investigate the abnormal phenotypes they cause at later developmental stages by producing clones of mutant cells failing to express Myosin VI at various times and in various tissues.

4. Experimental procedures

4.1. Generation of jar mutants and fly crosses

The stocks used in these experiments are: *C865* (Deng et al., 1997); jar^{mmw14} (Hicks et al., 1999); $y^{1}w^{-}$; *TM3*, Sb^{1}/*TM6B*, Tb^{+}; *w-*; *P{Δ2-3]Dr/w-*, *TM6*, *Tb*; Ly^{1}/*TM6B*, $P\{w^{+mW.hs} = UbiGFP.S65T\}$ *PAD2*, Tb^{1}; *Df(3R)crb87-5*, $st^{1}e^{1}$/*TM3*, Ser^{1}, (Bloomington Stock Center), UAS-Δ*ATPjar* (Pertrisch et al., 2003), *engrailed-gal4* (Brand A) *e22c* (Deng et al., 1999).

The *jar* mutants were generated by mobilising a single P element insertion located in the 5′ UTR of the *jar* locus in strain *C865*, which contains a P element *P[GawB]* at 95F on the third chromosome (*w-*; *P [Gal4 w +] Y*; *P [Gal4 w +]*), located at bp 306 in exon 1 (Fig. 1B) Homozygous mutant embryos and larvae were distinguished from their heterozygous siblings by using the fluorescent balancer chromosome Ly^{1}/*TM6B, GFP Tb*.

For the expression of dominant negative Myosin VI, virgin female of the *en-gal4* line were crossed with male *UAS-ΔATP-jar* flies. Statistical analysis used the chi square test ($P < 0.005$).

4.2. Molecular analysis of mutants

The new mutants jar^{R39} and jar^{R235} do not complement the mutant jar^{mmw14} ($jar^{mmw14}/jar^{R39/R235}$ heterozygotes are male sterile), therefore the mutations were potentially located in the same area as the 1 kb deletion in jar^{mmw14} (Fig. 1C). The precise location of the deletion in jar^{mmw14} was first identified by sequencing jar^{mmw14}/*TM3* heterozygous flies (Fig. 1C), and the mutations in jar^{R39} and jar^{R235} were identified by sequencing the deletion area of jar^{mmw14} (this contains only the copy of the mutant genes, as shown in Fig. 1C).

4.3. Generation of Myosin VI-GFP (PGM) DNA construct

The DNA construct expressing Myosin VI fused in-frame to Green Fluorescent Protein (GFP) was prepared by two cloning steps. In the first step the 0.8 kb *EGFP* gene was isolated from pEGFPN1 plasmid (Clontech), using *EcoRI* and *NotI* restriction sites, and cloned into a pUAST plasmid (restricted with the same enzymes) to form the pUAST-GFP plasmid. In the second step, a full-length cDNA encoding the EM3 isoform of Myosin VI (95F MHC) was cloned in the pUAST-GFP plasmid, connected in-frame with the *EGFP* gene at its 3′ end (see Fig. 8A). The 4.1 kb Myosin VI cDNA was amplified by proof-reading PCR, with a 5′ primer that added an *EcoRI* restriction site upstream of the initiator methionine, and a 3′ primer, designed to contain *AgeI* restriction site downstream of the Myosin VI cDNA, and connected in-frame with the *EGFP* gene.

The proof-reading PCR used the *pfu* turbo polymerase kit (Stratagene), according to the manufacturer's instructions. The PCR product was digested with *EcoRI* and *AgeI* and cloned into the pUAST-GFP plasmid (restricted with the same enzymes), to form the DNA construct: pUAST-Myosin VI-GFP (PGM) DNA construct. The DNA construct was injected into w^{k} fly embryos as described previously (Deng et al., 1999). The fly line selected for use in this experiment is PGM 45-1, as the insert is located on the X chromosome.

4.4. Mutant rescue

Transgenic flies, containing the Myosin VI cDNA fused in-frame to the *EGFP* gene (PGM), driven by a UAS (upstream activating sequence) target sequence, were generated by p element-mediated transformation. The PGM transgene was crossed with the *e22C-Gal4* line and with the mutant flies jar^{R39}/*TM3*, *Sb*, or jar^{R235}/*TM3* to create the fluorescent heterozygous fly lines: *PGM*; *e22C*; jar^{R39}/*TM3*, *Sb* and *PGM*; *e22C*; jar^{R235}/*TM3*, *Sb*. *e22C* fly line express the Gal4 protein ubiquitously during embryogenesis and hence triggers the expression of PGM throughout the embryo during late stages of embryogenesis, when the maternal supplies of Myosin VI begin to disappear. The fluorescent heterozygous flies were crossed with the non-fluorescent heterozygous flies, as described for jar^{R39}:

4.4.1. PGM; e22C; jar^{R39}/TM3, Sb X jar^{R39}/TM3, Sb

This cross created fluorescent and non-fluorescent progeny; each group will contain the same genotype composition, as described in the table on Fig. 8D, for the test group. In non-fluorescent flies, because the homozygous mutants are embryonic lethal and the flies homozygous for the balancer chromosome are lethal as well, only the heterozygous embryos are expected to survive, yielding

a survival rate of 50%. If the expression of PGM rescues the embryonic lethal phenotype, the fluorescent homozygous embryos will survive and the number of fluorescent larvae hatching from the eggs will be significantly higher than the non-fluorescent embryos. As a control the effect of PGM expression on the survival of embryos which are not homozygous Myosin VI mutants was examined by the following cross (described for *jar*^{R39}):

4.4.2. PGM; e22C; jar^{R39}*/TM3, Sb X TM3, Sb/TM6, Tb*

This cross created fluorescent and non-fluorescent progeny; each group will contain the same genotype composition, as described in the table in Fig. 8D, for the control group. Each group contains theoretically 75% viable embryos, heterozygous and non-mutant.

In every group a reciprocal cross was established in order to test the maternal contribution of PGM on the survival of the embryos. The fluorescent and non-fluorescent embryos obtained from every cross were selected separately (100 eggs from each group) and the survival of embryos was calculated as the number of larvae hatching from the eggs within the following two days.

4.5. PCR and RTPCR

mRNA was primed with oligo-p(dT)$_{18}$ and reverse transcribed by Superscript™ II (GIBCO BRL). When cDNA was used as a template and for PCR of small DNA fragments (up to 5 kb), the Qiagen PCR kit was used (201203). Large DNA fragments were amplified using the Expand Long Template PCR kit of Roche (1681834), according the manufacturers' instructions.

The primers used were: for *jar* mRNA: P1: gagttcgactc gactcatccaac; P517-1: atcacgatgacaactgcgaac; P1027: tagtgcgatatgtaaccaccgacc; TAN: catttccgaattcggcaagatcaa caagatccgg; MYC2: atttaccggtccttgtttctgcattgctgc. For *myosin 29D* mRNA: TRIF: aatcacagcttcagccacac; 529R: gtcccgacaagtggatcag. For ribosomal RNA: PR491: aagcccaagggtatcgacaac; PR492: attgaactcggcactggcaca. For *jar* genomic DNA: HKC865F: tgttgctacccattgcttttcaatc; 5k3C865: cgggctgaaaagggaaaag; C865 for: gcggatc caaatcttcttgctttgctg, C865 Rev: tttgaacaggaaactgaaacg, EXC2Rev: acatggaatagggtgcatgg, EXC2For: gtgcttgttgtt tttcgg, mmw14 delfor: tgcaggtgttgcagaagagtg; mmw14delrev: ttatccccttacccctattcc. For *jaguar* cDNA amplification: MYN: atttccgaattcttcgactcgactcatccaacg; and MYC2.

The PCR products obtained were isolated from Tris-acetate/Ethylenediaminetetra-acetate (TAE) gels, purified, and seqenced.

4.6. Antibodies

The Myosin VI monoclonal antibody 3C7 (Kellerman and Miller, 1992) was diluted 1:50 and Myosin VI polyclonal antibody was diluted 1:3. Nonmuscle Myosin II (Edwards and Kiehart, 1996) was diluted 1:50. Phalloidin (molecular probes, A12380) was diluted 1:50, rat anti-*Drosophila* E-Cadherin (Uemura, T.) was diluted 1:20. Alexafluor 568 conjugated anti mouse (molecular probes) was diluted 1:500, FITC-cojugated anti-mouse IgG and anti rabbit IgG was diluted 1:100. HRP conjugated anti-mouse IgG was diluted 1:500.

For the Western Analysis, 3C7 was diluted 1:200, and the anti-mouse secondary antibody diluted 1:10000. The YP control antibody (Bownes and Nothiger, 1981) was diluted 1:1000 with the HRP conjugated anti-rabbit IgG secondary antibody diluted 1:10000 (Promega).

4.7. Western analysis

20 embryos were homogenised in 40 μl of 2 × loading buffer. Western Blot was performed as described previously (Deng et al., 1999).

4.8. In situ antibody staining of embryos

Embryos were collected at four hour intervals after laying. They were dechorionated, fixed and devitilinated manually or with methanol. The staining of the embryos was performed according to standard protocols (Sullivan et al., 2000).

Acknowledgements

We are grateful to BBSRC for a studentship for KL, to the Darwin Trust and the B'nei Brith' Fellowship for a studentship and support respectively for HM, to Hilary Anderson for preparation of the manuscript and to George Tzolovsky and anonymous reviewers for comments on the paper.

References

Adams, M.D., et al., 2000. The genome sequence of *Drosophila melanogaster*. Science 287, 2185–2195.

Ahmed, Z.M., Morell, R.J., Riazuddin, S., Gropman, A., Shaukat, S., Ahmad, M.M., Mohiddin, S.A., Fananapazir, L., Caruso, R.C., Husnain, T., et al., 2003. Mutations of MYO6 are associated with recessive deafness, DFNB37. Am. J. Hum. Genet. 72, 1315–1322.

Avraham, K.B., Hasson, T., Steel, K.P., Kingsley, D.M., Russell, L.B., Mooseker, M.S., Copeland, N.G., Jenkins, N.A., 1995. The mouse Snellís waltzer deafness gene encodes an unconventional myosin required for structural integrity of inner ear hair cells. Nat. Genet. 11, 369–375.

Avraham, K.B., Hasson, T., Sobe, T., Balsara, B., Testa, J.R., Skvorak, A.B., Morton, C.C., Copeland, N.G., Jenkins, N.A., 1997. Characterization of unconventional MYO6, the human homologue of the gene responsible for deafness in Snell's waltzer mice. Hum. Mol. Genet. 6, 1225–1231.

Baker, J.P., Titus, M.A., 1998. Myosins: matching functions with motors. Curr. Opin. Cell Biol. 10, 80–86.

Bloor, J.W., Kiehart, D.P., 2002. *Drosophila* RhoA regulates the cytoskeleton and cell–cell adhesion in the developing epidermis. Development 129, 3173–3183.

Bohrmann, J., 1997. *Drosophila* Myosin VI is involved in intra- and intercellular transport during oogenesis. Cell. Mol. Life Sci. 53, 652–662.

Bownes, M., Nothiger, R., 1981. Sex determining genes and vitellogenin synthesis in *Drosophila* melanogaster. Mol. Gen. Genet. 182, 222–228.

Buss, F., Kendrick-Jones, J., Lionne, C., Knight, A.E., Cote, G.P., Luzio, J.P., 1998. The localization of myosin VI at the golgi complex and leading edge of fibroblasts and its phosphorylation and recruitment into membrane ruffles of A431 cells after growth factor stimulation. J. Cell Biol. 143, 1535–1545.

Buss, F., Arden, S.D., Lindsay, M., Luzio, J.P., Kendrick-Jones, J., Myosin, V.I., 2001. isoform localized to clathrin-coated vesicles with a role in clathrin-mediated endocytosis. Eur. Mol. Biol. Org. J. 20, 3676–3684.

Cho, N., Oh, Y., Hwang, S.Y., Han, D., Park, S.P., Yoon, J., Han, K., Baek, K., 1998. Promoter analysis of the *Drosophila* genes encoding TFIIB and TATA box-binding protein. Mol. Cells 8, 770–776.

Deng, W.M., Zhao, D., Rothwell, K., Bownes, M., 1997. Analysis of P[gal4] insertion lines of *Drosophila melanogaster* as a route to identifying genes important in the follicle cells during oogenesis. Mol. Hum. Reprod. 3, 853–862.

Deng, W., Leaper, K., Bownes, M., 1999. A targeted gene silencing technique shows that *Drosophila* Myosin VI is required for egg chamber and imaginal disc morphogenesis. J. Cell Sci. 112, 3677–3690.

Geisbrecht, E.R., Montell, D.J., 2002. Myosin VI is required for E-cadherin-mediated border cell migration. Nat. Cell Biol. 4, 616–620.

Hasson, T., Mooseker, M.S., 1994. Porcine Myosin-VI, characterization of a new mammalian unconventional myosin. J. Cell Biol. 127, 425–440.

Hasson, T., Gillespie, P.G., Garcia, J.A., MacDonald, R.B., Zhao, Y., Yee, A.G., Mooseker, M.S., Corey, D.P., 1997. Unconventional myosins in inner-ear sensory epithelia. J. Cell Biol. 137, 1287–1307.

Hicks, J.L., Deng, W.M., Rogat, A.D., Miller, K.G., Bownes, M., Class, V.I., 1999. unconventional myosin is required for spermatogenesis in *Drosophila*. Mol. Biol. Cell 10, 4341–4353.

Hirose, F., Yamaguchi, M., Handa, H., Inomata, Y., Matsukage, A., 1993. Novel 8-base pair sequence (*Drosophila* DNA replication-related element) and specific binding factor involved in the expression of *Drosophila* genes for DNA polymerase alpha and proliferating cell nuclear antigen. J. Biol. Chem. 268, 2092–2099.

Jacinto, A., Wood, W., Balayo, T., Turmaine, M., Martinez-Arias, A., Martin, P., 2000. Dynamic actin-based epithelial adhesion and cell matching during *Drosophila* dorsal closure. Curr. Biol. 10, 1420–1426.

Kelleher, J.F., Mandell, M.A., Moulder, G., Hill, K.L., L'Hernault, S.W., Barstead, R., Titus, M.A., 2000. Myosin VI is required for asymmetric segregation of cellular components during *C. elegans* spermatogenesis. Curr. Biol. 10, 1489–1496.

Kellerman, K.A., Miller, G.M., 1992. An unconventional myosin heavy chain gene from *Drosophila melanogaster*. J. Cell Biol. 119, 823–834.

Kellerman, K.A., Gardner, H.F., Miller, K.G., 1992. Expression pattern of the *Drosophila* 95F myosin heavy-chain gene. Mol. Biol. Cell Suppl. 3, 46–46.

Kiehart, D.P., Galbraith, C.G., Edwards, K.A., Rickoll, W.L., Montague, R.A., 2000. Multiple forces contribute to cell sheet morphogenesis for dorsal closure in *Drosophila*. J. Cell Biol. 149, 471–490.

Lantz, V.A., Miller, K.G., 1998. A class VI unconventional myosin is associated with a homologue of a microtubule-binding protein, cytoplasmic linker protein-170, in neurons and at the posterior pole of *Drosophila* embryos. J. Cell Biol. 140, 897–910.

Martin, P., Wood, W., 2002. Epithelial fusions in the embryo. Curr. Opin. Cell Biol. 14, 569–574.

Mermall, V., McNally, J.G., Miller, K.G., 1994. Transport of cytoplasmic particles catalysed by an unconventional myosin in living *Drosophila* embryos. Nature 369, 560–562.

Mermall, V., Miller, K.G., 1995. The 95F unconventional myosin is required for proper organization of the *Drosophila* syncytial blastoderm. J. Cell Biol. 129, 1575–1588.

Mermall, V., Post, P.L., Mooseker, M.S., 1998. Unconventional myosins in cell movement, membrane traffic, and signal transduction. Science 279, 527–533.

Melchionda, S., Ahituv, N., Bisceglia, L., Sobe, T., Glaser, F., Rabionet, R., Arbones, M.L., Notarangelo, A., Di Iorio, E., Carella, M., et al., 2001. MYO6, the human homologue of the gene responsible for deafness in Snell's waltzer mice, is mutated in autosomal dominant nonsyndromic hearing loss. Am. J. Hum. Genet. 69, 635–640.

Mohiddin, S.A., Ahmed, Z.M., Griffith, A.J., Tripodi, D., Friedman, T.B., Fananapazir, L., Morell, R.J., 2004. Novel association of hypertrophic cardiomyopathy, sensorineural deafness, and a mutation in unconventional Myosin VI (MYO6). J. Med. Genet. 41, 309–314.

Morris, S.M., Arden, S.D., Roberts, R.C., Kendrick-Jones, J., Cooper, J.A., Luzio, J.P., Buss, F., 2002. Myosin VI binds to and localises with Dab2, potentially linking receptor-mediated endocytosis and the actin cytoskeleton. Traffic 3, 331–341.

Oh, Y., Lee, C., Baek, K., Kim, W., Yoon, J., Han, K., Cho, N., 1999. Related an element with palindromic structure is required for the expression of TBP (TATA box-binding protein) gene in *Drosophila* melanogaster. Mol. Cells 9, 673–677.

Okada, T., Sakai, T., Murata, T., Kako, K., Sakamoto, K., Ohtomi, M., Katsura, T., Ishida, N., 2001. Promoter analysis for daily expression of *Drosophila* timeless gene. Biochem. Biophys. Res. Commun. 283, 577–582.

Oliver, T.N., Berg, J.S., Cheney, R.E., 1999. Tails of unconventional myosins. Cell Mol. Life Sci. 56, 243–257.

Petritsch, C., Tavosanis, G., Turck, C.W., Jan, L.Y., Jan, Y.N., 2003. The *Drosophila* Myosin VI Jaguar is required for basal protein targeting and correct spindle orientation in mitotic neuroblasts. Dev. Cell. 4, 273–281.

Rogat, A.D., Miller, K.G., 2002. A role for Myosin VI in actin dynamics at sites of membrane remodelling during *Drosophila* spermatogenesis. J. Cell Sci. 115, 4855–4865.

Sullivan, W., Ashburner, M., Hawley, R.S., 2000. *Drosophila* protocols. Cold Spring Harbor Laboratory, New York.

Wu, X., Jung, G., Hammer, J.A. 3rd, 2000. Functions of unconventional myosins. Curr. Opin. Cell Biol. 12, 42–51.

Wu, H., Nash, J.E., Zamorano, P., Garner, C.C., 2002. Interaction of SAP97 with minus-end-directed actin motor Myosin VI. J. Biol. Chem. 277, 30928–30934.

Young, P.E., Richman, A.M., Ketchum, A.S., Kiehart, D.P., 1993. Morphogenesis in *Drosophila* requires nonmuscle myosin heavy chain function. Genes Dev. 7, 29–41.